ASPECTS OF SWATH DESIGN AND EVALUATION

Alexander Ferguson Miller B.Eng.

Thesis Submitted for the Degree of Master of Science

Department of Naval Architecture and Ocean Engineering
University of Glasgow

September 1991

ProQuest LLC.
789 East Eisenhower Parkway
P.O. Box 1346
Ann Arbor, MI 48106 – 1346

DECLARATION

Except where reference is made to the work of others
this thesis is believed to be original.

ACKNOWLEDGEMENTS

The work described in this thesis formed the first joint Vickers Shipbuilding and Engineering Ltd / Glasgow University 'SWATH design and evaluation' project. The research was additionally funded by the Science and Engineering Research Council through the Marine Technology Directorate at the University.

The author would like to express his gratitude to all the staff of the Department of Naval Architecture and Ocean Engineering at the University, together with his colleagues in the Naval Architects Department at VSEL Barrow-in-Furness.

In particular the author wishes to acknowledge the supervision and support given by;

Professor D. Faulkner, John Elder Professor and Head of the Department of Naval Architecture and Ocean Engineering at Glasgow University.

Dr R.C. McGregor, Reader in the Department of Mechanical Engineering and until recently Senior Lecturer in the Department of Naval Architecture and Ocean Engineering at Glasgow University.

Dr A. Incecik, Superintendent of the Hydrodynamics Laboratory, Department of Naval Architecture and Ocean Engineering at Glasgow University.

Mr D. Downs and Mr J.A. Logan, of the Naval Architecture and Future Projects Department at VSEL Barrow-in-Furness.

Finally I would like to thank the other members of the University SWATH research team, past and present, for their advice and encouragement. I am especially indebted to Alistair Jones, James MacGregor and Eko Djatmiko, without whom the progression of this project would have been a considerably more daunting affair.

CONTENTS

LIST OF FIGURES

LIST OF TABLES

SUMMARY

This thesis describes research intended to extend and enhance the existing SWATH design capability developed at the University.

The thesis commences (Chapter 2) with a brief general review of all design aspects relevant to the balanced evaluation and comparison of monohull and SWATH vessels. SWATH vessel performance in each of these areas is analysed individually, and where possible quantified in relation to that of corresponding monohull ships. This chapter is intended to highlight the range and extent of the variations existing in SWATH / monohull design and operability characteristics.

Chapters 3, 4 and 5 of the thesis describe studies aimed at improving our understanding of the often neglected although fundamental aspects of damage stability, manoeuvring and wave induced global loading. These design topics were selected for investigation after the preliminary review highlighted shortfalls in the availability and reliability of relevant information.

Chapter 3 addresses the question of damage stability. Results from an extensive parametric study undertaken to explore the damage stability characteristics of SWATH vessels are presented and discussed. Secondly the relationships thus established between design geometry and damage stability are utilized in the construction of 'FSEP1'; a design program which estimates damaged stability characteristics at the preliminary design stage.

Chapter 4 investigates the manoeuvring performance of SWATH ships. Following a thorough literature survey, conventional (monohull) manoeuvring theory is applied and adapted to create a manoeuvring prediction tool for SWATH vessels; 'SWATHMAN'. This program will estimate required rudder areas in order to achieve a specified manoeuvring performance. Conversely the program will estimate the likely turning performance for a specified rudder area. The program incorporates propeller acceleration effects and caters for control fins mounted in and outwith the slipstream.

Chapter 5 reviews aspects of wave loading in the structural design of SWATH ships. It is widely acknowledged that wave induced side force leading to a transverse bending moment is the dominant form of environmental loading for these vessels. All available methods for the calculation / estimation of this force were therefore identified

and applied to the vessels T-AGOS 19 and the M.V. Patria. Short term extreme value prediction methods are applied in order to determine likely lifetime values of design extreme loading. Empirically derived estimates are compared with those produced by the application of rigorous three dimensional potential theory, and conclusions on the applicability of the methods are drawn.

Finally chapter 6 outlines a method for the overall mission based evaluation of alternative monohull and SWATH designs. This comparison is based on all relevant features of the two concepts. Features and characteristics of both hullforms are identified and assigned a priority level. The priority level assigned includes consideration of the vessel's intended role and operating profile. Through application of this technique the chapter aims to provide guidance for the designer selecting hullforms for both general and specific roles.

CHAPTER 1

INTRODUCTION

1.1 General

Small Waterplane Area Twin Hull (SWATH) vessels have now been around for almost 20 years. These vessels are a form of modified catamaran where the underwater form has been distorted to move the supporting buoyancy well below the surface of the sea. A typical SWATH vessel consists of two totally submerged torpedo like hulls upon which an above water cross structure is supported by means of long streamlined surface piercing struts.

Fig 1.1 illustrates the M.V. Halcyon which is typical of modern SWATH geometry.

Improved seakeeping performance was the rationale behind development of the concept. Since wave excitation forces decrease exponentially with depth, their effect on deeply submerged hulls is therefore minimal. Reductions in motion due to decreased wave forces, are further augmented by the low waterplane area inherent in the concept. This increases the natural periods of resonant motion outwith the peak energy ranges of ocean wave spectra. It also allows the possibility of manipulating the motion transfer functions to decouple heave, pitch and roll responses. The resulting vessels have demonstrated dramatically improved seakeeping performance over conventional monohulls and catamarans at both model and full scale. Indeed in full scale trials conducted by the U.S. Navy (Ref 1), the 220 tonne S.S.P. Kaimalino was found to have seakeeping performance equivalent to a monohull some fifteen times its displacement.

In addition to offering dramatically improved seakeeping performance, SWATH ships possess larger 'usable' deck areas than equivalent monohulls. This permits greater flexibility particularly for operations involving aircraft or requiring a moonpool. This feature combined with low platform motion makes SWATH ships ideally suited to missions requiring air capability or involving hydrographic survey, diving support, etc.

These benefits are not however achieved without penalty. The provision of twin hulls increases surface area and hence weight so reducing payload fractions while

increasing construction costs and frictional resistance. In addition the twin hulled configuration necessitates duplication of certain shipboard systems further increasing cost and complexity. These problems are compounded by the low waterplane area which introduces restrictions on payload and requires the provision of control fins together with extensive ballasting / deballasting arrangements.

From the foregoing it will be obvious that the SWATH concept must not be regarded as a panacea. If SWATH is to evolve the limitations of the concept must be recognized and where possible action taken to minimize their effect. When evaluating alternative design proposals the naval architect must balance and offset the advantages afforded by SWATH ships by their many drawbacks, in an effort to determine the vessel type best suited to a given role.

1.2 History and Development

Although SWATH ships are a relatively recent phenomenon, the naval architechtural principles embodied in the concept have been known and applied separately for centuries.

Seafarers and traditional shipwrights alike, have long recognized the relationship between deep submergence of buoyancy and seakeeping. The many deep draught coastal vessels existing worldwide are evidence of this appreciation. Logical extension of this principle ultimately led Lundborg (Ref 2) to patent a semi-submerged ship in 1880.

Unfortunately since stability is linked to waterplane area such designs are inherently unstable. The solution to this problem was most likely first devised by the Polynesian and Melanesian peoples of the Pacific. For these islanders the use of multi hulls to achieve speed whilst maintaining stability has been standard practice for centuries.

Combining Lundborg's semi-submerged ship with the 'technology' of the Pacific Islanders leads directly to the modern Small Waterplane Area Twin or Triple Hull (SWATH) ship.

Evolution of the SWATH concept during the 20th century is best traced through patent applications. Notable amongst these are American applications by Nelson (Ref 3) (1905), and Blair (Ref 4) (1930). Albin Nelson was the first to file for a patent on a

twin hulled semi-submerged ship resembling a modern SWATH form. His motivation was however not improved seakeeping, but rather the requirement of keeping the cargo cool. It was thus left to William Blair to identify seakeeping as the rationale for the concept. Blair was subsequently awarded a patent on a multi-hulled semi-submerged ship specifically designed to improve performance in a seaway. In spite of this it was another 13 years before the first practical SWATH designs appeared in 1943 when Frederick Creed (Ref 5) filed for British and American patents on aircraft carrier and salvage vessel designs.

The 1960's saw the introduction and development of low motion semi-submersible offshore drilling rigs by the oil industry. Continued growth of interest in these designs led to the design and construction of the medium waterplane area twin hull seabed operations vessel 'Duplus' in 1969 (Ref 6). She has operated successfully since then under the names 'Duplus', 'Jaramac 57' and more recently 'Twin Drill'.

Two years later in the U.S.A. Litton Industries produced the first manned SWATH demonstrator, the 6m long experimental 'Trisec 1' (Ref 7). By this time the United States Navy was heavily engaged in the design study for a semi submerged platform. It was this work which finally led to the construction and launch of the S.S.P. Kaimalino in 1973 (Ref 8). This was the world's first true Small Waterplane Area Twin Hull ship.

Twenty six such vessels today exist worldwide and a further nine are on order awaiting delivery. Notable amongst these is the 18,400 grt cruise liner Radisson Diamond, currently under construction at Rauma Yards in Finland. Upon completion she will be the worlds largest SWATH and first SWATH cruise liner. Also on order are six more SWATH T-AGOS ships. It is understood that the U.S. department of defence has placed orders for two more 3,500 ton ships and four 5,500 ton variants. In addition FBM Marine will shortly commence construction of a second fast displacement catamaran ferry, similar to their successful M.V. Patria.

Small Waterplane Area Twin Hull vessels are therefore no longer emerging technology. Nearly 20 years have passed since the launch of S.S.P. Kaimalino during which time SWATH technology has evolved rapidly to its present level. The expertise required to build and operate these vessels is currently available and applicable to a wide range of ship types and roles. It need no longer be confined to experiment tanks, demonstrators and prototypes.

Table 1.1 Outlines SWATH vessels built to date and / or currently under construction.

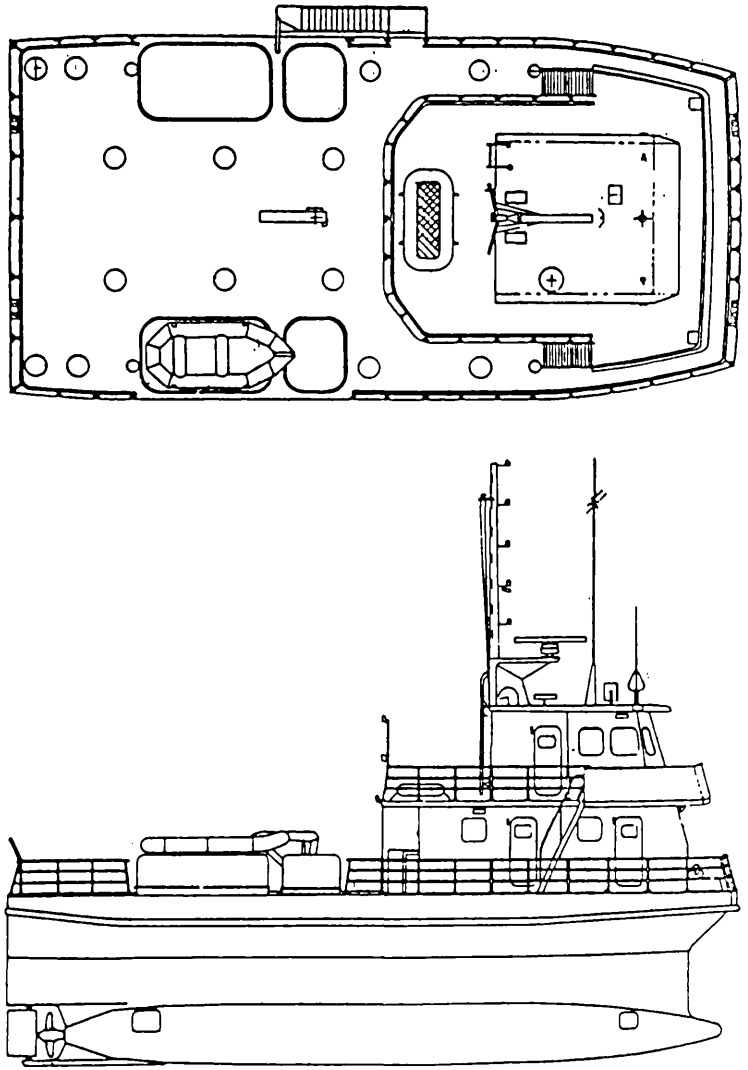

Fig 1.1 M.V. Halcyon

Vessel Name(s)	Year Completion	Country	Design Role	Length oa (metres)	Beam oa (metres)	Draught (metres)	Displacement (tonnes)	Speed (knots) Service / Max
Twin Drill (Duplus)	1969	Netherlands	Seabed Operations	47	17.06	5.5	1200	6 - 7 / 8
Trisec 1	1971	USA	Experimental	6.1	2.44	0.61	1.18	~ / 8
Kalmalino	1973	USA	Naval Workboat	27.1	14.17	4.66	193 / 224	~ / 18
Marine Ace I	1977	Japan	Experimental	12.35	6.5	1.55	18.4	~ / 17.3
Marine Ace II	1978	Japan	Experimental	12.35	6.5	1.55	22.2	~ / 15.4
Seagull	1979	Japan	Fast Ferry	35.9	17.1	3.15	343	23 / 27.1
Ohtori	1980	Japan	Hydrographic Survey	27	12.5	3.4	239	20.6 / ~
Kotozaki	1980	Japan	Hydrographic Survey	27	12.5	3.2	236	19 / 20.5
Betsy (Sauve Lino)	1981	Japan	Sport Fishing	19.2	9.1	1.9 - 2.13	39 - 49	18 / ~
Charwin	1983	USA	Scallop Fishing	~	~	~	100	~
Kaiyo	1984	Japan	Diving Support	61.5	28	6.3	3500	13.25 / 14.1
Halycon	1985	USA	Demonstration	18.29	9.14	2.13	43 - 57	18 / 22.4
Marine Wave	1985	Japan	Saloon luxury boat	15.1	6.2	1.6	25.4	16 / 18.2
Chubasco	1987	USA	Yacht	21.95	9.45	2.13	56 - 79	17 / 20
Sun Marina	1987	Japan	Cabin luxury boat	15.05	6.4	1.6	25.4	~ / 20.5
Samhach	1988	UK	Test Bed	6.6	2.83	0.84	3.5	~ / 5
Frederick Creed	1989	USA	Ocean Survey	20.4	9.75	2.6	80	25 / 29
Bay Queen	1989	Japan	Multi-purpose boat	18.6	6.8	1.6	~	~ / 20
Victorious / T-AGOS 19	1989	USA	SSV	70.7	28.65	7.54	3556	9.6 / ~
Patria	1989	UK	Fast Ferry	37	13	2.7	180	30 / 32
Navatek I	1989	USA	Day / Dinner Excursion	43	16	2.4 - 4.27	365	15 / 18
Seagull 2	1989	Japan	Fast Ferry	39.3	~	3.25	567	~ / 30
Ali	1990	UK	Creel Fishing / Trials	12	5	1.6	20	8 / ~
Diana	1990	Japan	Day Trip / Party	20.8	6.8	1.6	~	15 / 19.2
Hibiki	1990	Japan	SSV	67	29.9	7.5	3700	11 / ~
Theodore Von Karman	1991	USA	Experimental	31.7	10.05	~	~	10 / 18
	1991	Poland	Experimental	6.09	~	0.57	1.88	15.54
Abel / T-AGOS 20	Now Building	USA	SSV	70.7	28.65	7.54	3556	9.61 / ~
Radisson Diamond	Now Building	Finland	Cruise Liner	129	~	~	10-12,000 Est	~

Table 1.1 SWATH Vessels Existing Worldwide @ August 1991

1.3 Existing Design Capability

Traditionally ships are designed by the interpolation and extrapolation of knowledge and past practice. This process although conservative in approach, has over thousands of years evolved near optimal monohull designs. Unfortunately SWATH vessels are very different from conventional monohulls. The design techniques applied must therefore be modified accordingly.

SWATH vessels present the naval architect with many problems all of which must be solved effectively in order to create an efficient solution, i.e. a vessel which is able to compete favourably with a monohull designed for the same role. Unfortunately definition of the twin hull configuration requires a large number of variables with respect to geometry, structural design, carrying capacity, powering and motion response. Without the extensive design database available for monohulls, increased use must be made of first principles and iterative design methods. This approach has only recently been made feasible by modern developments in digital computing power which allow the relatively rapid generation, analysis and subsequent modification of designs.

Computer aided design tools for monohulls have been around for some time, however lack of demand coupled with an absence of relevant design data has until recently obviated the creation of such a system for SWATH ships. Increasing interest in the SWATH concept in the late '80's together with an expanding database of design information prompted J.R. MacGregor to develop a computer aided method for the preliminary design of SWATH vessels (Ref 9). When completed in 1989 these programs embodied the existing 'state of the art' in SWATH vessel design.

This thesis describes research aimed at extending and enhancing this capability.

1.4 Extension of Design Capability

A position has now been reached where the primary advantages and disadvantages of the concept are recognized and therefore no longer in dispute. Consequently attention may now be directed towards previously neglected aspects of the design and towards establishing a measure of the concepts overall performance relative to that of monohull counterparts.

In an effort to enhance the existing design capability, areas outwith the specification of the original design suite were identified. Following a brief review of general SWATH design aspects, the following were targeted for detailed investigation:-

1. Damage Stability
2. Manoeuvring
3. Environmental Loading

These areas were selected since in all three cases the different geometry of SWATH and monohull vessels leads to radically different behaviour.

Damage Stability was chosen since it is an area which frequently arouses concern amongst those unaccustomed to SWATH vessels. The low waterplane area allows rapid heeling / trimming upon flooding, however as demonstrated in Chapter 3 subsequent immersion of the cross deck structure arrests this trend quite satisfactorily.

Manoeuvring was similarly selected since it too is an area where SWATH geometry produces different characteristics to those of monohull ships. The long streamlined struts on SWATH ships produce directionally stable systems. This may not always be a disadvantage but does result in reduced manoeuvring performance at speed.

In direct contrast to monohull vessels the dominant global loading on SWATH ships is a transverse bending moment. Since it is recognized that the accurate evaluation of loading is an essential prerequisite to developing an efficient structure, environmental loading was considered in an effort to rationalize the many calculation methods and approximations available.

Finally an attempt was made to develop a framework for evaluating alternative monohull and SWATH designs. This led to the creation of a simplified method for the assessment of alternative designs proposals based on the idea of 'mission equivalence'.

1.5 Related Activities

Since completion of the 'DESIN' suite of programs in 1989, eleven SWATH vessels have been launched worldwide. Two of these were designed and built in Britain; the M.V. Patria, a 37 metre fast passenger ferry and the M.V. Ali, a 12 metre

SWATH demonstrator / fishing vessel.

The M.V. Patria was designed and built by FBM Marine on the Isle of Wight. The SWATH motor fishing vessel was designed and built privately in Glasgow through a syndicate headed by Dr J.R. MacGregor the creator of the 'DESIN' capability.

The author has been privileged to witness the construction of this vessel and to serve on the trials team which took the vessel to sea late in November 1990. During the period spanned by this research the author also participated in trials of 'Samhach' a 4 tonne SWATH demonstrator designed and constructed by Yarrows Shipbuilding Ltd. Results from these trials are however still undergoing analysis and are regrettably unavailable to date.

1.6 Format of Thesis

The thesis begins (Chapter 2) with a brief general review of all design aspects relevant to the balanced evaluation and comparison of monohull and SWATH vessels. No attempt is made to combine or relate the findings at this stage. A method for the overall mission based evaluation of monohull and SWATH vessels is instead presented in Chapter 6.

Chapter 3 addresses the question of damage stability. Results from an extensive parametric study undertaken to explore the damage stability characteristics of SWATH vessels are presented and discussed. Secondly the relationships established between design geometry and damage stability are utilized in the construction of 'FSEP1'; a design program which estimates damaged characteristics at the preliminary design stage.

Chapter 4 investigates the manoeuvring performance of SWATH ships. Following a thorough literature survey, conventional (monohull) manoeuvring theory is applied and adapted to develop a manoeuvring prediction tool for SWATH vessels; 'SWATHMAN'. This program will estimate required rudder areas in order to achieve a specified manoeuvring performance. Conversely the program will estimate the likely turning performance for a specified rudder area. The program incorporates propeller acceleration effects and caters for control fins mounted in and outwith the slipstream.

Chapter 5 reviews aspects of wave loading in the structural design of SWATH

vessels. It is widely acknowledged that wave induced side force leading to a transverse bending moment is the dominant form of environmental loading for these vessels. All available methods for the calculation / estimation of this force were therefore identified and applied to the vessels T-AGOS 19 and the M.V. Patria. Short term extreme value prediction methods are applied in order to determine likely lifetime values of design extreme loading. Empirically derived estimates are compared with those produced by the application of rigorous three dimensional potential theory, and conclusions on the applicability of the methods are drawn.

References to Chapter 1

1. Woolaver, D.A., and Peters, J.B., 'Comparitive Ship Performance Trials for the U.S. Coast Guard Cutters Mellon and Cape Corwin and the U.S. Navy Small Waterplane Area Twin Hull Kaimalino', DTNSRDC Report No 80/037, March 1980.

2. Lundborg, C.G., 'Construction of Ships', U.S. Patent No.234 794, 1880.

3. Nelson, A., 'Vessel', U.S. Patent No. 795 002, 1905.

4. Blair, W.R., 'Ocean Going Water Craft', U.S. Patent No. 753 399, 1930.

5. Creed, F.G., 'Improvements in and Relating to Floating Structures', U.K. Patent No 561 741, 1944.

6. 'Twin Hull Vessel DUPLUS for Netherlands Offshore Company', Reprinted from Holland Shipbuilders, February 1969.

7. Marbury, F., 'Small Prototypes of Ships - Theory and a Practical Example', Naval Engineers Journal ,October 1973.

8. Lang, T.G., Hightower, J.D., and Strickland, A.T., 'Design and Construction of the 190 Ton SSP', ASME Paper No 73-WA/Oct-2, 1973.

9. MacGregor, J.R., 'A Computer Aided Method for Preliminary Design of SWATH Ships', Ph.D. Thesis, Glasgow University, May 1989.

CHAPTER 2

ASPECTS OF DESIGN

2.1 Introduction

This chapter identifies and reviews design aspects relevant to the SWATH concept. SWATH vessel performance is analysed for each of these aspects individually, and where possible quantified in relation to that of corresponding monohull ships. At this stage no attempt is made to combine or relate the findings. A method for the objective overall evaluation of SWATH and monohull designs is instead presented in Chapter 6.

2.2 Seakeeping

The greatly enhanced seakeeping capabilities offered by SWATH vessels are now widely recognized. SWATH ships have demonstrated excellent motion response characteristics in model experiments (Ref 1-4), controlled tests on large demonstrators (Ref 5-8), and full scale trials (Ref 9-13). In addition observations on, and experiences with, working SWATH vessels (Ref 13-17) all confirm the concepts superior seakeeping performance. Indeed full scale trials (Ref 13) have shown that a SWATH ship may possess seakeeping equal to a monohull vessel some fifteen times its displacement - Fig 2.1.

Direct SWATH / monohull comparisons on an equal size basis, often penalize the SWATH on the grounds of increased build and operating cost. However these comparisons neglect the vastly increased seakeeping capabilities possessed by the SWATH ship. For missions requiring good seakeeping performance, e.g. Sonar Surveillance (SSV), Air or Diving Support, the increased capability afforded by the SWATH concept may allow a SWATH ship to perform the same role as a monohull of much greater size.

The accurate evaluation of seakeeping is therefore essential when comparing SWATH and monohulls vessels on a mission basis.

In order to evaluate the effect of seakeeping upon operability, it is usual to define

certain limiting criteria. These criteria stipulate the maximum significant amplitudes of motion and acceleration, deck wetness, slamming etc. which may be tolerated. In addition criteria relating to the operation of onboard equipment, including aircraft handling gear, may be specified for some missions. Kennel, Olson and McKreight (Ref 18-20) offer comprehensive lists of seakeeping criteria applicable to SWATH / Monohull evaluation.

Ref (18-24) describe mission based comparisons based on such criteria. In these studies theoretical techniques were used to evaluate the seakeeping characteristics for both SWATH and monohull designs. In each case the results were combined with sea spectral data, in order to evaluate the percentage of time that the limiting criteria were exceeded. This information enabled the calculation of percentage operability for each vessel operating a specified mission profile.

Fig 2.2 illustrates the principal characteristics of payload and seakeeping equivalent ships. These designs were derived by Kennel et al (Ref 18). In this study a SWATH and a monohull were first designed on the basis of equal payload. A seakeeping analysis was then performed and a second monohull design configured to possess seakeeping equivalent to the SWATH vessel. Fig 2.3 illustrates the percentage annual operability attained by each of these vessels performing both general and helicopter support duties in the North Atlantic.

Fig 2.4 presents a graphic illustration of the relative seakeeping performance of the 3605 Ton FFG7 frigate and a 3400 Ton SWATH design. To produce these diagrams Olson (Ref 19) applied specific seakeeping criteria in order to determine limiting wave heights for each combination of speed and heading. The results demonstrate the excellent seakeeping performance of the SWATH in head and beam seas, and a reduction in performance in following seas. In contrast the FFG7 performs best in following seas and worst in head seas. It will be noted that in general the limiting wave height is significantly greater for the SWATH which suffers no performance degradation in up to 35 feet waves at any speed for headings between 90 and 270 degrees.

Motions, deck wetness, speed and course maintenance are all significantly improved for SWATH ships. Slamming on the underside of the box structure may be worse than monohull slamming in extreme sea states. The phenomenon is not yet adequately understood, and reliable theoretical predictions of slam pressure are not yet available. Djatmiko (Ref 25) reviews currently available slam prediction techniques.

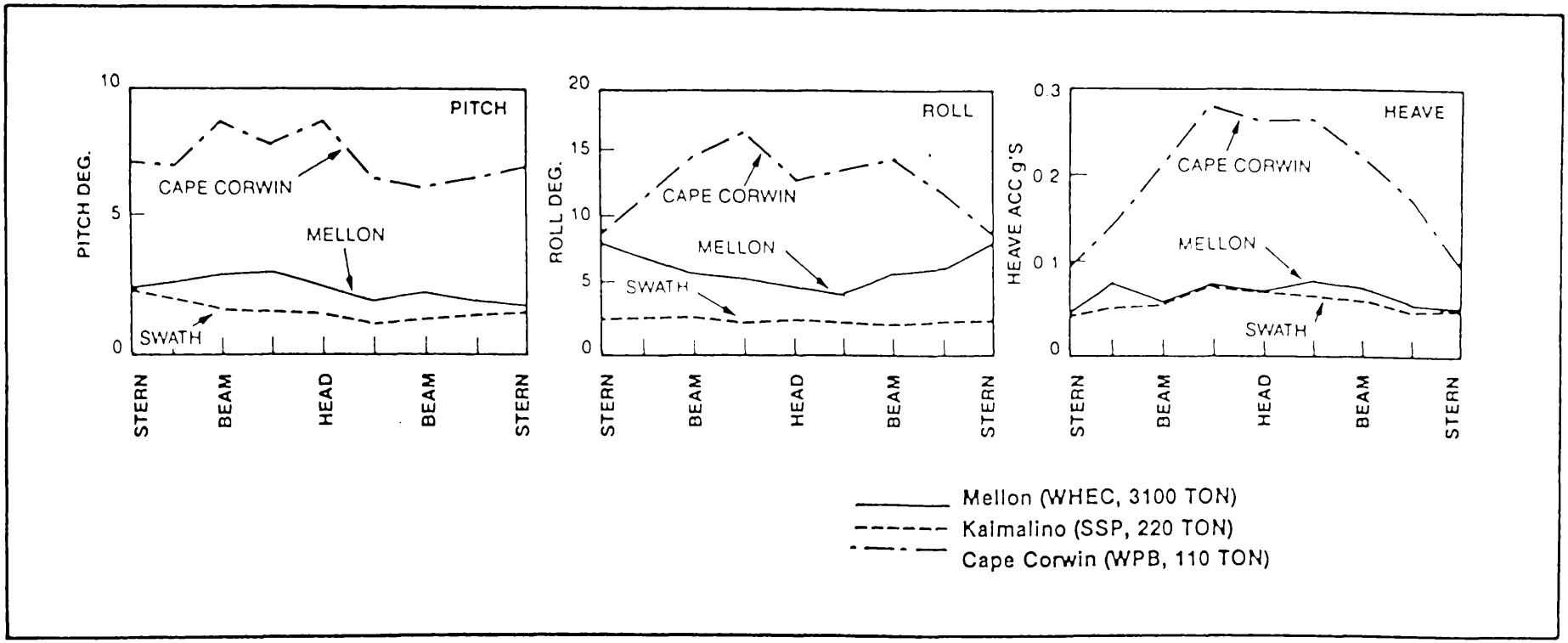

US Navy/Coast Guard seakeeping trials motions comparisons

Fig 2.1 SWATH / Monohull Motion Comparison

(Ref 13)

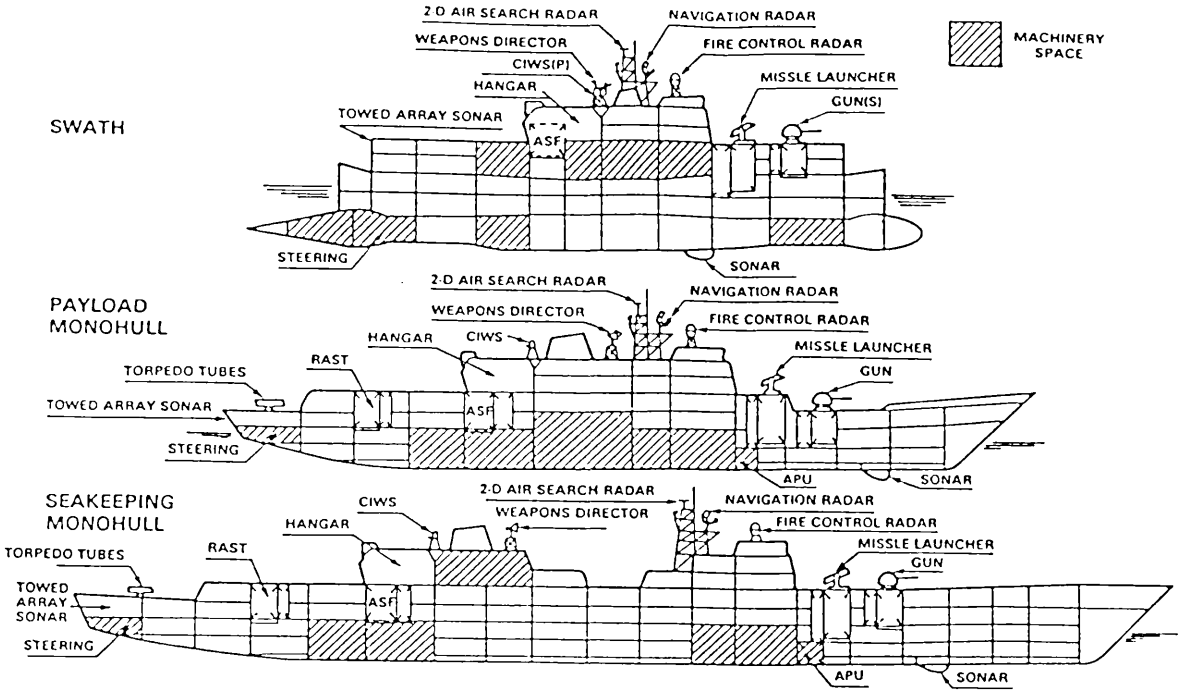

Inboard profiles

Principal characteristics

	Payload Monohull	SWATH	Seakeeping Monohull
LPB (ft)	420	310	584
LOA (ft)	455	380	619
Beam (ft)	49	90	62
Draft (molded, ft)	19	28	18
Light ship (incl. margin, LT)	4335	5380	7302
Full load (LT)	5373	7070	9116
Total volume (ft^3)	623797	817000	1184651
Sustained speed (knots)	26.6	25.0	26.0
Installed propulsion power (shp)	48500	48500	48500

Weight summary (LT)

	Payload Monohull	SWATH	Seakeeping Monohull
Weight groups			
1-structure	1834	2365	3782
2-propulsion	474	455	489
3-electric plant	319	337	388
4-command/surveillance	137	159	186
5-aux. systems	652	774	981
6-outfit/furnishings	382	445	610
7-armament	143	143	143
Light ship (incl. margin)	4335	5380	7300
Loads			
fuel-ship	795	1043	938
fuel-helo	70	70	70
mission loads	67	68	67
misc. loads	106	109	106
solid ballast	0	400	635
Full load	5373	7070	9116

Volume summary (ft^3)

	Payload Monohull	SWATH	Seakeeping Monohull
Space groups			
1-payload	84 185	84 185	89 789
2-personnel	109 358	109 358	111 526
3-ship support	161 361	242 204	259 252
4-machinery	251 201	324 560	290 248
5-voids	17 692	56 693	433 836
Total volume	623 797	817 000	1 184 651

Fig 2.2 Payload and Seakeeping Equivalent Ships

(Ref 18)

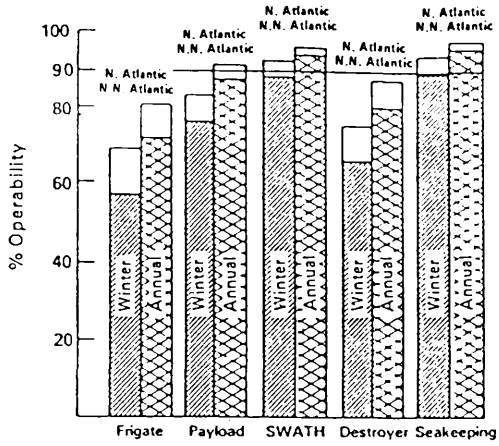

Percent Operability

	Frigate	Payload	SWATH	Destroyer	Seakeeping
Annual North Atlantic	81	91	96	87	97
Annual Northern North Atlantic	73	87	94	80	95
Winter North Atlantic	69	83	92	76	93
Winter Northern North Atlantic	57	76	88	66	89

Mobility percent operability by operating season/region

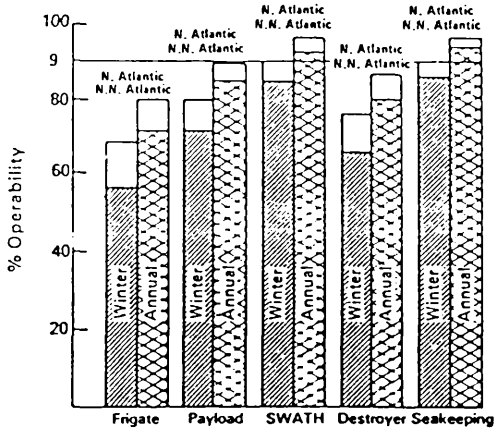

Percent Operability

	Frigate	Payload	SWATH	Destroyer	Seakeeping
Annual North Atlantic	80	89	95	86	95
Annual Northern North Atlantic	71	84	92	80	93
Winter North Atlantic	67	80	90	75	90
Winter Northern North Atlantic	55	71	84	65	85

Helo ops percent operability by operating region/season

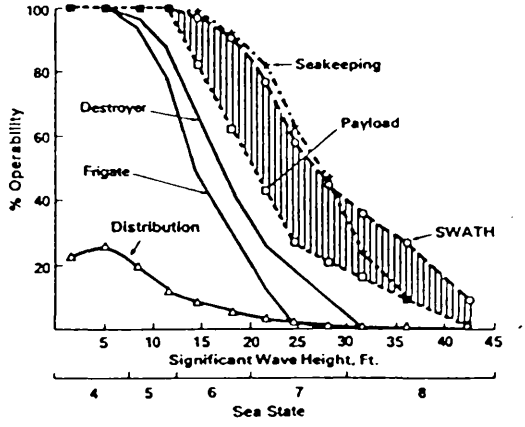

Mobility percent operability, northern North Atlantic—annual

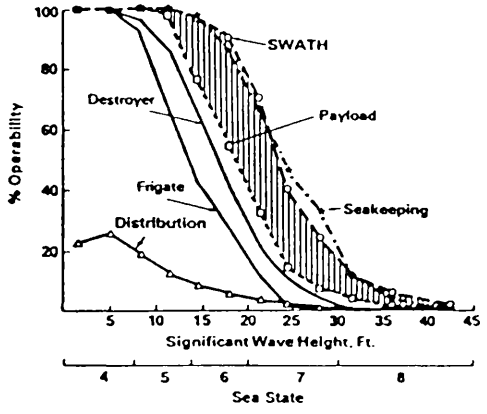

Helo ops percent operability, northern North Atlantic—annual

Fig 2.3 Operability Statistics for Several Monohull and SWATH Forms (Ref 18)

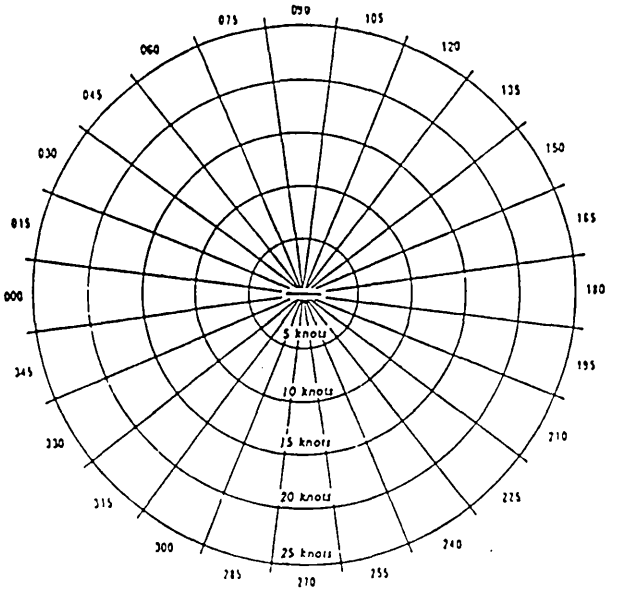

SEAKEEPING CONTOUR FOR THE FFG 7 IN SEAS

SEAKEEPING CONTOUR FOR A 3400 TON SWATH IN SEAS

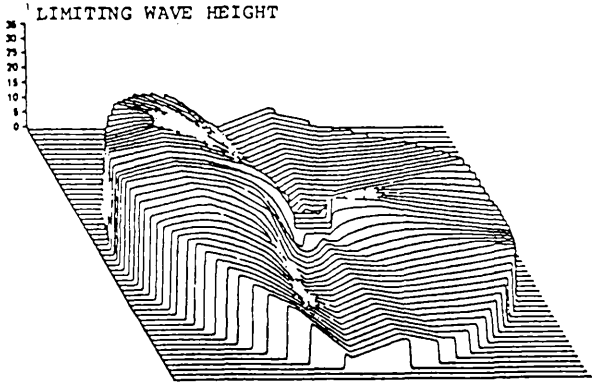

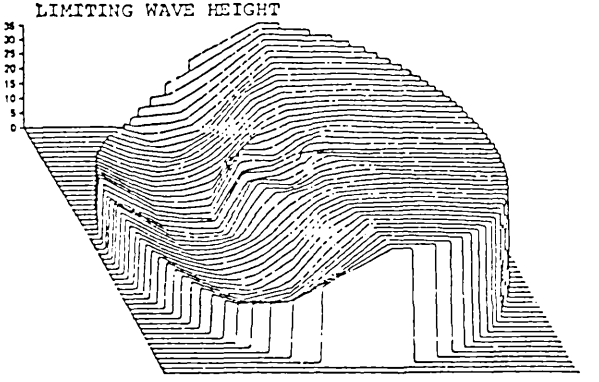

Fig 2.4 Seakeeping Contours - FFG7 Frigate and a 3400 Ton SWATH (Ref 19)

2.3 Principal Dimensions

The geometry of SWATH and monohull vessels is so very different that direct comparisons are difficult to make. The most important differences between the concepts are:-

- Length
- Beam
- Draught
- Freeboard
- Deck Area

Comparing vessels of equal displacement, the SWATH will be shorter with a greater beam, draught and freeboard than its monohull counterpart. The SWATH will also possess a larger usable deck area than the monohull, although total deck areas will probably be roughly equal.

These parameters obviously effect many constructional and operational characteristics of the vessel. Considerations of outfit arrangement and operation are however covered in other sections. Here attention is restricted to the effect upon interfacing ability which differences in the above parameters introduce. Interfacing performance may be measured in terms of the vessels ability to use existing port, repair and docking facilities etc.

Comparing vessels of equal displacement, the length of SWATH will generally be some 30-40% less than that of the monohull (Ref 26). In practice this has very little effect on interfacing ability. Minor advantages may occasionally arise in terms of being able to use shorter berths etc. Conversely the beam of SWATH vessels will generally be some 60-70% greater than for monohulls (Ref 26). This is unlikely to effect interfacing ability until such time as SWATH ship sizes reach the physical limits imposed by canals (notably the Panamanian) and that of existing repair facilities. Current estimates suggest the maximum size of SWATH able to transit the strategically important Panama canal will be around 10,000 Tonnes displacement (Ref 27). This size may be increased by distorting the geometry away from the optimum.

Increased draught will limit the number of ports which a large SWATH vessel will be able to use, similarly increased freeboard may pose problems when

loading/unloading at some quaysides. The constraint on freeboard is relatively minor however draught restrictions may pose problems in some localities. It is therefore recommended that careful consideration be given to any operability limitations imposed upon the SWATH option by increased draught.

Increased useful deck area is central to many of the operational roles for which SWATH ships are being proposed. The provision of large areas of uncluttered deck has many operational advantages but has no significant effect on the interfacing ability of the vessel other than obviously increasing air capability.

2.4 Operation Onboard Systems

On naval vessels these may be subdivided into Surface, Air and Underwater systems:-

Surface systems include weapon and sensor suites together with equipment boat and handling gear.

Air support systems comprise helicopter/aircraft handling equipment both on and below decks.

Underwater systems consist of both passive and active sonar devices where fitted.

Almost all the above systems operate more efficiently onboard SWATH vessels although exceptions to this rule may possibly exist in case of surface weapon systems.

Concern is often expressed that the high freeboard of SWATH may create difficulties during 'over the side' boat or equipment handling operations. These problems must however be balanced against the benefits resulting from reduced absolute and relative deck/waterline motion. The U.S. Navy have conducted extensive trials on S.S.P. Kaimalino (Ref 14,26) including handling of a two ton buoy. In practice no significant problems were encountered, indeed on one trial the S.S.P. Kaimalino managed to recover floating equipment from a seaway after a monohull some four times its displacement, had consistently failed to do so (Ref 26). Personal trials experience onboard a SWATH fishing vessel (Ref 12) reinforces this. On these trials a waverider buoy was launched and recovered in varying sea states without difficulty.

The operation of weapon and sensor suites is the other area over which concern is occasionally expressed. Weapon and sensor layouts have evolved to fit 'long thin' warships (Ref 26). With SWATH these must be changed to a 'short wide' format. This requires care if effectiveness is to be maintained. (Ref 28,29) address the subject of combat systems for advanced Naval Vehicles. The U.S. Navy have studied the effect of motion on the detection abilities of several radar systems. They conclude that the reduced motion of SWATH ships will significantly improve radar performance, perhaps to the point where a 2D system mounted on a SWATH will prove equivalent to a 3D system on a monohull (Ref 19). This allows reduced cost, increased reliability or greater effectiveness.

Reduced motion coupled with a large usable deck area combine to make the SWATH ship an ideal contender for missions requiring air capability. Standard helicopter and aircraft handling gear may be utilized onboard SWATH ships, further extending the range of sea states through which air capability may be maintained.

Reduced surge and yaw together with low radiated noise levels, dramatically increase the quality of signal received from SWATH towed sonar arrays. Similarly the effectiveness of deeply mounted hullborne sonar is increased, due to reduced motion, low background noise and the absence of slamming, aeration and bubble sweepdown.

Outside the field of naval applications, onboard systems are usually confined to lifting and boat handling gear. As noted SWATH ships present no problems in this area. In the cruise and ferry industry, the maintenance of passenger comfort may also be considered an onboard system. In this area the SWATH ship excels. Low motion and large regularly shaped deck areas, together with reduced noise and vibration from hull mounted engine / transmission, greatly improve passenger comfort levels.

2.5 Payload Fraction

SWATH vessels have inherently higher structural weight fractions than monohulls. The fraction of displacement available for payload is therefore correspondingly less. Fig 2.2 compiled from Ref 18 illustrates the principal particulars of both monohull and SWATH frigates designed to carry equal payload.

2.6 Endurance / Range

The endurance of a SWATH ship is likely to be less than that of a corresponding monohull for the same reason, i.e. the greater structural weight fraction effectively reduces the capacity of a SWATH ship to carry fuel and stores. Greater calm water resistance also results in reduced range, although reduced added resistance in waves may help to offset this.

2.7 Layout

In contrast with monohulls, most of the usable volume in SWATH vessels is concentrated above the water in the cross deck structure. On some large designs the engines are situated in the hulls, however in smaller vessels the hull space is generally only used for fuel and ballast tankage. Strut volume is often only used for access to the hulls.

Whilst this arrangement results in much void space, it does however present the designer with a large amount of regularly shaped space, which is easy and therefore cheap to outfit. Such a vessel lends itself easily to the highly efficient modularised pre-outfit techniques utilized by modern shipyards - Fig 2.5. The extreme regularity of form may even allow a degree of outfit module interchangeability between vessels. Such flexibility would greatly increase the capability of a modern fleet or navy, drastically reducing refit and repair times, possibly even allowing one vessel to perform a number of roles (Ref 19,30).

A more basic demonstration of the outfitting flexibility afforded by the SWATH concept is given by the choice of engine location (on larger vessels):-

On ferries and cruise ships the engines may be sited in the hulls, effectively isolating the passengers from noise and vibration. For sonar surveillance and other ships where acoustic signature is important, the process may be reversed, i.e. the engines may be located in the cross deck in order to minimize radiation of underwater noise. The choice of engine location will also effect GM values, hence the seakeeping characteristics, and the efficiency of the propulsive drivetrain.

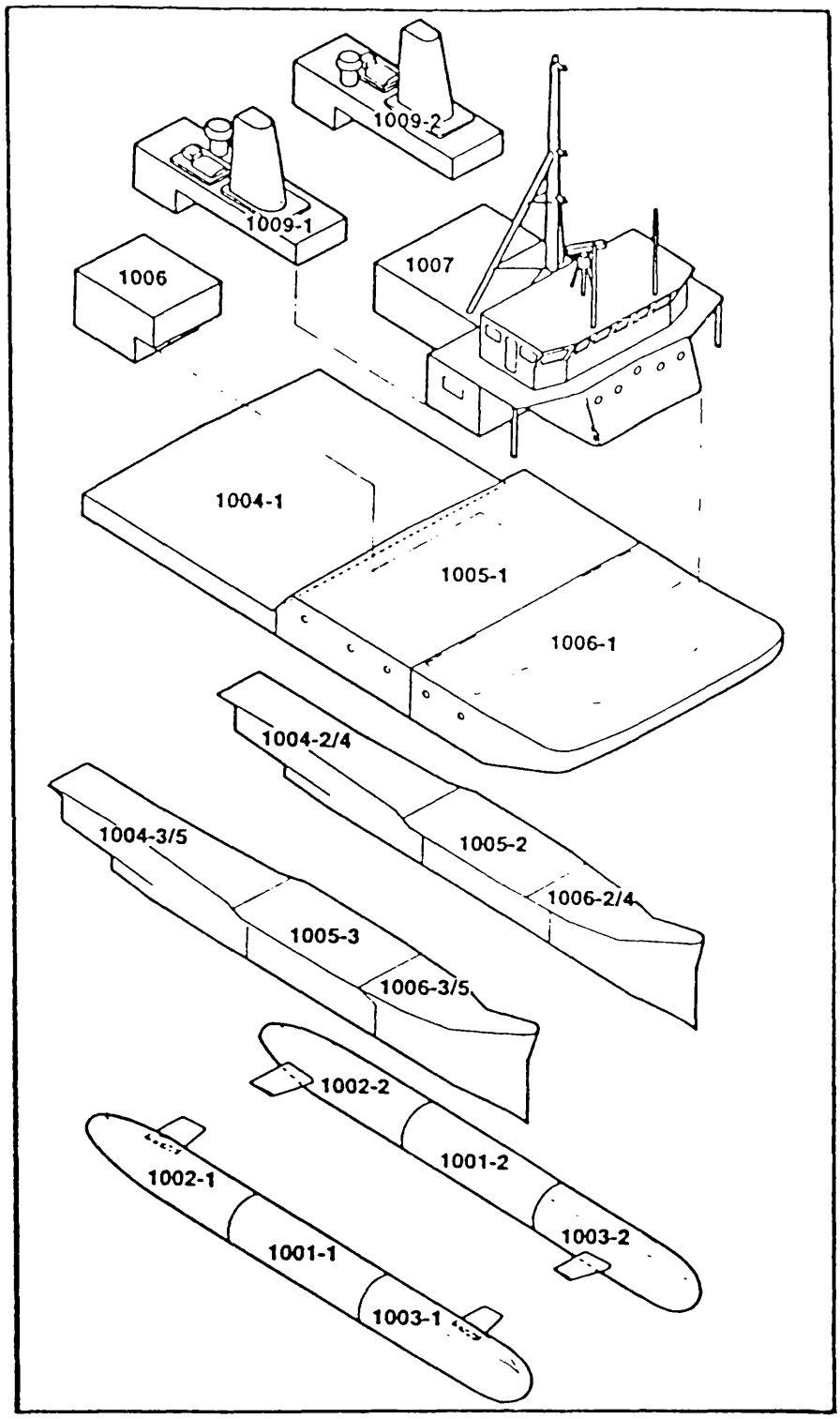

SWATH modular construction.

Fig 2.5 Potential SWATH Fabrication and Outfit Units (Ref 37)

2.8 Powering Requirements

SWATH ships typically possess about 60% greater wetted surface areas than monohulls of equal displacement (Ref 26). Frictional resistance is therefore higher. Wavemaking resistance is roughly equal for equivalent sized vessels, however it is possible to optimize the geometry of the lower hullforms to minimize this component (Ref 31). The total resistance in calm water is therefore usually greater for SWATH ships, however with careful design the resistance may be significantly reduced to levels close or equal to monohull values (Ref 31,32). Table 2.1 indicates the sensitivity of resistance to hull shape.

Although the SWATH ship has greater calm water resistance the hullform geometry provides ample opportunity to optimize wave making resistance for a given speed as illustrated in Fig 2.6. In addition the added resistance component due to waves is significantly less for SWATH vessels (Ref 33). This feature may result in a vessel whose total resistance in waves is less than that of monohull equivalents (Ref 34).

Windage and wind resistance are both greater for SWATH vessels of normal form than for equivalent sized monohulls.

When mission and operational profile considerations are included, it may be seen that the powering requirements of equivalent sized SWATH and monohull vessels are, overall broadly similar. For missions where seakeeping considerations dictate the size of vessel, it will be noted that the smaller mission equivalent SWATH requires less power than a monohull designed for the same role (Ref 35).

2.9 Cost

This element may be broken down into at least three groups:-

- Design
- Construction
- Operation

Due to the novelty presently attached to the concept, design costs will usually be greater for a SWATH vessel. Some uncertainties still exist regarding environmental

loading on the vessel and the transfer of stress throughout the structure. It is however anticipated that as knowledge of, and confidence in, the concept increase, the differential between monohull and SWATH design costs will decrease. Indeed it is possible that the regular shapes present in SWATH geometry will ultimately aid detailed design of outfit, so reducing overall design costs.

Construction costs for SWATH vessels are currently higher than for monohulls. This is largely due to the greater surface area and hence material and welding that are required. However it must be remembered that for missions where size is dictated by seakeeping, an "equivalent" SWATH will be considerably smaller than its monohull counterpart. An "equivalent" SWATH may therefore require less material, less fabrication, smaller engines etc. In addition the regular geometry of SWATH forms presents many opportunities to increase build efficiency including the adoption of automated panel line techniques. These factors may combine to reduce SWATH build costs to the same level or less, than those of an "equivalent" monohull. Olson (Ref 19) suggests that build costs for mission equivalent vessels are already within 5-10 %, with even smaller differences in the life cycle costs.

Increased calm water resistance combined with higher maintenance costs resulting from duplicated equipment will result in greater operational costs for a SWATH of equal length or displacement to a monohull. However as noted, a mission equivalent SWATH may be considerably smaller than the monohull. This factor combined with reduced (relative to monohulls) added resistance, may reduce operating costs for SWATH ships to the same levels or less than those of mission equivalent monohulls.

2.10 Reliability

Reliability must be assessed using perceived relative values relating to both hull structure and machinery. Owing to the novelty of the concept and remaining uncertainties surrounding the structural design of SWATH ships, the perceived reliability of SWATH structures is less than for monohulls. In this context 'structural performance' must be considered. This parameter is unseen and therefore often forgotten, however its effect upon build and life cycle costs should not be underestimated. Meyerhoff (Ref 38) offers a concise review of SWATH structural aspects while Chapter 5 of this thesis investigates the predominant wave loads acting.
In contrast the perceived reliability of machinery on SWATH ships is greater due to the increased duplication of systems required onboard such vessels.

Changes in Effective Power Obtained with 'Deep' Draught Contoured Hulls

Displacement (t)	Hullform	Code	Hull Dimensions (m) Breadth	Depth	% Change in Baseline EHP 15 kt	17 kt	20 kt	25 kt
1000	Midships Bulge	Cokebottle	4.149	2.963	-22.6	-0.74	15.2	7.9
	Complex Hull	Dogbone	3.712	2.652	-6.04	11.1	-1.79	-2.28
2000	Midships Bulge	Cokebottle	5.477	3.912	-23.3	-5.6	28.38	15.12
	Complex Hull	Dogbone	4.799	3.428	-6.43	10.32	2.28	-4.48
3000	Midships Bulge	Cokebottle	6.461	4.615	-19.63	-25.97	36.89	21.26
	Complex Hull	Dogbone	5.66	4.043	5.82	-10.36	4.41	-6.08
4000	Midships Bulge	Cokebottle	7.254	5.182	-15.88	-32.31	42.42	26.77
	Complex Hull	Dogbone	6.358	4.541	20.47	-16.67	7.53	-5.9
5000	Midships Bulge	Cokebottle	7.935	5.668	-14.02	-36.54	42.76	31.39
	Complex Hull	Dogbone	6.979	4.985	32.78	-20.85	8.85	-5.57

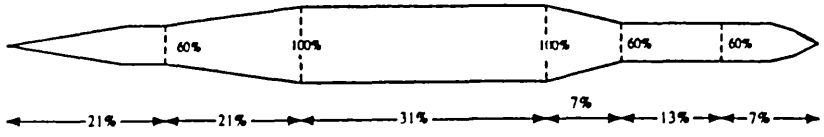

Typical Slow Speed Hullform (cokebottle)

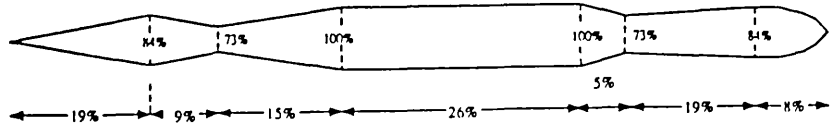

High Speed Hullform (dogbone)

Table 2.1 The Influence of Contoured Hulls on SWATH Resistance

(Ref 36)

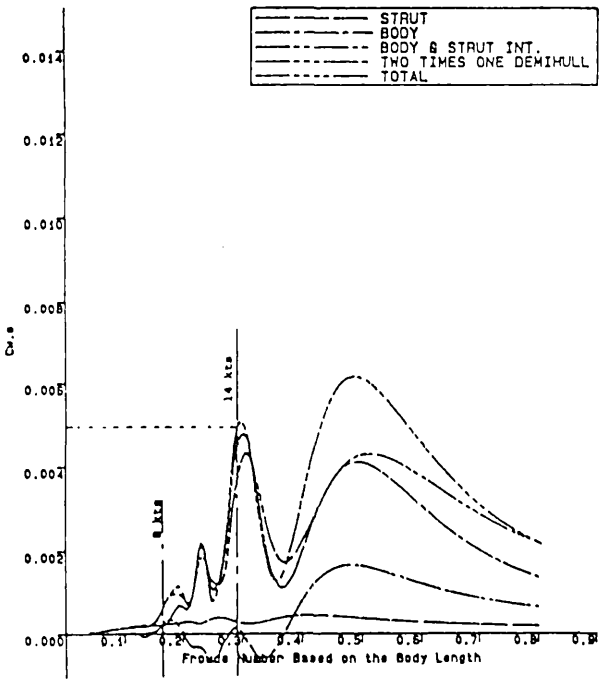

Wave Resistance Coefficients of a 2405 tonne SWATH vs Fn
Draft (6.85m), SD (1.5m). Non-Contoured Circular Cross Sec.

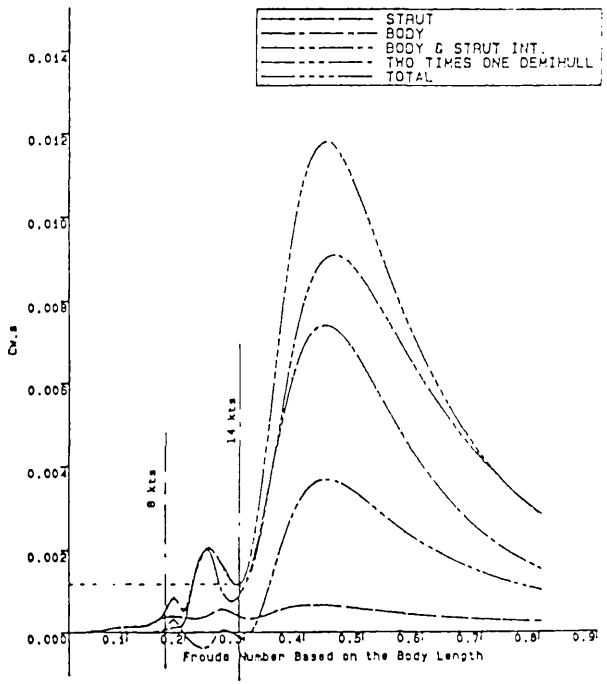

Wave Resistance Coefficients of a 2405 tonne SWATH vs Fn
Draft (7.40m), SD (1.94M). Contoured Square Cross Sec. Hull

Fig 2.6 The Influence of Contoured Hulls on SWATH Wavemaking
(Ref 31)

2.11 Habitability

Habitability is improved onboard SWATH vessels compared to monohulls. Motion is reduced, decks are drier, noise and vibration are often less where the engines are located in the hulls.

2.12 Motion Control

One of the inherent disadvantages of low waterplane area is that small changes in displacement produce large changes in draught. As a result more extensive ballasting systems are required on SWATH vessels. The inclusion of counter flooding systems is also of greater priority on SWATH ships.

In addition some means of controlling pitch whilst underway is required. The aerodynamic phenomenon resulting in pitching moments on airships was first observed by Munk in 1924 (Ref 39). Chapman (Ref 40) then noted the phenomenon manifest itself as a bow down pitch moment on SWATH ships at speed in 1974. The now familiar "Munk moment" must be counteracted by fixed or active control fins (Ref 41,42). Almost all SWATH vessels built to date are fitted with such fins which are usually mounted between the hulls at the stern.

Provision of any control surface and mechanism obviously increases cost, however this increase may be offset by the increased build cost of a potentially larger mission equivalent monohull. Increased complexity is never desirable, but despite doubts concerning the consequences of control system failure, the experiences of those operating the Japanese vessels Marine Ace, Seagull, Kohtozaki, Ohtori and Kaiyo should be considered. These vessels are fitted with rudimentary control systems only, yet all have been, and are still operating without problems (Ref 5,11,17).

2.13 Survivability

Survivability may be considered in two parts:-

- Signature
- Resilience to attack

Signature may be further subdivided into:-

- Infra Red
- Acoustic
- Radar

The infra red signatures of SWATH and monohull vessels are largely similar. Locating the engines in the hulls of SWATH ships may slightly reduce the infra red signature, however locating the engines in the above water cross deck will greatly reduce the acoustic signature. This reduction is potentially extremely useful, particularly for sonar surveillance vessels. The reduction in self generated background noise significantly enhances the performance of both hull mounted and towed sonar arrays.

Radar signatures of SWATH vessels are likely to be greater than those of equivalent sized monohulls. High freeboard and regular "boxy" shapes readily reflect radar waves. It must be remembered however that mission equivalent SWATH's are likely to be considerably smaller than their monohull counterparts. These smaller ships may then possess radar signatures equal or less than the mission equivalent monohull.

A vessels resilience or ability to withstand attack depends on many factors. One of the key factors is the separation and duplication of onboard systems. This is necessary to ensure that the ship is not crippled by one relatively small strike in a critical area. SWATH vessels inherently possess large reserves of system redundancy and duplication. One of a SWATH ships most important assets is the provision of two independent propulsion and manoeuvring systems, located on opposite sides of the vessel. In an emergency / survival situation the ship may therefore be operated as effectively two parts albeit with greatly reduced mobility and manoeuvring performance. A small monohull may be completely disabled by one strike on the engine room or steering gear. It is almost impossible to conceive of a scenario where one strike would produce the same effect on a SWATH ship.

Damage resistance to strikes by missile,torpedo and mine is therefore likely to be better for SWATH vessels than for monohulls. This is due to redundancy / duplication and the remote locations of personnel and systems.

2.14 Stability

Transverse stability of SWATH vessels is excellent, due to the large transverse separation of waterplane areas and the great increase in immersed volume, and hence righting moment, that results from immersion of the haunch and box structure (Ref 9). Concern is often expressed regarding the damage stability characteristics of SWATH ships. Low waterplane area does result in rapid initial heeling/trimming upon flooding, however subsequent immersion of the cross deck structure arrests these trends quite satisfactorily. Counter flooding may effectively be used to return the vessel to an even keel. The effects of flooding upon the stability characteristics of SWATH vessels have now been well studied by analytical and experimental means (Ref 43-45). Chapter 3 indicates there is no cause for concern regarding the damage stability of SWATH vessels. Indeed it seems likely that SWATH ships possess survivability which is at least equal to that of monohulls.

It is important to note that SWATH ships may not meet existing stability criteria, particularly those relating to initial heeling. This is a consequence of the criteria being developed exclusively for monohull ships. It does not necessarily mean that SWATH vessels suffer inferior stability or damage stability characteristics, merely that these characteristics are different. This need not be a problem but is a feature off which the designer should be aware.

2.15 Manoeuvrability

Concern has often been expressed regarding the manoeuvrability of SWATH vessels. The long streamlined hulls and struts combine to form a very directionally stable system. This stability combined with problems of rudder location has in the past given rise to fears of unmanoeuvrable vessels.

Chapter 4 of this thesis addresses SWATH manoeuvring. In addition many experiments have been performed at DTNSRDC (Ref 46-51) to investigate the problem. Based on the results of these studies, there is no undue cause for concern. SWATH vessels can possess turning performance equivalent to comparable monohulls (Ref 51), together with excellent slow speed manoeuvring capabilities due to the availability of large amounts of differential thrust from widely spaced propellers. SWATH's also offer the possibility of providing quite exceptional stationkeeping and docking performance by linking main and thruster power to an active control system.

2.16 Conclusions

The preceding pages are intended to highlight the range and extent of the variations existing in SWATH / monohull design and operability characteristics. It will be noted that the principal advantages / disadvantages of the SWATH concept are now recognized and therefore no longer in dispute. Consequently attention may now be directed towards previously neglected aspects of the design and towards establishing a measure of the concepts overall performance relative to that of monohull counterparts.

On this basis chapters 3, 4 and 5 of the thesis describe studies aimed at improving our understanding of the less 'fashionable', although no less fundamental subjects of SWATH damage stability, manoeuvring and wave induced global loading. These design aspects were selected for investigation after a preliminary review highlighted shortfalls in the availability and reliability of relevant information.

Finally chapter 6 outlines a method for the overall mission based evaluation of alternative monohull and SWATH designs, in an attempt to provide guidance for the designer engaged in selecting hullforms for a given role.

References to Chapter 2

1. E.B. Djatmiko, 'Experimental Investigation into SWATH Ship Motions and Loadings', MSc Thesis, Department of Naval Architecture, Glasgow University, 1987.

2. Chun, H.H., Grygorowicz, M. and Kobylinski, L., 'Small Model Experiments of SWATH Concept', Proceedings International Conference on SWATH Ships and Advanced Multi-Hulled Vessels II, London, November, 1988.

3. Djatmiko, E.B., Chun, H.H., McGregor, R.C. and MacGregor, J.R., 'Hydrodynamic Behaviour of a SWATH Fishing Vessel', Proceedings, CSME Mechanical Engineering Forum, University of Toronto Campus, Canada, June 1990.

4. Choung M. L., and Curphey,R.M., 'Prediction of Motion, Stability, and Wave Load of Small Waterplane Area, Twin Hull Ships', Trans SNAME, Vol 85,1977, pp94-130.

5. Oshima, M., Narita, H. and Kunitake, Y., 'Experiences with 12 Meter Long Semi-Submerged Catamaran (SSC) 'Marine Ace' and Building of SSC Ferry for 445 Passengers', Proceedings AIAA/SNAME Advanced Marine Vehicles Conference, Baltimore, Maryland, USA, 1979.

6. Luedeke, G. Jr., Montague, J., Posnansky, H. and Lewis, Q., 'The RMI SD-60 SWATH Demonstartion Project', Proceedings International Conference on SWATH Ships and Advanced Multi-Hulled Vessels, London, April, 1985.

7. Luedeke, G. Jr. and Montague, J., 'RMI's Small-Waterplane-Area-Twin-Hull (SWATH) Boat Project', The SNAME, San Diego Section, USA, November, 1984.

8. Coe, T. J., 'A Technical Evaluation of the 60 Foot SWATH Ship Halcyon to Determine Utility in Coast Guard Operations', Proceedings Intersociety Advanced Marine Vehicles Conference, Washington, June, 1989.

9. Fein ,J.A., McCreight, K.K., and Kallio,J.A., 'Seakeeping of SSP Kaimalino', Proceedings AIAA/SNAME Advanced Marine Vehicles Conference, San Diego, California, U.S.A., April, 1978.

10. The Editor of the Fast Ferry Int., 'First FBM Marine FDC 400 on Trials', Fast Ferry International, December, 1989.

11. Narita, H., and Mabuchi, Y., 'Design and Full Scale Test Results of Semi-Submerged Catamaran (SSC) Vessels', Proceedings 1st International Marine Systems Design Conference (ZMSDC) , London 1982.

12. McGregor, R. C. , 'Report on the Full Scale Trials of the 20 tonne SWATH Fishing Vessel - M.V. Ali', Marine Technology Report in Preparation , @ June, 1991.

13. Woolaver, D.A., and Peters, J.B., 'Comparitive Ship Performance Trials for the U.S. Coast Guard Cutters Mellon and Cape Corwin and the U.S. Navy Small Waterplane Area Twin Hull Kaimalino', DTNSRDC Report No 80/037, March 1980.

14. Hightower, J.D., and Seiple,R.L., 'Operational Experiences with the SWATH Ship S.S.P. Kaimalino', Proceedings AIAA/SNAME Advanced Marine Vehicles Conference, San Diego, California, U.S.A., April, 1978.

15. Drummond, S.E., 'Sixteen Years of SWATH Operations',Proceedings, Intersociety Advanced Marine Vehicles Conference, Arlington, VA, USA, June 1989

16. Kelley, T.D.,'Actual Experiences with US SWATH Designs', Proceedings International Conference on SWATH Ships and Advanced Multi-Hulled Vessels II, RINA, London, Nov. 1988.

17. Mabuchi, T., Kunitake, Y. and Nakamura, H., 'A Status Report on Design and Operational Experiences with the Semi-Submerged Catamaran (SSC) Vessels', Proceedings International Conference of SWATH Ships and Advanced Multi-Hulled Vessels , London, April, 1985.

18. Kennell, C., White, B.L. and Comstock, E.N., 'Innovative Naval Design for North Atlantic Operations', Transactions, SNAME, Vol. 93, pp. 261-281, 1985.

19. Olson, S.R., 'The Military Utility of the Small Waterplane Area Twin Hull (SWATH) Concept', Proceedings, AIAA/SNAME Advanced Marine Vehicles Conference, San Diego, California, April, 1978.

20. McCreight, K.K., 'Assessing the Seaworthiness of SWATH Ships',Transactions SNAME, Vol. 95, pp. 189-214, 1987.

21. Olson, LCDR S.R,'An Evaluation of the Seakeeping Qualities of Naval Combatants', Naval Engineers Journal, February, 1978.

22. Olson, LCDR S.R,'Seakeeping- and the SWATH Design', U.S. Naval Institute, Proceedings, March, 1978.

23. Comstock, E.N., Bales, S.L. and Gentile, D.M., 'Seakeeping Performance Comparison of Air Capable Ships', Naval Engineers Journal, ASNE, April, 1982.

24. McCreight, K.K. and Stahl, R.G.,'Recent Advances in the Seakeeping Assessment of Ships', Naval Engineers Journal, ASNE, May 1985.

25. Djatmiko, E.B., 'Comparitive Evaluation of some Slamming Prediction Methods for SWATH Type Vessels', Departmental Report, Department of Naval Architecture, University of Glasgow, March 1991.

26. Gore, J.L., "SWATH Ships", Naval Engineers Journal, February, 1985.

27. Cannon, T.R., and McKesson, C.B., 'Large SWATHS A Discussion of the Diminishing Returns of Increasing Ship Size', Proceedings AIAA 8th Advanced Marine Systems Conference, San Diego, California, U.S.A., Sept,1986.

28. Weiss, I.M. and Cross, R.G.,'Ship Motion Effects on Gun Fire Control System Design, Naval Engineers Journal, ASNE, Vol. 91, No. 5, pp. 75-80, October 1979.

29. Meeks, T.L., Graham, C. and Hu, R.C., 'Combat Systems for the Advanced Naval Vehicles Concept Evaluation', Naval Engineers Journal, ASNE, Vol. 90, No. 5, pp. 65-72, October, 1978.

30. Abbott, J.W., 'Modular Payload Ships in the U.S. Navy', Transactions SNAME, Vol. 85, pp. 350-395, 1977.

31. Chun, H.H., 'Theoretical and Experimental Studies on the Resistance of SWATH Ships', PhD Thesis, Department of Naval Architecture, Glasgow University, 1988.

32. Chun, H.H., McGregor, R.C. and Ferguson, A.M., 'Wave Making Resistance Characteristics of SWATH Ships', Proceedings International Conference on SWATH Ships and Advanced Multi-Hulled Vessels II, RINA, London, November, 1988.

33. Chun, H.H. and McGregor, R.C., 'Added Resistance of SWATH Models in Uniform Waves', Proceedings Intersociety Advanced Marine Vehicles Conference and Exhibit, Washington D.C., USA, June 1989.

34. Chun, H.H., McGregor, R.C., and Chung,J.H., 'Experiments on the Added Resistance of SWATH Models in Regular Head Waves', Proceedings of the 19th ITTC, Madrid, Spain, September 1990.

35. Kaysen, H.D., 'SWATH AGS Deep Ocean Survey Ship', The SNAME, The Chesapeake Section, October, 1985.

36. MacGregor, J.R., 'A Computer Aided Method for Preliminary Design of SWATH Ships', Ph.D. Thesis, Glasgow University, May 1989.

37. Gupta, S.K., and Schimdt, T.W., 'Developments in SWATH Technology', Naval Engineers Journal, May 1986, pp171-187.

38. Meyerhoff, W.K. et al, Report of Commitee V.4. "Novel Design Concepts - SWATH", Proceedings of the 10th International Ship and Offshore Structures Congress,Vol. 2, Lyngby, Denmark, August, 1988.

39. Munk, M.M., 'The Aerodynamic Forces on Airship Hulls', Report No 184, National Advisory Comitte for Aeronautics, 1924.

40. Chapman, R.B., 'Sinkage and Trim of SWATH Demihulls', Proceedings AIAA/SNAME/USN, Advanced Marine Vehicles Conference , San Diego, California, 1974.

41. Wu, J.Y. and McGregor, R.C., 'SWATH Seakeeping in the Presence of Control Fins', Proceedings 5th International High-Speed Surface Craft Conference, Southampton, England, May, 1986.

42. Caldeira-Seraiva, F., and Clarke, D., 'The Design of Compensators for Control of SWATH Motions', International Conference on SWATH Ships and Advanced Multi-Hulled Vessels II, RINA, London, November, 1988.

43. Nehrling, B.C., 'An Experimental Investigation into the Stability and Motions of a Damaged SWATH Model', Proceedings of STAB'90 - the Fourth International Conference on the Stability of Ships and Ocean Vehicles , Naples, September, 1990.

44. Miller, A.F., 'Aspects of Damaged Stability in the Computer Augmented Design Process for SWATH Vessels', Proceedings of STAB'90 - the Fourth International Conference on the Stability of Ships and Ocean Vehicles, Naples, September 1990.

45. Papanikolaou, A., Zaraphonitis, G., Koskinas, C. and Savvas, J., 'On the Stability of a SWATH Ferry in Calm Water and in Waves', Proceedings of STAB'90 - the Fourth International Conference on the Stability of Ships and Ocean Vehicles,Naples,September,1990.

46. Whalen, J.E., and Kahn, L.A., 'SWATH Dynamic Simulation Model', Operations Research Inc, Technical Report 1093 January 1977.

47. Fein, J.A., and Waters, R.T., 'Rotating Arm Experiments for SWATH 6A Manoeuvring Predictions' , DTNSRDC SPD Report 0698-01, July 1976.

48. Fein, J.A., 'Rotating Arm Experiments for the Stable Semi-Submerged Platform (SSP) Manoeuvring Prediction', DTNSRDC SPD Report 0698-02, September 1977.

49. Hart, C.J. et al, 'Rotating Arm Experiment for an Extended Strut SWATH Ship as Represented by SWATH 6E' , DTNSRDC SPD Report 0698-03,September, 1983.

50. Fein, J.A., ' The Application of Rotating Arm Data to the Prediction of Advanced Ship Manoeuvring Characteristics', Proceedings 18th American Towing Tank Conference, Maryland August,1977.

51. Waters, R.T., and Fein, J.A., 'Manoeuvrability of SWATH Ships', Proceedings of 19th American Towing Tank Conference, Ann Arbour, July 1980.

CHAPTER 3

DAMAGE STABILITY

3.1 Introduction

One of the greatest drawbacks associated with SWATH vessels is their inherent sensitivity to changes in weight or flooding. This is unfortunately a natural consequence of low waterplane area and an unavoidable limitation of the concept.

Despite this sensitivity surprisingly little work has been published in the field of SWATH damage stability. Betts (Ref 1) highlighted the oversight in 1988, however regardless of prompting little has been published since then.

Papanikolau et al (Ref 2) and Nehrling (Ref 3) describe theoretical and experimental studies in SWATH stability in papers presented at STAB'90 - The Fourth International Conference on the Stability of Ships and Ocean Vehicles. The study described here was also presented at that conference in September 1990 (Ref 4). In addition Goldberg and Tucker (Ref 5,6) offer stability and buoyancy criteria designed to ensure that SWATH ships possess damage stability equivalent to a monohull.

These few references represent the full extent of currently available information on the topic. With these exceptions published information on SWATH damage stability is restricted to brief observations in scattered sources.

3.2 Aims and Objectives

It is clearly desirable to include consideration of a vessels ability to survive damage when evaluating design proposals. Conventional damage stability software packages capable of handling the novel geometry of the SWATH form are available however all existing programs require detailed design information and are both time and labour intensive. When the Naval Architect is faced with the task of evaluating large numbers of alternative design proposals for a given vessel, the value of a tool providing fast, first estimates of damage stability becomes clear. Ideally, such a tool should be quick to use and require only preliminary design data.

This chapter describes the creation of such a design tool and its development from parametric study through to completed design program. The program enables the user to quickly and easily assess the damage stability characteristics of Small Waterplane Area Twin Hull (SWATH) ships at the preliminary design stage.

The chapter also seeks to demonstrate that SWATH vessels possess acceptable damage stability characteristics and to reassure potential SWATH ship operators that survivability for SWATH vessels is likely to be at least comparable to that for monohulls.

3.3 Approach Adopted

3.3.1 The Parametric Study

In order to provide such a capability the links between design geometry and survivability must be explored and relationships between the two established. To this end, a parametric study was selected as the most suitable vehicle for the first part of the work. Results from this study were then analysed and mathematically defined to allow the construction of a program which predicts damaged behaviour at the earliest stages of the design process.

The first stage was to create a 'family' of SWATH vessels, that is, vessels whose principal dimensions and geometrical proportions are closely related. These vessels are not geosims in the true sense but share the same basic proportions for the main design variables : for instance, hull/strut length ratios, strut setback, nose and tail run-in, run-out etc. The computer program 'DESIN' (Ref 7) was used to synthesize this family of ships for five displacements in the range 1000 to 5000 tonnes. It is felt that this displacement range covers most likely SWATH newbuildings in the foreseeable future.

Simple circular hulls with elliptical noses and paraboloidal tails were chosen for all five designs. All designs had 'short' struts (80% of hull length) supporting a standard cross structure of depth equal to one deck plus structure. The length of the cross structure was equal to that of the struts without any overhang forward or aft. A linear sheer was incorporated into the wet deck (the underside of the box) over the forward 25% of its length. Fig 3.1 shows a typical bodyplan for a vessel in the study. The resulting designs are the most basic SWATH forms likely to be considered in practice. Their main attribute is simplicity of construction, and the coincidence of longitudinal

centres of buoyancy and gravity afforded by the short single strut arrangement. This is desirable in reducing coupled heave and pitch motions. The final reason for their selection was to maintain continuity with existing work utilizing the same hullforms (Ref 8).

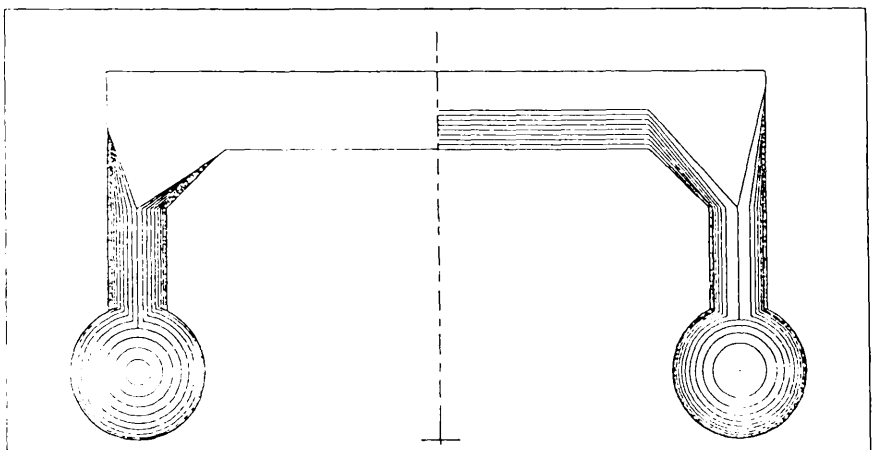

Fig 3.1 Typical Bodyplan Drawing for a Vessel in the Study

For each displacement, vessels were created with one of two different box clearance values and one of three different compartment lengths. The values of box clearance chosen were selected to correspond with values proposed by Lamb in 1987 for contouring and platforming modes of operation for SWATH vessels (Ref 9). These values form the upper and lower ends of the range of feasible wet deck/waterline clearances. All vessels were idealised to have uniform bulkhead spacing and therefore equal compartment spacing throughout their length. This simplifying assumption, whilst clearly unrealistic was made in order to reveal trends and patterns in the results which might otherwise have remained hidden.

Bulkhead spacings of 6.25%, 8.33% and 12.5% of the vessels length were selected for all designs. These values were selected after careful consideration of current SWATH design subdivision practice. The percentage values chosen gave compartments of length approximating to the upper, lower and intermediate values of compartment length currently considered suitable by contemporary SWATH designers.

The only remaining 'ship' variable considered was operating draught. For each design displacement flooded stability calculations were carried out at three draughts, corresponding to design displacement and design displacement +/- 5%. The resulting range of 10 % design displacement, whilst low by conventional standards, was considered sufficiently large to cover the operating envelope of most SWATH vessels.

It is recognized that many other parameters have a significant effect on the damaged stability of SWATH vessels. However, it must be appreciated that for reasons of sheer logistics, the number of variables must be kept low since in a study of this kind, each additional variable has a multiplying effect on the size of the study.

Variations in KG, the vertical height of the vessels centre of gravity, were additionally investigated by means of a separate parametric sub-study. This was undertaken after the main study was complete. The results from the sub-study were then developed in the form of correction factors. The format for the sub study was identical to that of the main study, but utilized far fewer design variables.

Table 3.1 gives the main dimensions of vessels used in the investigation while Fig 3.2 illustrates the main parametric study outline.

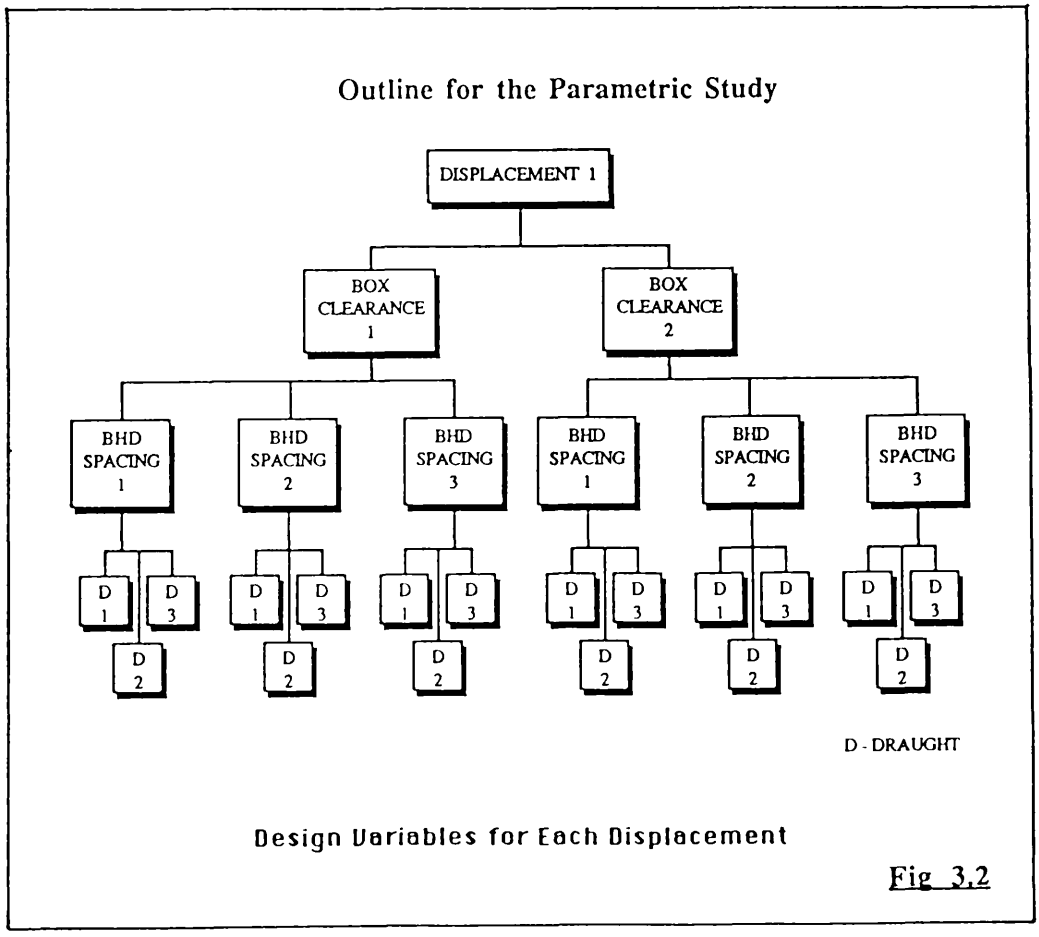

Fig 3.2

Design Displacement tonnes	1000	2000	3000	4000	5000
Hull and Strut Geometry					
Hull Length	71.747	82	83.558	86.97	89.78
Ellipsoidal Nose Length	21.524	24.6	25.067	26.091	26.934
Paraboloidal Tail Length	17.937	20.5	20.889	21.743	22.445
Hull Diameter	3.116	4	4.897	5.5	6.016
Strut Length	57.398	65.6	66.846	69.58	71.824
Elliptical Nose Length	20.089	22.96	23.396	24.353	25.138
Parabolic Tail Length	20.089	22.96	23.396	24.353	25.138
Strut Thickness	0.917	1.5	1.964	2.399	2.798
Design Draught	4.674	6	7.346	8.25	9.024
Hull Centreline Spacing	21.244	22	23.92	24.4	25.484
Box Clearance Values					
Upper	3.4	4.27	4.91	5.38	5.94
Lower	2.21	2.77	3.17	3.48	3.88
Compartment Lengths					
6.25 % Hull Length	4.48	4.94	5.22	5.44	5.61
8.33 % Hull Length	5.98	6.58	6.96	7.24	7.48
12.5 % Hull Length	8.96	9.88	10.44	10.88	11.22
Intact GM Values	2.124	2.268	2.392	2.44	2.548
VCG Values	9.417	10.066	10.863	11.193	11.986

All Dimensions in Metres Unless Otherwise Stated

Table 3.1 Design Data for the Vessels used in the Parametric Study

Once the variables associated with the ship were determined, attention was focussed on suitable damage scenarios. For each bulkhead spacing, compartments were successively flooded singly and in pairs, fore, aft and amidships, port and starboard around the vessel. In keeping with U.S. Navy practice (Ref 8) no horizontal subdivision was incorporated. The vessel was therefore free to flood up to the main (bulkhead) deck. Transverse flooding to the longitudinal centreline was assumed. In addition a standard flooding permeability value of 0.95 was selected for all compartments. Although it is generally accepted that these assumptions are unrealistic, they do provide a useful degree of conservatism in the results. It is therefore considered that the resulting ten flooding conditions represent most foreseeable damage conditions which a vessel may reasonably be expected to survive.

These variables were selected because they were considered the most fundamental. They provide a sound foundation around which the study can be later expanded to consider the effects of variations in many other parameters. The main parametric study was thus established with five variables and a final total of some 900 permutations.

3.3.2 Calculation and Analysis Procedure

A parametric study of this nature is constrained by its very size to be computer based. Several commercial damage stability packages were considered for the task, including SIKOBS, SFOLDS and the University of Southampton's Wolfson Unit programs. In the end the Wolfson Unit software was selected, primarily because of its availability and perceived user- friendliness.

Wolfson software was used to calculate the effect of the ten different flooding scenarios on each of the ninety combinations of vessel design features. The resulting mass of 'raw' damage stability data was processed and analysed exhaustively using micro computer based spreadsheet and graphics packages. Heel and trim were plotted against flooding extent for every combination of flooding location. Equilibrium draughts, changes in draught, maximum GZ values after flooding, and areas under two sections of the flooded GZ curves were also plotted against combinations of flooding location, extent and operating displacement. Complete GZ curves were plotted for all damage cases and the results overlaid to display trends of flooded behaviour.

After careful study of a 'testcase' vessel the five quantities; heel, trim, maximum GZ and area under the GZ curve for the two regions 0-45 degrees and 0-20 degrees

were selected to represent and define a vessels response to flooding.

For every combination of design parameter and flooding scenario, plots of these five values against flooding extent were prepared. The resulting curves were then mathematically defined using regression routines and the polynomial coefficients of the equations thus produced were stored. It is these equations which form the database which allowed construction of the Flooded Stability Estimation Program "FSEP1" .

Full results are presented in Appendix A in the form of these equations.

3.4 Discussion of Damaged Stability

The testcase vessel selected had a design displacement of 4000 tonnes and a wet deck/waterline clearance of 3.48 m corresponding to the lower bound for a contouring mode of operation. This ship was selected arbitrarily for no other reason than that its combination of geometrical parameters combined to produce a vessel of fairly realistic proportions. Some results from the analysis of this vessel are presented here together with some brief general observations on the trends exhibited in the study overall.

3.4.1 Effect of Increasing Flooding Extent

Effect on GZ curves : For asymmetric flooding the GZ curve is shifted 'fwd and down' as expected - Fig 3.3-3.5. However, for symmetrical flooding resulting in trim alone we find that the righting lever GZ opposing forced heeling actually increases with flooding for initial heel angles - Fig 3.6 and 3.7. This is due to early immersion of the haunch and cross deck structure caused by the flooding induced trim. The subsequent rise in waterplane area increases stability and hence raises GZ. Above 25 degrees heel this immersion is relatively constant for all cases regardless of initial trim, GZ therefore reduces with flooding as expected. It may be seen from the curves that flooding forward produces greater changes in GZ than flooding aft. This phenomenon is due to the greater volume/length ratios of the forward compartments and to the presence of sheer on the forward wet deck. These factors combine to increase the heeling/trimming moment and reduce the restoring moment produced by immersion of the cross deck. Indeed it will be noted that results are unavailable for 25% symmetrical flooding forward. It seems likely that the excessive trim induced pushed the problem outwith the Wolfson Unit program's limit of operation.

Effect on Heel and Trim : Heel and trim increase almost linearly with flooding extent for all flooding cases. Flooding forward or aft results in much smaller heel angles than damage amidships, since the accompanying trim tends to immerse the cross deck and increase stability. Flooding forward results in values of heel and trim which are slightly higher than those resulting from equivalent damage aft. This is due to the increased volume of the forward compartments and the presence of sheer on the wet deck reducing restoring forces for a given inclination. Slight trimming was observed for flooding amidships. This is most probably due to slight shifts in the relative positions of the longitudinal centres of flotation, buoyancy and gravity - Fig 3.8 and 3.9

Effect on Max GZ : Increasing the extent of flooding reduces the maximum value of the righting lever GZ possessed by the damaged vessels. This is most noticeable for asymmetric flooding amidships when the reduction is almost linear with increased flooding. When damage occurs towards the ends of the ship the onset of the reduction is delayed.This is due to immersion of the cross structure caused by trim - Fig 3.10.

Effect on Area under the GZ Curve : The energy required to heel a damaged vessel to a given angle is represented by the area under the GZ curve. This area was found to decrease with flooding as anticipated - Fig 3.11. As for maximum GZ the reduction was again greatest for asymmetric damage amidships, while trim induced immersion of the cross structure delayed the onset of the reduction where damage occurred at the vessels extremities. This immersion is particularly significant for symmetrical flooding. Indeed it was discovered that area under the GZ curve in the region 0-20 degrees was actually increased rather than decreased for these cases - Fig 3.12.

3.4.2 Effect of Increasing Operating Displacement

Effect on GZ curves : Increasing operating displacement i.e. draught, results in a general 'fwd and down' shift of the GZ curve. The shape of the curve remains relatively constant in the 10% displacement range studied, while maximum GZ values reduce by approx 6% on average over this range. Fig 3.13 - 3.17 illustrate this.

Effect on Heel and Trim : Equilibrium values of heel and trim reached after damage vary non uniformly with changes in operating draught. Increasing draught may increase or decrease heel and trim depending on the extent and location of flooding. This erratic behaviour is due to variations in immersion of the cross deck, resulting from the coupled effects of heel and trim combined with initial draught. In general for pure heel and pure trim, increasing draught reduces the equilibrium angle reached as more of the

cross deck is immersed for a given inclination. The variations noted are illustrated in Figs 3.18 - 3.25.

Effect on Area under the GZ Curve : In general increasing operating draught results in an almost linear reduction in area under the curve. However in the case of asymmetric flooding amidships the area under the first part (0-20 degrees) increases with small amounts of flooding. This is again due to earlier immersion of the cross deck structure increasing stability. For greater damage extents and larger forced heel angles (above 20 degrees), this immersion is relatively constant regardless of initial operating draught. Figs 3.26 - 3.35 illustrate the behaviour observed.

3.4.3 Effect of Increasing Design Displacement

Heel and trim resulting from damage both increase with increasing vessel size. This phenomenon is due to the volume of flooding and hence the heeling/trimming moment increasing at a faster rate than does the restoring moment. Since the vessels in the study were not true geosims the ratio of (waterplane area * beam) / enclosed volume does not remain constant with increasing size. Simple calculations verify this explanation while Fig 3.36 and 3.37 illustrate the phenomenon.

N.B. Only 3 displacements are shown for clarity. In Fig 3.36 no heel is shown for 25% flooding of the 1000 tonne design. It appears that this scenario resulted in a condition outwith the Wolfson Unit programs limit of operation.

Maximum GZ and area under the GZ curve both decrease as normal with increasing design displacement although the total righting moment (Displacement * GZ) naturally increases. Flooding effects on max GZ and area the GZ curve are relatively unaltered by changes in displacement.

3.4.4 Effect of Increasing Box Clearance

Increasing box clearance results in later immersion of the cross structure, this effectively increases equilibrium heel and trim for a given flooding condition. In general maximum GZ values are increased although the total area under the curve is always reduced.

For small vessels with low box clearances, small amounts of flooding immerse the cross deck structure increasing the maximum values of GZ experienced. In these cases

increasing box clearance reduces immersion of the cross deck structure and therefore reduces the maximum values of GZ opposing forced heeling.

For more extensive flooding, the equilibrium angle of heel is sufficient to immerse the cross deck structure for both high and low box clearance designs. For these cases vessels designed with high wet deck / waterline clearances ultimately demonstrate the greatest resistance to heeling, i.e. the largest GZ's.

The extent of flooding at which this change in behaviour occurs reduces with increasing design displacement. This is most probably due to the rise in heel associated with increasing design displacement. Note:- For vessels of design displacement greater than 3000 tonnes, increasing box clearance increases maximum GZ for all flooding extents.

Figs 3.38 - 3.40 Illustrate the effect of box clearance on the max GZ values attained.

3.4.5 Effect of Increasing KG

Variations in the position of the vertical centre of gravity were not investigated in the main parametric study for logistical reasons. The parameter was however deemed sufficiently important that a limited sub study was undertaken to evaluate its influence. Preliminary investigation based upon a restricted data set indicates the following trends.

Increasing the height of the vertical centre of gravity 5% above the design value used in the main study produces the following effects:-

Equilibrium Heel angle Increases 10%
Equilibrium Trim angle Increases 2%
Maximum GZ value Decreases 5%
Area under GZ curve (0-45degrees) Decreases 5%
Area under GZ curve (0-20degrees) Decreases 11%

Similarly reducing the KG by 5% has an equal and opposite effect upon the results.

It must be stressed that these results were obtained from limited analysis on a very restricted data set. They are therefore offered for guidance only and should be applied with caution.

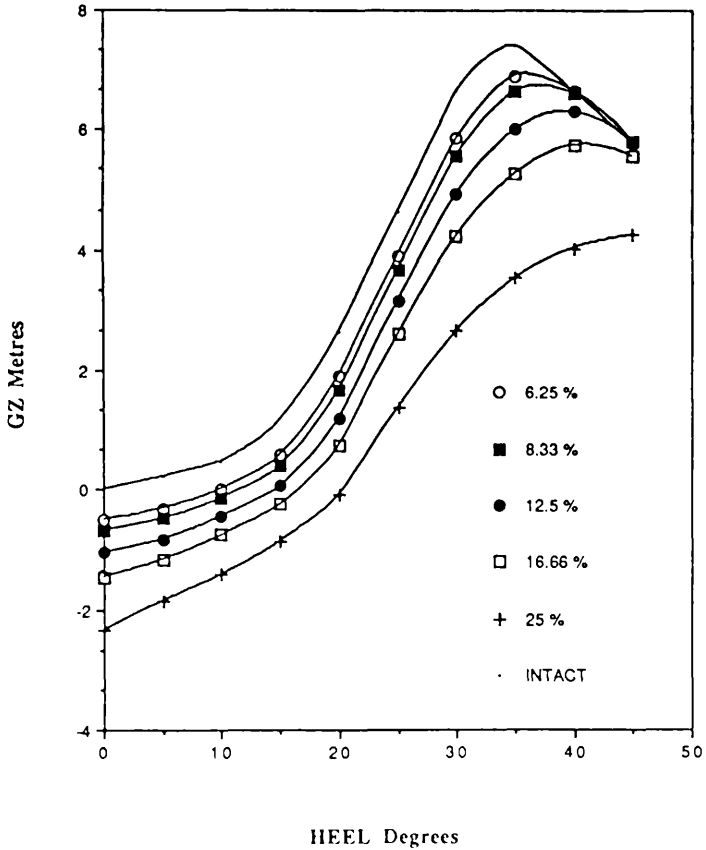

Fig 3.3 Variation of GZ with Flooding Extent. Flooding Stb Amidships.

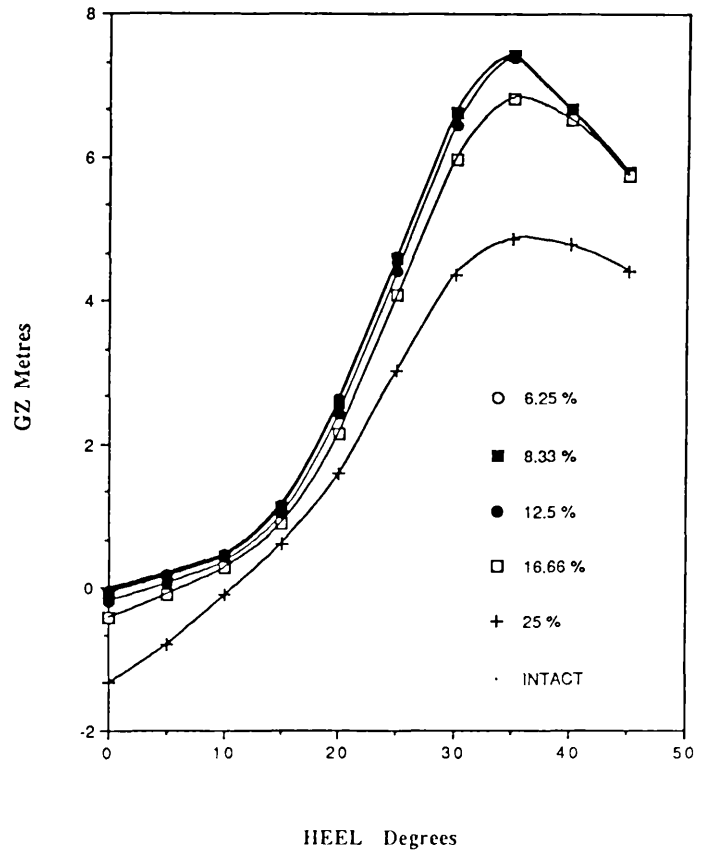

Fig 3.4 Variation of GZ with Flooding Extent. Flooding Stb Only Aft.

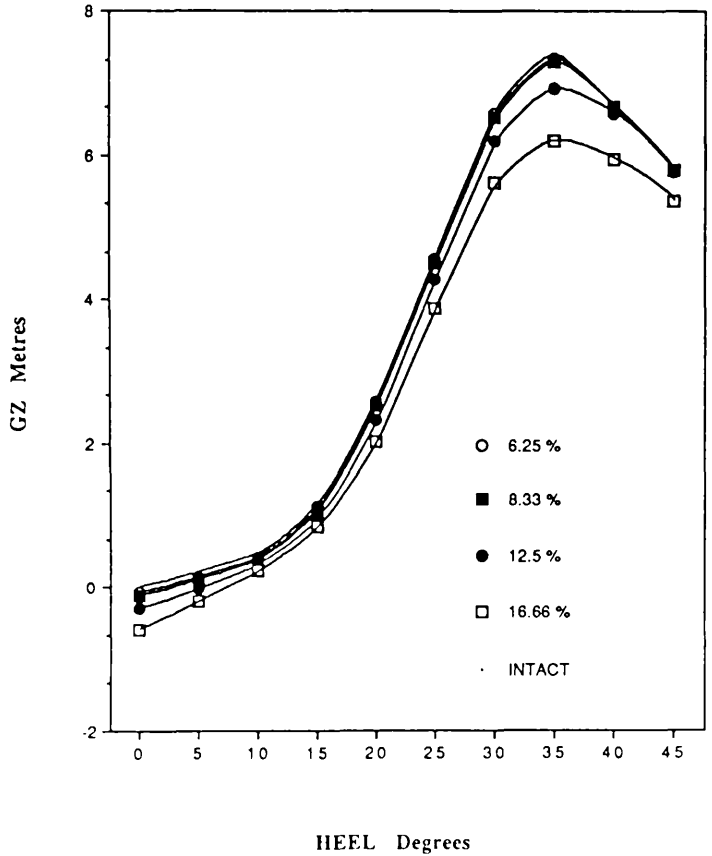

Fig 3.5 Variation of GZ with Flooding Extent, Flooding Stb Only Fwd.

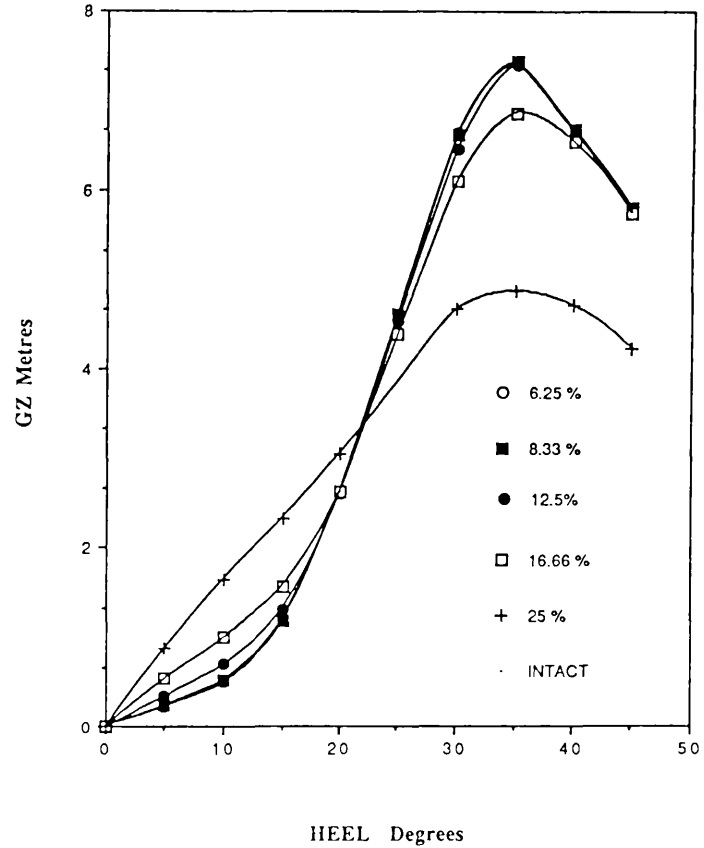

Fig 3.6 Variation of GZ with Flooding Extent, Flooding Port and Stb Aft.

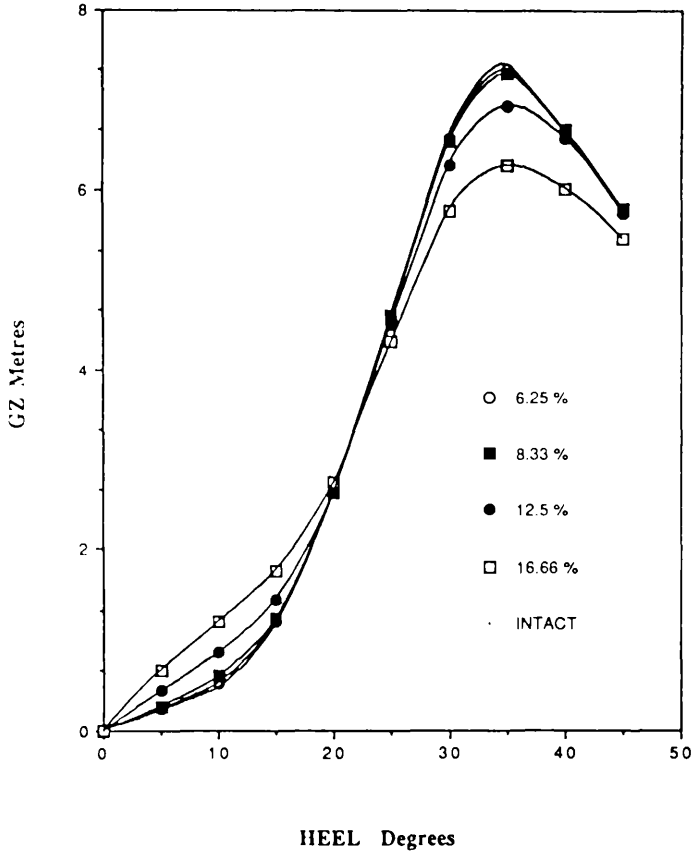

Fig 3.7 Variation of GZ with Flooding Extent, Flooding Port and Stb Fwd.

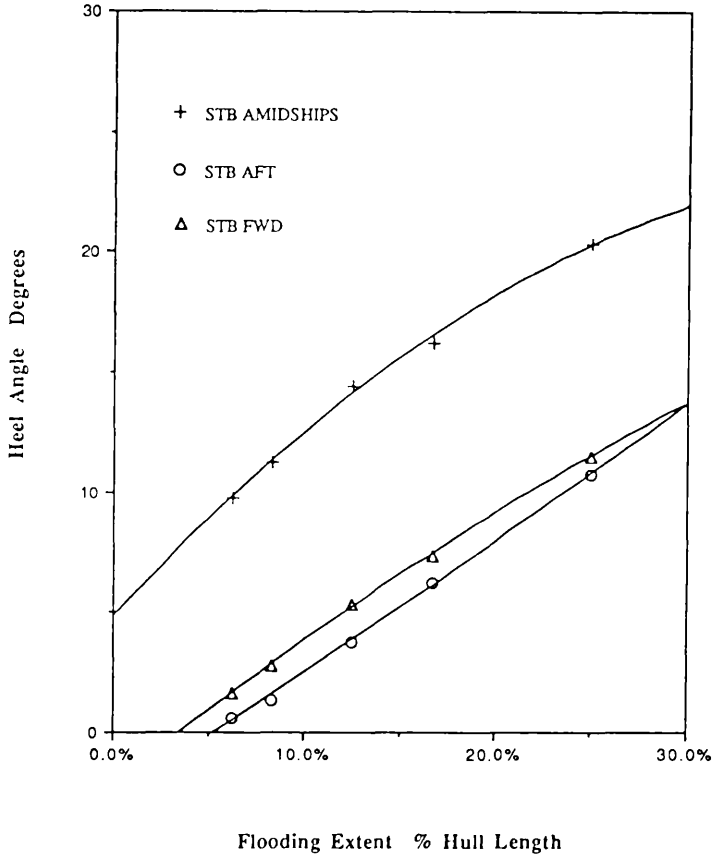

Fig 3.8 Heel / Flooding Extent

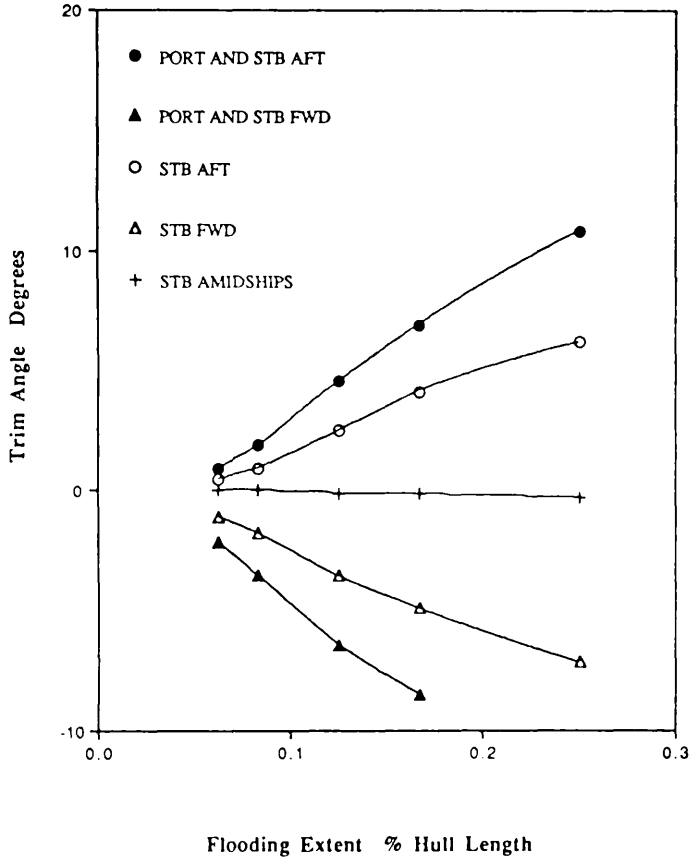

Fig 3.9 Trim / Flooding Extent

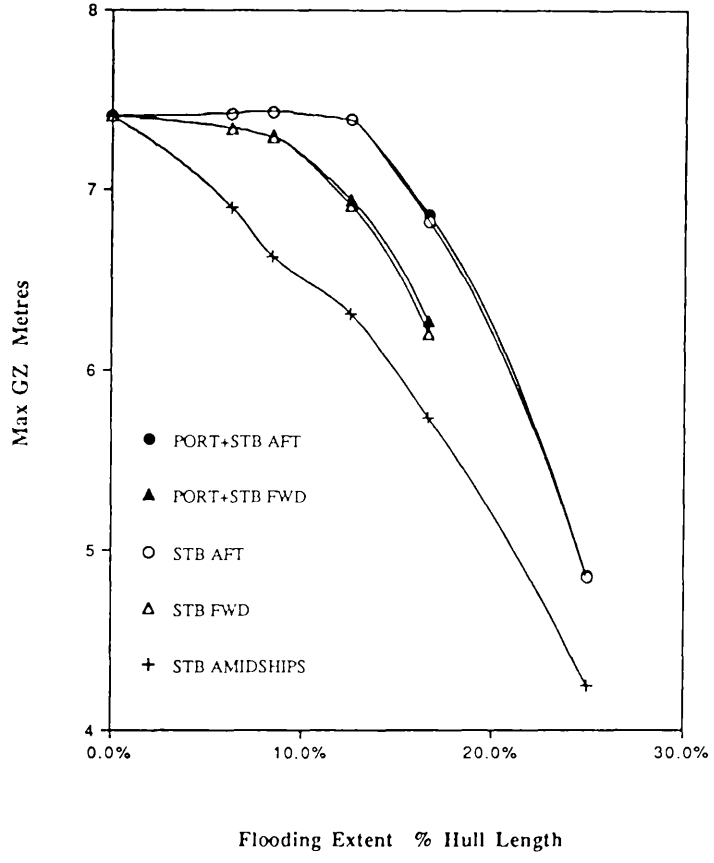

Fig 3.10 Maximum GZ / Flooding Extent

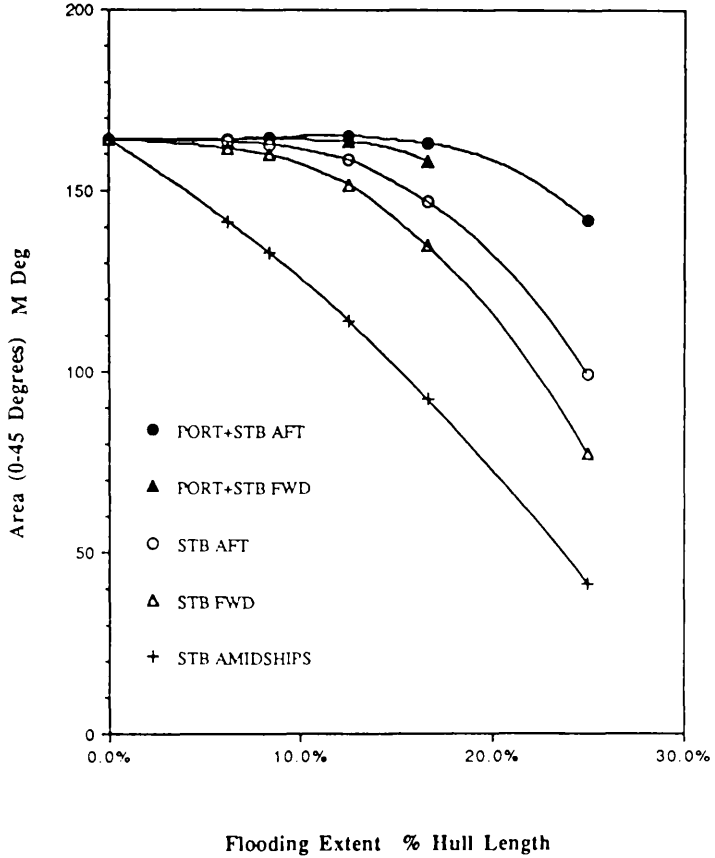

Fig 3.11 Area Under GZ Curve / Flooding Extent

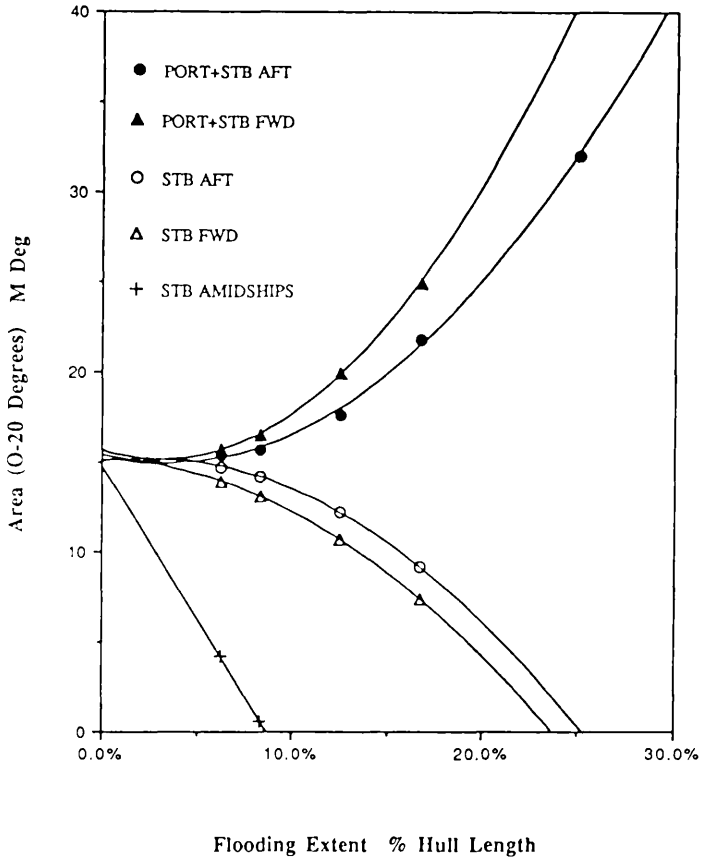

Fig 3.12 Area under GZ Curve / Flooding Extent

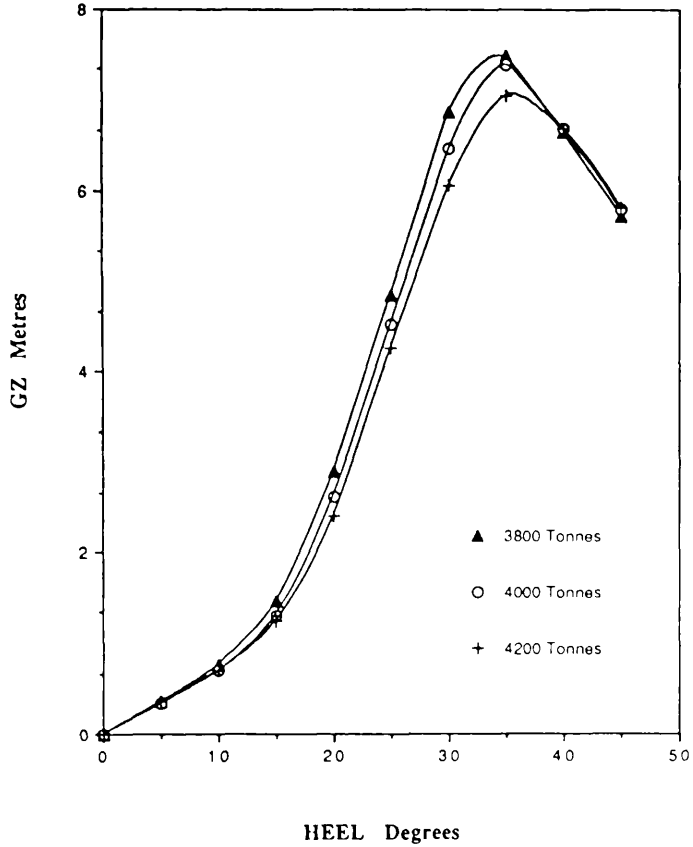

Fig 3.13 GZ / Heel / Operating Displacement, 12.5% Flooding Port and Stb Aft

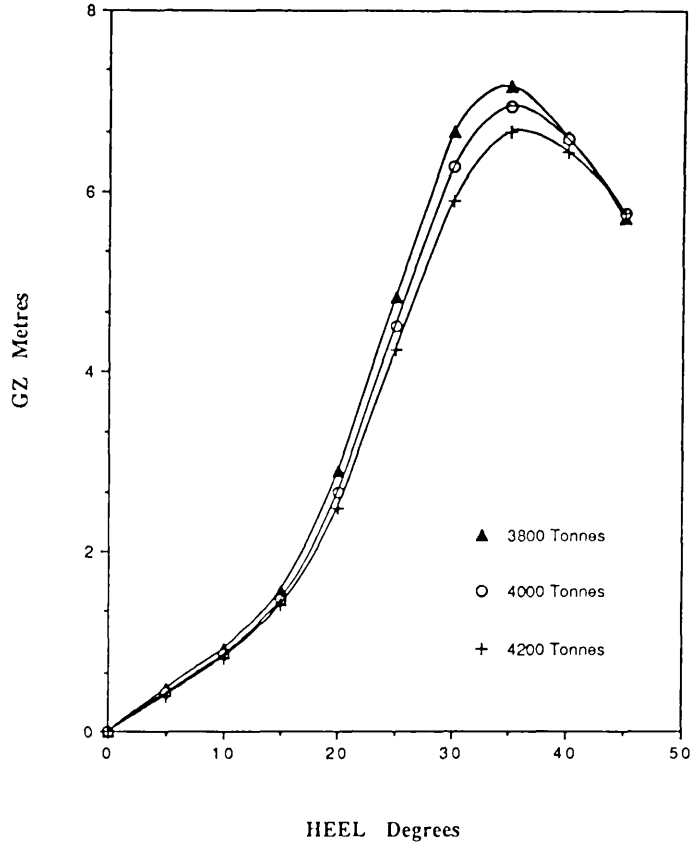

Fig 3.14 GZ / Heel / Operating Displacement, 12.5% Flooding Port and Stb Fwd.

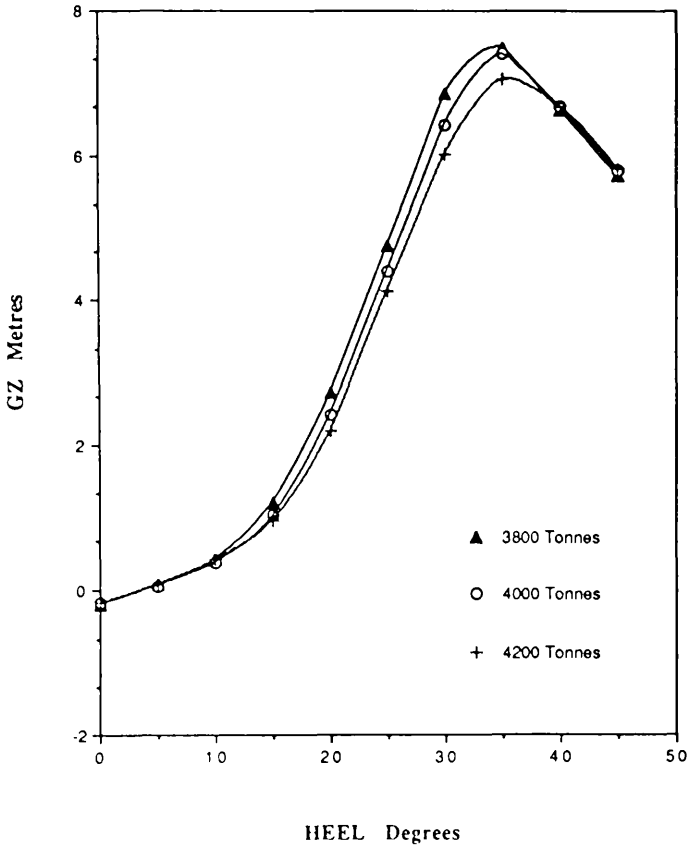

Fig 3.15 GZ / Heel / Operating Displacement, 12.5% Flooding Stb Only Aft

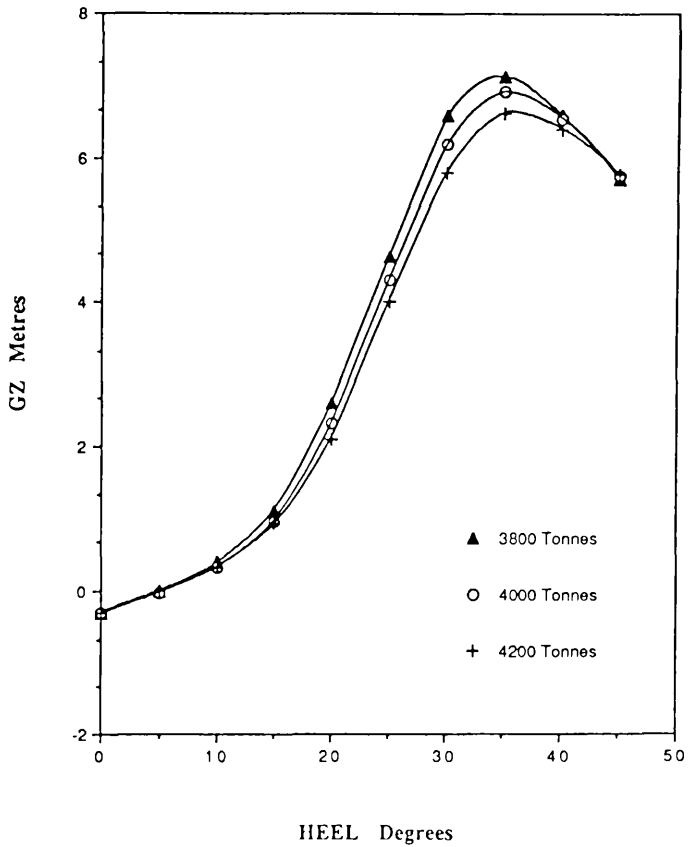

Fig 3.16 GZ / Heel / Operating Displacement, 12.5% Flooding Stb Only Fwd.

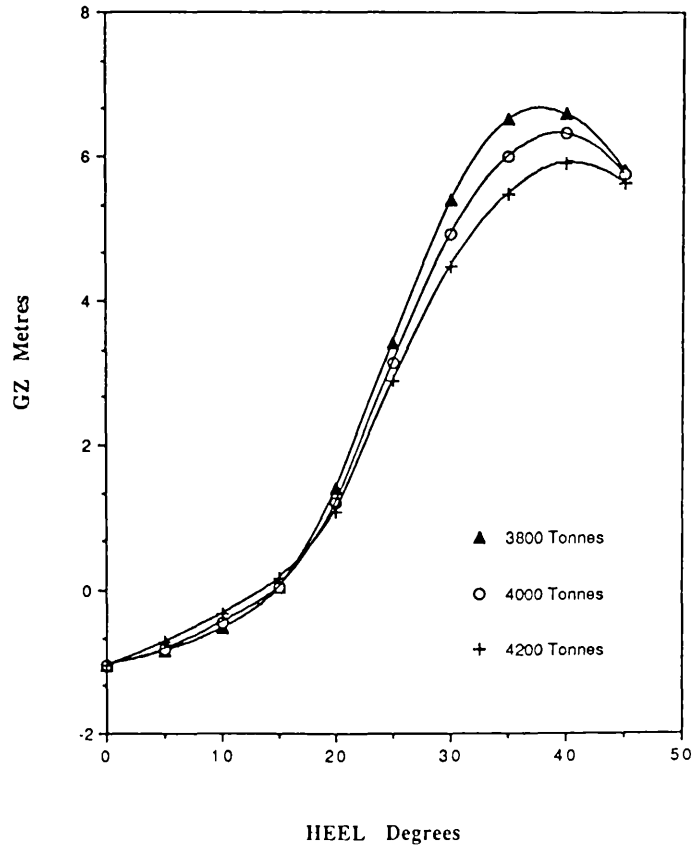

Fig 3.17 GZ / Heel / Operating Displacement, 12.5% Flooding Stb Amidships

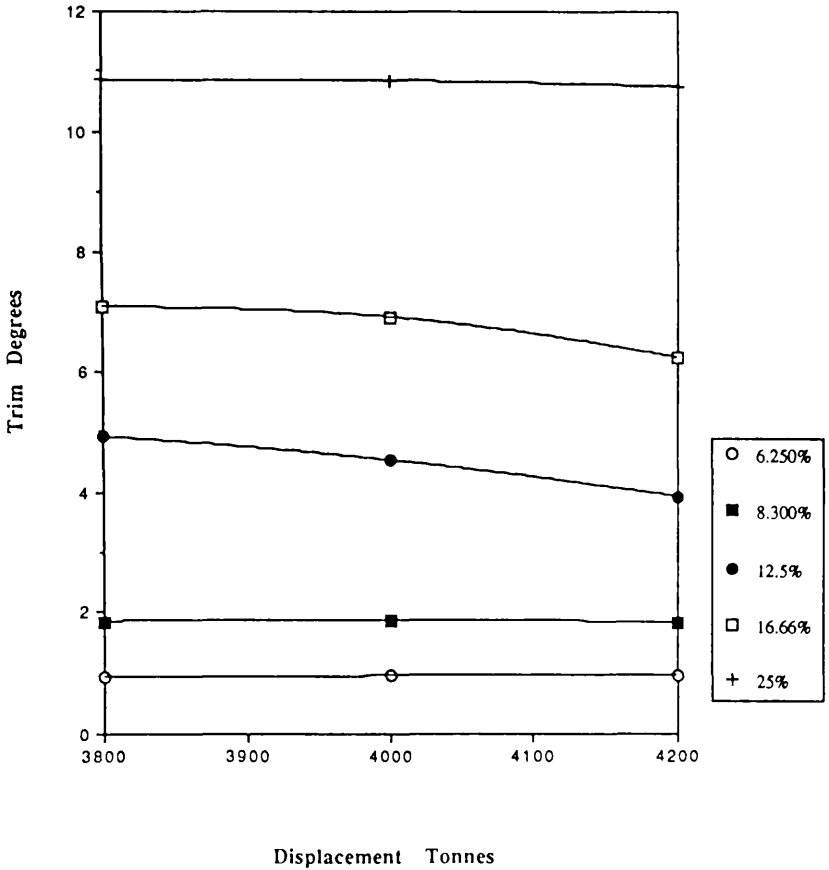

Fig 3.18 Trim / Operating Displacement
% Extent of Flooding - Port+Stb Aft

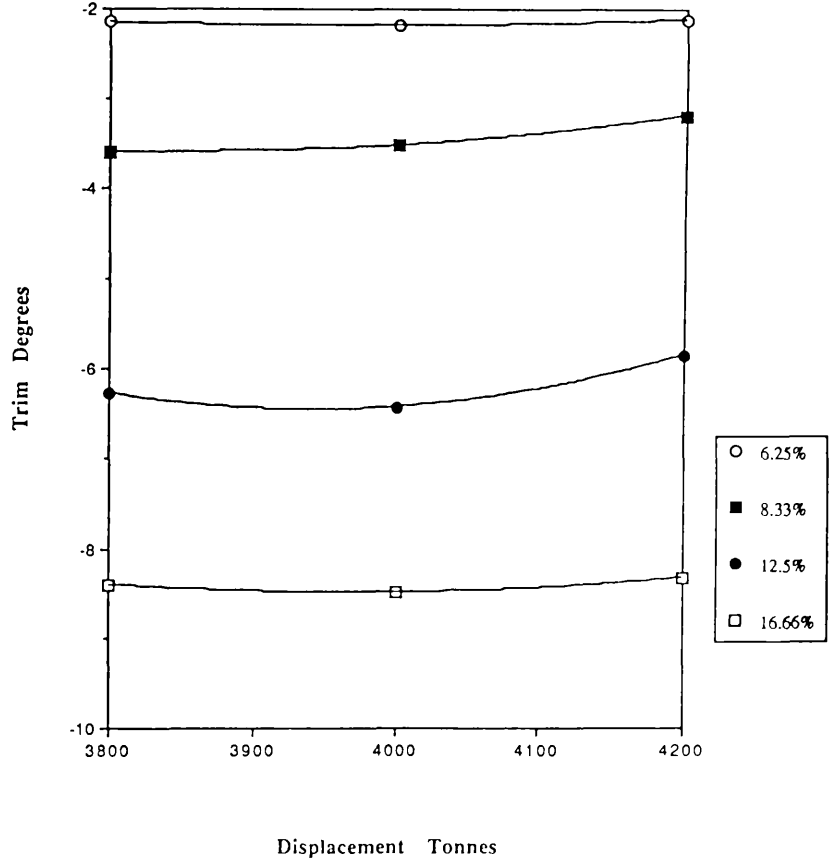

Fig 3.19 Trim / Operating Displacement
% Extent of Flooding - Port+Stb Fwd

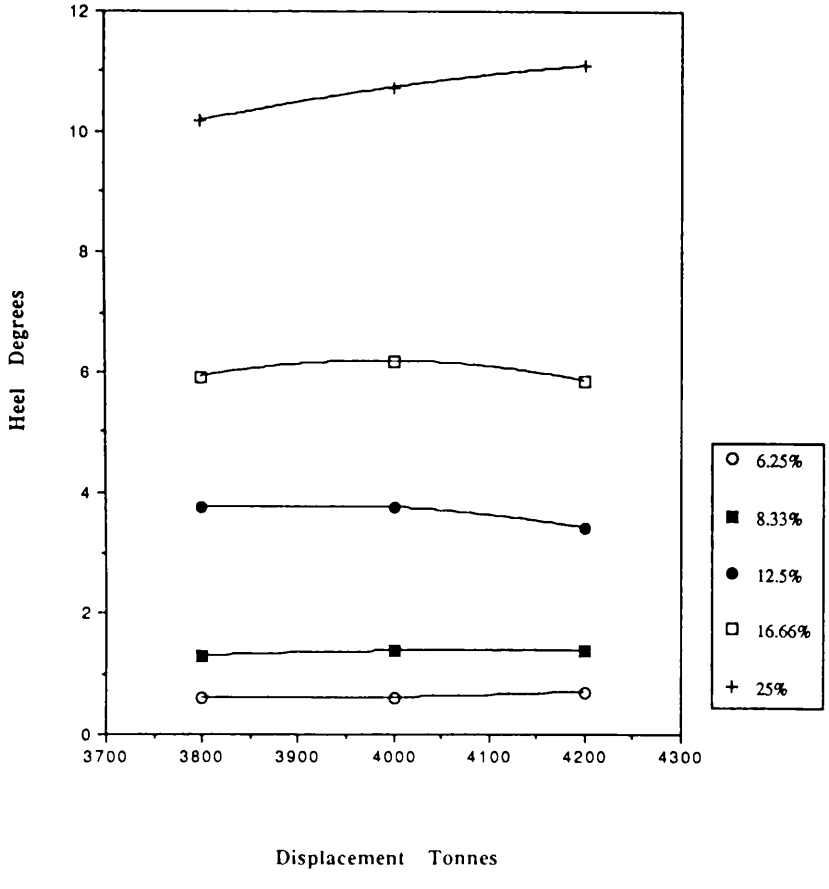

Fig 3.20 Heel / Operating Displacement
% Extent of Flooding - Stb Aft

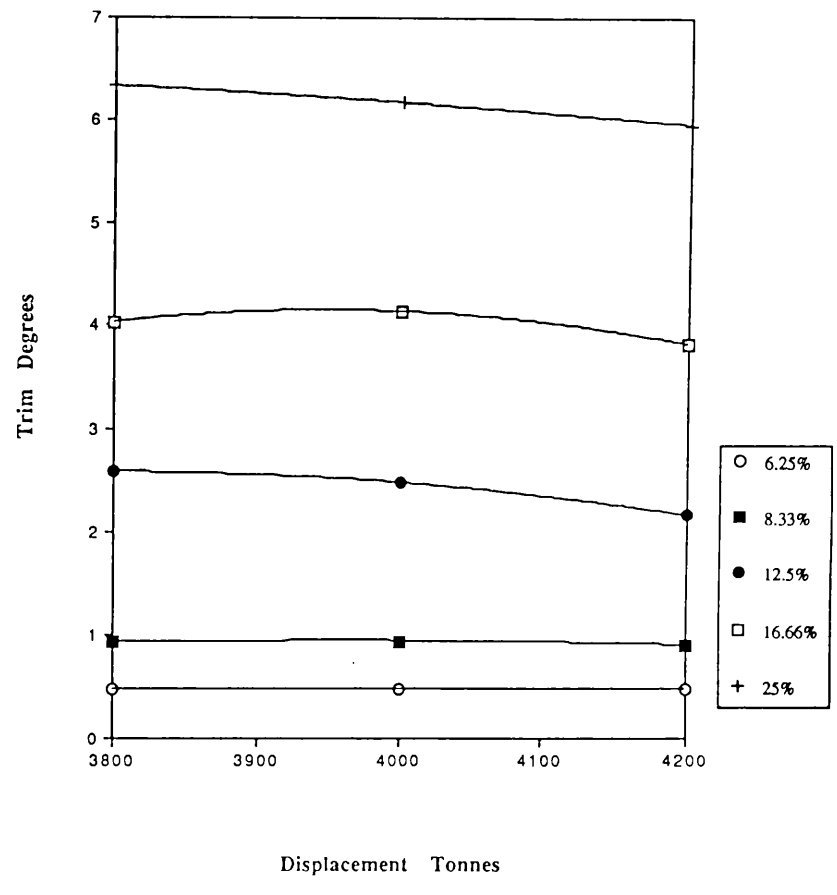

Fig 3.21 Trim / Operating Displacement
% Extent of Flooding - Stb Aft

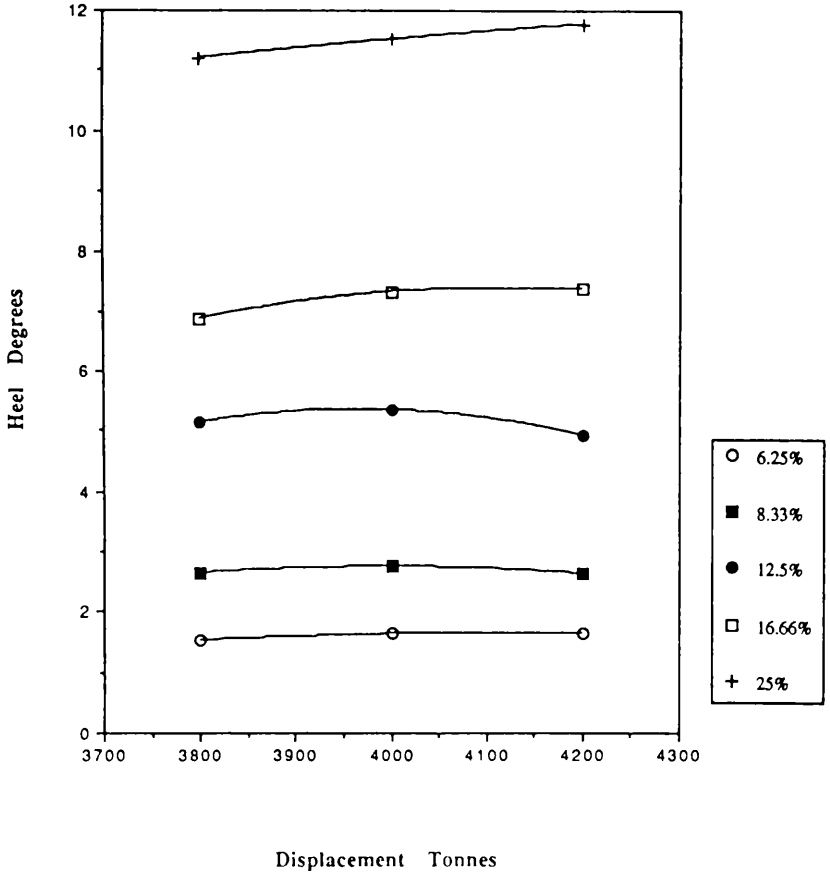

Fig 3.22 Heel / Operating Displacement
%Extent of Flooding - Stb Fwd

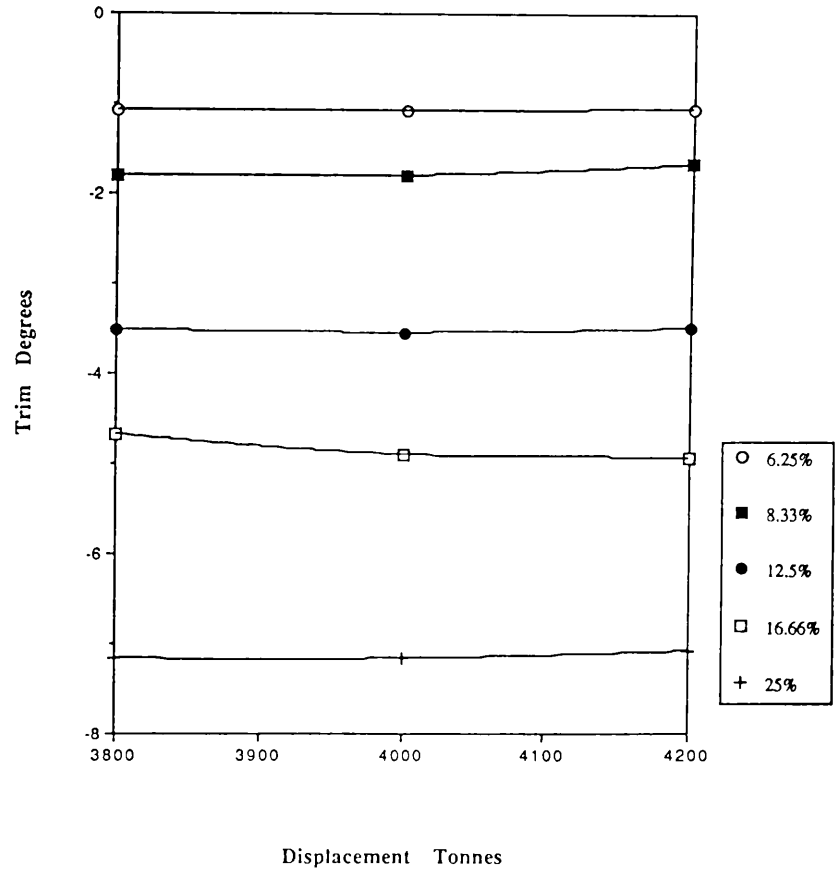

Fig 3.23 Trim / Operating Displacement
% Extent of Flooding - Stb Fwd

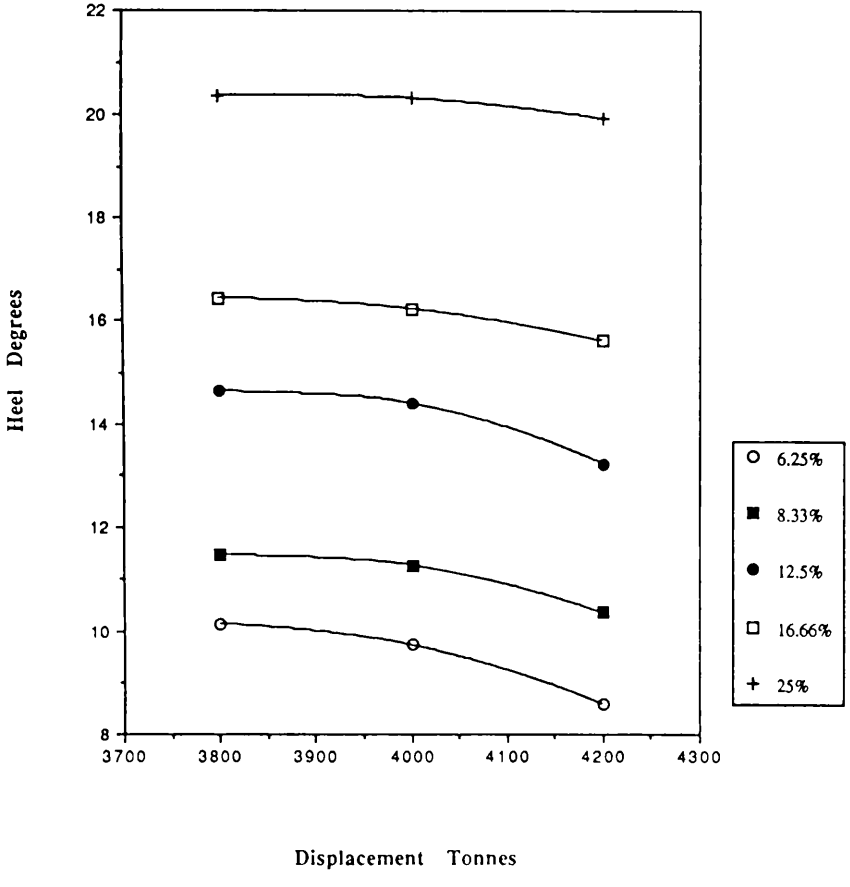

Fig 3.24 Heel / Operating Displacement
% Extent of Flooding - Stb Amidships

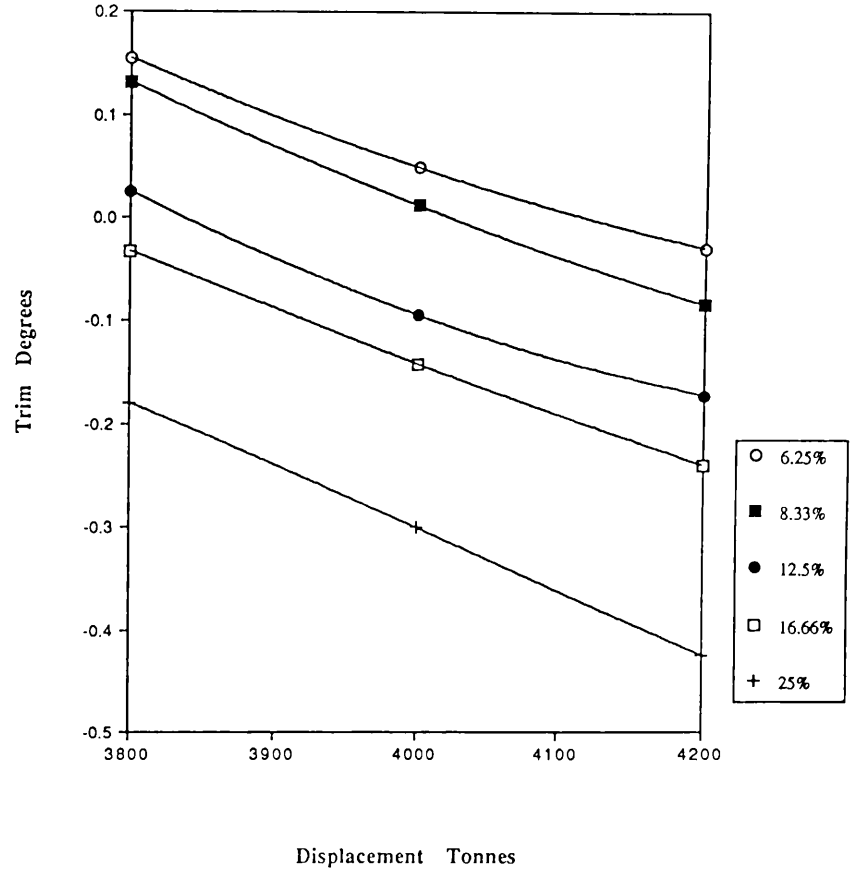

Fig 3.25 Trim / Operating Displacement
% Extent of Flooding - Stb Amidships

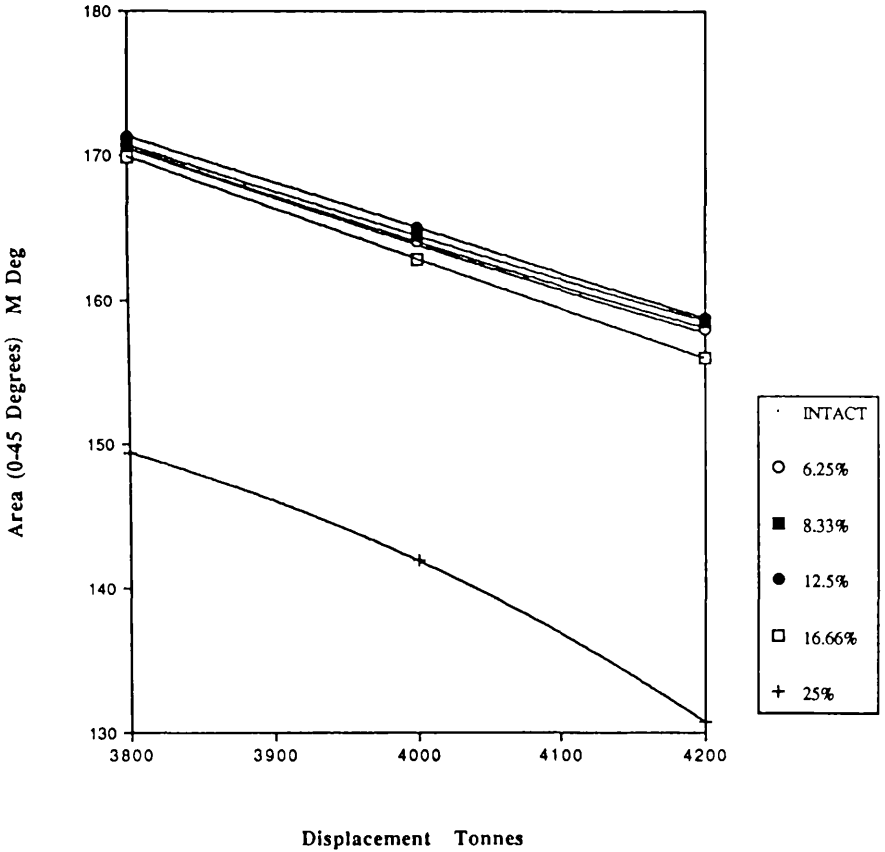

Fig 3.26 Area Under the GZ Curve / Draught
% Extent of Flooding - Port+Stb Aft

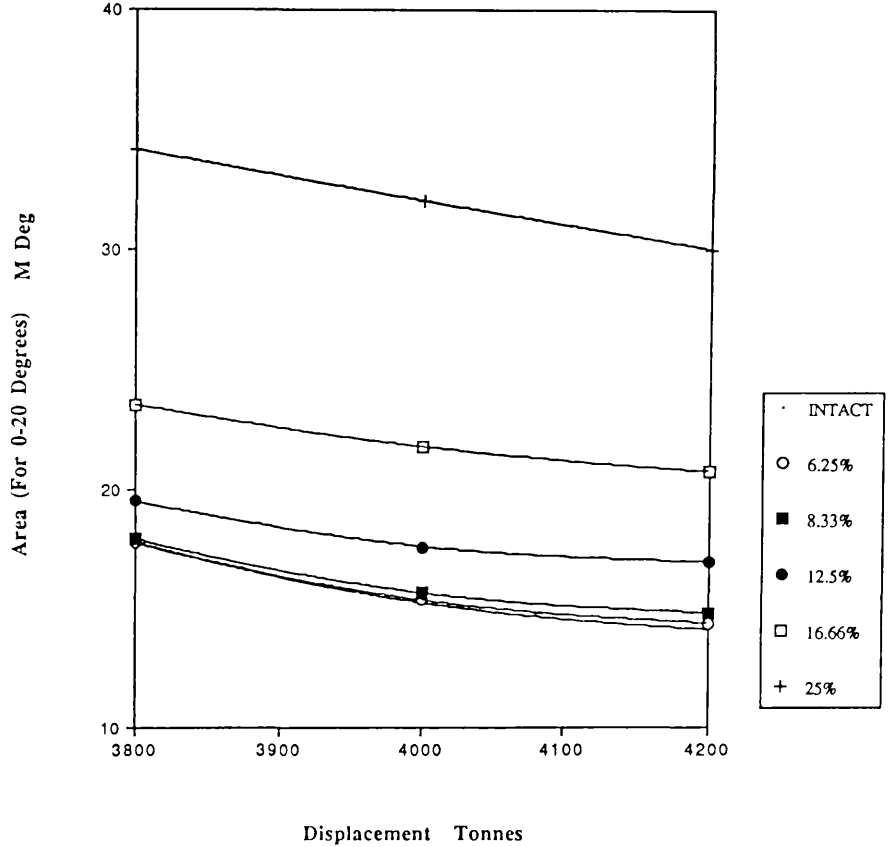

Fig 3.27 Area Under the GZ Curve / Draught
% Extent of Flooding - Port+Stb Aft

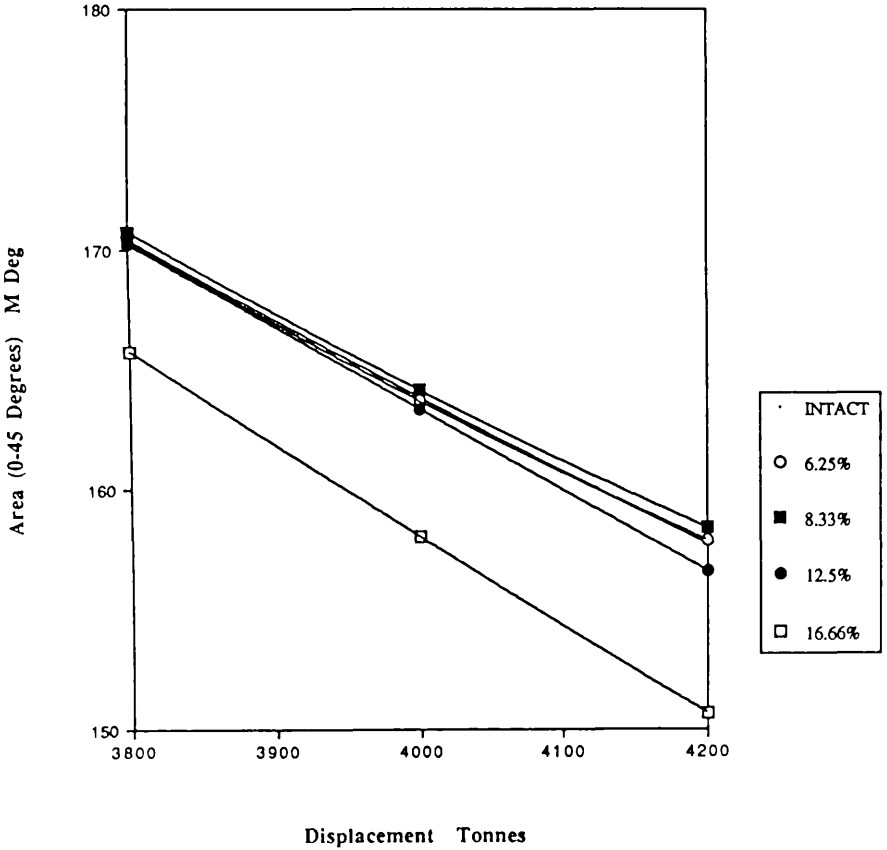

Fig 3.28 Area Under GZ Curve / Draught
% Extent of Flooding - Port+Stb Fwd

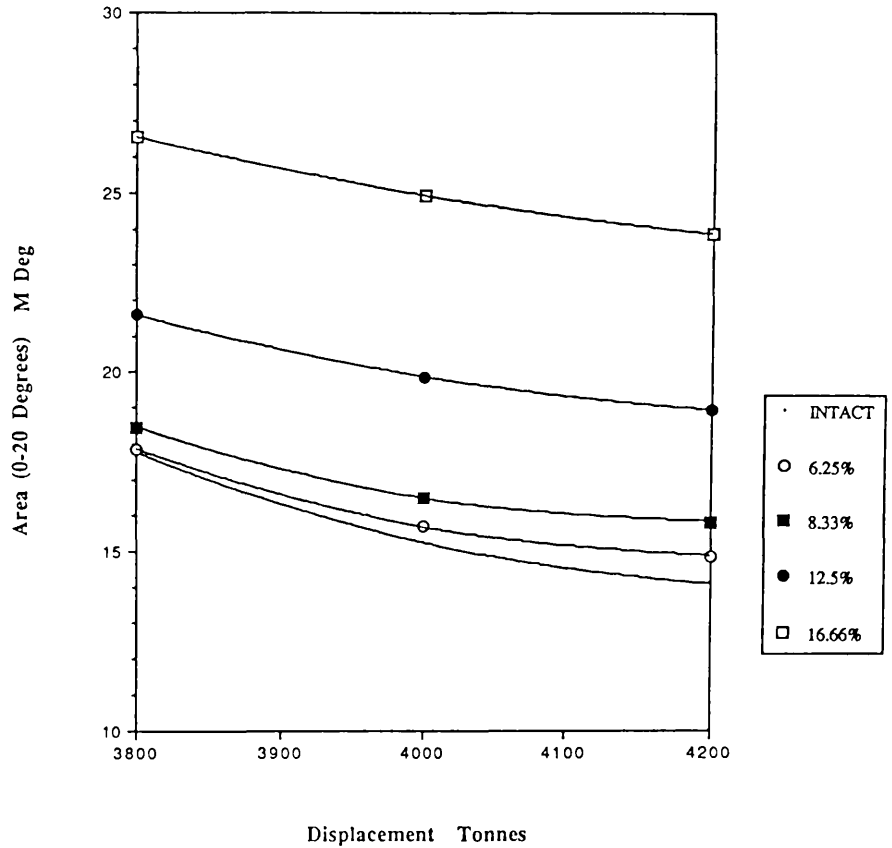

Fig 3.29 Area Under GZ Curve / Draught
% Extent of Flooding - Port+Stb Fwd

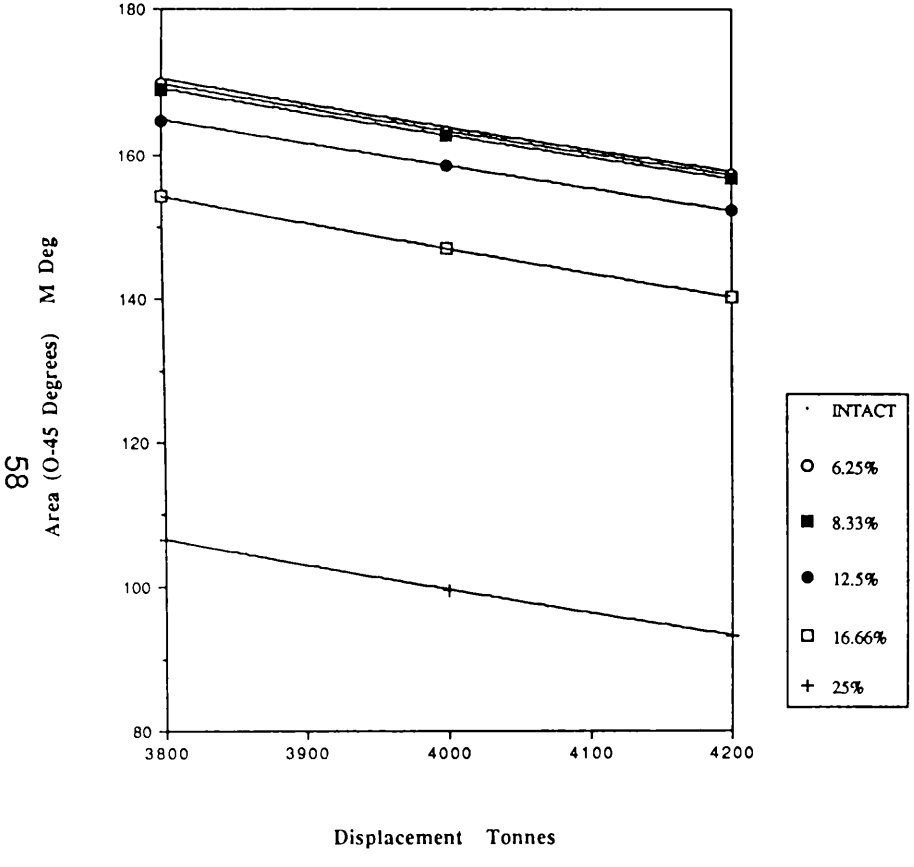

Fig 3.30 Area Under GZ Curve / Draught
% Extent of Flooding - Stb Aft

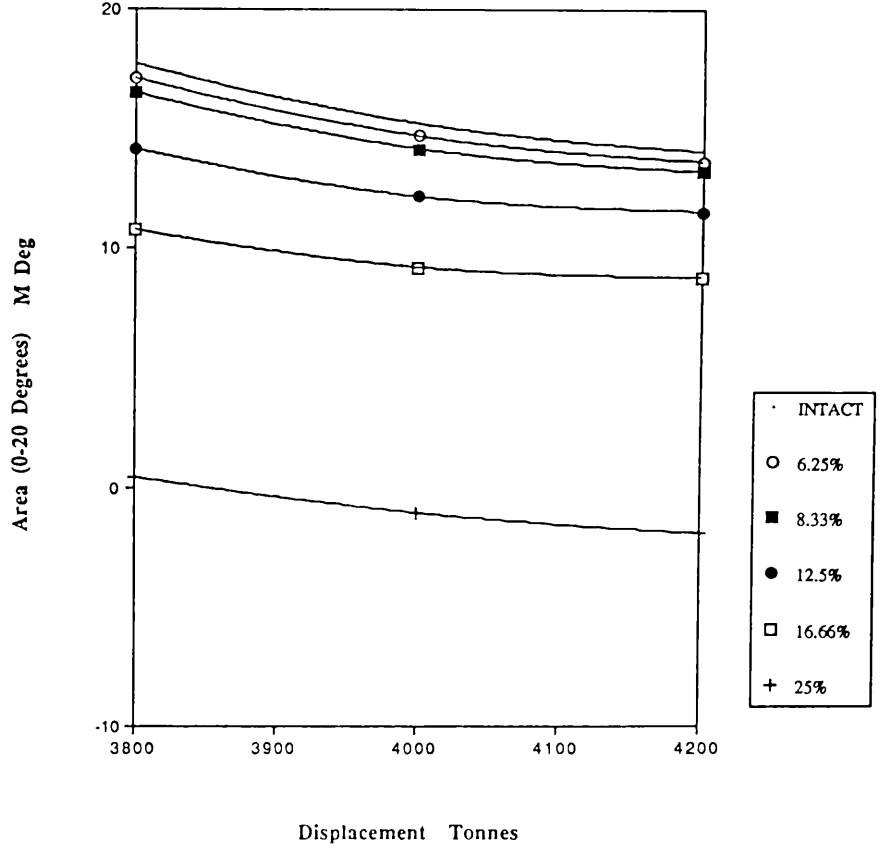

Fig 3.31 Area Under the GZ Curve / Draught
% Extent of Flooding - Stb Aft

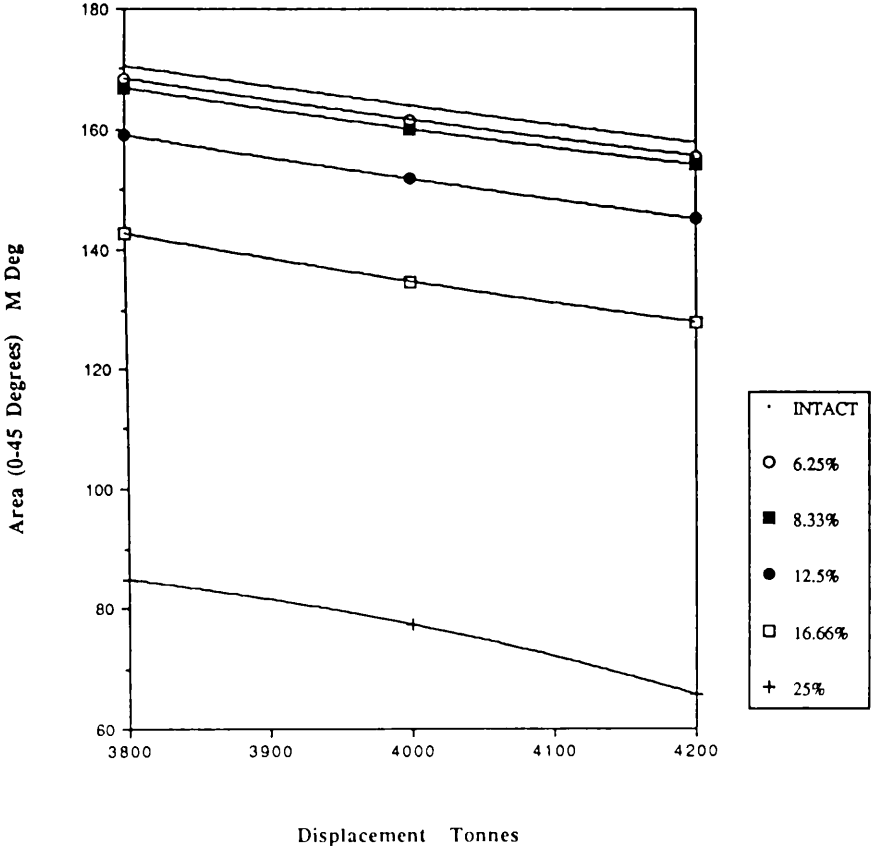

Fig 3.32 Area Under the GZ Curve / Operating Displacement
% Extent of Flooding - Stb Fwd

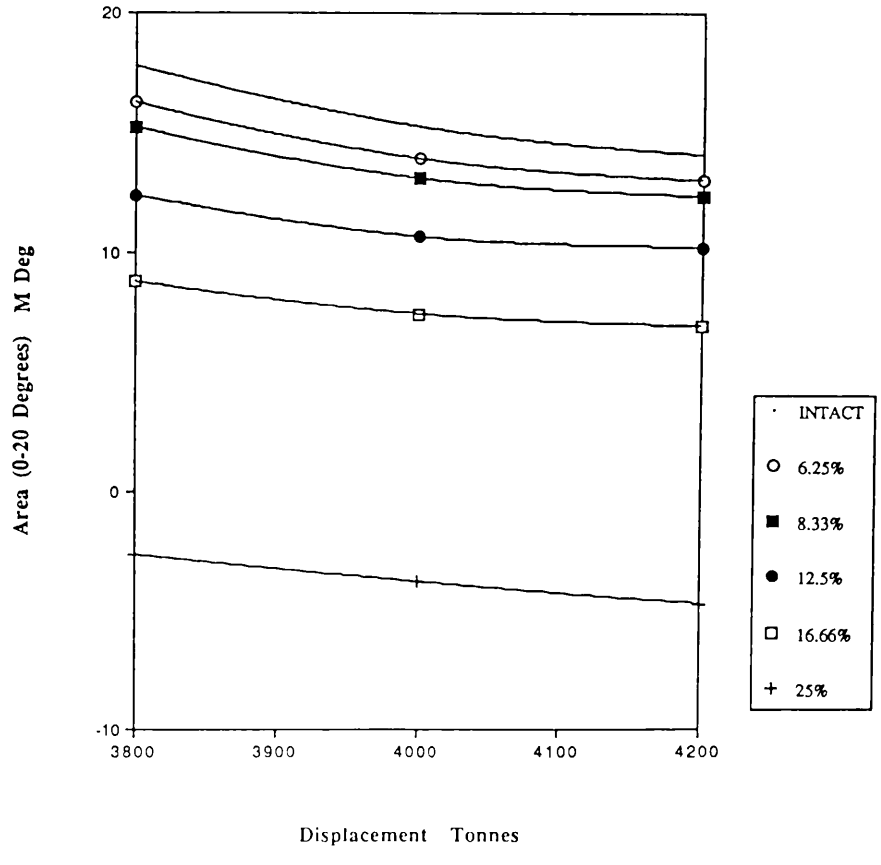

Fig 3.33 Area Under the GZ Curve / Draught
% Extent of Flooding - Stb Fwd

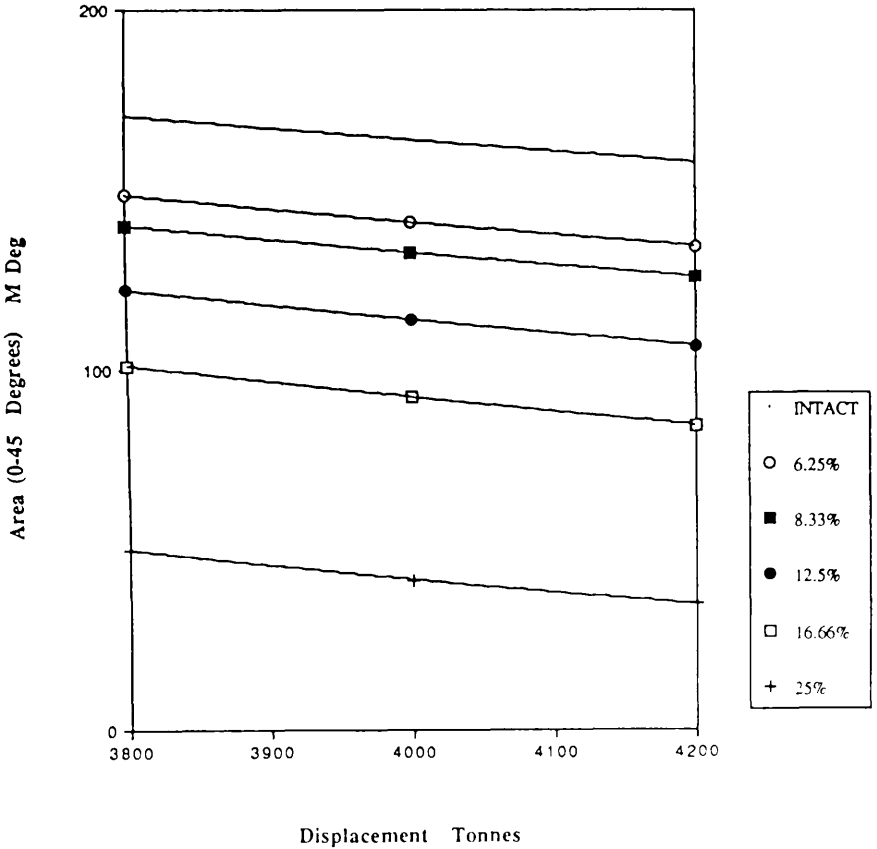

Fig 3.34 Area Under the GZ Curve / Draught
% Extent of Flooding - Stb Amidships

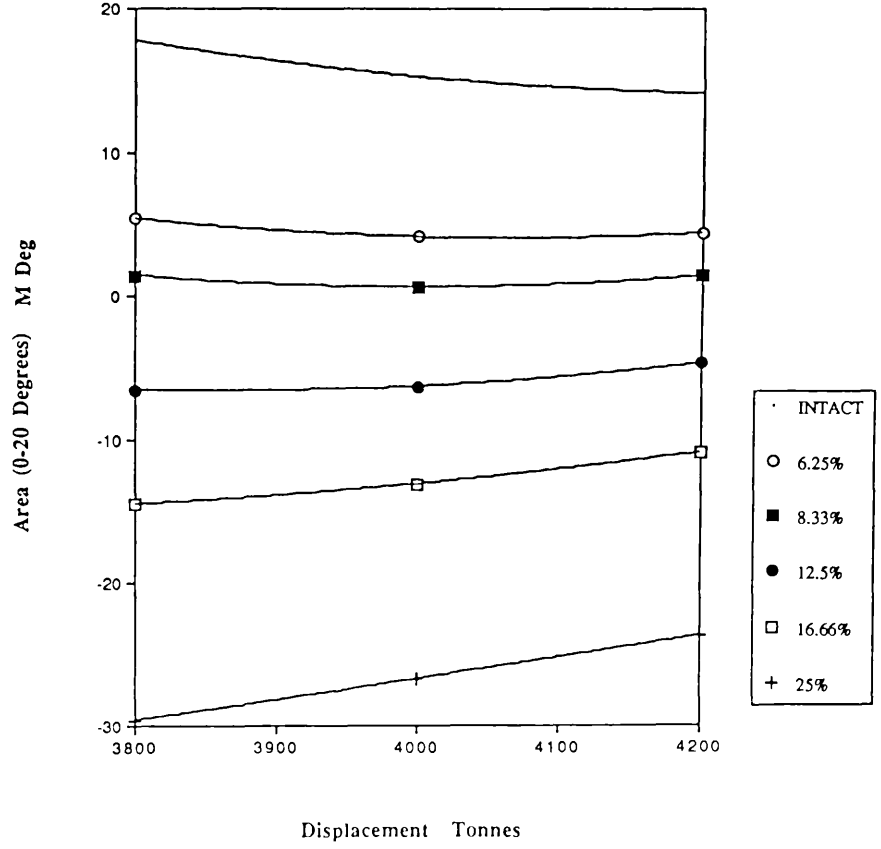

Fig 3.35 Area Under the GZ Curve / Draught
% Extent of Flooding - Stb Amidships

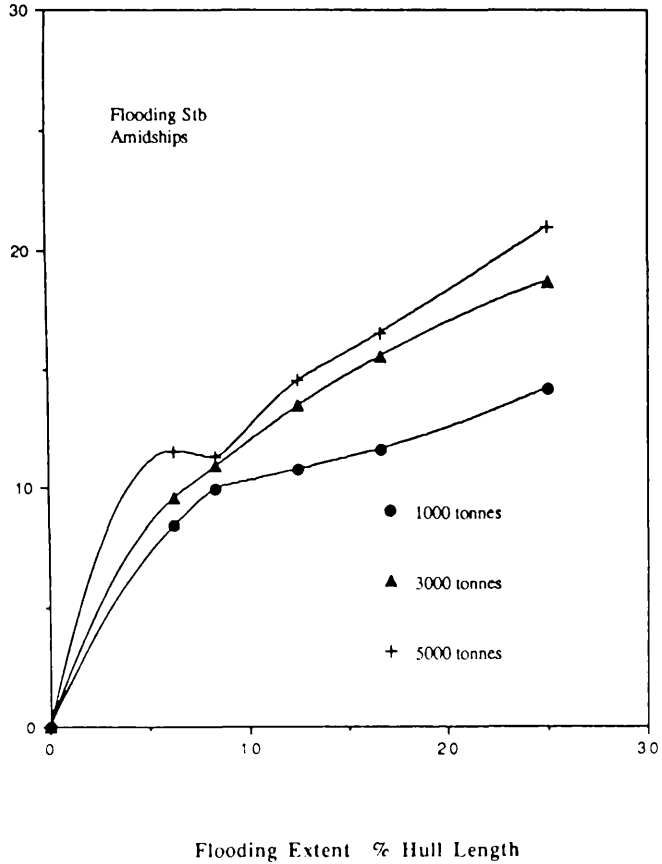

Fig 3.36 Heel / Flooding Extent / Displacement

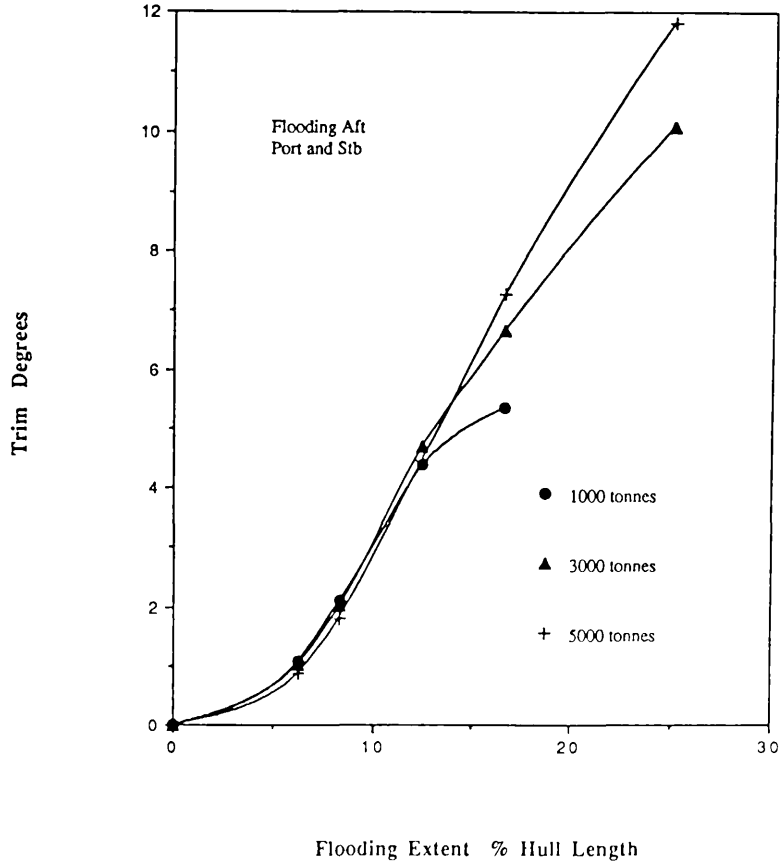

Fig 3.37 Trim / Flooding Extent / Design Displacement

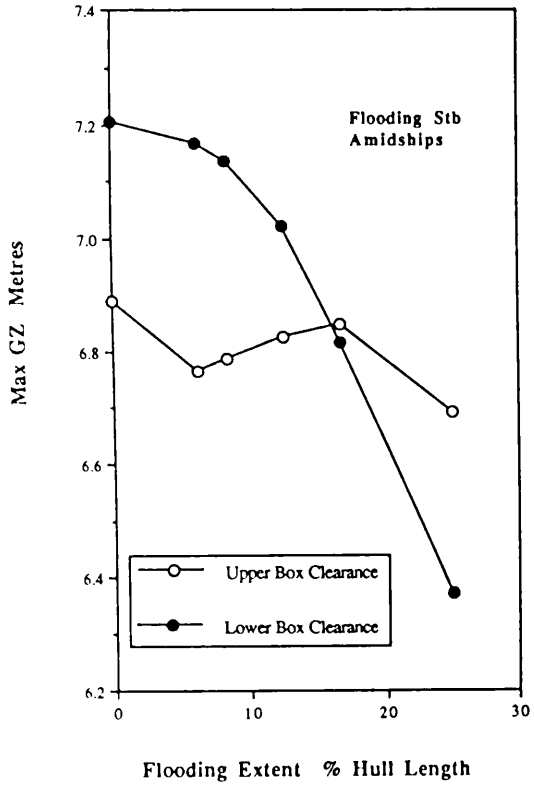

Fig 3.38 Max GZ / Box Clearance (1000t Design Displacement)

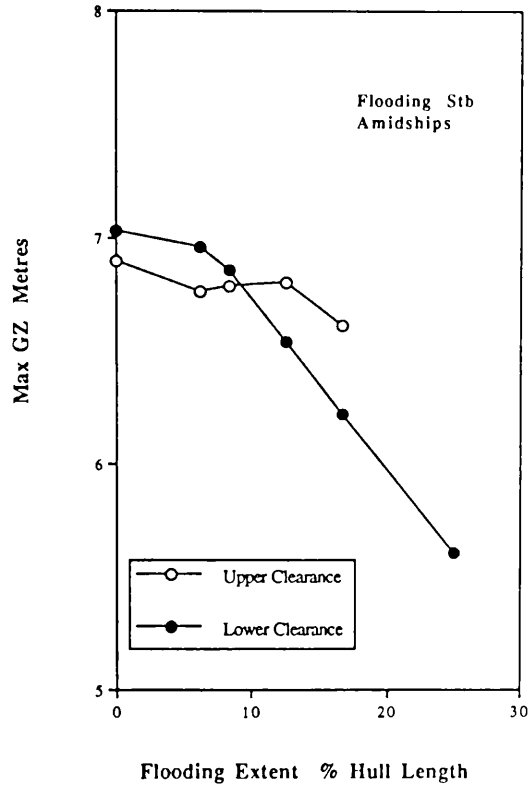

Fig 3.39 Max GZ / Box Clearance (2000t Design Displacement)

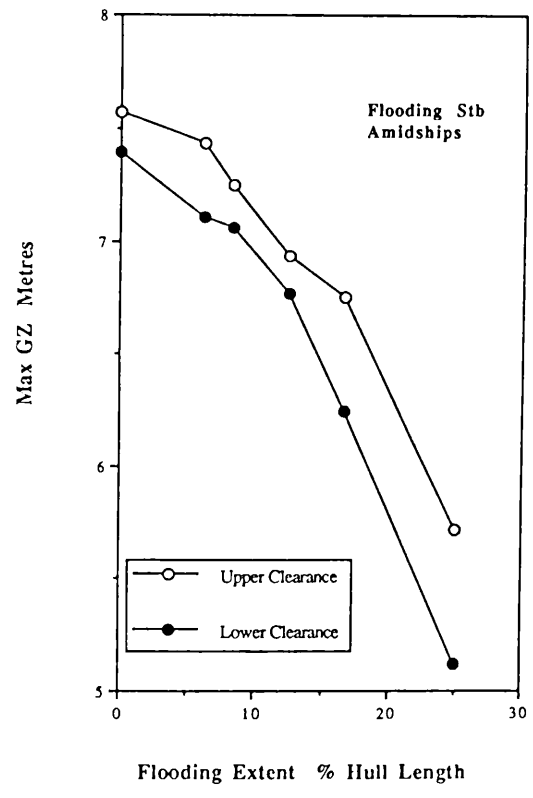

Fig 3.40 Max GZ / Box Clearance (3000t Design Displacement)

3.4.6 Summary and Survivability Considerations

It becomes immediately obvious that the size and shape of the vessel's haunches i.e. wet deck / strut interface, are of major importance to the way the vessel responds once damaged.

In the case of symmetrical flooding fore and aft it was discovered that stability actually increased with flooding. This is due to immersion of the haunch and wet deck induced by the trim. The resulting increase in waterplane area provides sufficient additional stability to counteract the negative influence of flooding.

Since asymmetric flooding in these locations leads to rapid loss of stability, development of fast counter flooding measures must assume a high priority for designers.

Whilst many of the trends observed in the results were intuitively anticipated their verification is not without value. Similarly the value of demonstrating probable post flooding magnitudes for heel, trim etc. should not be underestimated.

Some representative flooded stability results for a 4000 tonne SWATH ship are presented in Table 3.2. The values shown in this table confirm the excellent "survivability" of the SWATH concept while Fig 3.41 illustrates some damaged waterlines in an effort to demonstrate the physical significance of the values given.

HEEL Degrees

Flooding Extent	Port + Stb Aft	Port + Stb Fwd	Stb Only Aft	Stb Only Fwd	Stb Amidships
6.25%	0	0	0.665	1.636	9.74
8.33%	0	0	1.37	2.751	11.271
12.50%	0	0	3.75	5.344	14.412
16.66%	0	0	6.19	7.331	16.236
25%	0	0	10.71	11.508	20.309

TRIM Degrees

Flooding Extent	Port + Stb Aft	Port + Stb Fwd	Stb Only Aft	Stb Only Fwd	Stb Amidships
6.25%	0.946	2.183	0.475	1.087	0.049
8.33%	1.873	3.526	0.936	1.798	0.012
12.50%	4.527	6.432	2.485	3.551	-0.095
16.66%	6.911	8.481	4.132	4.899	-0.141
25%	10.826	12.39	6.17	7.167	-0.301

Max GZ Metres

Flooding Extent	Port + Stb Aft	Port + Stb Fwd	Stb Only Aft	Stb Only Fwd	Stb Amidships
6.25%	7.421	7.342	7.42	7.342	6.897
8.33%	7.434	7.295	7.434	7.294	6.633
12.50%	7.387	6.944	7.388	6.913	6.313
16.66%	6.86	6.27	6.825	6.199	5.741
25%	4.862	3.808	4.854	4.101	4.25

Table 3.2 Selected Flooded Stability Results for the 4000 tonne Testcase Vessel.

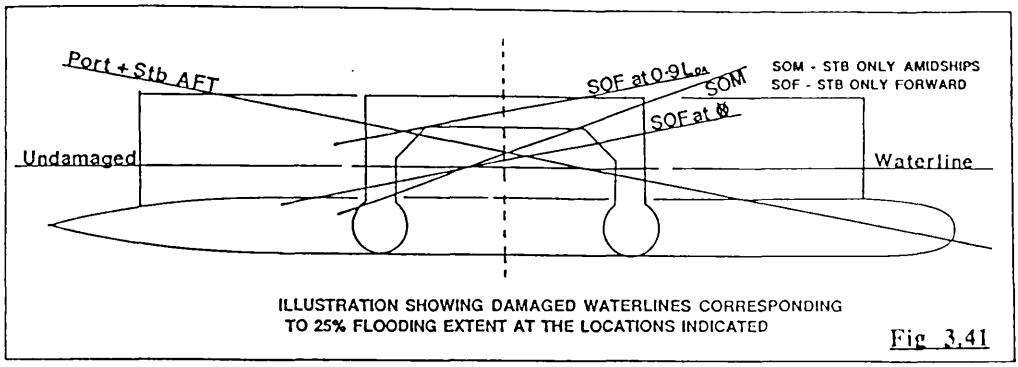

ILLUSTRATION SHOWING DAMAGED WATERLINES CORRESPONDING TO 25% FLOODING EXTENT AT THE LOCATIONS INDICATED

Fig 3.41

Current US Navy stability and buoyancy criteria for advanced marine vehicles (Ref 8) identify the principal constraints on SWATH survivability to be:-

1. Maximum initial heel after flooding of not more than 20 degrees
2. The main deck edge remains above water at all points

The vessel analysed was found to just exceed the first criteria for 25% flooding amidships. In addition the large trim caused by extreme flooding at the vessels ends was found to slightly immerse the main deck as illustrated in Fig 3.41. This immersion was however only slight and the results should perhaps be put in perspective by stating that they resulted from an extreme flooding condition :- 25% of the vessels length flooded with 95% permeability. Such a extreme condition is highly unlikely ever to occur in service.

It should be noted that the testcase vessel was a 'low' box clearance design. Equivalent flooding in a 'high' clearance design will result in greater initial heel but drier decks.

Based on this analysis it appears that the greatest threat to the survivability of a damaged SWATH vessel is damage to structure and superstructure caused by unforeseen green sea loads. Careful consideration should therefore be given to the possibility of these loads when designing SWATH vessels. Other logical priorities for designers in the field include the development of fast counter flooding techniques in an attempt to combat initial heel and trim.

Whilst the above results are valuable, undoubtedly the greatest benefit of the study stems from the provision of a large database of SWATH damage stability information. It is this database which subsequently allowed the construction of the Flooded Stability Estimation Program 'FSEP1'.

3.5 'FSEP1'- A Flooded Stability Estimation Program

3.5.1 Structure of 'FSEP1'

'FSEP1' is the first stage of a program which allows estimation of a SWATH vessel's flooded stability at the preliminary design stage. That is only basic geometry details are used in the evaluation.

The program requires the user to input for his design, operating displacement, wet deck/waterline clearance, location and extent of flooding as a percentage of vessel length.

Given this information 'FSEP1' will estimate the likely angles of heel and trim after flooding and produce probable values of Max GZ and the area under the GZ curve for the two regions 0-45 and 0-20 degrees.

Essentially 'FSEP1' relies on an iterative interpolation technique to produce results. The program searches an extensive database for values bounding the required input condition. Using the polynomial coefficients contained in this database the program calculates values for the bounding conditions and interpolates between these to find values for the design condition. This process is repeated in a 'nested' fashion until finally output is produced for the required input condition.

3.5.2 Validation of 'FSEP1'

Results from the program have been checked against actual flooded stability data at three levels :-

Level 1 - For the first stage of the validation process flooded stability calculations were performed for ship files which were already defined , that is using designs which were utilized in the construction of the 'FSEP1' database. This effectively fixed box clearance and limited operating displacement to within +/- 5% . Flooding extent was of course fully variable within the 0-25 % program range. Fourteen flooding combinations were evaluated at this level and the results compared with those from 'FSEP1'. These comparisons are presented in Tables 3.3 and 3.4.

Level 2 - The second level of validation again utilized existing ship definitions which this time were uniformly 'distorted' within the computer to give vessels of intermediate displacements whilst still retaining 'family' proportions for the main dimensions. This allowed investigation of larger changes in displacement whilst still retaining a relatively fixed box clearance (either an upper or a lower bound value). Eighteen flooding combinations were evaluated and the results compared with those from 'FSEP1' - Tables 3.5 - 3.7.

Level 3 - The existing ship definitions were distorted uniformly in the horizontal and longitudinal directions but not in the vertical. The influence of varying box clearance on the accuracy of 'FSEP1' 's predictions could then be assessed. At this level it is possible to investigate fairly large changes in all input parameters whilst still remaining loosely within the envelope of 'family' proportions. Twenty four flooding combinations were evaluated and the results compared with those from 'FSEP1' as shown in Table 3.8 - 3.10.

At the first level of validation the predictions made by the program match closely the values calculated by the commercial software. Maximum errors are 0.4 degrees for heel, 1.35 degrees for trim and 0.1 metres in the estimation of maximum GZ. Areas under the GZ curve were calculated to within 0.125 MetreRadians (m rad) in all cases. It should be noted that the maximum error of 1.35 degrees for trim is unrepresentative. The next largest trim error is 0.53 degrees.

Comparison of calculated and estimated values at the second level of validation show similar good agreement. Maximum errors experienced were 1.5 degrees in heel and 0.6 degrees in trim. Maximum GZ was estimated to within 0.45 metres in all cases and areas under the GZ curve were estimated to within 0.604 m rad. Once again it should be noted that the 0.604 m rad figure is unrepresentative - the next highest error being 0.204 m rad.

As expected the errors experienced at the third validation level were slightly larger. Maximum errors were however still only of the order of 2 degrees for both heel and trim values whilst the maximum error in predicting maximum GZ was 0.7 metres. Interestingly the estimates of area under the GZ curve show rather better agreement with calculated values than do those at the second validation level. This tends to reinforce the view that 0.604 m rad is unrepresentative of error at the second level validation.

The program appears to perform worst when estimating trim for flooding amidships. This shortfall is most likely due to poor representation of the interaction between the longitudinal centres of gravity and buoyancy.

Overall the figures produced are encouraging, however it must be remembered that all three validation levels utilized ships from the same 'family' of designs. Once outside the envelope of 'family' proportions it can be expected that the error figures will rise substantially. Despite this it is anticipated that with a little flexibility on the part of the user, the program will give meaningful results for vessels of geometry quite far removed from the 'family' tested here.

The program is sufficiently accurate for the intended preliminary design stage.

3.5.3 Extension of 'FSEP1'

With 'FSEP1' valuable foundations for a computer aided damage stability estimation tool have been laid. The program should be regarded as a first stage in the development of computer assisted damage stability estimation for SWATH vessels.

Since the value of the program is linked directly to the size of the database, further studies on the effect of beam, strut flare and internal subdivision would all be extremely beneficial. Extension of the program to consider such additional design information should be readily possible leading to the development of a sophisticated design tool. As previously noted a limited investigation into the effects of varying KG has already been undertaken. Results from this investigation may be applied directly to 'FSEP1' predictions, or they may be incorporated within the programs iterative loop structure. This has already been done to effectively create 'FSEP2' , however to date this second stage in the programs development remains unvalidated.

Expansion would best be tackled using commercial damage stability software mounted on a mainframe computer. Alternatively customized or tailor made software should be specially created to produce the required results quickly and easily.

DISPLACEMENT	BOX CLEARANCE	DMGE CONDITION	HEEL	TRIM	MAX GZ	∫ GZ 0-45	∫ GZ 0-20	
Tonnes	Metres		Degrees	Degrees	Metres	M Rad	M Rad	
975	3.4	20% Port +Stb Aft	0	7.607	6.696	3.043	0.529	CALCULATED
			0	8.139	6.661	3.013	0.51	"FSEP1"
			0	**-0.532**	**0.035**	**0.03**	**0.019**	DIFFERENCE
		20% Stb Midships	16.227	-0.056	6.85	2.443	0.052	CALCULATED
			16.338	-0.095	6.827	2.436	0.042	"FSEP1"
			-0.111	**0.039**	**0.023**	**0.007**	**0.01**	DIFFERENCE
1025	3.4	20% Port +Stb Aft	0	7.573	6.735	2.995	0.492	CALCULATED
			0	8.923	6.631	2.974	0.494	"FSEP1"
			0	**-1.35**	**0.104**	**0.021**	**-0.002**	DIFFERENCE
		20% Stb Midships	16.175	-0.217	6.84	2.402	0.047	CALCULATED
			15.982	-0.285	6.802	2.408	0.148	"FSEP1"
			0.193	**0.068**	**0.038**	**-0.006**	**-0.101**	DIFFERENCE
2925	3.17	10% Stb Midships	11.937	0.072	---	---	---	CALCULATED
			12.338	0.07	6.99	2.594	0.114	"FSEP1"
			-0.401	**0.002**	**---**	**---**	**---**	DIFFERENCE
		10% Stb Only Fwd	3.944	-2.573	7.383	2.963	0.284	CALCULATED
			3.7	-2.489	7.325	3.088	0.285	"FSEP1"
			0.244	**-0.084**	**0.058**	**-0.125**	**-0.001**	DIFFERENCE
		10% Port +Stb Fwd	0	-4.911	7.39	3.062	0.368	CALCULATED
			0	-4.506	7.34	3.055	0.372	"FSEP1"
			0	**-0.405**	**0.05**	**0.007**	**-0.004**	DIFFERENCE

Table 3.3 Level 1 Validation for "FSEP1" Program

DISPLACEMENT	BOX CLEARANCE	DMGE CONDITION	HEEL	TRIM	MAX GZ	∫GZ 0-45	∫GZ 0-20	
Tonnes	Metres		Degrees	Degrees	Metres	M Rad	M Rad	
3075	3.17	10% Stb Midships	11.625	-0.056	---	---	---	CALCULATED
			11.902	-0.05	6.804	2.488	0.102	"FSEP1"
			-0.277	**-0.006**	---	---	---	DIFFERENCE
		10% Stb Only Fwd	3.718	-2.409	7.137	---	---	CALCULATED
			3.67	-2.448	7.124	2.856	0.253	"FSEP1"
			0.048	**0.039**	**0.013**	---	---	DIFFERENCE
		10% Port +Stb Fwd	0	-4.463	7.137	---	---	CALCULATED
			0	-4.469	7.139	2.964	0.341	"FSEP1"
			0	**0.006**	**-0.002**	---	---	DIFFERENCE
4875	3.88	4% Port +Stb Aft	0	0.285	7.571	2.76	0.238	CALCULATED
			0	0.062	7.61	2.749	0.22	"FSEP1"
			0	**0.223**	**-0.039**	**0.011**	**0.018**	DIFFERENCE
		4% Stb Only Fwd	0.656	-0.494	7.548	2.743	0.227	CALCULATED
			0.763	-0.543	7.629	2.716	0.216	"FSEP1"
			-0.107	**0.049**	**-0.081**	**0.027**	**0.011**	DIFFERENCE
5125	3.88	4% Port +Stb Aft	0	0.298	7.591	2.624	0.194	CALCULATED
			0	-0.004	7.569	2.623	0.188	"FSEP1"
			0	**0.302**	**0.022**	**0.001**	**0.006**	DIFFERENCE
		4% Stb Only Fwd	0.708	-0.492	7.582	2.606	0.185	CALCULATED
			0.714	-0.485	7.565	2.608	0.185	"FSEP1"
			-0.006	**-0.007**	**0.017**	**-0.002**	**0**	DIFFERENCE

Table 3.4 Level 1 Validation for "FSEP1" Program

DISPLACEMENT	BOX CLEARANCE	DMGE CONDITION	HEEL	TRIM	MAX GZ	∫ GZ 0-45	∫ GZ 0-20	
Tonnes	Metres		Degrees	Degrees	Metres	M Rad	M Rad	
2400	4.567 ACTUAL 4.27 USED	19% Stb Only Aft	5.945	4.184	6.796	2.661	0.233	CALCULATED
			7.462	4.801	6.762	2.487	0.154	"FSEP1"
			-1.517	**-0.617**	**0.034**	**0.174**	**0.079**	DIFFERENCE
		19% Stb Midships	18.04	0.177	6.544	2.094	0.014	CALCULATED
			17.78	-0.06	6.24	1.981	0.013	"FSEP1"
			0.26	**0.237**	**0.304**	**0.113**	**0.001**	DIFFERENCE
2500	4.567 ACTUAL 4.27 USED	19% Stb Only Aft	6.735	4.579	6.739	2.568	0.195	CALCULATED
			7.449	4.839	6.809	2.52	0.163	"FSEP1"
			-0.714	**-0.26**	**-0.07**	**0.048**	**0.032**	DIFFERENCE
		19% Stb Midships	18.535	0.088	6.466	1.992	0.009	CALCULATED
			17.855	-0.039	6.321	1.994	0.012	"FSEP1"
			0.68	**0.127**	**0.145**	**-0.002**	**-0.003**	DIFFERENCE
2600	4.567 ACTUAL 4.27 USED	19% Stb Only Aft	7.357	4.887	6.656	2.482	0.168	CALCULATED
			7.435	4.878	6.857	2.554	0.772	"FSEP1"
			-0.078	**0.009**	**-0.201**	**-0.072**	**-0.604**	DIFFERENCE
		19% Stb Midships	18.865	0.002	6.297	1.888	0.006	CALCULATED
			17.931	-0.019	6.403	2.007	0.002	"FSEP1"
			0.934	**0.021**	**-0.106**	**-0.119**	**0.004**	DIFFERENCE
3350	3.356 ACTUAL 3.48 USED	11% Stb Only Fwd	3.169	-2.447	7.291	3.022	0.339	CALCULATED
			4.125	-2.803	7.107	2.781	0.226	"FSEP1"
			-0.956	**0.356**	**0.184**	**0.241**	**0.113**	DIFFERENCE
		11% Stb Midships	12.084	0.213	7.128	2.588	0.12	CALCULATED
			13.074	-0.047	6.693	2.357	0.074	"FSEP1"
			-0.99	**0.26**	**0.435**	**0.231**	**0.046**	DIFFERENCE

Table 3.5 Level 2 Validation for "FSEP1" Program

DISPLACEMENT	BOX CLEARANCE	DMGE CONDITION	HEEL	TRIM	MAX GZ	∫ GZ 0-45	∫ GZ 0-20	
Tonnes	Metres		Degrees	Degrees	Metres	M Rad	M Rad	
3500	3.356 ACTUAL 3.48 USED	11% Stb Only Fwd	3.799	-2.705	7.2	2.914	0.285	CALCULATED
			4.075	-2.782	7.152	2.802	0.232	"FSEP1"
			-0.276	**0.077**	**0.048**	**0.112**	**0.053**	DIFFERENCE
		11% Stb Midships	12.611	0.119	6.85	2.471	0.094	CALCULATED
			13.303	-0.011	6.738	2.369	0.072	"FSEP1"
			-0.692	**0.13**	**0.112**	**0.102**	**0.022**	DIFFERENCE
3650	3.356 ACTUAL 3.48 USED	11% Stb Only Fwd	4.167	-2.813	7.093	2.811	0.247	CALCULATED
			4.024	-2.761	7.196	2.823	0.237	"FSEP1"
			0.143	**-0.052**	**-0.103**	**-0.012**	**0.01**	DIFFERENCE
		11% Stb Midships	12.746	0.024	6.493	2.355	0.08	CALCULATED
			13.531	0.026	6.784	2.381	0.07	"FSEP1"
			-0.785	**-0.002**	**-0.291**	**-0.026**	**0.01**	DIFFERENCE
4350	3.703 ACTUAL 3.88 USED	15% Stb Only Aft	5.736	3.672	7.405	2.753	0.194	CALCULATED
			5.122	3.346	6.951	2.581	0.184	"FSEP1"
			0.614	**0.326**	**0.454**	**0.172**	**0.01**	DIFFERENCE
		15% Stb Only Fwd	6.756	-4.411	6.819	2.594	0.178	CALCULATED
			6.451	-4.327	6.483	2.443	0.187	"FSEP1"
			0.305	**-0.084**	**0.336**	**0.151**	**-0.009**	DIFFERENCE

Table 3.6 Level 2 Validation for "FSEP1" Program

DISPLACEMENT	BOX CLEARANCE	DMGE CONDITION	HEEL	TRIM	MAX GZ	∫ GZ 0-45	∫ GZ 0-20	
Tonnes	Metres		Degrees	Degrees	Metres	M Rad	M Rad	
4500	3.703 ACTUAL 3.88 USED	15% Stb Only Aft	5.677	3.593	7.213	2.672	0.178	CALCULATED
			5.148	3.382	7.0761	2.644	0.194	"FSEP1"
			0.529	**0.211**	**0.1369**	**0.028**	**-0.016**	DIFFERENCE
		15% Stb Only Fwd	6.989	-4.515	6.629	2.504	0.166	CALCULATED
			6.191	-4.229	6.639	2.523	0.193	"FSEP1"
			0.798	**-0.286**	**-0.01**	**-0.019**	**-0.027**	DIFFERENCE
4650	3.703 ACTUAL 3.88 USED	15% Stb Only Aft	5.35	3.367	6.968	2.593	0.17	CALCULATED
			5.173	3.417	7.191	2.706	0.205	"FSEP1"
			0.177	**-0.05**	**-0.223**	**-0.113**	**-0.035**	DIFFERENCE
		15% Stb Only Fwd	6.945	-4.465	6.423	2.42	0.159	CALCULATED
			5.931	-4.132	6.795	2.603	0.2	"FSEP1"
			1.014	**-0.333**	**-0.372**	**-0.183**	**-0.041**	DIFFERENCE

Table 3.7 Level 2 Validation for "FSEP1" Program

DISPLACEMENT	BOX CLEARANCE	DMGE CONDITION	HEEL	TRIM	MAX GZ	∫ GZ 0-45	∫ GZ 0-20	
Tonnes	Metres		Degrees	Degrees	Metres	M Rad	M Rad	
2400	4.028	18% Stb Only Aft	5.89	4.152	6.826	2.7	0.233	CALCULATED
			6.695	4.338	6.843	2.563	0.179	"FSEP1"
			-0.805	**-0.186**	**-0.017**	**0.137**	**0.054**	DIFFERENCE
		18% Stb Midships	17.005	0.108	6.454	2.134	0.022	CALCULATED
			16.959	-0.08	6.346	2.051	0.198	"FSEP1"
			0.046	**0.188**	**0.108**	**0.083**	**-0.176**	DIFFERENCE
2500	4.028	18% Stb Only Aft	6.448	4.461	6.76	2.612	0.202	CALCULATED
			6.714	4.392	6.897	2.598	0.187	"FSEP1"
			-0.266	**0.069**	**-0.137**	**0.014**	**0.015**	DIFFERENCE
		18% Stb Midships	17.212	-0.236	6.18	2.031	0.018	CALCULATED
			17.032	-0.056	6.422	2.067	0.019	"FSEP1"
			0.18	**-0.18**	**-0.242**	**-0.036**	**-0.001**	DIFFERENCE
2600	4.028	18% Stb Only Aft	6.76	4.659	6.666	2.53	0.18	CALCULATED
			6.732	4.446	6.951	2.632	0.195	"FSEP1"
			0.028	**0.213**	**-0.285**	**-0.102**	**-0.015**	DIFFERENCE
		18% Stb Midships	17.175	-0.072	5.997	1.925	0.016	CALCULATED
			17.106	-0.031	6.498	2.083	0.018	"FSEP1"
			0.069	**-0.041**	**-0.501**	**-0.158**	**-0.002**	DIFFERENCE
2400	3.489	18% Stb Only Aft	5.998	4.325	6.66	2.687	0.232	CALCULATED
			6.273	4.073	6.806	2.625	0.207	"FSEP1"
			-0.275	**0.252**	**-0.146**	**0.062**	**0.025**	DIFFERENCE
		18% Stb Midships	16.247	-0.007	6.131	2.107	0.028	CALCULATED
			15.803	-0.149	6.283	2.114	0.032	"FSEP1"
			0.444	**0.142**	**-0.152**	**-0.007**	**-0.004**	DIFFERENCE

Table 3.8 Level 3 Validation for "FSEP1" Program

DISPLACEMENT	BOX CLEARANCE	DMGE CONDITION	HEEL	TRIM	MAX GZ	∫ GZ 0-45	∫ GZ 0-20	
Tonnes	*Metres*		Degrees	Degrees	Metres	M Rad	M Rad	
2500	3.489	18% Stb Only Aft	6.213	4.49	6.563	2.601	0.209	CALCULATED
			6.349	4.168	6.853	2.657	0.213	"FSEP1"
			-0.136	**0.322**	**-0.29**	**-0.056**	**-0.004**	DIFFERENCE
		18% Stb Midships	16.14	-0.091	5.781	1.991	0.025	CALCULATED
			15.923	-0.122	6.364	2.13	0.03	"FSEP1"
			0.217	**0.031**	**-0.583**	**-0.139**	**-0.005**	DIFFERENCE
2600	3.489	18% Stb Only Aft	6.042	4.404	6.444	2.521	0.195	CALCULATED
			6.425	4.264	6.899	2.69	0.219	"FSEP1"
			-0.383	**0.14**	**-0.455**	**-0.169**	**-0.024**	DIFFERENCE
		18% Stb Midships	15.773	-0.17	5.545	1.874	0.024	CALCULATED
			16.044	-0.094	6.445	2.146	0.028	"FSEP1"
			-0.271	**-0.076**	**-0.9**	**-0.272**	**-0.004**	DIFFERENCE
3350	4.577	13% Stb Midships	12.465	0.229	7.425	2.534	0.091	CALCULATED
			10.222	0.021	6.731	2.111	0.025	"FSEP1"
			2.243	**0.208**	**0.694**	**0.423**	**0.066**	DIFFERENCE
		13% Port+Stb Fwd	0	-4.823	7.364	3.187	0.514	CALCULATED
			0	-6.807	7.11	2.804	0.326	"FSEP1"
			0	**1.984**	**0.254**	**0.383**	**0.188**	DIFFERENCE
3500	4.577	13% Stb Midships	14.312	0.222	7.13	2.414	0.052	CALCULATED
			16.252	0.06	6.784	2.123	0.025	"FSEP1"
			-1.94	**0.162**	**0.346**	**0.291**	**0.027**	DIFFERENCE
		13% Port+Stb Fwd	0	-5.505	7.348	3.073	0.446	CALCULATED
			0	-6.71	7.13	2.828	0.337	"FSEP1"
			0	**1.205**	**0.218**	**0.245**	**0.109**	DIFFERENCE

Table 3.9 **Level 3 Validation for "FSEP1" Program**

DISPLACEMENT	BOX CLEARANCE	DMGE CONDITION	HEEL	TRIM	MAX GZ	∫ GZ 0-45	∫ GZ 0-20	
Tonnes	Metres		Degrees	Degrees	Metres	M Rad	M Rad	
3600	4.577	13% Stb Midships	15.387	0.162	6.944	2.305	0.034	CALCULATED
			16.272	0.085	6.818	2.131	0.026	"FSEP1"
			-0.885	**0.077**	**0.126**	**0.174**	**0.008**	DIFFERENCE
		13% Port+Stb Fwd	0	-6.139	7.279	2.971	0.395	CALCULATED
			0	-6.614	7.151	2.852	0.348	"FSEP1"
			0	**0.475**	**0.128**	**0.119**	**0.047**	DIFFERENCE
3350	3.967	13% Stb Midships	13.312	0.225	7.238	2.512	0.081	CALCULATED
			15.097	-0.045	6.596	2.183	0.041	"FSEP1"
			-1.785	**0.27**	**0.642**	**0.329**	**0.04**	DIFFERENCE
		13% Port+Stb Fwd	0	-5.302	7.27	3.152	0.479	CALCULATED
			0	-6.534	7.036	2.862	0.351	"FSEP1"
			0	**1.232**	**0.234**	**0.29**	**0.128**	DIFFERENCE
3500	3.967	13% Stb Midships	14.557	0.155	6.915	2.39	0.05	CALCULATED
			15.232	-0.006	6.644	2.194	0.04	"FSEP1"
			-0.675	**0.161**	**0.271**	**0.196**	**0.01**	DIFFERENCE
		13% Port+Stb Fwd	0	-5.194	7.217	3.045	0.424	CALCULATED
			0	-6.468	7.071	2.883	0.358	"FSEP1"
			0	**1.274**	**0.146**	**0.162**	**0.066**	DIFFERENCE
3600	3.967	13% Stb Midships	15.207	0.077	6.648	2.277	0.037	CALCULATED
			15.366	0.033	6.692	2.204	0.039	"FSEP1"
			-0.159	**0.044**	**-0.044**	**0.073**	**-0.002**	DIFFERENCE
		13% Port+Stb Fwd	0	-6.375	7.112	2.946	0.384	CALCULATED
			0	-6.403	7.105	2.904	0.366	"FSEP1"
			0	**0.028**	**0.007**	**0.042**	**0.018**	DIFFERENCE

Table 3.10 Level 3 Validation for "FSEP1" Program

3.6 Conclusions

The project aimed to establish links between survivability and vessel geometry and to utilize this information by constructing a program to estimate damage stability using only preliminary design information.

Through an extensive parametric study, the damaged stability characteristics of SWATH vessels have been investigated. Complete damage stability calculations have been performed for 900 combinations of initial ship condition and flooding scenario.

Results from these calculations have been processed and analysed exhaustively. The data obtained illustrates the dominance of cross structure effects on SWATH damage stability. Overall the results confirmed what was intuitively expected, initial flooding leads to rapid heeling/triming which eases upon the immersion of the cross deck structure and the subsequent massive rise in waterplane area and hence stability. From the data collected to date it appears that SWATH vessels possess acceptable damaged stability characteristics, and indeed survivability which is likely to be ultimately superior to that of an equivalent monohull. It should be noted that the maximum angle of heel attained by the testcase vessel was only fractionally greater than 20 degrees. This corresponded to asymmetric flooding amidships of extent equal to 25 % of the vessels length. Clearly this is an extreme damage condition and one which very few conventional monohull vessels could hope to survive.

Using the database created, a program has been developed which allows the user to estimate at the preliminary design stage, a vessels ability to survive in the event of it sustaining damage leading to partial flooding. This program has been validated, using flooded stability results calculated using commercial software, for a variety of combinations of design parameter.

In addition a limited investigation into the effects of varying the height of the vessels centre of gravity has been performed. Results from this investigation have been incorporated in the above program.

This project was intended to provide the foundations for a computer augmented damage stability estimation tool for SWATH vessels. With the creation and validation of 'FSEP1' and 'FSEP2' this aim has been accomplished.

References to Chapter 3

1. Betts, C.V., 'A Review of Developments in SWATH Technology', Proceedings Second International Conference on SWATH Ships and Advanced Multi-Hulled Vessels, RINA, London, November, 1988.

2. Papanikolaou, A., Zaraphonitis, G., Koskinas, C. and Savvas, J., 'On the Stability of a SWATH Ferry in Calm Water and in Waves', Proceedings of STAB'90 - the Fourth International Conference on the Stability of Ships and Ocean Vehicles,Naples,September,1990.

3. Nehrling, B.C., 'An Experimental Investigation into the Stability and Motions of a Damaged SWATH Model', Proceedings of STAB'90 - the Fourth International Conference on the Stability of Ships and Ocean Vehicles , Naples, September, 1990.

4. Miller, A.F., 'Aspects of Damaged Stability in the Computer Augmented Design Process for SWATH Vessels', Proceedings of STAB'90 - the Fourth International Conference on the Stability of Ships and Ocean Vehicles , Naples, September, 1990.

5. Goldberg, L.L. and Tucker, R.G., 'Current Status of U.S. Navy Stability and Buoyancy Criteria for Advanced Marine Vehicles', Proceedings AIAA/SNAME Advanced Marine Vehicles Conference, San Diego, California, February, 1974.

6. Goldberg, L.L. and Tucker, R.G.., 'Stability and Bouyancy Criteria for Low Waterplane Catamarans', Proceedings Society of Aeronautical Weight Engineers, May, 1972.

7. MacGregor, J.R., 'A Computer Aided Method for Preliminary Design of SWATH Ships', Ph.D. Thesis, Glasgow University, May, 1989.

8. MacGregor, J.R., Simpson, R.R. and Norton, P., 'Parametric Studies in the Design of SWATH Ships', Proceedings AIAA Intersociety Advanced Marine Vehicles Conference, Washington, June, 1989.

9. Lamb, G.R., 'Some Guidance for Hull Form Selection for SWATH Ships', Marine Technology, vol. 25 no. 4, SNAME, October, 1988.

CHAPTER 4

MANOEUVRING

4.1 Introduction

Since the advent of the Small Waterplane Area Twin Hull concept, considerable effort has been directed towards improving our understanding of the hydrodynamic forces and moments acting upon such hullforms. Since the primary reason for the very existence of SWATH ships is their excellent seakeeping performance, it is perhaps not surprising that most of this effort has been aimed at predicting and quantifying ship motions in a seaway. Many thousands of hours of research and computational time have been spent developing and continuously refining mathematical tools aimed at the prediction and evaluation of SWATH seakeeping and hydrodynamic loading.

In contrast relatively little effort has been devoted to the study, prediction and control of SWATH ship motion in the horizontal plane; i.e. their manoeuvring characteristics.

4.2 Aims and Objectives

The objectives for this phase of the project were threefold :-

1. To provide a greater understanding of the manoeuvring characteristics of Small Waterplane Area Twin Hull vessels.

2. To develop a tool to assist in the preliminary design of rudder area and location for SWATH vessels in order to to ensure adequate turning performance.

3. To extend the database of manoeuvring information available, and provide some limited validation of the above tool, by the collection of full scale manoeuvring data using the 20 tonne SWATH fishing vessel "Ali" (Ref 1).

4.3 Outline of Approach Adopted for the Study

In order to meet the study objectives the following workplan was devised : -

1. A comprehensive survey of all existing available literature on SWATH manoeuvring.

2. A review of currently accepted monohull manoeuvring theory.

3. The creation of a FORTRAN computer program incorporating algorithms based on adaptations of accepted monohull theory.

4. Full Scale Trials on the SWATH fishing vessel "Ali"

4.4 Literature Review

4.4.1 General SWATH Manoeuvring Considerations

The bulk of available literature (Ref 2-10) originates from the David Taylor Naval Ship Research and Development Centre and largely concerns model tests performed on rotating arm devices. These experiments were performed to calculate hydrodynamic force and moment derivatives for vessels in a large number of combinations of initial ship condition and rudder configuration. It is anticipated that the resulting database will allow construction of a manoeuvring simulation tool for SWATH vessels. The DTNSRDC simulation tool is however as yet unfinished, or at least generally unavailable.

Very little full scale operational information is available (Ref 11-14) at present although it is hoped this situation will alter as the number of SWATH vessels in service worldwide increases over the next few years. Study of published information, although limited, nonetheless allows several interesting conclusions to be drawn.

SWATH vessels are by nature of their geometry inherently directionally stable. The centroid of the projected area of the struts is generally aft of the centre of gravity of the vessel, it therefore takes a large side force to initiate a turn at speed. Consequently larger rudders and heavier steering gear must be employed than on equivalent monohulls. However directional stability is an advantage for missions requiring a

steady course, particularly in oblique seas. It is especially advantageous if towing a sonar array since the signals from the array will be less confused and thus easier to interpret. Due to this inherent directional stability and the problem of rudder location on SWATH vessels, close attention must be paid to the design of the steering mechanism in order to ensure that the ship possesses adequate turning performance.

Fein (Ref 3) states that there is no inherent advantage in single or twin struts for manoeuvring, it is merely the size and location of rudders that determine the turning ability of SWATH vessels.

The SWATH form presents a number of unique problems when it comes to siting rudders and steering gear. Naturally this has led to the development of several innovative configurations for control surfaces. These are covered in Section 4.4.2.

Due to the transverse separation of propellers, low speed manoeuvrability on SWATH ships using differential thrust is excellent. It is noted that S.S.P. Kaimalino turns within her own length at very low speeds (Ref 3). Vessels equipped with bow thrusters should be able to turn on the spot. The possibility exists of providing exceptional stationkeeping or docking performance using bow thrusters linked to differential thrust from controllable pitch propellers under active automatic control. Controllable pitch propellers and/or electric transmission is recommended for applications requiring good low speed manoeuvring. With fixed pitch propellers and a conventional drivetrain, unacceptable strains would be placed on gearboxes due to the constant forward/reverse shifts that would be required.

At higher speeds turning performance may be improved by employing canards to bank the vessel into the turn. The resulting asymmetric drag created, results in sharper turns. S.S.P. Kaimalino has reported reductions in tactical diameter of the order of 20 % using this method. Similarly deployment of a retractable "turning foil" has been found to yield benefits. Not surprisingly trim also has an important effect on turning performance particularly on designs with surface piercing rudders.

Turning performance is dependent on speed. At 23 knots the tactical diameter of the S.S.C. Seagull was found to be twice that at 13 knots (Ref 13). This is due to flow patterns along the hull varying considerably with Froude Number. Tank tests (Ref 8) reveal that the manoeuvring derivatives are less speed dependent for a long strut design (SWATH6E) than for the short strut SWATH 6A. Consequently the turning radius of SWATH6E was found not to vary with speed.

With careful design of the control surfaces, turning performance of SWATH ships can be made comparable to that of equivalent monohulls. The often quoted ratio of tactical diameter / ship length is misleading for comparison purposes, since the length of an "equivalent" SWATH is less than its monohull counterpart.

4.4.2 Rudder Configurations

SWATH hullforms present the naval architect with several options when designing control surfaces. Unlike conventional monohull ships several possibilities exist for both the location and type of control surface used to manoeuver and stabilize the vessel.

Traditionally in monohulls the rudder(s) is / are placed right aft, usually directly behind the propeller(s). In this location the rudder exerts maximum turning moment for a given force due to its distance aft of the LCG . The turning force exerted by the rudder is further increased by the increase in flow velocity induced by the propeller(s). This increased flow velocity is particularly important at low speed and when trying to manoeuver from stationary, since without flow there can be no sideforce generated by the hull or rudder. Combined with the presence of suitable otherwise unusable space in the stern directly above for siting steering gear, this location then provides an ideal and hence almost universal solution to the problem for monohulls.

For SWATH ships the answer is not so simple. The same considerations apply, however the lack of suitable protected mounting positions for the rudders, coupled with the problem of locating steering gear, has resulted in a number of innovative solutions.

With "long" strut designs, i.e. designs where the strut length equals or overhangs the lower hull aft, a traditional solution with rudder behind the propeller and steering gear housed in the hull and strut is normal. For "short" strut designs the obvious arrangement is to incorporate the rudder into the trailing edge of the strut. However this solution produces low turning efficiency and necessitates a much larger (by virtue of its location unbalanced) rudder requiring larger and heavier steering gear. Without propeller induced flow over the rudder this arrangement also suffers in its ability to manoeuver at zero speed.

Without accurate prediction and simulation techniques, proper comparison of the relative performance of these variants must inevitably come from extensive / expensive model tests and to a lesser degree from full scale experiences. Engineers at the DTNSRDC performed several such experiments during the late 1970's Ref 2-10.

The following briefly describes the most common steering arrangements for SWATH vessels together with the advantages and disadvantages associated with each. The basic configurations are illustrated in Fig 4.1.

Strut Rudder

As the name suggests this type of rudder (described above) forms part of the strut of the ship. A movable section is incorporated into the trailing edge of the struts controlled by steering gear in the cross deck or in the struts themselves. This is the simplest solution and therefore the cheapest. This solution also adds least drag to the vessel. Unfortunately the configuration is ineffective at both low and high speeds, since at low speeds there is no benefit gained from the locally increased flow velocity due to propellers, and at high Froude No's the waterline dips towards the stern of the vessel, reducing wetted-effective rudder area. Consequently greatly increased rudder areas are required to ensure adequate turning performance. Since by the nature of the configuration, it is impossible to balance strut rudders, very large powerful steering gear is required with attendant cost and weight penalties.

Extended Strut Rudder Aft Propeller

Following traditional (monohull) practice this is the most common arrangement for long strut designs. The flow induced by the propeller increases effectiveness and allows a relatively small rudder to provide adequate turning and directional control. For short strut designs however this is not a practical answer since the provision of a "strut extension" to carry the rudder would increase drag and cost unacceptably. The problem of rudder protection should also be addressed for ships utilizing this configuration. The turning diameter is approximately 30% less for configurations with the rudder behind the screw, and speed loss in the turn is greater but the same turning diameter is achieved for a smaller rudder deflection, therefore the speed loss effect is counteracted.

(Surface Piercing) Spade Rudder Forward of Propeller

This type of rudder is a combination of the two configurations described above. It offers a compromise for "short strut" vessels where the provision of a rudder behind the propeller is not practical. The rudder is located above the hull just forward of the propellers to take advantage of the accelerated flow induced by the screws. The steering gear must be located in the lower hulls which produces access problems, however since these rudders can be balanced, unlike strut mounted types, this steering gear may be of minimum dimensions. If required the rudder may be surface piercing, allowing the possibility of providing additional lateral support above the waterline.

In model tests the configuration was found to provide adequate turning performance for reasonable rudder areas. In the case of surface piercing variants effectiveness was found to decrease with speed as for strut rudders. Locating the rudder forward of the screw obviously degrades the flow into the propeller. At best this will result in slightly worse propulsive efficiency, however in some model tests rudder ventilation occurred for helm angles greater than 25 degrees. If frequent use of extreme helm is anticipated, then consideration should be given to the provision of diesel electric propulsion since conventional drivetrains will be adversely affected by the fluctuating forces created.

Canards

These closely resemble a cross between conventional ships rudders and fin stabilizers. This is perhaps not surprising since this is exactly the role they are designed to fulfil. Generally mounted inboard of the twin hulls in clear protected water at the stern of the ship, they provide combined control of vertical and horizontal motion.

Since only one set of fins are required the designer saves ship drag and weight. Against these savings must be set the additional complexity and cost of the control system required. Further, in the event of a breakdown of this system independent manual control of vertical and horizontal motion may not be possible. The configuration also suffers from interaction between roll, sway and yaw at low encounter frequencies, this is particularly noticeable in following seas. Otherwise the configuration resembles and shares the same pros and cons as the non surface piercing variant of the spade rudder described above.

Turning Foil

This is perhaps the most novel approach to the problem. The device consists of a vertical foil normally housed in a trunk in the forward hull/strut. When a turn is required the foil is lowered/hinged into position beneath the hull which is on the inside of the desired turn. The increased drag produced by the foil acts with the created sideforce to yaw the vessel into the turn.

The device is primarily intended to assist turns initiated by other methods. It cannot be the sole manoeuvring device aboard a ship since it cannot be used in shallow or confined waters. It does however have several interesting features including the cancellation of side forces created by conventional aft rudders which push the ship sideways out the turn when helm is first applied.

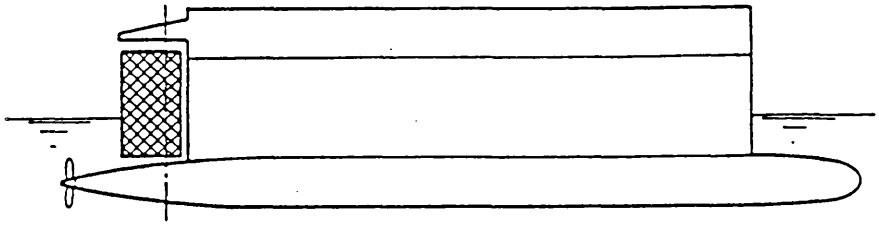

Strut Rudder

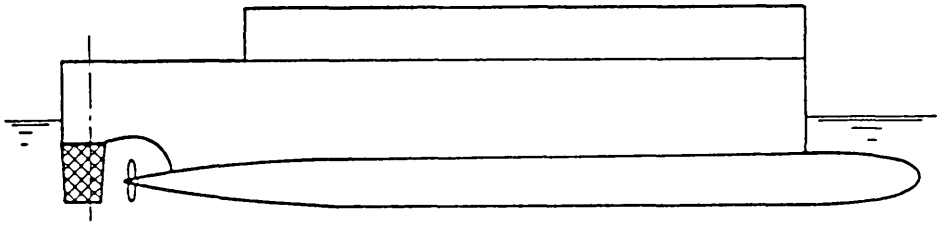

Extended Strut Rudder Aft Propeller

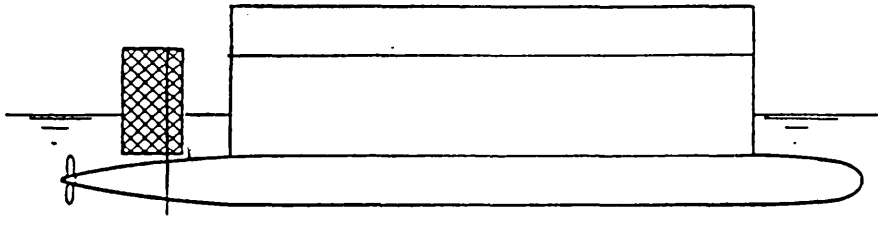

Surface Piercing Spade Rudder Fwd of Propeller

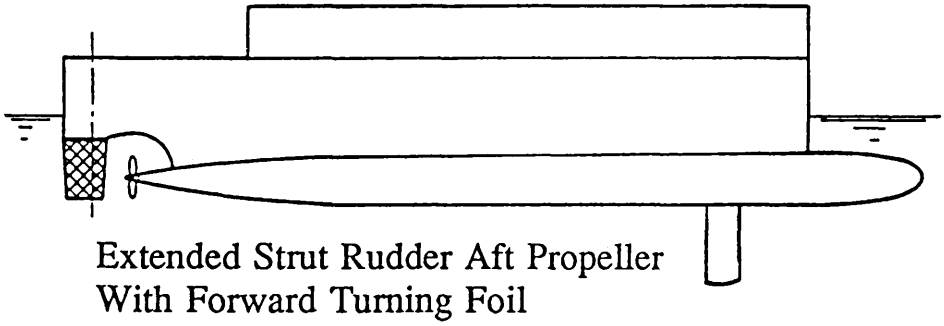

Extended Strut Rudder Aft Propeller
With Forward Turning Foil

Fig 4.1 Rudder Configurations Applicable to SWATH Vessels

4.5 Manoeuvring Theory

SWATHMAN is based upon manoeuvring theory developed for monohull vessels. Much of this theory is founded upon linear approximations and semi-empirical expressions developed from analysis of experimental data. It is anticipated that the symmetrical nature of SWATH geometry will readily lend itself to study utilizing theory developed in this way. It is therefore fully expected that calculations based upon this theory will be equally valid for SWATH vessels as for those of monohull form.

4.5.1 Mathematical Modelling

In this analysis the ship is considered to be a rigid body, with only three degrees of freedom in surge, sway and yaw. Ship motions in the other degrees of freedom, roll, pitch and heave are neglected. It is convenient to describe the motion in terms of a Eulerian system of axes coincident with amidships. This co-ordinate system is illustrated in Fig 4.2 together with the basic nomenclature used.

Thus the equations of motion are :-

$$X = m\left(\dot{u} - rv - x_G r^2\right)$$
$$Y = m\left(\dot{v} + ur + x_G \dot{r}\right)$$
$$N = I_z \dot{r} + mx_G(\dot{v} + ru)$$

(Eqn 4.1)

The terms on the right hand side are the inertial responses whilst those on the left are the hydrodynamic forces and moments acting on the ship.

The hydrodynamic forces and moments, X,Y and N acting on the ship due to motions in the three degrees of freedom surge, sway and yaw are usually expressed as perturbations about a steady ahead speed. The hydrodynamic forces and moments are then assumed to be directly proportional to these perturbation quantities. This procedure and its limitations are more fully described in Ref 15 and 16.

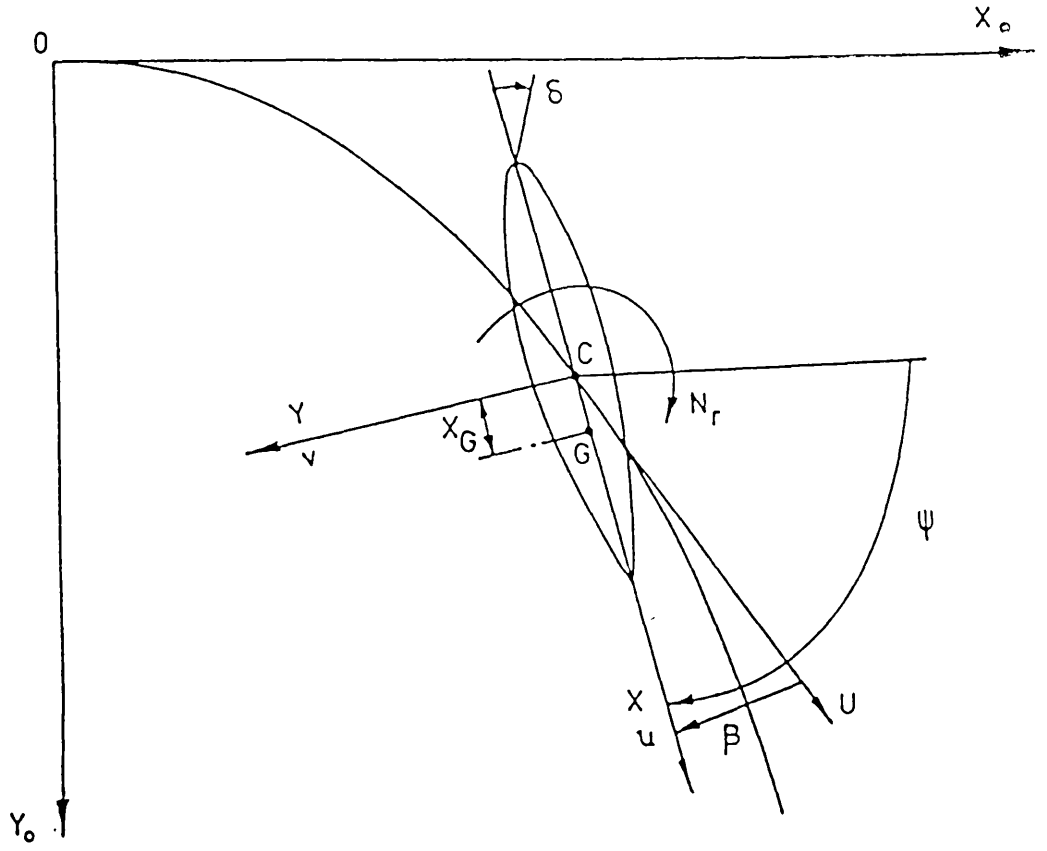

Co-ordinate Axes Fixed in Ship

X	Hydrodynamic Force acting on ship due to Surge
Y	Hydrodynamic Force acting on ship due to Sway
N	Hydrodynamic Moment acting on ship due to Yaw
u	Longitudinal Velocity of Ship
v	Lateral Velocity of Ship
r	Yaw Rate of Vessel
δ	Rudder Deflection Angle
β	Drift Angle
Ψ	Heading Angle
m	Mass of Vessel
X_G	Distance fwd of ammidships of vessels centre of gravity
I_Z	Moment of Inertia about ammidships of vessel

Fig 4.2 Co-ordinate Axes System Adopted for Mathematical Modelling Including Basic Nomenclature

$$T'_1 T'_2 = \frac{(Y'_{\dot{v}} - m')(N'_{\dot{r}} - I'_z) - (Y'_{\dot{r}} - m'x'_G)(N'_{\dot{v}} - m'x'_G)}{Y'_{\dot{v}}(N'_r - m'x'_G) - N'_{\dot{v}}(Y'_r - m')}$$

$$T'_1 + T'_2 = \frac{(Y'_{\dot{v}} - m')(N'_r - m'x'_G) + (N'_{\dot{r}} - I'_z)Y'_v - (Y'_{\dot{r}} - m'x'_G)N'_v - (N'_{\dot{v}} - m'x'_G)(Y'_r - m')}{Y'_v(N'_r - m'x'_G) - N'_v(Y'_r - m')}$$

$$T'_3 = \frac{(N'_{\dot{v}} - m'x'_G)Y'_\delta - (Y'_{\dot{v}} - m')N'_\delta}{N'_v Y'_\delta - Y'_v N'_\delta}$$

$$T'_4 = \frac{(N'_{\dot{r}} - I'_z)Y'_\delta - (Y'_{\dot{r}} - m'x'_G)N'_\delta}{(N'_r - m'x'_G)Y'_\delta - (Y'_r - m')N'_\delta}$$

$$K' = \frac{N'_v Y'_\delta - Y'_v N'_\delta}{Y'_v(N'_r - m'x'_G) - N'_v(Y'_r - m')}$$

$$-K'_v = \frac{(N'_r - m'x'_G)Y'_\delta - (Y'_r - m')N'_\delta}{Y'_v(N'_r - m'x'_G) - N'_v(Y'_r - m')}$$

$$T' = T'_1 + T'_2 - T'_3$$

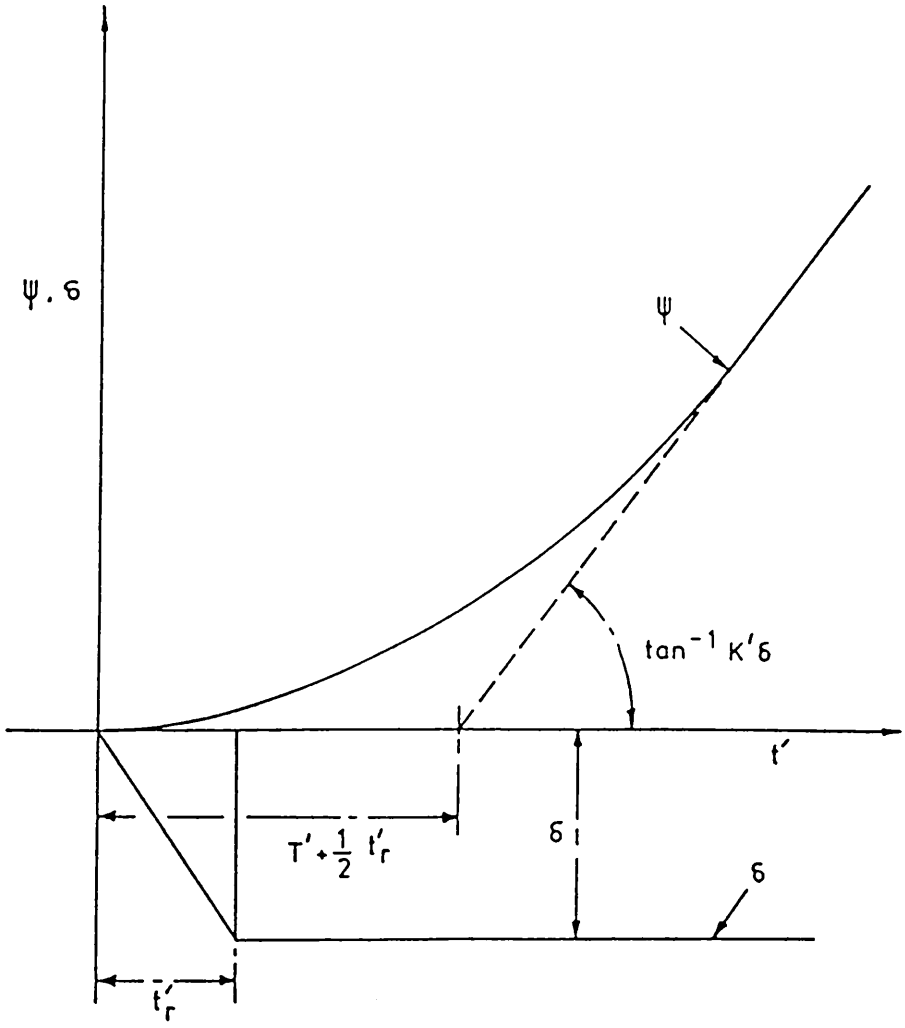

Fig 4.3 Definition of Coefficients K' and T'

Neglecting non-linear terms these equations may be expressed as :-

$$X = X_{\dot{u}}\dot{u} + X_u \Delta u$$
$$Y = Y_{\dot{v}}\dot{v} + Y_v v + Y_{\dot{r}}\dot{r} + Y_r r$$
$$N = N_{\dot{v}}\dot{v} + N_v v + N_{\dot{r}}\dot{r} + N_r r$$

(Eqn 4.2)

Where

$$Y_{\dot{v}} = \frac{\partial Y}{\partial \dot{v}} \quad and \quad Y_v = \frac{\partial Y}{\partial v} \qquad \text{etc.}$$

These partial derivatives are the constants of proportionality between the hydrodynamic forces and the perturbation quantities, hence the terms proportional to acceleration perturbations are known as the acceleration derivatives,

$$X_{\dot{u}}, Y_{\dot{v}}, Y_{\dot{r}}, N_{\dot{v}}, N_{\dot{r}}$$

and those proportional to the velocity perturbations are known as the velocity derivatives,

$$X_u, Y_v, Y_r, N_v, N_r$$

Expressing Equations 4.1 in terms of the perturbation quantities and discarding all but linear terms in order to maintain consistency with Equations 4.2, we obtain the usually accepted form of the linearised equations of motion :-

$$\begin{aligned}
(X_{\dot{u}} - m)\dot{u} + X_u \Delta u &= 0 \\
(Y_{\dot{v}} - m)\dot{v} + Y_v v + (Y_{\dot{r}} - mx_G)\dot{r} + (Y_r - mu_0)\, r &= 0 \\
(N_{\dot{v}} - mx_G)\dot{v} + N_v v + (N_{\dot{r}} - I_z)\dot{r} + (N_r - mx_G u_0)\, r &= 0
\end{aligned} \qquad \text{(Eqn 4.3)}$$

It will be observed that the first equation, which describes the surge response of the vessel is now decoupled from the other two. Since it therefore has no effect on the transverse motion of the ship, it is neglected and attention focused on the other pair.

Forces and moments due to rudder deflection have been omitted from the foregoing analysis. These are considered separately later. At present it is sufficient to assume that

deflection of a rudder will result in a side force and moment which are directly proportional to the angle of deflection.

Incorporating the rudder terms and nondimensionalising we obtain the usual form of the linearised equations of motion used in steering and manoeuvring calculations:-

$$\begin{aligned}
(Y'_{\dot{v}} - m')\dot{v}' + Y'_{v}v' + (Y'_{\dot{r}} - m'x'_G)\dot{r}' + (Y'_{r} - m')r' + Y'_{\delta}\delta &= 0 \\
(N'_{\dot{v}} - m'x'_G)\dot{v}' + N'_{v}v' + (N'_{\dot{r}} - I'_z)\dot{r}' + (N'_{r} - m'x'_G)r' + N'_{\delta}\delta &= 0
\end{aligned}$$

(Eqn 4.4)

Where :-

$$Y'_{\dot{v}} = Y_{\dot{v}} / 0.5\rho L^3$$
$$Y'_{\dot{r}} = Y_{\dot{r}} / 0.5\rho L^4$$
$$N'_{\dot{v}} = N_{\dot{v}} / 0.5\rho L^4$$
$$N'_{\dot{r}} = N_{\dot{r}} / 0.5\rho L^5$$
$$Y'_{v} = Y_{v} / 0.5\rho L^2 u$$
$$Y'_{r} = Y_{r} / 0.5\rho L^3 u$$
$$N'_{v} = N_{v} / 0.5\rho L^3 u$$
$$N'_{r} = N_{r} / 0.5\rho L^4 u$$
$$Y'_{\delta} = Y_{\delta} / 0.5\rho L^2 u^2$$
$$N'_{\delta} = N_{\delta} / 0.5\rho L^3 u^2$$

$$v' = v / u$$
$$r' = rL / u$$
$$\dot{v}' = \dot{v}L / u^2$$
$$\dot{r}' = \dot{r}L^2 / u^2$$
$$t' = tu / L$$
$$m' = \rho\nabla / \tfrac{1}{2}\rho L^3$$
$$I'_Z = I_Z / \tfrac{1}{2}\rho L^5$$
$$X'_G = X_G / L$$

The above form expresses the equations of motion as a pair of simultaneous first order differential equations, where the constant coefficients are the dimensionless acceleration and velocity derivatives.

Nomoto postulated (Ref 17) that these equations may be written as a pair of decoupled second order equations :-

$$\begin{aligned}
T'_1T'_2\dddot{r}' + (T'_1 + T'_2)\ddot{r}' + \dot{r}' &= K'\dot{\delta} + K'T'_3\ddot{\delta}' \\
T'_1T'_2\ddot{v}' + (T'_1 + T'_2)\dot{v}' + v' &= K'_v\delta + K'_vT'_4\dot{\delta}'
\end{aligned}$$

(Eqn 4.5)

It is common practice in the analysis of trial manoeuvers, both at full scale and with free running models, to use a more simple expression than equation 4.5.

Nomoto first proposed (Ref 17) that :-

$$T'r' + r' = K'\delta$$

(Eqn 4.6)

Eqn 4.6 may be used instead of equation 4.5. This simplification is extremely useful but has limitations on its applicability.

The coefficients used in these equations are detailed in Fig 4.3.

4.5.2 Manoeuvring Criteria

The foregoing analysis forms the basis for the manoeuvring criteria adopted by the SWATHMAN program.

Turning Ability

It is usual to describe the turning behaviour of a ship in terms of its turning circle. Values of advance, transfer and diameter are often quoted as a means of quantifying a vessels inherent directional stability. However most vessels turn with a diameter of two-three times the ship length whether stable or unstable, so that the final turning behaviour is not a very useful means of determining the manoeuvrability of a ship.

As an alternative to considering the turning circle, initial turning ability of the ship will be examined immediately after rudder activation. Since deviations from a straight course are small, the linear theory developed in the preceding section may be used with confidence.

A more suitable definition of turning ability may be taken as the change in heading angle per unit helm angle applied after the ship has travelled one ship length.
N.B. for comparative purposes e.g. in Section 4.8, turning diameters are often used since they are often the only model / full scale manoeuvring results available.

Fig 4.3 illustrates heading response / helm angle variation.

The heading response may be obtained by solving the first part of equation (4.5) for this rudder time history, together with zero rate and heading angle initial conditions, as follows:-

$$\frac{\Psi(t)}{\delta} = K'\left[\begin{array}{l} t' - (T'_1 + T'_2 - T'_3) + t'_r / 2 \\ + \dfrac{(T'_1 - T'_3)T'^{2}_1}{(T'_1 - T'_2)t'_r}\left(e^{t'_r / T'_1} - 1\right)e^{-t'/T'_1} \\ - \dfrac{(T'_2 - T'_3)T'^{2}_2}{(T'_1 - T'_2)t'_r}\left(e^{t'_r / T'_2} - 1\right)e^{-t'/T'_2} \end{array}\right]$$

(Eqn 4.7)

From equation (4.6) for the same helm input :-

$$\frac{\Psi(t)}{\delta} = K'\left[t' - T' + t'_r / 2 + \frac{T'^{2}}{t'_r}\left(e^{t'_r / T'} - 1\right)e^{-t'/T'}\right]$$

(Eqn 4.8)

Study of equations (4.7) and (4.8) confirms that both solutions tend to a similar asymptote if :-

$$T' = T'_1 + T'_2 - T'_3$$

If the time for the rudder movement tends to zero, and non-dimensionalised time is set to t=1, (which is equivalent to moving one ship length), then Eqns (4.7) and (4.8) become:-

$$\frac{\Psi(t)}{\delta} = K'\left[\begin{array}{l} 1 - (T'_1 + T'_2 - T'_3) \\ + \dfrac{(T'_1 - T'_3)}{(T'_1 - T'_2)}T'_1 e^{-1/T'_1} \\ + \dfrac{(T'_2 - T'_3)}{(T'_1 - T'_2)}T'_2 e^{-1/T'_2} \end{array}\right]$$

(Eqn 4.9)

and

$$\frac{\Psi(t)}{\delta} = K'\left[1 - T' + T'e^{-1/T'}\right]$$

(Eqn 4.10)

Norrbin (Ref 18) first introduced the idea of a turning index and he used Equation (4.10) to denote what he termed the "P" No. This is the heading change per unit helm angle for one ship length travelled, described in terms of the Nomoto indices K' and T'

Norrbin suggested a value for $P > 0.3$, however Norrbin and Nomoto later suggested that in the case of large tankers this requirement may be relaxed to $P > 0.2$. From analysis of results to date and considering the fact that SWATH vessels are shorter than "equivalent" monohulls it is recommended that $P > 0.2$ be taken as standard for SWATH vessels.

A value of P=0.3 is equivalent to a 10 degree change in ship heading angle in one ship length, when the helm is placed hard over (30 degrees or more rudder deflection).

Equation (4.10) may be expanded into the following form:-

$$P = \frac{\Psi(t)}{\delta} = \frac{1}{2}\frac{K'}{T'}\left[1 - \frac{1}{3T'} + \frac{1}{12T'^2} - \frac{1}{60T'^3} + \ldots\right] \qquad \text{(Eqn 4.11)}$$

and when T' is large this reduces to:-

$$P \approx \frac{1}{2}\frac{K'}{T'} \qquad \text{(Eqn 4.12)}$$

Dynamic Stability

For a linear dynamic system to be stable it is necessary for the roots of the characteristic equation to be negative. In most ship manoeuvring problems these roots are usually real, so that this requirement is satisfied if the time constants are positive. The condition for stability therefore reduces to :-

$$Y'_v(N'_r - m'x'_G) - N'_v(Y'_r - m') > 0 \qquad \text{(Eqn 4.13)}$$

This may alternatively be expressed :-

$$\frac{N'_r - m'x'_G}{Y'_r - m'} > \frac{N'_v}{Y'_v} \qquad \text{(Eqn 4.14)}$$

This latter inequality is useful in explaining the requirement for dynamic stability . It simply indicates that the centre of pressure in pure yaw should be ahead of the centre of pressure in pure sway if the ship is to be dynamically stable.

Turning Diameter

Whilst the terminal turning behaviour of a vessel should not, on its own, be used to define its manoeuvring performance, the information is nonetheless not without value. A vessels turning diameter is the most often quoted result from full scale manoeuvring trials, due most likely to the relative ease of measurement and the easily understood physical significance of the value. Similarly current regulations require that this information is permanently displayed in the wheelhouse of most vessels and it is certainly a quantity the prospective operator of a SWATH vessel will wish to know. For these reasons a routine was incorporated into SWATHMAN program in order to enable the calculation of turning radii for specified degrees of helm.

From previously developed linear theory and an analysis of turning behaviour (Ref 16). For dynamically stable vessels the steady radius of turning, R is given by :-

$$\frac{R}{L} = -\frac{1}{\delta}\frac{Y'_v(N'_r - m'x'_G) - N'_v(Y'_r - m')}{Y'_v N_\delta - N'_v Y'_\delta} \qquad \text{(Eqn 4.15)}$$

Where L is the length of the vessel.

4.5.3 Estimation of Ship Derivatives

From the foregoing it is obvious that the acceleration and velocity derivatives must be known or at least approximated before any predictions on the manoeuvring capability of a ship may be made. Several techniques are currently employed to determine these values.

Model Testing

For ship forms, model tests remain to date the most reliable means of determining the acceleration and velocity derivatives. Captive model testing, using either a planar motion mechanism or a rotating arm is the standard technique. Such experiments are however time consuming and costly, requiring the exclusive use of a large specialised purpose built facility. It would clearly be a great advantage if the derivatives could be calculated directly e.g. using strip theory.

Strip Theory

This is applied with some success in the case of aircraft and with missiles, where the body geometry is dominated by wings and fins. Unfortunately, the slender body theory and strip methods used do not give accurate results for ship forms, since there are no large flat stabilising surfaces and the flow around the hull is greatly altered by viscosity effects.

Since model testing is impractical and direct evaluation is not feasible, recourse is often made to semi-empirical techniques.

Semi-Empirical Methods

Several attempts have been made to derive empirical expressions relating the velocity derivatives to ship geometry. These formulae were derived after analysis of experimental results obtained on planar motion and rotating arm devices.

In the following formulae:-

L - Ship Length Between Perpendiculars

B - Beam of Vessel

T - Draught of Vessel

Cb- Block Coefficient

In 1970 Wagner Smitt (Ref 19) proposed :-

$$Y'_v = -5.0\left(\frac{T}{L}\right)^2 = -\Pi\left(\frac{T}{L}\right)^2 .(1.59)$$

$$Y'_r = +1.02\left(\frac{T}{L}\right)^2 = -\Pi\left(\frac{T}{L}\right)^2 .(-0.32)$$

$$N'_v = -1.94\left(\frac{T}{L}\right)^2 = -\Pi\left(\frac{T}{L}\right)^2 .(0.62)$$

$$N'_r = -0.65\left(\frac{T}{L}\right)^2 = -\Pi\left(\frac{T}{L}\right)^2 .(0.21) \qquad \text{(Eqn 4.16)}$$

While in 1971 Norrbin (Ref 15) suggested:-

$$Y'_v = -\Pi\left(\frac{T}{L}\right)^2\left[+1.69 + 0.08\frac{C_B}{\Pi}\frac{B}{T}\right]$$

$$Y'_r = -\Pi\left(\frac{T}{L}\right)^2\left[-0.645 + 0.38\frac{C_B}{\Pi}\frac{B}{T}\right]$$

$$N'_v = -\Pi\left(\frac{T}{L}\right)^2\left[+0.64 - 0.04\frac{C_B}{\Pi}\frac{B}{T}\right]$$

$$N'_r = -\Pi\left(\frac{T}{L}\right)^2\left[0.47 - 0.18\frac{C_B}{\Pi}\frac{B}{T}\right] \qquad \text{(Eqn 4.17)}$$

and in 1981 Inoue (Ref 20) recommended :-

$$Y'_v = -\Pi\left(\frac{T}{L}\right)^2\left[1.0 + \frac{1.4}{\Pi}C_B\frac{B}{T}\right]$$

$$Y'_r = -\Pi\left(\frac{T}{L}\right)^2\left[-\frac{1}{2}\right]$$

$$N'_v = -\Pi\left(\frac{T}{L}\right)^2\left[\frac{2.0}{\Pi}\right]$$

$$N'_r = -\Pi\left(\frac{T}{L}\right)^2\left[\frac{1.04}{\Pi} - \frac{4.0}{\Pi}\frac{T}{L}\right] \qquad \text{(Eqn 4.18)}$$

Examination of these formulae reveals discrepancies in the values obtained for the four velocity derivatives. This is most likely due to variations in the experimental data and regression techniques applied.

In an attempt to clarify the situation Clarke (Ref 21) performed a multiple regression analysis of all available data. His results are summarised in the following expressions for velocity and acceleration derivatives:-

Clarke Offers (Ref 21) :-

$$\frac{-Y'_v}{\Pi\left(\frac{T}{L}\right)^2} = 1 + 0.40C_B B / T$$

$$\frac{-Y'_r}{\Pi\left(\frac{T}{L}\right)^2} = -1/2 + 2.2B / L - 0.08B / T$$

$$\frac{-N'_v}{\Pi\left(\frac{T}{L}\right)^2} = 1/2 + 2.4T / L$$

$$\frac{-N'_r}{\Pi\left(\frac{T}{L}\right)^2} = 1/4 + 0.039B / T - 0.56B / L$$

(Eqn 4.19)

$$\frac{-Y'_v}{\Pi\left(\frac{T}{L}\right)^2} = 1 + 0.16C_B B / T - 5.1(B / L)^2$$

$$\frac{-Y'_r}{\Pi\left(\frac{T}{L}\right)^2} = 0.67B / L - 0.0033(B / T)^2$$

$$\frac{-N'_v}{\Pi\left(\frac{T}{L}\right)^2} = 1.1B / L - 0.041B / T$$

$$\frac{-N'_r}{\Pi\left(\frac{T}{L}\right)^2} = 1/12 + 0.017C_B B / T - 0.33B / L$$

(Eqn 4.20)

Fin Corrections to Hull Derivatives

The following fin effects must be added to ship derivatives given by the previous expressions (Equations 4.16 - 4.20) :-

$$Y'_{v\,fin} = -\gamma Y'\delta$$

$$Y'_{r\,fin} = -\tfrac{1}{2} Y'_{v\,fin}$$

$$N'_{v\,fin} = -\tfrac{1}{2} Y'_{v\,fin}$$

$$N'_{r\,fin} = \tfrac{1}{4} Y'_{v\,fin}$$

(Eqn 4.21)

Where the flow straightening coefficient γ may be taken as 0.3 (Ref 22).

4.5.4 Estimation of Rudder Derivatives

The side force Y created by the rudder is calculated on the basis that the rudder acts like a low aspect ratio wing, so that :-

$$Y = \tfrac{1}{2}\rho c^2 A C_L$$

Where c is the flow velocity over rudder, A is the rudder area and Cl is the lift coefficient for the rudder section.

Non-Dimensionalising gives :-

$$Y' = \left(\frac{A}{LT}\right)\left(\frac{T}{L}\right) C_L \left(\frac{c}{u}\right)^2$$

The force / helm angle is therefore :-

$$Y'_{\delta} = \left(\frac{A}{LT}\right)\left(\frac{T}{L}\right)\left(\frac{\partial C_L}{\partial \delta}\right)\left(\frac{c}{u}\right)^2$$

(Eqn 4.22)

The flow velocity ratio term is dependent on whether the rudder is subject to propeller induced accelerated flow. For rudders outwith propeller affected flow the ratio:-

$$\left(\frac{c}{u}\right) = \left[\frac{V_A}{V_S}\right]$$

Where Vs is the ship speed and Va is the flow speed into rudder. This simply reduces to (1-w) where w is the taylor wake fraction for the hullform.

For rudders subject to propeller accelerated flow (Ref 16) the ratio becomes :-

$$\left(\frac{c}{u}\right)^2 \approx \left\{1 + \%_{Area}\left[\left(\frac{V_A(ACL)}{V_S}\right)^2 - 1\right]\right\}$$

(Eqn 4.23)

Where (%Area) is the proportion of rudder area subject to the accelerated flow, and ACL the flow acceleration due to the propeller.

The Lift Curve Slope Coefficient for the rudder is harder to define. Classical theory (Ref 20) is available to calculate the quantity from first principles given a knowledge of the aspect ratio for the control surface. However this theory was developed for fins operating in free stream without complications imposed by the proximity of hull structure and associated disturbances in the flow.

After analysis of results obtained using this method proved disappointing, it was decided to fix the value of lift curve coefficient for all control surfaces. The value chosen was selected after study and comparison of results obtained for several SWATH forms with full scale data. A value was chosen which was found to give acceptable results for a range of vessels when utilising equations (4.19 and 4.20).

This approximation removes the effect of rudder aspect ratio from the calculation procedure. This is unlikely to effect results for low aspect ratio rudders behind the propellers, but may introduce small errors when determining side force due to high aspect ratio surface piercing strut rudders.

This unfortunate effect is counteracted by the incorporation of a mirror imaging factor into the calculation. This is primarily designed to model the increase in effective aspect ratio which occurs due to the proximity of perpendicular hull surfaces and rudder fences in the case of surface piercing variants equipped with such devices. This factor may also be used to modify the "effective" lift curve slope coefficient in the case of very high values of rudder aspect ratio.

For the above cases the standard value of lift curve slope coefficient is modified according to the following formulae (Ref 16) :-

$$\left(\frac{\partial C_L}{\partial \delta}\right)_{Modified} = \left(\frac{\partial C_L}{\partial \delta}\right)_{Std} \left[1 + \left(\frac{1-K}{K}\right)\left(1 - \frac{\partial C_L / \partial \delta}{1.8\,\Pi}\right)\right]^{-1} \qquad \text{(Eqn 4.24)}$$

Where K is the imaging factor for the rudder.

The moment due to application of rudder is therefore equal to :-

$$N'_\delta = -\left(\frac{RDIST}{LOA}\right) Y'_\delta \qquad \text{(Eqn 4.25)}$$

Where RDIST is the distance of the rudders aft amidships and LOA is the ship length.

4.6 Development of 'SWATHMAN' Program

A manoeuvring prediction tool for SWATH vessels was created incorporating suitably modified adaptations of currently accepted monohull practice.

The resulting tool allows the user to determine the size of rudder required for a given vessel in order to provide adequate manoeuvring performance. The program can cope with rudders fore and aft of the propellers and will check the directional stability for a given design in addition to estimating the likely turning performance and heel angles for specified degrees of helm.

The program in common with all computer programs may be broken down into a number of easily understood algorithms. These algorithms are illustrated in flowchart form in Fig 4.4.

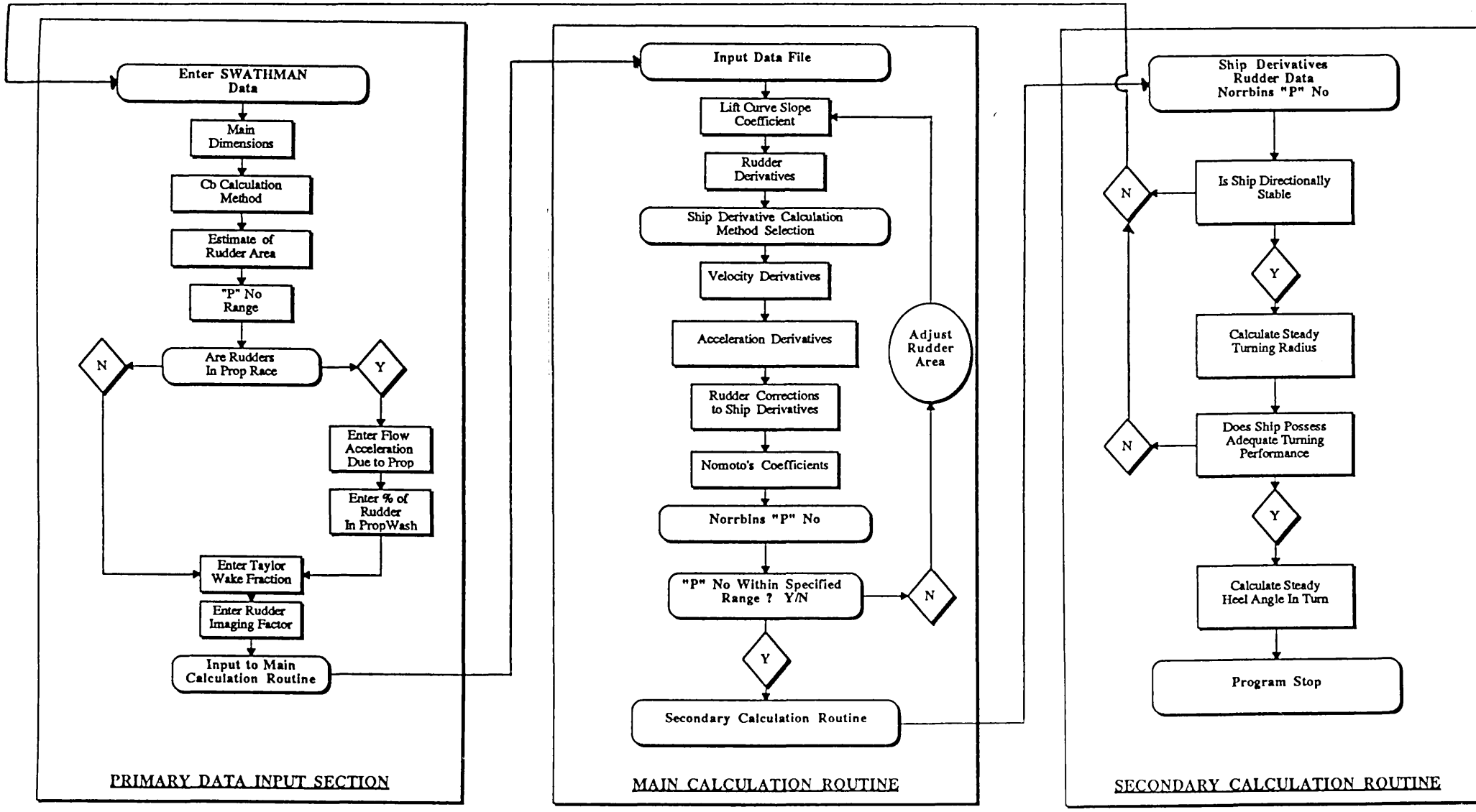

Fig 4.4 SWATHMAN Algorithm Flow Diagram

The first stage is to input the main geometrical details of the vessel. For those values which may be unknown at the design stage, such as the mass moment of inertia, default values are available. These default values are based upon regression fits of data from existing designs, and are selected according to the main dimensions of the required vessel.

Next an "effective" block coefficient is required, the user is given three options :-

I. Input a previously calculated value
II. Select a value based on hull and strut dimensions
III. Select a value based on hull dimensions only

Option II is the most intuitively realistic assuming a value is unavailable. Option III is included for use at the very early design stage when dimensions of the strut may be unknown, e.g. when comparing strut type rudders hung on short struts against traditional configurations utilising overhanging struts.

The program then requests bounding values defining the acceptable range for Norrbin's "P" No. For the benefit of users unfamiliar with this index the program reminds us that values of "P" No in the range 0.2 - 0.4 are usual for normal vessels.

A first estimate of rudder area and location is next requested, a default value for area is again available for inexperienced users.

At this stage the option of siting the rudders in or out of the propeller slipstream is given and the user is asked what proportion, if any, of the rudder is subject to this slipstream. Using this information together with values for the Taylor Wake Fraction and a flow acceleration term - either input by user or default values, (derived from T-AGOS 19 data (Ref 23), and Kaimalino data (Ref 7)), the program calculates the ratio of flow velocity over the rudder to the ship speed. This value combined with the lift curve slope for the rudder section, allows estimation of the side force generated by the rudder.

The lift curve slope for the rudder section was initially calculated from first principles by the method given by Whicker and Fehlner (Ref 24) for low aspect ratio wings. However after comparison of the manoeuvring predictions obtained by this method and full scale trial results for the M.V. Patria, it was found that greater accuracy

could be attained by utilising a fixed coefficient of 1.301 per Rad. This value was reached after extensive analysis of full scale data and model test results together with published comparisons and predictions utilizing Clarke's regression routines from several early versions of the 'SWATHMAN' program. The lift curve slope may be modified to allow for imaging effects (where present) by means of an effective mirror imaging coefficient.

At this stage the program calculates "Clarke's Propulsive Coefficient". It was Clarke (Ref 21) who suggested that the product :-

$$\left(\frac{\partial C_L}{\partial \delta}\right)\left(\frac{c}{u}\right)^2$$

may be assumed constant. Clarke suggested a value of 3.0 as typical for single screw vessels of normal form. The program displays this product and allows the user to change its value if so required.

The rudder derivatives are calculated and the program moves on to consider the ship derivatives. These may be calculated by any one of four semi-empirical techniques according to Wagner Smitt (Ref 19), Norrbin (Ref 15), Inoue (Ref 20) or Clarke (Ref 21). Alternatively the user may input his own values as found from model tests or ship motion packages.

Once the ship derivatives are evaluated the corrections due to the fins / rudders are calculated and the derivatives modified accordingly if required.

The final stage of the first iteration is completed by calculating Nomoto's turning coefficients (Ref 17) and Norrbin's "P" Number (Ref 18). If this "P" No falls outwith the range initially specified by the user the rudder is resized automatically and further iterations performed until the condition is met.

Once the "P" number falls within the specified range the program offers the user the option of checking the vessels dynamic stability . If the vessel is found to be unstable three options are given:-

I. Proceed with the unstable design
II. Attempt to stabilize it by changing overall vessel dimensions
III. Attempt to stabilize it by changing rudder dimensions only .

Final values of rudder area and corresponding "P" Number are displayed at this stage and the option given to accept or modify the value of rudder area.

When acceptable values are reached the user may proceed to calculate the likely steady turning radius for his vessel equipped with the chosen rudders. Finally the program estimates the probable value of heel angle attained whilst executing a turn of specified radius.

This program entitled 'SWATHMAN3' (SWATH MANoeuvring version 3) has been validated for a number of designs at model and full scale, including the SWATH M.F.V. Ali. The program has also been used in an attempt to quantify the effect of rudder type / location upon turning performance.

4.7 Full Scale Trials

Limited full scale manoeuvring performance trials were conducted utilising the 20 tonne SWATH fishing vessel "Ali" . This vessel is a basic SWATH form of single "short strut" design. The rudders are incorporated into the trailing edge of the struts. Details of the vessel and its rudders can be found in Ref 1 and in Table 4.1.

The manoeuvring evaluation formed part of the overall trials program conducted on this vessel during December 1990. These trials were sponsored by the Science and Engineering Research Council through the Marine Technology Directorate at Glasgow University, together with Vickers Shipbuilding and Engineering Limited, Yarrows Shipbuilders Limited and YARD Ltd.

The primary objective of the trials was to collect data on resistance, propulsion and seakeeping, in an effort to validate predictions from various theoretical tools and model tests. Owing to a lack of time and the difficulty of conducting accurate manoeuvring trials, a comprehensive evaluation of the manoeuvring characteristics of the ship was not attempted. Evaluation of the vessels manoeuvrability was instead limited to subjective observations on its response to the helm and to measurement of turning circles. In the absence of sophisticated position fixing equipment these circles were defined by measurement of the distance travelled (approximately the circumference neglecting transfer effects) together with the time taken and the compass heading relative to the bearing when commencing the turn. From this information the Tactical Diameter can be calculated with reasonable accuracy for a given helm angle and speed .

The most obvious characteristic of the vessel was the directional stability which it possessed. Despite noticeable yawing in bow quartering seas the overall course remained straight, with little or no correction to the helm necessary. As anticipated for a vessel with strut rudders medium to high speed manoeuvring ability was fairly poor.

Some preliminary results from the turning trials are presented in Table 4.2 and Fig 4.6, 4.9 and 4.12. Full analysis of the data collected during these trials is still incomplete. Complete results from the trials will be presented once available (Ref 25).

4.8 'SWATHMAN' Results and Program Validation

A program now exists which allows the user to predict for any given design of SWATH vessel, the rudder area and configuration required to provide that vessel with acceptable manoeuvring performance. In addition the program will estimate turning characteristics and re-design the rudder as required to meet specific requirements.

In an effort to validate 'SWATHMAN' the program was run for seven "real life" vessels for which full scale manoeuvring trials information was available. The names and main particulars of these seven ships are given in Table 4.1.

For each of these seven vessels the program was utilized in two alternative ways:-

Firstly the program was required to determine suitable rudder areas in order to satisfy a previously specified turning performance.

Secondly the program was used to simulate the likely manoeuvring performance of the vessels "as built". In this case real values of rudder area were input together with likely prevailing flow conditions for the region around the rudder.

In addition several studies were made into the effects of varying flow conditions around the rudder, free surface imaging and mirroring effects. Clarkes regression routines were used for all the above comparisons. The effect of calculating manoeuvring derivatives using different regression routines was also briefly investigated. Turning diameter forms the basis for all these comparisons since it is the most often published result from model and full scale trials.

Vessels Name	Patria	Kaimalino	Halcyon	Marine Ace	Seagull	Ohtori	Ali
Year of Build	1989	1973	1985	1977	1979	1980	1990
Builder	FBM Cowes	USCG	RMI Inc	Mitsui	Mitsui	Mitsui	Private
Purpose/Role	Fast Ferry	Workboat	Demostrator	Demostrator	Fast Ferry	Hydrographic	Creel Fishing
Length Over All	37.00	26.41	18.29	12.34	35.90	27.00	12.00
Hull Length	32.00	24.38	16.13	10.47	31.50	24.00	10.48
Strut Length	32.00	14.17	16.78	7.31	32.14	24.00	8.90
Hull Centreline Spacing	10.00	12.19	7.47	5.30	13.50	8.00	4.00
Load Draught	2.70	4.66	2.13	1.55	3.15	3.40	1.60
Maximum Hull Diameter	1.85	1.97	1.52	1.24	2.95	2.30	1.00
Maximum Strut Width	1.00	0.91/1.2	0.75	0.57	1.25	0.60	0.60
Load Displacement (tonnes)	180.00	193.00	50.00	18.40	343.00	239.00	20.00
Type of Rudders	Aft Props on Overhang	Aft Props on Overhang	Aft Props on Overhang	Aft Props on Overhang	Aft Props on Overhang	Aft Props on Overhang	Fwd Props Strut Hung
Rudder Height/Span	-	4.42	1.20	0.75	1.50	1.48	0.68 (1)
Rudder Chord Length	-	0.88	0.70	0.45	0.84	0.8 (mean)	0.60
Total Rudder Area	1.12	3.89	0.84	0.34	1.26	1.38	0.41
Data Source (Ref)	11	7	26	14	14	28	1
Full Scale Trials Results							
Turn Diameter @ 35 Degrees Helm	240-280	229-282	90-100 (2)	66.00	200.00	165-330	120.00
Data From Reference No	11	2	26,27	14	13	28	25

(1) Submerged at Load Draught

All Dimensions in Metres Unless Otherwise Stated

(2) @ 30 Degrees Helm

Table 4.1 Main Particulars of Vessels Used in the Validation of the SWATHMAN Program

Vessel Name	Patria	Kaimalino	Halcyon	Marine Ace	Seagull	Ohtori	Ali
Type of Rudders	Aft Props on Overhang	Aft Props on Overhang	Aft Props on Overhang	Aft Props on Overhang	Aft Props on Overhang	Aft Props on Overhang	Fwd Props Strut Hung
Actual Rudder Area	1.12	3.89	0.87	0.34	1.26	1.38	0.41
Rudder Area used for Prediction	1.12	3.89	0.84	0.34	1.26	1.38	0.41

Turn Diameter @ 35 Degrees Helm							
Full Scale Trials Results	240-280	229-282	90-100	66	200	165-330	120
SWATHMAN Program Prediction	240	220	98	58	142	132	112

SWATHMAN Prediction Conditions							
% Rudder In Flow	75	40	75	75	75	75	-
Flow Acceleration Due to Propeller	1.8	1.8	1.8	1.8	1.8	1.8	0
Mirror Imaging Factor Applied	1.0	1.0	1.0	1.0	1.0	1.0	1.5

Comment	Rudder NACA Section 15	High Span Only 40% In Propwash	Figures for 30 Deg Helm Only	Prog selected A=0.3 m**2 Giving TD=66 m	Trial Fig may not be @30 Deg Helm	Prog selected A=1.21m**2 Giving TD=148 m	Only Vessel Fitted with Strut Hung Rudders

All Dimensions in Metres Unless Otherwise Stated

Fig 4.2 Turning Performance - A Comparison of Actual and Predicted Values

Figures 4.5, 4.6 and 4.7 present 'SWATHMAN' predictions of minimum turning diameters / rudder area for the vessels Patria, Ali, and Kaimalino. It will be noted that the predictions agree well with values measured on full scale trials.

Figures 4.8, 4.9 and 4.10 present 'SWATHMAN' predictions of turning performance (Turn Diameter / Helm Angle) for the vessels Patria, Ali and Halcyon. Good agreement with measured values is again observed.

Fig 4.11, 4.12, and 4.13 demonstrate the influence upon manoeuvring performance of rudder imaging effects. This phenomenon occurs where the proximity of large flat areas close to and perpendicular to rudders produce an increase in rudder efficiency. The effect may be likened to a mirroring and therefore an increase in "effective" area. A mirror imaging factor of 2 corresponds to full imaging in the hull while the other end of the foil is subject to normal crossflow conditions. A value of 1.7 would probably be more appropriate for a circular hulled SWATH where a gap opens up at larger angles of attack. Ventilation at the free surface may reduce this still further for surface piercing variants, therefore a value of 1.5 was selected for calculations relating to the M.V. Ali. The results obtained for this vessel indicate this approximation to be not unreasonable. Where rudder fences (perpendicular projections designed to counteract ventilation) are fitted the imaging factor may in theory be infinite. In practice this will never happen although values of 3 and 4 are feasible.

Fig 4.12 and 4.13 demonstrate how imaging effects may combine to increase the efficiency of surface piercing strut hung rudders (fitted with fences) to the almost the same level as those mounted aft in the propeller slipstream.

Fig 4.14 and 4.15 illustrate the influence of propeller induced flow acceleration on rudder effectiveness. As expected efficiency increases markedly with increased flow velocity. This explains the considerable difference in turning performance / rudder area for vessels fitted with rudders forward and aft of the propellers.

Fig 4.16 and 4.17 quantify the increases in turning performance that may be obtained by changing the proportion of rudder area subject to propeller accelerated flow. It may be deduced from Fig 4.17 that only 25-35 % of S.S.P. Kaimalino's rudder is in accelerated flow. Examination of relative rudder and propeller dimensions for the vessel does in fact confirm this rather unusual situation.

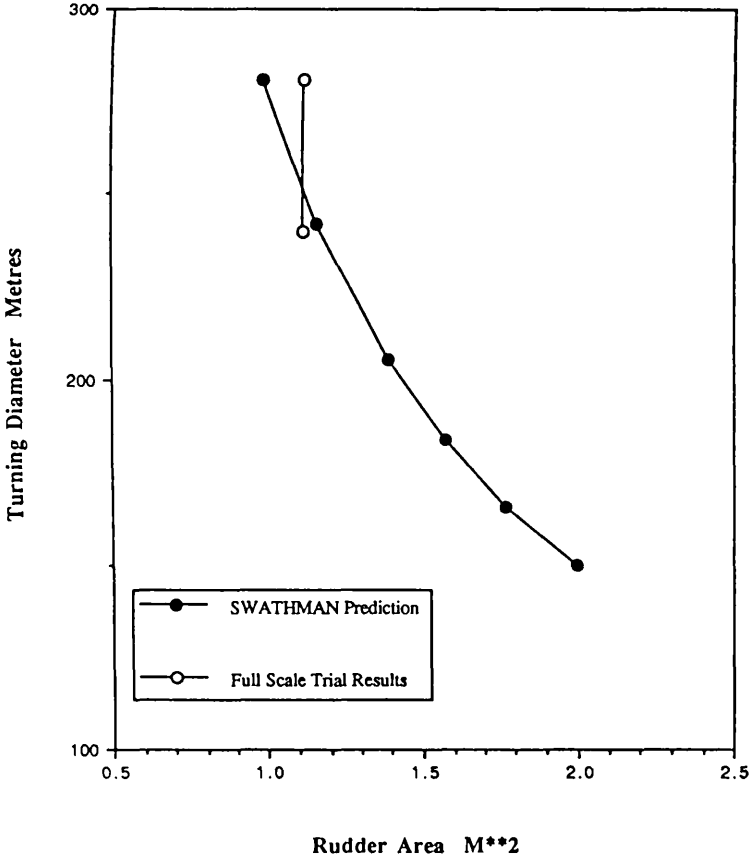

Fig 4.5 M.V. Patria - Turning Diameter / Rudder Area.

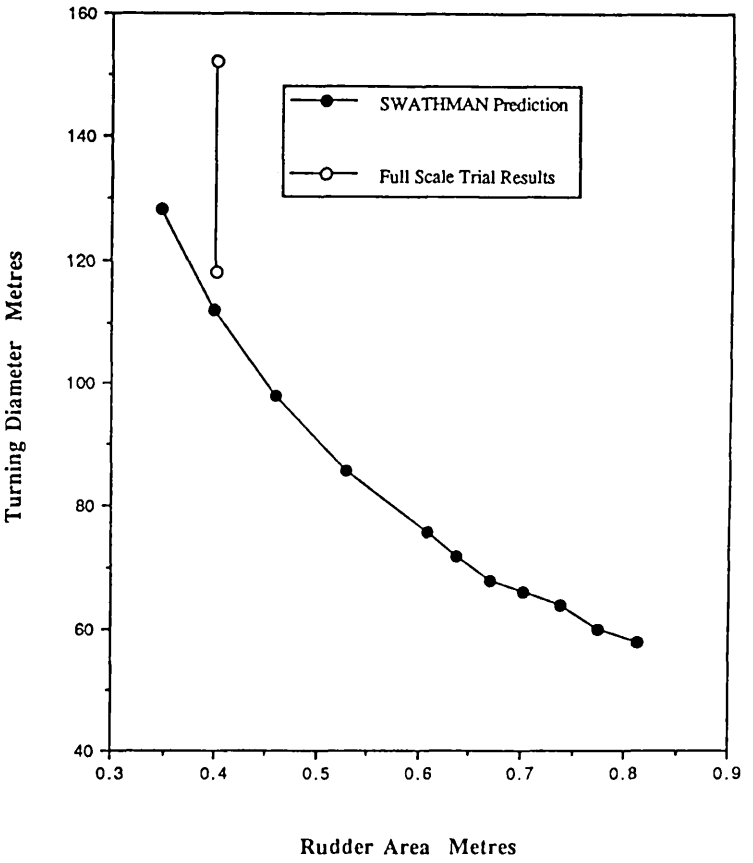

Fig 4.6 M.V. Ali - Turning Diameter / Rudder Area.

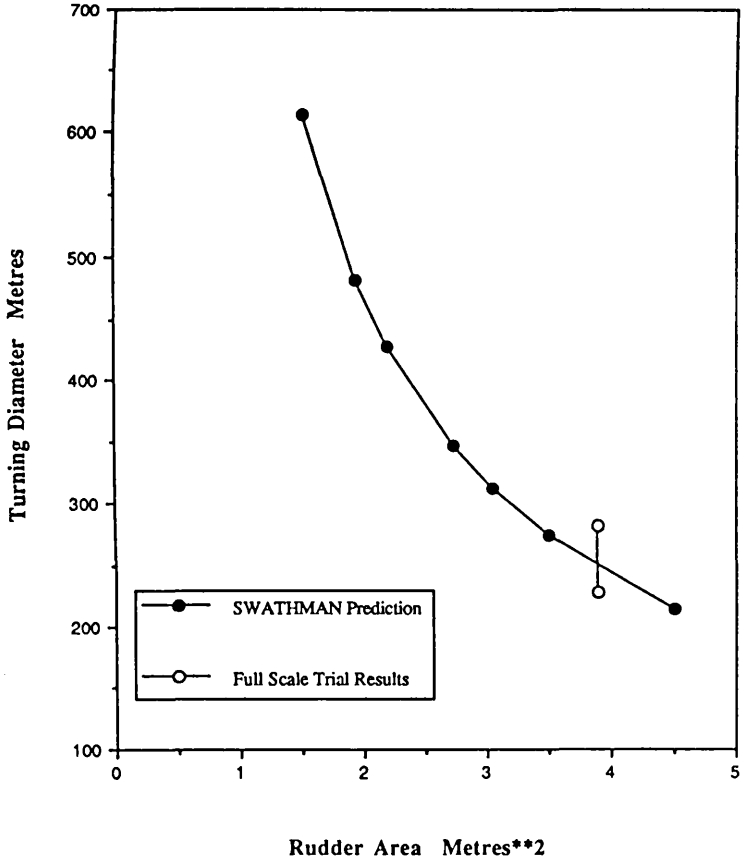

Fig 4.7 S.S.P. Kaimalino - Turning Diameter / Rudder Area.

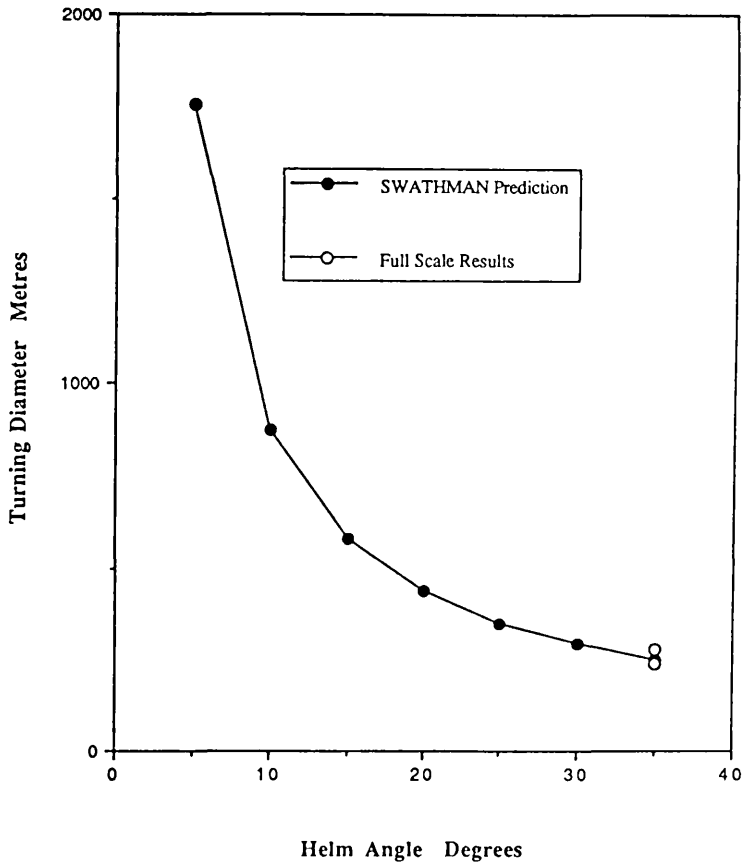

Fig 4.8 M.V. Patria - Turning Diameter / Helm Angle.

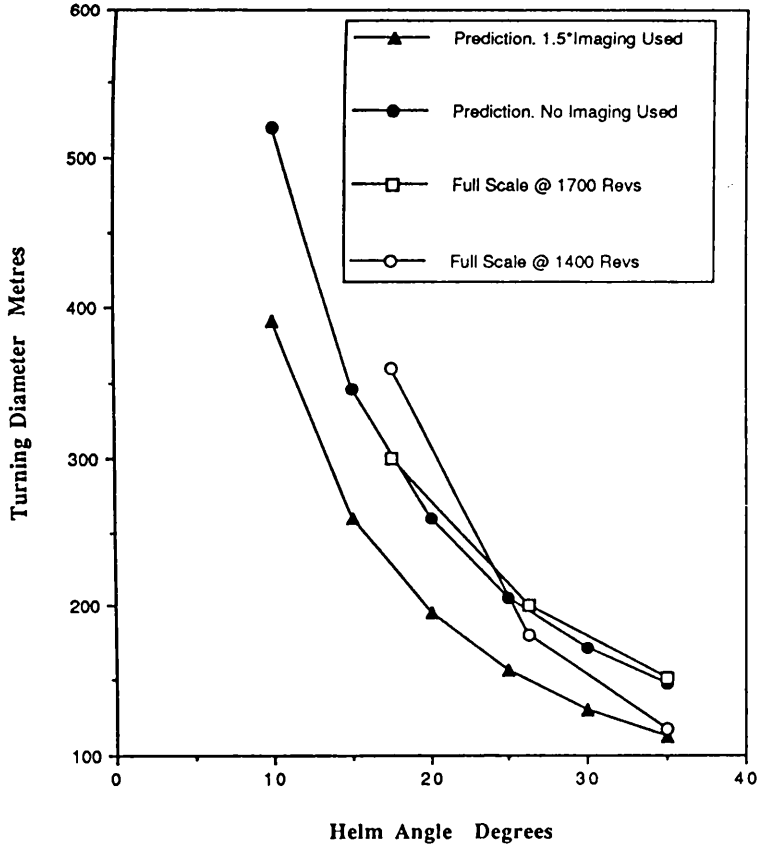

Fig 4.9 M.V. Ali - Turning Diameter / Helm Angle.

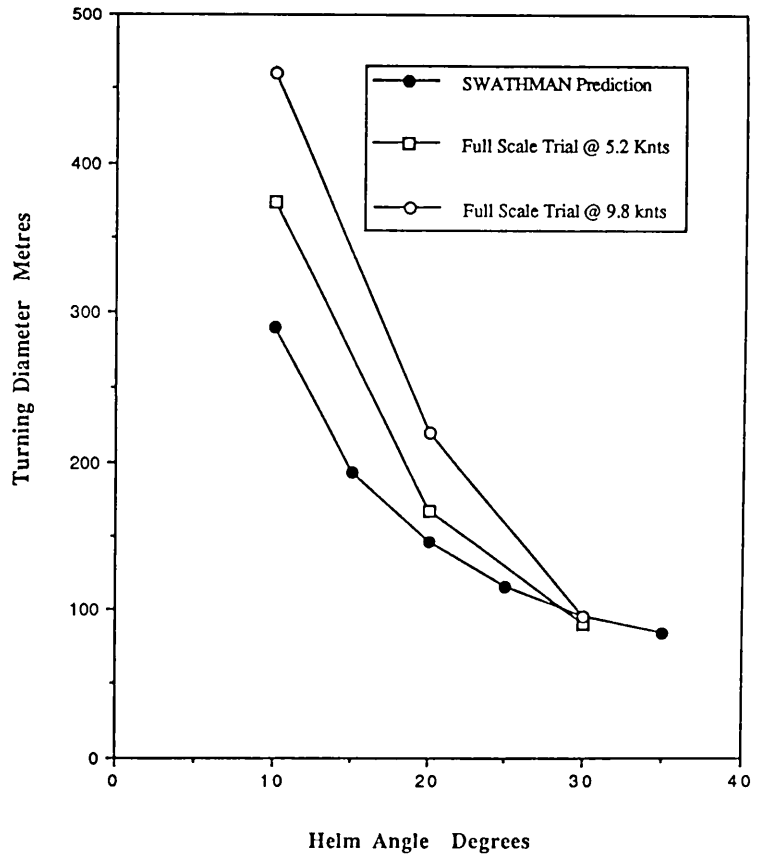

Fig 4.10 M.V. Halcyon - Turning Diameter / Helm Angle.

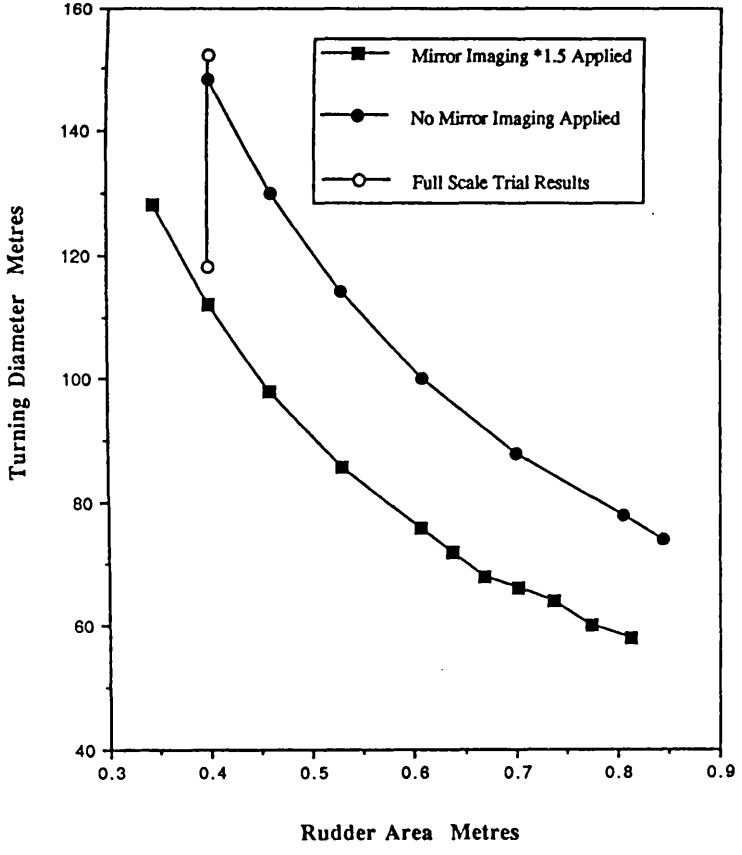

Fig 4.11 Turning Diameter / Rudder Area / Mirror Imaging Factor. (M.V. Ali)

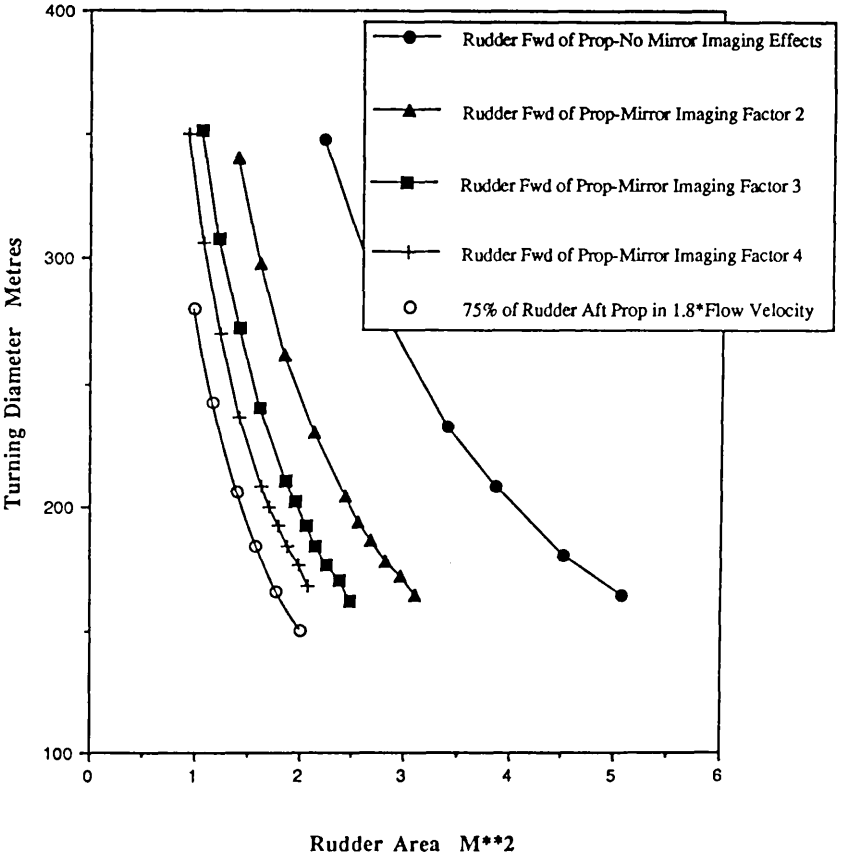

Fig 4.12 Turning Diameter / Rudder Area / Mirror Imaging Factor. (Patria Hullform fitted with Rudders Fore and Aft of Propellers)

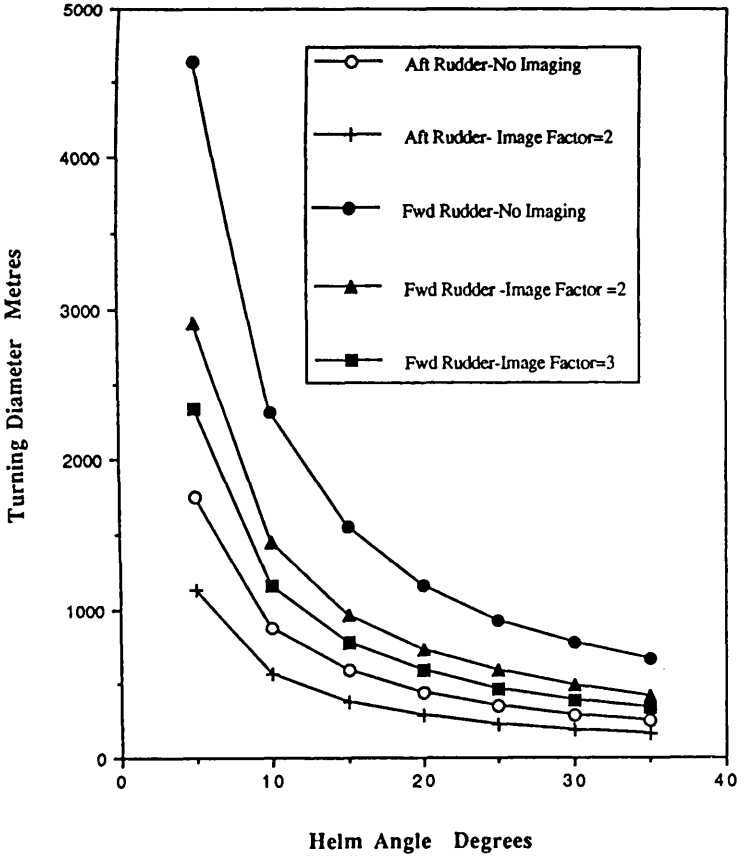

Fig 4.13 Turning Diameter / Helm Angle / Mirror Imaging Factor. (Patria Hullform - Rudders Fore and Aft of Propellers)

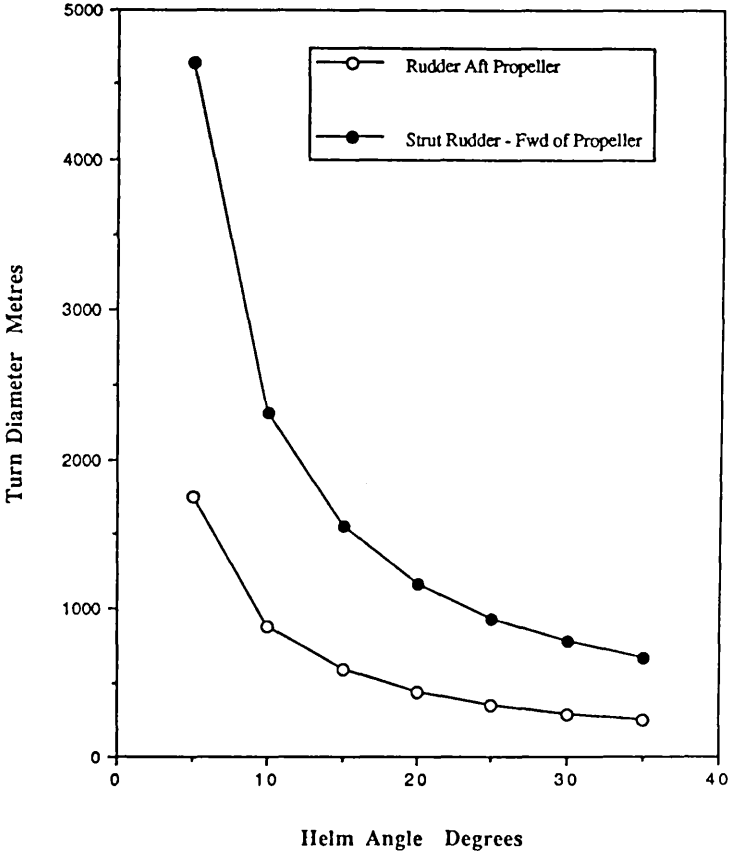

Fig 4.14 Patria Hullform - Rudders Fore & Aft of Propellers. Turning Diameter / Helm Angle. No Imaging Effects.

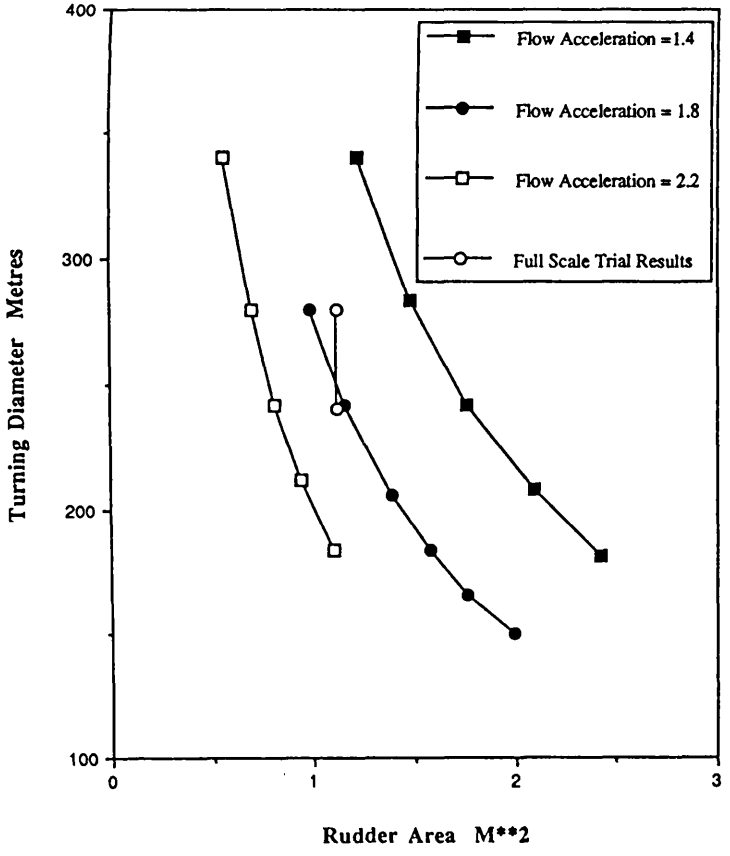

Fig 4.15 Turning Diameter / Propeller Flow Acceleration. (M.V. Patria)

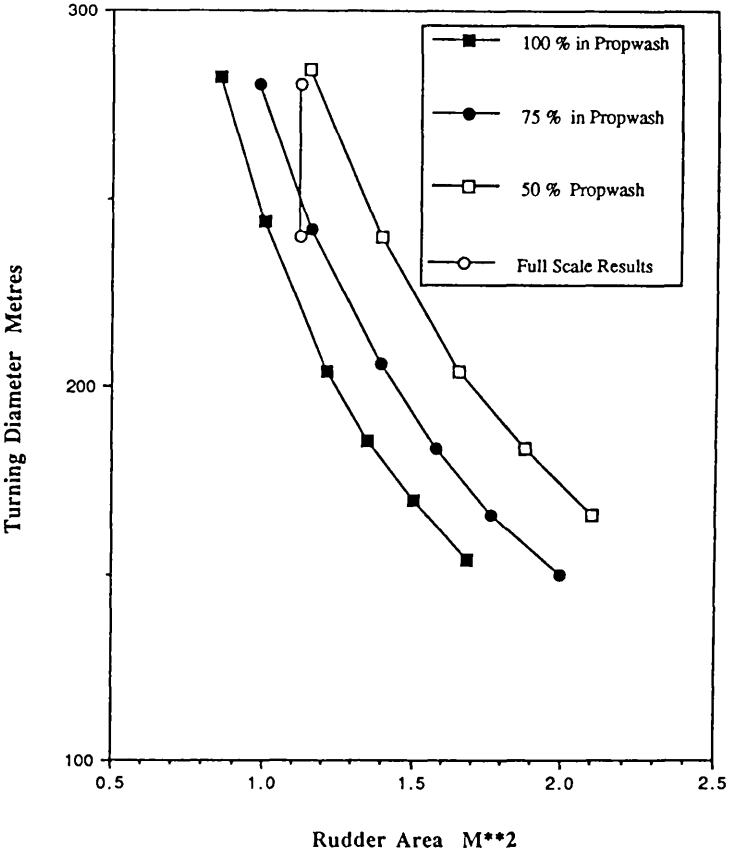

Fig 4.16 M.V. Patria - Turning Diameter / Rudder Area, % of Rudder in Propeller Accelerated Flow.

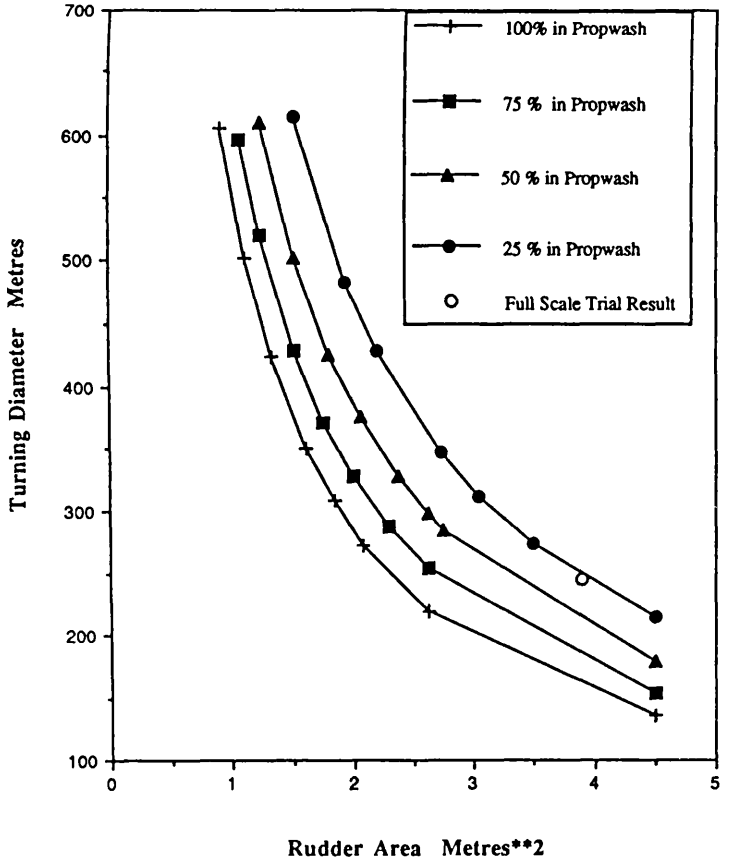

Fig 4.17 S.S.P. Kaimalino - Turning Diameter / Rudder Area, % of Rudder in Propeller Accelerated Flow.

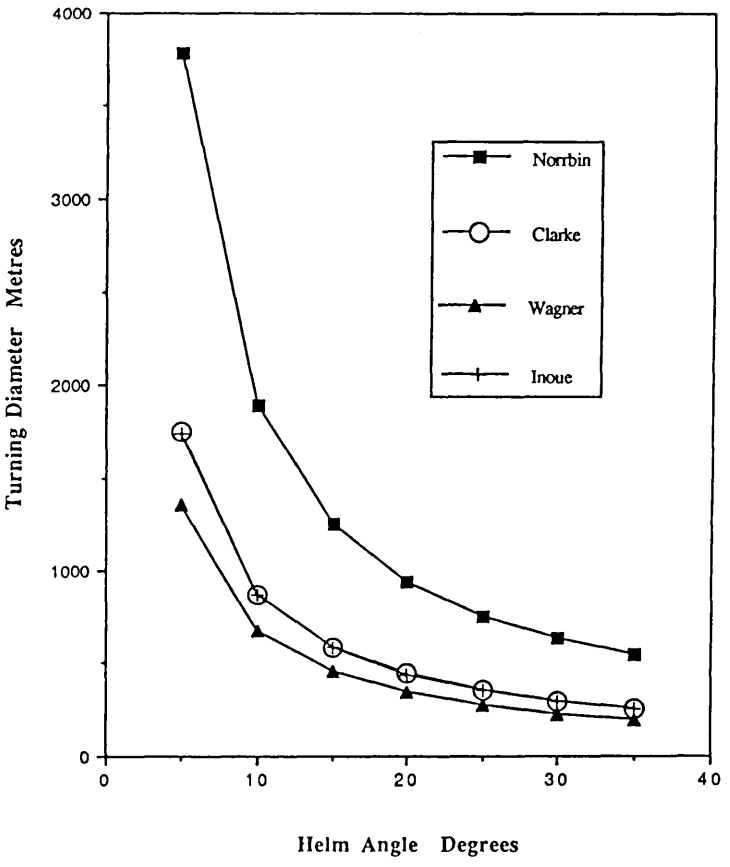

Fig 4.18 M.V. Patria - Turning Diameter / Helm Angle, Simulations due to Clarke, Wagner, Norrbin and Inoue.

Fig 4.18 presents a comparison of turning performance for the M.V. Patria. The four simulations presented represent four alternative regression data fits, attributable to Clarke, Wagner, Norrbin and Inoue respectively. As shown in Fig 4.18, manoeuvring performance predictions due to Clarke and Inoue are almost identical. The simulation attributable to Wagner Smitt shows reasonable agreement with this pair however it will be noted that the prediction using Norrbins equations is very different. This is most likely due to the quality of data and regression techniques applied by Norrbin in formulating (Equations 4.17).

A comparison of 'SWATHMAN' predictions with full scale trials data for all seven vessels is summarised in Table 4.2.

The predictions obtained tend to underestimate turning diameter slightly, this was particularly noticeable in the case of the two Japanese vessels, S.S.C. Seagull and Ohtori. Overall however predictions from the program were found to agree fairly closely with full scale trial results. This may be expected in the case of the M.V. Patria whose geometry was used to calibrate the derivative calculation routines. However the good agreement observed between the predictions and trial results for the other six vessels confirms the validity of the approach.

It should be noted that all predictions were obtained assuming the ships centre of gravity to be at amidships. This clearly unrealistic assumption was made to provide consistency, since actual values of longitudinal centre of gravity (LCG) were not available for all vessels. The generally observed underprediction of turning diameters is most likely due to this assumption, since moving the LCG forward results in a more stable ship, i.e. one which is more difficult to turn. Tests confirm this; it was found that moving the LCG forward 2 metres increased the turning diameter of S.S.C. Seagull by 54 metres to 196 metres.

It is particularly interesting to note the close simulation of the turning performance of M.V. Ali. This vessel was the only one of the seven to be fitted with strut rudders, i.e. rudders sited unconventionally outwith the propeller race.

4.9 Future Work

Future work on the 'SWATHMAN' program would most profitably be directed

towards incorporating the non linear speed dependence of the derivatives. Such work may be based on an experimental or theoretical analysis of the relationships between Froude number and the derivatives, or upon a first principles theoretical approach to the determination of the manoeuvring derivatives. At present the former approach appears the most likely to be successful.

Further work on the interference effects between hulls would also be worthwhile. Since there is little information available at present, a series of model tests devised to determine the relationships between hull separation and the manoeuvring derivatives would be most valuable.

The incorporation of shallow water effects would be relatively easily accomplished and certainly not without value.

The program could be interfaced with one of the many commercially available ship manoeuvring simulators. In this way pilots may be given the opportunity of "test sailing" designs not yet built. Such simulators usually require data in the form of manoeuvring derivatives, since these derivatives are an integral part of the output from 'SWATHMAN' it should be a relatively simple matter to provide an interface module for the program.

4.10 Conclusions

The manoeuvring characteristics of SWATH vessels have been studied, demonstrated and simulated. This was achieved by means of literature review, full scale tests and the development of a manoeuvring prediction tool incorporating the best elements of currently available and accepted manoeuvring theory, suitably adapted for the novel geometry of the SWATH form.

Principal conclusions from the literature review may be summarised as follows :-

1. SWATH vessels are inherently very directionally stable. This is an advantage for missions requiring good course keeping in rough seas e.g. Sonar Surveillance Vessels.

2. In spite of this SWATH vessels can possess turning diameters equivalent to

comparable monohulls. However this can only be achieved by careful design of the control surfaces.

3. Slow speed manoeuvring is excellent due to the availability of large amounts of differential thrust from widely spaced propellers.

4. Unlike monohulls turning performance is very speed dependent for most SWATH designs. Turning diameters increase with speed as we move from the medium to high speed range, particularly for designs with surface piercing rudders.

A manoeuvring prediction program was developed for SWATH vessels operating in the low to medium speed range. This program determines the rudder size required for a given vessel, and estimates the resulting turning performance for that vessel. The program may be applied to SWATH vessels fitted with rudders both in and out of the propeller slipstream and possessing widely different resistance and propulsive characteristics.

The program has been run for a number of existing SWATH designs for which full scale trials information is available. The results/predictions from the program were found to agree closely with the actual values observed on trials.

In addition full scale manoeuvring trials on the 20 ton SWATH fishing vessel "Ali" have been conducted and data on the turning performance collected. This data will be analysed and the results reported in due course.

References to Chapter 4

1. MacGregor, J.R., Bose, N., and Small, G., 'Design and Construction of a Small Waterplane Area Twin Hull (SWATH) Vessel', Proceedings of World Symposium on Fishing Gear and Fishing Vessel Design, St Johns, Newfoundland , Canada, Nov 1988.

2. Waters, R.T., and Fein, J.A., 'Manoeuvrability of SWATH Ships', Proceedings of 19th American Towing Tank Conference, Ann Arbour, July 1980.

3. Fein, J.A., 'Vertical and Horizontal Plane Control of SWATH Ships', Proceedings of 7th Ship Control Symposium.

4. Whalen, J.E., and Kahn, L.A., 'SWATH Dynamic Simulation Model', Operations Research Inc, Technical Report 1093 Jan 1977.

5. Lee, C.M. , 'Theoretical Prediction of Motion of SWATH Ships in Waves', DTNSRDC Report 76-0046 Dec 1976.

6. Fein, J.A., and Waters, R.T., 'Rotating Arm Experiments for SWATH 6A Manoeuvring Predictions' , DTNSRDC SPD Report 0698-01, July 1976

7. Fein, J.A., 'Rotating Arm Experiments for the Stable Semi-Submerged Platform (SSP) Manoeuvring Prediction' , DTNSRDC SPD Report 0698-02, September 1977.

8. Hart, C.J. et al, 'Rotating Arm Experiment for an Extended Strut SWATH Ship as Represented by SWATH 6E' , DTNSRDC SPD Report 0698-03,September 1983.

9. Fein, J.A., 'The Application of Rotating Arm Data to the Prediction of Advanced Ship Manoeuvring Characteristics', Proceedings 18th American Towing Tank Conference, Maryland August,1977.

10. Eda, H. et al, Report of the Technical Commitee on Steering and Manoeuvring, Proceedings 18th American Towing Tank Conference, Maryland August,1977.

11. Warren, N., Private Communication - A.F. Miller regarding manoeuvring performance on trials of the M.V. "Patria". Nov 1990.

12. Nethercote, W.C.E. et al, 'Manoeuvring of SWATH ships', Proceedings of 20th American Towing Tank Conference, Hoboken, New Jersey, July 1983.

13. Narita, H., and Mabuchi, Y., 'Design and Full Scale Test Results of Semi-Submerged Catamaran (SSC) Vessels', Proceedings 1st International Marine Systems Design Conference (ZMSDC) , London 1982.

14. Oshima, M., et al, 'Experiences with 12m Long Semi Submerged Catamaran (SSC) "Marine Ace" and Building of SSC Ferry for 446 Passengers', Proc. AIAA/Sname Advanced Marine Vehicles Conference, Baltimore, Maryland, Oct 1979.

15. Norrbin, N.H., 'Theory and Observations on the Use of a Mathematical Model for Ship Manoeuvring in Deep and Confined Waters', Meddelanden SSPA No 68, 1971 (Sweden).

16. Mandel, P., 'Ship Manoeuvring and Control', Principles of Naval Architecture, SNAME , 1967, pp 463-606.

17. Nomoto,K.,Taguchi,T.,Honda,K.,and Hirano,S., 'On the Steering Qualities of Ships', International Shipbuilding Progress, Vol 4. No 35, July 1957.

18. Norrbin, N., 'Zig-Zag Test Technique and Analysis with Preliminary Statistical Results', SSPA Allmann Report, No 12 1965.

19. Wagner Smitt, L., 'Steering and Manoeuvring Full Scale Model Tests', European Shipbuilding 1970(19) No 6 and 1971(2) No 1.

20. Innoe, S., Hirano, M., Kijima,K., 'Hydrodynamic Derivatives on Ship Manoeuvring', International Shipbuilding Progress , Vol 28, No 321, May 1981.

21. Clarke, D., Gedling, P., and Hine,G., 'The Application of Manoeuvring Criteria in Hull Design Using Linear Theory', Proceedings of the RINA Spring Meetings, London,1982.

22. Nomoto, K., 'Researches on the Manoeuvrability of Ships in Japan', Society of Naval Architects of Japan, 60th Anniversary Series Publication 1966, Vol. 11.

23. Kim, K.-H., and Reed , A.M., 'Propeller Design of U.S. Navy's SWATH T-AGOS19',

24. Whicker, L.F., and Fehlner, L.F., 'Free Stream Characteristics of a Family of Low Aspect Ratio Control Surfaces', DTMB Report 933, May 1958.

25. McGregor, R. C. , 'Report on the Full Scale Trials of the 20 tonne SWATH Fishing Vessel M.V. Ali', Marine Technology Report in Preparation , September 1991.

26. Luedeke, G., et al , 'The RMI SD-60 SWATH Demonstration Project - Addendum', Proceedings RINA First International Conferance on SWATH Ships and Advanced Multi-Hulled Vessels, London, 1985.

27. Coe, T. J., 'A Technical Evaluation of the 60 Foot SWATH Ship Halcyon to Determine Utility in Coast Guard Operations', Proc. Intersociety Advanced Marine Vehicles Conference, Washington, June 1989.

28. Adachi, T., Araki, T., and Kan,T., 'Initial Design of Semi-Submerged Catamarans', Journal of Kansai Society of Naval Architects No 185, June 1982.

CHAPTER 5

ENVIRONMENTAL LOADING

5.1 Introduction

One of the greatest drawbacks of SWATH geometry is the high (relative to a monohull) structural weight fraction. This is due to the increased surface area / volume ratio associated with the vessels. Since structure comprises the largest single weight group of any vessel, and on SWATH may be up to 40% of the displacement, it is obvious that reductions in structural weight significantly improve the capability of the ship. Increases in the capability of the vessel may result from the increased payload and therefore range afforded by reductions in structural weight. Alternatively if the savings in structural weight are allowed to reduce ship displacement, then overall ship construction and operation costs may be reduced.

Structural design commences with an understanding of the loads and load paths through the structure. An accurate definition of the governing loads is therefore essential in order to design a ship with adequate but not excessive structural integrity.

Unfortunately traditional design approaches cannot be applied to the unconventional SWATH form. Current SWATH structural design criteria are therefore still largely empirical, although there are few SWATH ships in service which can provide feedback.

Without the extensive database of full scale experience, available for monohulls, it is necessary to use theoretical methods and model tests for the prediction of loading. The predictions obtained are applied together with wave spectral analysis techniques and finite element analysis in an effort to determine suitable structural scantlings for a given SWATH vessel.

Considerable uncertainty still exists regarding the reliability of currently available prediction techniques.This study aims to review and compare available methods and to determine the current 'state of the art' in SWATH wave load prediction.

5.2 Loading Definition

The 'primary', or governing, global loads on a SWATH vessel are:-

1. Side Force *Fy*
2. Vertical Shear Force *Vz*
3. Transverse Bending Moment *Mx*
4. Yaw Splitting Moment *Mz*

These are illustrated in Fig 5.1.

In direct contrast with monohulls, where the dominant loading is longitudinal bending, the primary loading for SWATH vessels is a transverse bending moment across the connecting deck and struts. This bending moment is primarily due to wave induced side forces on the hulls and struts. In addition still water bending moments, due to non uniform weight / buoyancy distributions, increase the 'prying' moment. The situation is aggravated where a twin hull vessel is operated in oblique seas, when longitudinally non uniform distributions of wave induced side load result in yaw splitting moments.

The other global loads which govern design are the vertical shear forces across the box structure. These forces consist of two parts due to the dead load weight of the box with acceleration effects, and to differential heaving of the twin hulls. The dead load weight of the box produces shear loads which maximize at the box strut intersection and fall to zero at the ship centreline. The differential loads due to heaving are constant across the box span.

Longitudinal bending moments and pitch torsional moments occur too, due to differential instantaneous buoyancy forces acting on the twin hulls. In addition longitudinal and transverse shear forces in the cross deck structure result from the wave induced side force and differential surging of the twin hulls in quartering seas. However these loadings are relatively insignificant and may be considered as 'secondary' global loads.

It has now been well established, by means of extensive model testing together with full scale trials on the S.S.P. Kaimalino, that maximum transverse bending moments occur when a SWATH vessel is at, or near zero speed in beam seas (Ref 1).

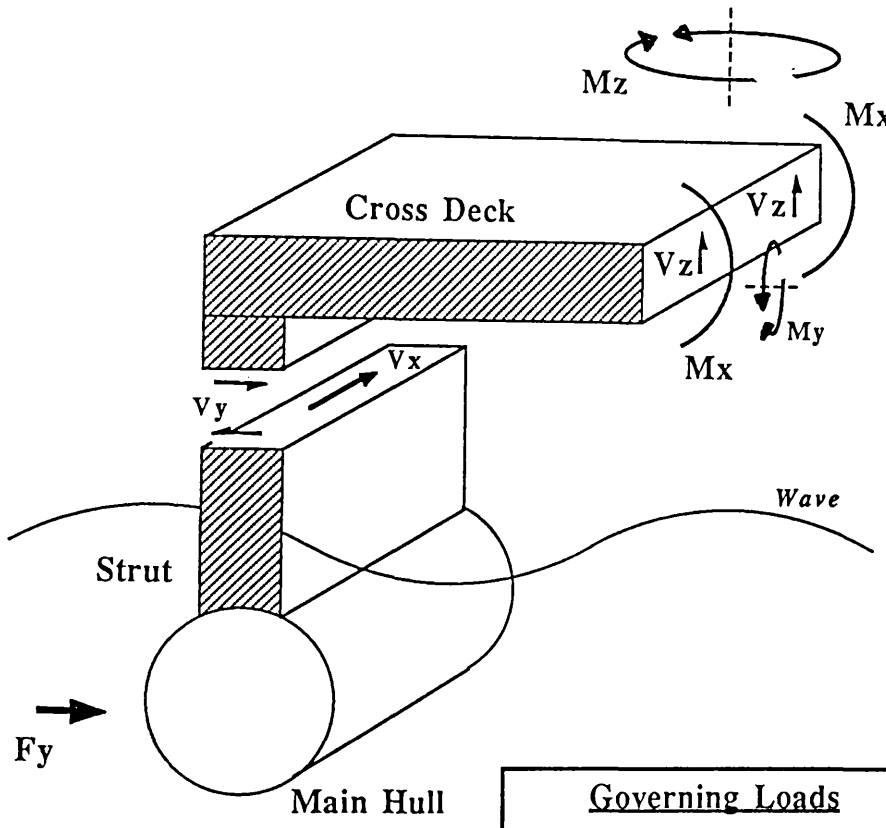

Governing Loads

Fy	Wave Induced Side Force
Mx	Transverse Bending Moment
Mz	Yawing Bending Moment
Vz	Vertical Shear Force

Fig 5.1 Schematic Representation of a SWATH Illustrating the Global Loadings Present

Since the yaw torsional moments are greatest for headings between 15 and 45 degrees off the beam (Ref 2). It is therefore likely that these yawing moments will combine with the transverse moment to define limiting sea states for vessels operating in bow quartering seas (Ref 3,4).

Results to date indicate that wave induced side load on SWATH forms reaches a maximum for wavelengths 3-4 times the underwater beam of the vessel (Ref 5). In addition it has been noted that maximum sideload may vary by a factor of two depending on ship configuration.

Side load is found to be relatively unaffected by changes in hull separation, however it increases rapidly with increasing draught (Ref 5). Increasing draught also increases the lever arm for cross deck bending moment, (assuming the wet deck/waterline clearance remains constant). Wave induced bending moments are therefore worse on SWATH vessels than on conventional catamarans, the requirements of seakeeping and structural weight reduction proving to some extent conflicting.

From the foregoing it will be realised that the reliable prediction of wave induced side load is vital. One of the principal thrusts of the U.S. Navy's development effort has been to determine the magnitude of this load and to develop a method for predicting the maximum lifetime values likely to be experienced (Ref 6).

In this study attention has therefore been focused on the prediction of wave induced side load and associated cross deck transverse bending moment. The prediction of loading response by experimental, analytical and empirical means is discussed, and techniques for the evaluation of short term and lifetime extreme values are introduced.

5.3 Techniques Available

5.3.1 Structural Response Measurements from Model Tests

Despite the development of several analytical techniques, model tests remain the most reliable means of predicting wave loading on SWATH ships. Model tests are to date the only way of investigating changing wave patterns due to the "tunnel" effects in catamaran and SWATH vessels. In addition they have until very recently been the only way of incorporating speed effects.

The most extensive program of tests to date was carried out at the David Taylor Naval Ship Research and Development centre during the 1970's. Eleven single strut SWATH configurations were tested together with two tandem strut full scale vessels including the SSP Kaimalino. On completion of testing two of the single strut models were converted to tandem strut configurations and retested. In this way data for 15 vessels was collected.This work has been well reported and results are freely available (Ref 6-13). The experiments covered vessels ranging in size from 3,000 -100,000 tonnes displacement. It was the results from these tests together with analytical predictions utilizing 2D theory, that Sikora et al (Ref 6-8) used to develop their 'standard' algorithm for the prediction of side loads on SWATH ships.

A similar program of work was undertaken by the joint Canadian / Netherlands SWATH Ship Project. Collaboration between the Defence Research Establishment Atlantic DREA of Canada and MARIN (Netherlands) led to the development of an algorithm for predicting design side load based on the results of model tests on approximately 10 single strut designs. This algorithm is incorporated in the SWATH concept exploration model developed by Nethercote et al (Ref 14,15). Predictions from the algorithm are believed to be reliable , but unfortunately both the algorithm and the test data from which it was derived remain unpublished.

Model tests in Britain have been limited to those tests performed at the Admiralty Research Establishment at Haslar (Ref 16) and the University of Glasgow's Hydrodynamics Laboratory (Ref 17-20). Three vessels of tandem and single strut configuration have been tested at Glasgow while the emphasis at ARE Haslar has been on a single strut model closely based on a U.K. MOD Sonar Surveillance Vessel design. Both sets of tests were principally designed to provide validation of analytical prediction tools under development.

Mitsui Engineering and Shipbuilding have built more SWATH vessels than any other organisation. The company have conducted many loading tests at model and full scale. Despite this hardly any information is freely available from Japanese sources (Ref 21,22).

5.3.2 Analytical Evaluation of Response

Theoretical predictions of wave load are generally developed in conjunction with predictions of motions, since these two problems are closely related. The prediction of these loads was initially pioneered by Lee and Curphey at the David Taylor Naval Ship

Research and Development Center (DTNSRDC) during the 1970's (Ref 9,23,24). The method they developed is closely based on the analytical method previously developed at the centre for catamarans.

Although the techniques have evolved significantly since, the method offered by Lee and Curphey (Ref 9) still offers acceptably accurate results for the limiting condition (zero speed in beam seas), and is less intensive in terms of computer time than other methods. For these reasons it remains to date one of the "industry standards".

All currently available methods for the prediction of wave loads on SWATH structures, rely on one of two approaches :-

1. 2D Strip Theory
   (Using source sink distribution techniques or approximate methods)

2. 3D Panel Theory
   (Always based on source sink distribution techniques)

In the following pages both these approaches are introduced and briefly described, together with brief general statements on their relative merits.

2D Strip Theory

This was the approach adopted by Lee and Curphey. Essentially it involves splitting the vessel into a number of two dimensional transverse "strips". The wave pressure distribution and the total wave load is then derived by integrating the pressure on each of these discrete elements along the complete vessel.

In order to predict structural responses by this technique there are five components of wave and motion induced load which must be evaluated :-

a) Body Mass or Inertia Force,
b) Incident Wave or Froude-Krylov Force,
c) Diffracted Wave Force,
d) Hydrodynamic Force, due to body motion and
e) Hydrostatic Restoring Force, due to body motion.

The first of these is calculated directly from the mass and acceleration of the body, whereas the remaining components are derived by integrating the corresponding pressure distributions acting on each "strip" over the wetted surface of the vessel.

The pressure distributions, due to wave acceleration and rigid body motions, may be found directly from the solution of diffraction and radiation potentials respectively. Alternatively a method such as the small body approximation (Ref 25) may be utilized to estimate the wave forces. This approach allows reasonable estimates of wave loadings to be produced quickly and cheaply at the feasibility stage of the design process.

The resulting force components are then superimposed taking phase angle in to account in order to determine the total structural load acting on the structure.

In order to simplify the problem, so that 2D strip theory may be applied to twin hull vessels, the following assumptions were proposed by Lee and Curphey [24]:-

1. The hulls are assumed symmetrical about the vertical centre plane and to possess longitudinal symmetry, therefore, only the sway, heave and roll modes of motions are excited by incident beam waves,

2. Without pitching or yawing motion, the three-dimensional loading problem has been simplified into loadings on an equivalent two-dimensional body,

3. The ship is approximated by uniform twin cylinders having cross sectional shape equal to a representative section (usually midship section) of the ship analysed,

4. The prediction is limited to loads exerted in the transverse cross section plane. Thus, only the the vertical bending moments, horizontal shear forces and vertical shear forces are considered in beam seas.

The above technique incorporating wave diffraction and body motion may be used to predict the dynamic structural loading on a twin hull ship with or without forward speed at any heading. However in the 2D method no account is taken of interaction or interference effects between the strips. Despite this, analytical predictions using this method at DTNSRDC have been compared with a large number of experimental and several full scale test results. Good correlation has been observed confirming the basic validity of the developed analytical method (Ref 9).

3D Panel Theory

This technique is similar to the 2D method but as the name suggests, account is also taken of vessel and wave motion in the third dimension. The vessel is subdivided into a number of three dimensional panels rather than 2D strips. In this way non uniform pressure distributions may be incorporated. The 3D approach allows consideration of a greater range of hullforms than 2D "strip" techniques.

The pressure distribution on each panel, due to wave acceleration and rigid body motions, is evaluated by solving diffraction and radiation potentials respectively. The application of 3D theory is relatively new, since the vastly increased requirements (over 2D methods) for computing power have been unavailable until relatively recently.

Programs utilizing this approach are now available (Ref 26,27,28). The 'MARCHS' suite recently developed at Glasgow University is a good example of its kind. These programs will predict first and second order wave forces (moments) for any type of vessel operating at arbitrary headings in regular waves, with or without forward speed.

These programs represent the current 'state of the art' in wave loading prediction tools. Their primary advantages over 2D methods are their versatility with respect to hullform configuration and their ability to solve problems including torsional loads. Quartering seas can be more accurately dealt with using 3D methods. Given the present advances in computer power it seems probable that these programs will shortly supersede those based on 2D strip theory and become the new "industry standards".

Hydro-Elasticity Theory

A substantially different approach to those previously discussed was developed at Brunel University (Ref 28-33). This approach is based on generalised linear hydroelasticity theory and finite element modelling techniques.

The major difference between this approach and seakeeping-based load prediction methods is that the structure is treated as an elastic one, whereas in seakeeping based approaches the vessel as regarded as a rigid body.

The method can be considered to consist of two parts; a "dry"part and a "wet" part.

The first step involves determining the structural properties of the vessel including

detailed information on the mass, damping and stiffness of the structure in the dry or vacuo mode. A finite element package is utilised to determine these quantities and thence the dynamic characteristics of the structure in the absence of external forces.

Once the "dry" dynamic characteristics of the vessel are known the vessel is analysed in waves (external forces) to determine the generalised fluid loading on the structure. This "wet" analysis is performed using a 3D source sink distribution panel method which considers the influence of forward speed.

This analytical prediction method has recently been extensively improved to account for the effects of non-linear fluid forces and extended to assess response behaviour in the time domain (Ref 33). The method has been employed to analyse the structural responses (ie. displacement, distortions, bending moments, shearing forces, torsional moments and stresses) of an idealised flexible SWATH travelling in regular waves (Ref 30-33).

Hydro-Elasticity theory is by far the most complex technique to be employed in the effort to predict wave induced loadings on a SWATH structure. As such it may be assumed that the technique will provide accurate estimates for these loadings, however the method has several serious drawbacks. Some authorities suggest that although promising in concept, it is probable that mass-inertia, added mass and damping effects caused by rigid body motion are large enough to negate the effects of those due to deformations of the vessel.

The method is extremely heavy on computer time and the programs are reported to be "user-unfriendly" requiring a skilled operator with detailed knowledge of the structural properties of the testcase vessel. They cannot therefore be used at the feasibility stage of the design process, rather they should be regarded as a checking routine for the final design. This severely limits the applicability of the software in the design environment.

5.3.3 Spectral Analysis Techniques

The techniques previously described predict the instantaneous loading experienced by a vessel subject to previously defined wave conditions. In order to predict likely values for the maximum lifetime loading on the structure, operational profiles for the vessel must be taken into consideration along with the magnitude of sea states and their probability of occurrence.

Several techniques exist to determine this value. Sikora et al (Ref 6-8) applied the following method to predict the once in a lifetime maximum loading likely to be experienced by a given vessel. The extreme value or once-in-a-lifetime maximum loading is defined as the loading which is exceeded once in the lifetime of the ship.

For any given vessel the operating mode may be defined in terms of its speed, heading relative to the waves and the sea conditions in which it operates. The sea conditions are generally described in terms of wave heights and spectral shapes (fully developed, rising sea, swells etc). The probability of operating in any one mode is the product of each of these individual probabilities. This probability value depends on the role and operating environment for which the vessel was designed. For each operating mode there exists a unique amplitude response spectrum corresponding to that combination of sea and operating condition. This amplitude response spectrum is given by the product of the relevant wave spectrum and response amplitude operators for that operating mode. (The response amplitude operator or RAO is defined as the Ship Response Amplitude / Wave Amplitude). Accordingly, each response function defines an amplitude probability distribution where the number of cycles in each of these distributions is equal to the time spent in that operating mode multiplied by the wave encounter frequency for that spectrum.

For a narrow banded response and normally distributed exciting function , each response function may be described in terms of a Rayleigh distribution of response magnitude and corresponding number of cyclic responses. The number of response cycles exceeding specified limits may then be determined from the area under sectors of this curve. Using this technique, an exceedence curve of response may be derived for each and every operating mode. The total lifetime response spectrum is given by the summation of all these individual spectra. From this final spectrum the extreme value loading is calculated as the loading which is exceeded once in the lifetime of the ship.

From the foregoing it will be realised that evaluation of maximum lifetime loading using long term prediction techniques is a complex and lengthy procedure. The reliability of the method is also questionable. Alternatively predictions based on short term wave statistics are comparatively readily available and therefore frequently used.

Ochi (Ref 34) has demonstrated the value of prediction techniques based on short term wave statistics. A simplified short term extreme value prediction method was therefore adopted for this study. The technique and equations used are detailed in Appendix C.

5.3.4 Empirical Algorithms

The first algorithm for the prediction of wave induced side force on SWATH ships was derived by Sikora et al (Ref 6). This was based on a series of model tests undertaken at DTNSRDC. Using the same database the American Bureau of Shipping have produced their own loading algorithms for SWATH vessels. These are presented in the form of a "Preliminary Guide for Building and Classing of Small Waterplane Area Twin Hull (SWATH) Vessels" . This guide, which remains unpublished at the time of writing (September 1991), is to date the only specific attempt by a classification society to predict SWATH vessel loadings.

In addition Det norske Veritas have recently updated their Rules for the Classification of High Speed and Light Craft. The revised rules now contain formulae suitable for estimating the accelerations and loading on fast displacement craft including SWATH vessels.

Sikora et al suggest that the Maximum Lifetime value of the Wave Induced Side Force on the structure may be taken as :-

$$F = \Delta D T L \text{ Tons} \qquad \text{(Eqn 5.1)}$$

Where :-

Δ = Displacement (ton)

$D = 1.55 - 0.75 \tanh(\Delta / 11000)$

$T = 0.532 \text{ draft (ft)} / \left(\sqrt[3]{\Delta}\right)$

$L = 0.75 + 0.35 \tanh(0.5 L_s - 6.0)$

$L_s = \text{strut length (ft)} / \left(\sqrt[3]{\Delta}\right)$

This force may be taken to act at a point at half draught,

The Maximum Wave Induced Transverse Bending Moment acting on the cross deck structure is therefore :-

$$BM = \Delta DTL.X \quad \text{Tonsft}$$

(Eqn 5.2)

Where :-

$$X = (\text{Height of Section} - \text{Draft} / 2)$$

These values correspond to a ship operating for 3600 days in a severe portion of the North Atlantic at random headings.

In addition to these wave loads, buoyancy forces due to the hull and struts together with dead loads may contribute to the transverse bending moment depending on the geometry.

Horizontal Torsional Moments can be calculated by multiplying the side force defined above by the strut length and a "torque arm factor" of between 0.05 and 0.25 dependent on heading (Ref 7).

The maximum wave induced differential Shear Force in the cross deck structure may be assumed to be 1/4 of the side force for conceptual designs (Ref 7).

It should be noted that these algorithms were obtained from regression fits on data obtained from model tests on 15 SWATH models for the range 3000-30,000 tonnes displacement. The algorithm is therefore strictly only valid for vessels of 3000 tonnes or more displacement. In practice, as will be seen later, the algorithms may be applied with reasonable accuracy to vessels of much smaller displacement, however in these cases the results must be treated with some caution.

Chalmers (Ref 2) reports the following refinements to the work of Sikora et al for tandem strut designs. The maximum expected side force in 20 years life with 180 days/year spent at sea (3600 days) is :-

$$F = \Delta DTLg \quad kN/m$$

(Eqn 5.3)

Where :-

g = gravitational acceleration

Δ = Displacement (ton)

$D = 1.55 - 0.75\tanh(\Delta / 11000)$

$T = 0.532\text{draft (ft)} / \left(\sqrt[3]{\Delta}\right)$

$L = -0.725 + 2.989\tanh\left(L_e / 24\right)$

$L_e = L_s + 0.5(L_{lh} - L_s)(D_h / t)(1 - 0.1G / D_h)$

L_s = strut length (ft) $/ \left(\sqrt[3]{\Delta}\right)$

L_{lh} = lower hull length $/ \left(\sqrt[3]{\Delta}\right)$

D_h = lower hull diameter $/ \left(\sqrt[3]{\Delta}\right)$

G = gap between struts $/ \left(\sqrt[3]{\Delta}\right)$

t = draught $/ \left(\sqrt[3]{\Delta}\right)$

For single and twin strut vessels,

Torsional (Yawing) Moment on the vessel : -

$$M_T = 0.13F_{MAX}L_s \qquad \text{(Eqn 5.4)}$$

Shear Force in the Cross Deck Structure : -

$$SF = 0.25F_{MAX} + 1.25\ g\ M_{b/2} \qquad \text{(Eqn 5.5)}$$

Where $M_{b/2}$ = half the box mass

This force is greatest in the region just inboard of the haunch.

Both these formulae were deduced from unpublished US sources.

In addition Chalmers recommends that the vessel be designed to withstand Vertical (Pitch) Torsional moments resulting from grounding on two diagonally opposite corners. This is the most important accidental loading and will provide the most severe values of torsional moment experienced by the vessel.

Chalmers also offers some suggestions for combining primary loadings.
These are summarised for the headings given in Table 5.1.

Wave Heading	Beam	Bow / Quartering	Head / Following
Loading			
Transverse Bending	Design	0.8 Design	0.15 Design
Shear Force	Design	Design	Design
Horizontal Torsion	0.25 Design	Design	0.10 Design
Longitudinal Bending	0.15 Design	0.8 Design	Design

Table 5.1 Suggested Combination Factors for Wave Induced Loads

(Ref 2)

A vessel should be designed for the worst combination of these loads.

The above algorithms are intended for use at the preliminary or concept design stage, ie. once the main dimensions have been decided. However in many cases the designer will also require an estimate of loading at the feasibility stage of the design process, i.e. before the main dimensions are selected. To this end University College London (UCL) derived the following formula (Ref 35) based upon a regression analysis of published data,

$$F = K \times \Delta^{0.77}$$

(Eqn 5.6)

Where K= 7.94 for single struts and 4.26 for tandem struts.

It will be shown later that this formula is only applicable to vessels in the range 3000 tonnes displacement and upwards. This to be expected since it was derived from regression analysis of data for vessels of that size.

For smaller vessels, RMI Ltd, the designers and builders of the 60 tonne SWATH demonstrator 'Halcyon', have estimated the maximum side force on a vessel of this size to be around 0.95-1.0 times the displacement (Ref 36,37).

$$F = (0.95 - 1.0)\Delta$$

(Eqn 5.7)

The RMI estimate agrees surprisingly well with the maximum life time value of side load for a 3000 tonne SWATH vessel given by Sikora et al (Ref 6) as equal to 0.94 times displacement.

These algorithms together with those formulae presented in the ABS "Preliminary Guide for Building and Classing of Small Waterplane Area Twin Hull (SWATH) Vessels" and the recently available DNV formulae, represent the full extent of currently available semi-empirical techniques specifically intended for predicting the wave induced global loadings on Small Waterplane Area Twin Hull ships.

5.4 Classification Society Approaches

5.4.1 American Bureau of Shipping

A.B.S. are to date the only classification society to have formulated rules dedicated to SWATH vessels. The rules remain to date unpublished and exist only in a limited circulation document entitled "Preliminary Guide for Building and Classing of Small Waterplane Area Twin Hull (SWATH) Vessels" (Ref 38). Unlike the Lloyds catamaran and DnV fast craft rules (Ref 39-41), the ABS SWATH guide applies only to steel construction and there are no limits on length, speed or operability.

The guide states that "the SWATH should be analysed for structural adequacy in a seaway using anticipated loads, including gravity loads together with environmental loads due to the effects of waves. The wave loads are required to be determined from ship motion response in realistic sea conditions." Vessels to be classed for unrestricted

service are to be analysed using wave loads determined from seakeeping analysis based on typical North Atlantic Sea spectra. This condition may be relaxed for vessels operating in a limited region.

Wave and motion induced loads are calculated using a program developed at ABS. These programs are based on two dimensional source-sink distribution methods. These account for hydrodynamic interaction between the hulls, to compute hydrodynamic coefficients and wave forces, and solve for the six degrees of freedom, motions of the vessel oscillating in regular waves of unit amplitude.

The analysis is performed at zero speed only since model tests indicate that the critical loads are maximized in this condition. The RAO's of the critical loads are then combined with relevant sea spectra to obtain load spectra from which short term extreme values can be easily predicted .

ABS identify side force and prying moment together with splitting (yawing) moment as the critical loading cases. In-plane axial stresses in the box (due to side force) and struts (due to inline and dead loads) are generally not considered for concept level structural design studies. Torsional loads have also been shown to produce negligible stresses and are therefore neglected at this stage.

In addition to the direct evaluation method described above, the new guide offers concept level design algorithms for the major global loads. These algorithms are derived from U.S. Navy model test data and consequently bear close resemblance to those offered by Sikora et al (Ref 6-8).

5.4.2 Lloyds Register of Shipping

Lloyds Register of Shipping do not at present have rules specifically applicable to SWATH forms. However their Provisional Rules for the Classification of High Speed Catamarans (Ref 39) (Provisional @ 31/9/90) are in theory applicable to all alluminium passenger carrying catamarans where, in general, the length of the catamaran exceeds 15 metres and the speed exceeds 20 knots.

The following are extracts from the rules:-

"For the purpose of the Rules, a catamaran is defined as a craft with two hulls, of either symmetric or asymmetric form, linked by a bridging structure".

"The craft may be of the displacement, semi-planing or wave piercing types."

Since these definitions obviously encompass SWATH vessels, it must be assumed that the rules are applicable. It must be remembered that a SWATH ship is merely a form of modified catamaran.

General Considerations

1. For craft exceeding 65 metres in length or 45 knots the loading and scantling determination methods given in the Rules must be supplemented by direct calculation techniques.

2. For vessels where Speed/(Square root of the Waterline Length) is outside the range 3.6-10.8 , the loads must be specially considered.

3. Craft built and classed in accordance with the Rules are assigned an operational envelope , based on speed, wave height and corresponding displacements. (See Appendix D of this thesis)

4. Alternative methods of determining the accelerations and loads will be specially considered by Lloyds if based on model tests, full scale measurements or generally accepted theories.

5. The accelerations of fast displacement craft e.g. SWATH's will be specially considered based upon model tests, full scale measurements or generally accepted theories.

N.B. The rules do not offer any formulae suitable for the determination of the accelerations of fast displacement craft e.g. SWATH vessels.

Global Loads on the Cross-Deck Structure

Twin Hull Transverse Bending Moment (about a longitudinal axis),

$$M_B = 2.5\Delta b a_v \quad \text{kNm}$$

(Eqn 5.8)

Twin Hull Torsional Connecting Moment (about a transverse axis),

$$M_T = 1.25\Delta L_S a_v \quad \text{kNm}$$

(Eqn 5.9)

Vertical Shear Force (at the cross-deck centreline),

$$Q = 2.5\Delta a_v \quad \text{kNm}$$

(Eqn 5.10)

Where:-

- a_v Vertical Accel'n in 'g' at the LCG (Long Centre of Gravity).
- b Transverse Separation of the two hulls in m
- L_s Waterline length in m (not less than 0.86 Length oa)
- Δ Ship Displacement in tonnes

It is instructive to note that the rules offer no empirical formulae for the direct calculation of horizontal (yawing) torsional moments. This loading has been identified by the U.S. Navy and the A.B.S. as one of the two most important for SWATH vessels (Ref 3,7,8). This omission points to the light planing/semiplaning catamaran heritage of the rules and leads to the inevitable conclusion that the other formulae must be treated with caution when applied to SWATH forms. In addition it should be noted that these rules do not provide algorithms suitable for the determination of the vertical accelerations of fast displacement craft, these values must be found by other means e.g model tests or full scale measurements.

5.4.3 Det norske Veritas

DNV do not have rules specifically intended for SWATH vessels either. The 1985 "Rules For The Classification of High Speed Light Craft" (Ref 40) have however

recently been substantially revised and updated (Jan 1991) to cover fast displacement craft including SWATH's. (Ref 41).

These rules cover the design and construction of high speed and light craft constructed in steel, aluminium or fibre composites.

For the purposes of these rules high speed craft are defined as vessels with Froude No's greater than 0.7. Light craft are vessels designed for light displacements compared with steel ships loaded in accordance with ILLC convention. Thus a light craft is defined as a vessel with a full load displacement not more than :-

$$\Delta = (0.13LB)^{1.5} \quad \text{tonnes}$$

(Eqn 5.11)

For catamarans the breadth of the tunnel at load waterline is to be deducted from B. Vessels with displacements in excess of the above requirements are to be classed in accordance with the rules for steel ships.

Many small SWATH vessels fall into the above categories, particularly those built in aluminium for the purpose of carrying passengers.

In common with Lloyds Register, craft built and classed in accordance with the DNV rules are assigned an operational envelope, based on speed, wave height and corresponding displacements. Details of these service restrictions may be found in Appendix D. It is interesting to note that the 1991 rules include more precise definitions of these operability limits than the previous (1985) rules. This presumably reflects a greater awareness on the part of DNV of the increasing range of applications and "rough water" roles now envisaged for catamarans and SWATH's.

Global Loads on the Cross-Deck Structure

The 1991 Rules offer two methods for estimation of transverse bending moment on the cross structure of a "catamaran" :-

1. For Planing and Semi-Planing craft in the Planing Mode,

Transverse Bending Moment in the Cross Deck Structure :-

$$M_T = \frac{\Delta a_{cg} b}{s} \quad kNm$$

(Eqn 5.12)

Where :-

a_{cg}	Design Vertical Acceleration in m/s**2
b	Transverse Separation of Hull Longitudinal Centrelines in m
s	Factor 4-8 Depending on Service Restriction (See Appendix D)
Δ	Fully Loaded Displacement in tonnes

This was the only formulae offered in the 1985 version of the same rules. Although it is not really applicable to displacement SWATH forms, it is included here because of its similarity to the Lloyds formulation. It is also demonstrated in Appendix F that incorporating suitable values of acceleration into this formula may produce reasonable values of transverse bending moment.

2. For High speed Displacement craft and Semi-Planing craft operating in the Displacement mode, DnV offer two formulae for the calculation of transverse bending moment. The first is acceleration based in its approach while the other relies on a static analysis of the forces acting.

DnV require the Twin Hull Transverse Bending Moment to be taken as the greater of:-

$$M_y = M_{y0}\left(1 - a_{cg}\right) \quad kNm$$

$$M_y = M_{y0} + F_y\left(Z - 0.75T\right) \quad kNm$$

(Eqn 5.13 , 5.14)

Where:-

$$a_{cg} = k\frac{C_w}{L}\left(0.85 + 0.25\frac{V}{\sqrt{L}}\right)g_0 \qquad ms^{-2}$$

(Eqn 5.15)

L, B, and T are the vessels length, beam and draught in metres.

C_w = Wave Coefficient for HS Displacement Craft
= 0.08L for unrestricted service

M_{y0} = Still Water Transverse BM kNm

Z = Height of Cross Structure NA above base in m

V = Vessel Speed in knots

F_y = Horizontal Splitting Force on Hull kNm

$$= 0.1L^2C_1C_2\left(1 - 0.1\frac{V}{\sqrt{L}}\right)\left(53 - \frac{L}{0.5B}\right) \text{ kNm}$$

(Eqn 5.16)

$$C_1 = 1.6 - \frac{6}{\sqrt{L}}$$

$$C_2 = 70 / \left(\frac{L}{T}\right)^{1.5}$$

An approximation for the still water transverse bending moment acting on a typical SWATH vessel is given in Appendix E.

The formulae given in the 1991 rules for shear force and pitch connecting moment remain unchanged from the acceleration based formulae given in 1985 : -

Shear Force in the Cross Deck Structure : -

$$S = \frac{\Delta a_{cg}}{q}$$

(Eqn 5.17)

q - Factor 3-6 Depending on Service Restriction (See Appendix D)

The limiting case given by these formulae corresponds to a condition where one hull is completely out of the water and its full static weight is supported by the transverse moment.

Pitch Connection (Torsional) Moment on Cross Deck Structure : -

$$M_P = \frac{\Delta a_{cg} L}{8}$$

(Eqn 5.18)

This Moment corresponds to a docking condition where the hulls are supported at diagonally opposite corners on points (Loa/4) fore and aft of the LCG respectively.

In common with the Lloyds rules no direct calculation method is offered for the evaluation of horizontal (yawing) torsional moment.

5.5 Comparison of Prediction Techniques

In order to compare prediction techniques it is necessary to select 'testcase vessels'. The SWATH M.V. Patria and the T-AGOS 19 were identified for this purpose since:-

1. They are feasible designs representative of two very different displacement ranges. Extensive geometric and structural details are available for both vessels.

2. The M.V. Patria is built in aluminium with a design speed of 30 knots. The vessel is therefore covered by the Lloyds and DnV rules for design and classification of high speed catamarans .

3. Extensive experimental and theoretical analysis of the T-AGOS 19 design has already been performed at DTNSRDC. Results are therefore already available for comparative purposes.

4. It seems likely, given the availability of information, that both vessels are destined to play an important part in later stages of the integrated structural design program for SWATH vessels currently underway at the University.

Once these vessels were adopted attention was focused on prediction techniques.

Since model testing was outwith the scope of this study, published experimental results were obtained. Unfortunately no suitable tests were ever performed on the model of the M.V. Patria. Adequate information is however available for the T-AGOS 19 and several other SWATH ships.

Secondly an attempt was made to evaluate transverse side load in beam seas directly by using the 3D 'MARCHS' suite of programs and by an approximate method developed for the study. ABS predictions of side load based on 2D theory for the T-AGOS 19 were also obtained.

Short term spectral analysis was then applied to both experimentally and analytically derived side load response data. In this way the most probable extreme and design extreme values of wave induced side load were obtained. These predictions were compared directly with the design values derived empirically using published algorithms and classification society approaches.

5.5.1 Experimental Results

Table 5.2 taken from Ref 6-8 summarises the results of studies undertaken at DTNSRDC. These studies were primarily designed to provide data to allow the development of the side force algorithm by Sikora et al (Ref 6). It will be noted that the data relates only to vessels in the 3000-30,000 ton displacement range for which the algorithm was developed. Results for vessels of design displacement outwith this range were Froude scaled up or down accordingly. The figures given relate to a vessel operating for 3600 days at random headings in a severe portion of the North Atlantic.

Model	Displacement [Tons]	Draft [1]	Strut Length [1]	Side Force / Displacement		% Difference
				Experiment	Algorithm (Ref 6)	
Single Strut per Side						
DTRC-A	3046	1.88	10.92	0.865	0.778	-10.0
Dav.Lab. N	3000	2.11	13.65	1.476	1.496	1.3
Dav.Lab. W	3000	2.11	13.65	1.623	1.496	-7.8
DTRC-81	3400	1.94	12.27	1.239	1.090	-12.0
T-AGOS 19	3500	1.63	12.52	0.896	0.960	7.1
NUC-Single	3900	1.80	16.68	1.157	1.356	17.2
DTRC-IVN	4000	1.75	14.32	1.086	1.244	14.5
DTRC-IVT	4000	2.04	14.32	1.525	1.451	-4.9
DTRC-I	22000	1.41	15.63	0.644	0.671	4.2
DTRC-CVW	30000	1.50	16.15	0.674	0.701	4.0
DTRC-CVN	30000	1.50	16.15	0.823	0.701	-14.8
Twin Strut per Side						
Kaimalino	3000	2.64	4.59 fwd 4.17 aft	0.814 [2]	0.809	-0.6
Dav.Lab.2	3000	2.11	5.21fwd 5.56 aft	0.892	0.844	-5.4
Marine Acc	3000	1.94	4.01 fwd 4.48 aft	0.533 [2]	0.586	9.9
NUC-Tandem	3900	1.80	4.58 fwd 4.58 aft	0.464	0.544	17.2

[1] - Dimension = Length(ft) / Cube root of displacement (ton)
[2] - Full Scale Trials 190 ton and 18.4 ton respectively

Table 5.2 Maximum Lifetime Sideload - Predictions Derived from Model Test Data against Values from Sikora's Algorithm. (Ref 8)

Experimentally derived RAO side load data for the T-AGOS 19 is presented in Fig 5.2 together with analytical predictions. This information (obtained from Ref 45) was combined with the short term spectral analysis technique described in Appendix C in order to predict the most probable extreme and design extreme loads based upon experiments. These values are given in Table 5.3 along with analytically derived predictions.

The design extreme value of 2609 tonnes predicted is 18% less than the experimental prediction published by DTNSRDC (Ref 7). This difference is surprisingly large. However since the simplified spectral analysis applied results in more severe conditions than those adopted by DTNSRDC the discrepancy must be attributable to differences in experimental procedure, only and not to differences in the spectral analysis techniques adopted.

5.5.2 Analytically Evaluated Results

The wave induced side force acting on T-AGOS 19 and the M.V. Patria was evaluated directly by :-

1. Utilising the 3D 'MARCHS' suite of programs
2. The approximate method described in Appendix G

Fig 5.2 presents analytical predictions of RAO for T-AGOS 19 using both these methods and also the 2D prediction tool used by the American Bureau of Shipping.

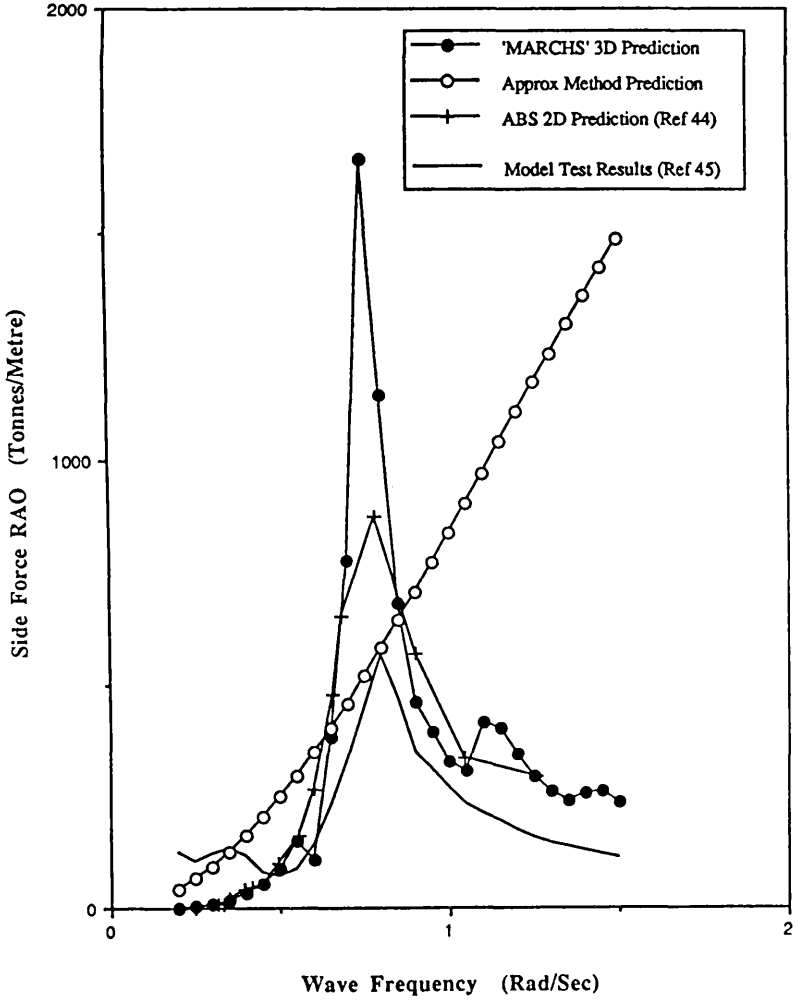

Fig 5.2 Wave Induced Side Load RAO's for T-AGOS 19.

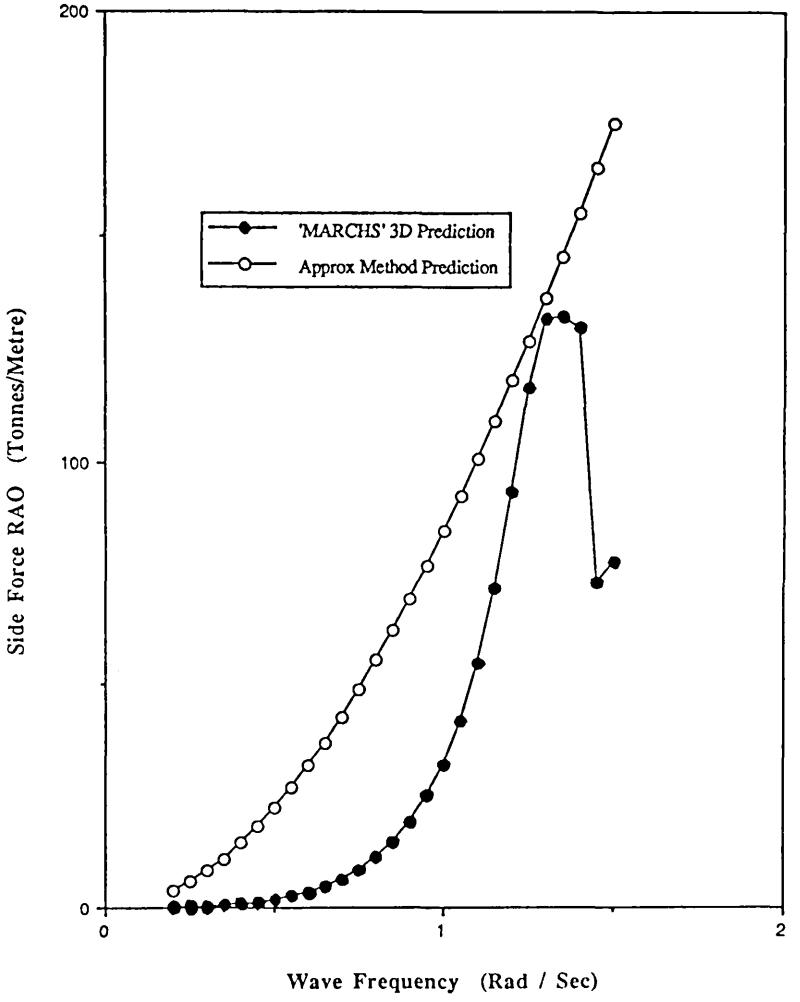

Fig 5.3 Wave Induced Side Load RAO's for the M.V. Patria.

In general good correlation is observed between the 3D 'MARCHS' and 2D ABS predictions, although the peak value predicted by 'MARCHS' is considerably higher than that given by ABS.

It will be noted that the approximate method developed provides reasonable if conservative estimates of RAO up to the wave frequency corresponding to the peak values of the 2D and 3D predictions. The simple theory used takes no account of diffraction effects, the resulting predictions therefore continue to rise with increasing wave frequency.

Fig 5.3 illustrates similar behaviour for the M.V. Patria.

Table 5.3 presents the most probable extreme and design extreme values of side load for T-AGOS 19 and the M.V. Patria. These values were derived using analytically determined RAO data together with the short term spectral analysis technique described in Appendix C.

Vessel	T-AGOS 19		M.V. Patria	
RAO derived from :-	Most Probable Extreme [1]	Design Extreme Value [2]	Most Probable Extreme [1]	Design Extreme Value [2]
'MARCHS' Prog	3709	4743	131	168
Approx Method [3]	3428	4384	329	421
Experiment [4]	2040	2609	-	-

[1] - Probability of exceedance = 63.2%
[2] - Probability of exceedance = 1.0%
[3] - See Appendix G
[4] - Published RAO data (Ref 45)

All Loads in Tonnes

N.B. All values derived using indicated RAO's and the short term spectral analysis described in Appendix C.

Table 5.3 Directly Evaluated Short Term Extreme Value Predictions of Side Load.

For T-AGOS 19 surprisingly good agreement was noted between those values derived using 'MARCHS' and those derived by the approximate method. Indeed the design extreme values predicted were within 8%. In contrast the extreme value predictions for the M.V. Patria were found to be wildly different. In this case the approximate method led to extreme value predictions some two and a half times those derived using 'MARCHS'.

This result is disappointing if not entirely unexpected. The difference in prediction accuracy may be traced to the behaviour of the calculated RAO curves in the region corresponding to the peak energy density for the Pierson Moskowitz wave spectrum. In the case of T-AGOS 19 the 'MARCHS' and the approximate method curves lie close together, however the corresponding RAO curves for the M.V. Patria lie comparatively far apart. The spectral analysis technique applied effectively amplifies this discrepancy which results in the effect observed.

5.5.3 Empirically Derived Results

For comparative purposes all available algorithms were applied to both vessels. The amount of scatter in the results highlights the importance of applying relevant algorithms developed for the displacement range under consideration.

Predictions of side force and transverse bending moment on the cross structure, are presented in Table 5.4 and Fig 5.4 for T-AGOS 19, and in Table 5.5 and Fig 5.5 for the M.V. Patria. It should be noted that DnV (1,2) relate to predictions obtained using equations 5.16 and 5.13 respectively.

N.B. Two of the formulae are acceleration based in their approach and give values of total (wave induced + dead load) bending moment directly, i.e. without separate prediction of wave induced side load. In these cases the side force has been calculated indirectly, subtracting the still water bending moment as indicated in Tables 5.4 and 5.5

A prediction of transverse bending moment for Patria based on the 1985 DnV Rules / (1991 DnV Rules Planing craft formulae) is also included for interest in Appendix F. It will be noted that the old (planing craft) formulae gives reasonable results for Patria *if* used with a valid estimate of vertical acceleration. The 1985 DnV rules provide no formulae from which a valid estimate for a displacement form could be obtained. It should be noted that no such formula yet exists within the Lloyds 1990 Provisional Rules for the Classification of High Speed Catamarans.

Sikora, ABS, Lloyds and RMI figures for bending moment are calculated assuming that wave induced side force acts at half draught. The two DnV estimates are based on the assumption that this force acts at a point 0.75 * draught above the keel. This difference in approach points to the generalised (not specifically SWATH) heritage of the DNV rules. Given the deeper than usual distribution of buoyancy on a SWATH , it seems likely that wave forces will act at a point below that suggested by DnV.

Tables 5.4 and 5.5 were compiled using the 3/4 draught values given in the DnV rules, however it is worth noting that adopting a standard moment arm of 4.05m for Patria and 11.32m for T-AGOS, raises the DnV total bending moments from 820 Tm to 964 Tm (+17%) for Patria and from 46419 Tm to 54917 Tm (+18%) for T-AGOS. Similarly adopting the standard value of moment arm, reduces the value of side force (found indirectly from DnV's directly calculated, acceleration based, total BM value) from 357 to 298 Tonnes (-20%) for Patria and from 2505 to 2088 Tonnes (-20%) for T-AGOS 19.

Considering each vessel in turn:-

T-AGOS 19 - 3500 Tonnes Displacement

Predictions obtained using the algorithms from Sikora and ABS proved similar as expected. Since these formulae were derived from analysis of vessels in the displacement range which includes T-AGOS, the predictions may be assumed to be accurate. The formulae derived by UCL for this displacement range also provided a reasonable, if conservative, estimate (27% greater than that predicted by Sikora).

Neither Lloyds nor DnV rules are applicable to a vessel of T-AGOS's type. Application of formulae from these rules therefore proved futile, resulting in predicted values of side force 32% above, 39% and 68% below that given by Sikora.

Interestingly the elementary formula from RMI provided a reasonable estimate; just 4% above that given by Sikora. This correlation is surprising since the estimate was derived from model test data in Patria's displacement range, and since none of the other algorithms appear to be applicable to both displacement ranges.

M.V. Patria - 180 Tonnes Displacement

As anticipated the UCL design estimate proved invalid for a vessel in Patria's size range. Estimates from Sikora and ABS were again substantially similar, both giving slightly higher values than those produced by the formulae from RMI, Lloyds and the non-acceleration based DnV formulae. This is reasonable given that the Sikora based algorithms were derived for vessels greater than 3000 Tonnes displacement operating for 3600 days in a severe portion of the North Atlantic at random headings. In contrast the RMI, Lloyds and DnV predictions are for small craft operating within specified restrictions on wave height etc.

T-AGOS 19 - 3556 Tonnes Displacement

Algorithm Source	Sikora	ABS	DNV	DNV	Lloyds	RMI	UCL
Algorithm Eqn No							
Acceleration	-	-	-	5.15	5.15 (N.B. DnV)	-	-
Side Force	5.1	5.3	5.16	-	-	5.7	5.6
Bending Moment	5.2	5.2	5.14	5.13	5.8	5.2	5.2
Vertical Acceleration	-	-	-	8.1 m/s**2	8.1 m/s**2	-	-
Side Force	3407 T	3193 T	4509 T	2088 T (2) 2505 T (3)	1098 T (2)	3556 T	4322 T
Moment Arm - Main Dk(1)	11.32 m	11.32 m	9.435 m (4)	11.32 m	11.32 m	11.32 m	11.32 m
BM Due To Side Force	38567 Tm	36148 Tm	51042 Tm (1) 42544 Tm (4)	n/a	n/a	40254 Tm	48925 Tm
Still Water BM (See Appendix C)	3875 Tm	3875 Tm	3875 Tm	3875 Tm	3875 Tm	3875 Tm	3875 Tm
Total Transverse BM	42442 Tm	40023 Tm	54917 Tm (1) 46419 Tm (4)	27512 Tm	16304 Tm	44129 Tm	52800 Tm

N.B. - DnV and Lloyds rules are not strictly applicable to a vessel of this displacement.

All Forces and Moments in Tonn
All to Nearest Tonne

Note:- (1) - Assuming 'F' acts at Draught/2
(2) - Indirectly from (Total BM-3875)/11.32
(3) - Indirectly from (Total BM-3875)/9.435
(4) - DnV Assume 'F' acts at 0.75 Draught

Table 5.4 Empirically Derived Design Side Force and Bending Moment on T-AGOS 19.

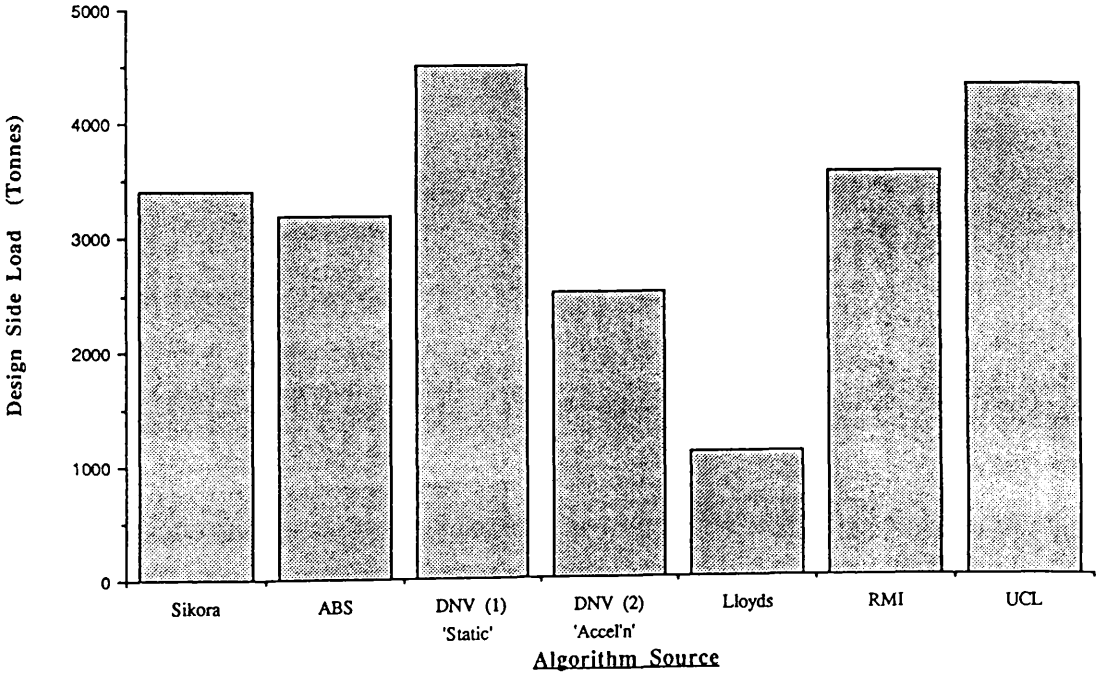

Fig 5.4 Comparison of Empirically Derived Design Side Force on T-AGOS 19

M.V. Patria - 180 Tonnes Displacement

Algorithm Source	Sikora	ABS	DNV	DNV	Lloyds	RMI	UCL
Algorithm Eqn No							
Acceleration	-	-	-	5.15	5.15 (N.B. DnV)	-	-
Side Force	5.1	5.3	5.16	-	-	5.7	5.6
Bending Moment	5.2	5.2	5.14	5.13	5.8	5.2	5.2
Vertical Acceleration	-	-	-	15.4 m/s**2	15.4 m/s**2	-	-
Side Force	247 T	271 T	216 T	298 T (2) 357 T (3)	155 T (2)	180 T	1066 T
Moment Arm - Main Dk (1)	4.05 m	4.05 m	3.375 m (4)	4.05 m	4.05 m	4.05 m	4.05 m
BM Due To Side Force	1000 Tm	1097	875 Tm (1) 730 Tm (4)	n/a	n/a	729 Tm	4317 Tm
BM Due To Dead Loads (See Appendix C)	90 Tm	90 Tm	90 Tm	90 Tm	90 Tm	90 Tm	90 Tm
Total Transverse BM	1090 Tm	1187 Tm	964 Tm (1) 820 Tm (4)	1296 Tm	720 Tm	819 Tm	4407 Tm

N.B. - Sikora, ABS and UCL Algorithms are not strictly applicable to a vessel of this displacement.

All Forces and Moments in Tonn
All to Nearest Tonne

Note :- (1) - Assuming 'F' acts at Draught/2
(2) - Indirectly from (Total BM-90)/4.05
(3) - Indirectly from (Total BM-90)/3.375
(4) - DnV Assume 'F' acts at 0.75 Draught

Table 5.5 Empirically Derived Design Side Force and Bending Moment on the M.V. Patria.

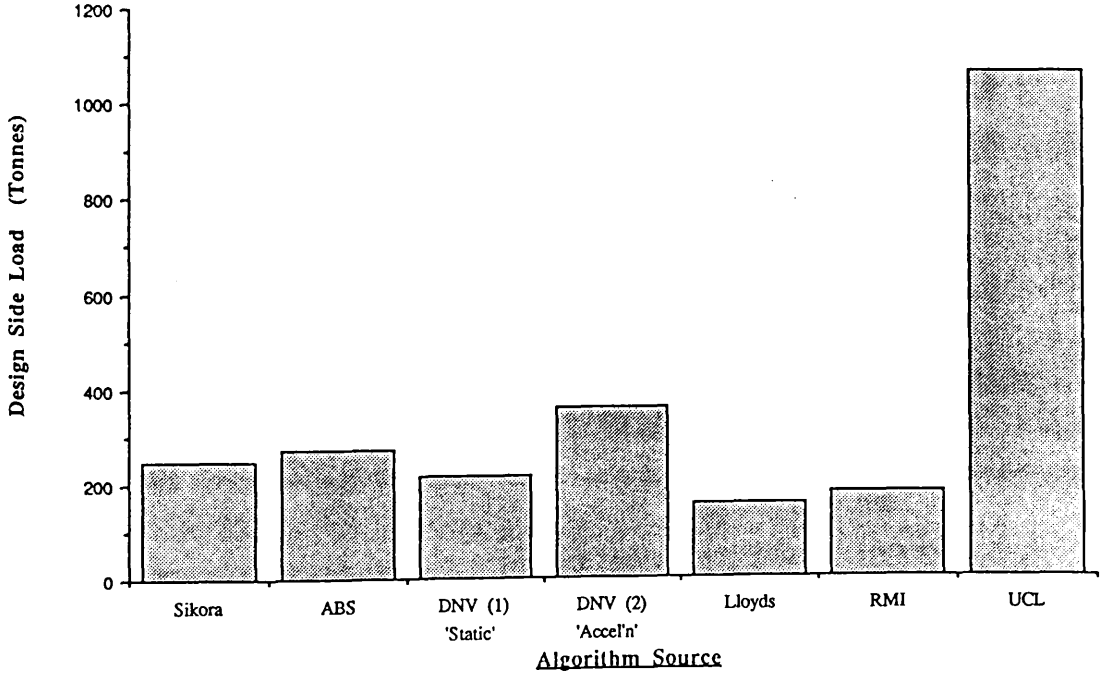

Fig 5.5 Comparison of Empirically Derived Design Side Force on M.V. Patria

5.5.4 Overall Comparison of Results

Fig 5.6 presents a comparison of experimentally, analytically and empirically derived values of wave induced side load acting on T-AGOS 19.
N.B. DnV (1,2) relate to predictions obtained using equations 5.16 and 5.13 respectively. Expt (3,4) corresponds to predictions obtained using published (Ref 45) RAO values, and those obtained direct from DTNSRDC (Ref 8).

At first glance there appears to be little correlation, however if we neglect the non applicable acceleration based Lloyds (Eqn 5.8) and DnV (Eqn 5.13) predictions, the picture becomes clearer. Adopting the DTNSRDC experimental value of 3186 tonnes as the benchmark or datum further simplifies matters. The Sikora and ABS formulae (Eqns 5.1 and 5.2) were developed at DTNSRDC for vessels in this size range. The correlation observed between these predictions and the experimental result is therefore reassuring if unremarkable.

The RMI estimate (Eqn 5.7) agrees reasonably well with the experimental datum selected. As previously noted the crude UCL formula (Eqn 5.6) proved overconservative although adequate for its intended role at the feasibility stage of the design process.

Similarly the non acceleration based DnV approach (Eqn 5.16) produced a value of 4509 tonnes - 41% greater than the datum. Interestingly 'MARCHS' and the approximate method yielded values of 4743 and 4384 tonnes respectively.

Based on these results it appears that direct evaluation using the 'MARCHS' suite of programs and the developed approximate method, results in overprediction of the design extreme side load by almost 48% and 38% respectively. This overprediction is most probably caused by adopting unrealistically severe sea conditions in the spectral analysis approach applied. If the severe sea state adopted in the method is to be retained, it is perhaps more realistic to relax the statistical probability of exceedance requirements. Relaxing these requirements leads to most probable extreme values, 16% and 8% above that found experimentally.

For the M.V. Patria, design extreme value predictions obtained using 'MARCHS' agree well with the Lloyds, RMI and acceleration based DnV predictions.

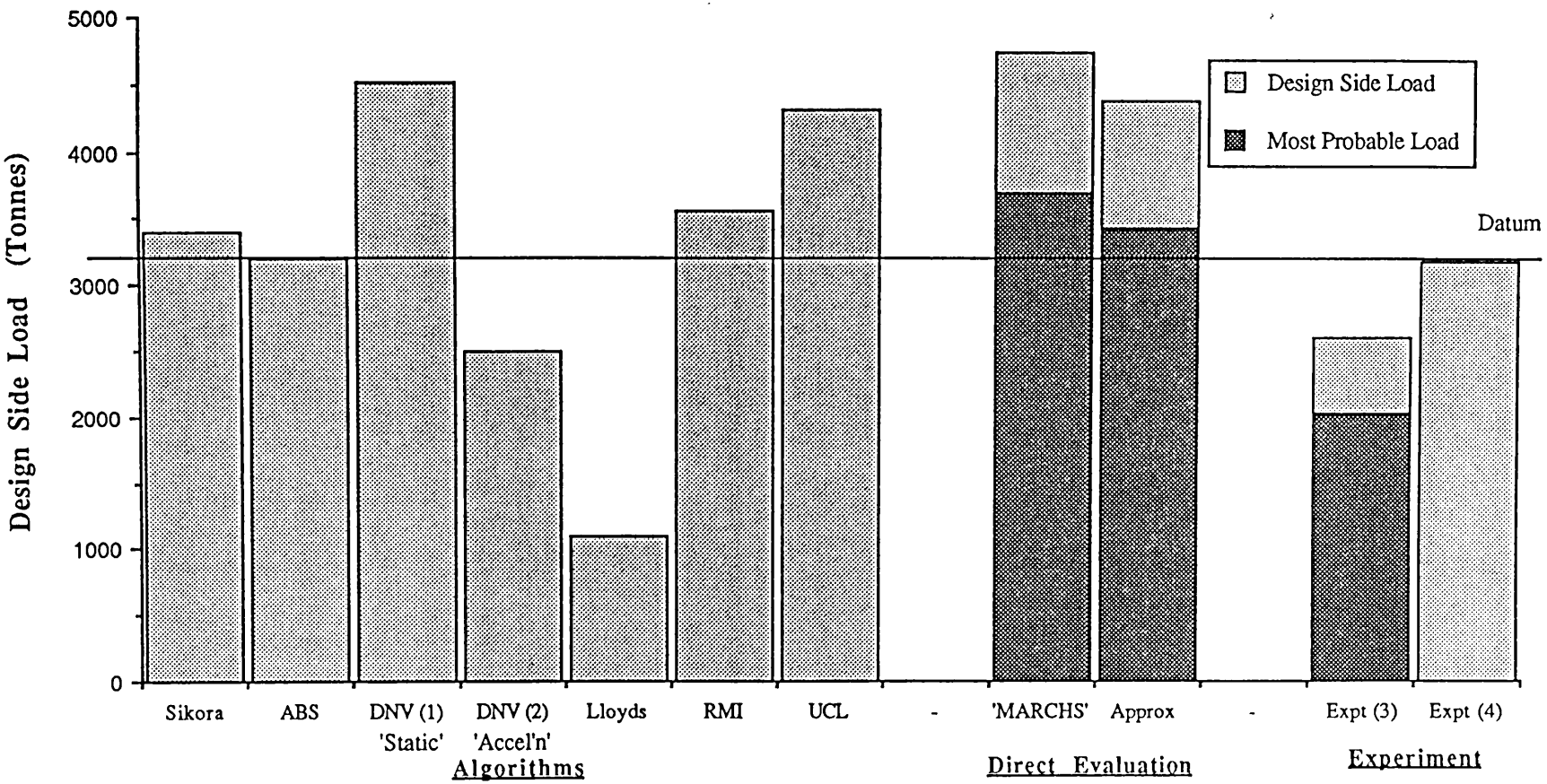

Fig 5.6 Comparison of Experimentally, Analytically and Empirically Derived Design Side Force on T-AGOS 19

In addition to the comparisons performed for this study, Sikora et al (Ref 6-8) have compared predictions obtained using their algorithm with many experimental results. These comparisons are presented in Table 5.2. The predictions generally correlate well with the experimental values, average error being only of the order of 9%.

5.6 Conclusions

1. A thorough review of the techniques employed to predict wave induced global loadings on SWATH ships has been undertaken. The principal methods have been explored and applied to produce predictions of extreme design side load on two very different vessels, namely the 3556 tonne S.S.V. T-AGOS 19 and the 180 tonne passenger ferry, the M.V. Patria.

2. The results obtained were on the whole encouraging. For vessels in the T-AGOS size range it appears that the capability presently exists to predict design extreme values of wave induced side load with reasonable certainty. For vessels in the M.V. Patria's size range, this is unfortunately not the case. However it must be remembered that the structural scantlings of these vessels are nearly always driven by considerations of secondary loading. The accuracy of presently available estimates is therefore quite adequate for design purposes.

3. The 3D 'MARCHS' motion and loading prediction programs performed well for the limiting condition tested here (zero speed in beam seas). These programs appear to offer considerable promise in the light of their capability to explore directional waves and ship speed effects.

4. SWATH ships are still not adequately catered for by the classification societies. ABS are to date the only society to propose rules suitable for the design of general SWATH vessels.

5. Based on the results of this study the author concludes that currently available methods for predicting extreme design global loads on SWATH ships are satisfactorily accurate for design purposes. The author subsequently recommends that attention be redirected towards incorporating the effect of weather and trade routing into the calculations, and to the investigation of structural response and stress transfer within the vessel.

References to Chapter 5

1. Gupta, S.K., and Schimdt, T.W., 'Developments in SWATH Technology', Naval Engineers Journal, May, 1986, pp171-187.

2. Chalmers, D.W., 'Structural Design Aspects of SWATH Ships', Lecture 14 presented to WEGEMT , Delft, Holland, 1989.

3. Shin, Y.S., Kotte, E., Thayamballi, A. and Unger, D., 'Analysis Procedure of Hydrodynamic Load and Fatigue Life Prediction for SWATH Ships in Waves', Proceedings of AIAA Intersociety Advanced Marine Vehicles Conference, Washington, June, 1989.

4. Shin, Y.S., Torng, J.M., and Ng, R., 'Correlation of Motion and Wave Induced Loads on a 3,000 ton SWATH Ship', ABS Technical Report, February, 1986.

5. Gore, J.L., 'SWATH Ships', Naval Engineers Journal, February, 1985.

6. Sikora, J.P., Dinsenbacher, A.L. and Beach, J.E. 'A Method for Estimating Lifetime Loads and Fatigue Lives for SWATH and Conventionall Monohull Ships', Naval Engineers Journal, May, 1983, pp63-85.

7. Sikora, J.P., 'Some Design Approaches for Reducing the Structural Weight of SWATH Ships', Proceedings of the RINA 2nd International Conference on SWATH Ships and Advanced Multi-Hulled Vessels, London, November, 1988.

8. Sikora, J.P. and Dinsenbacher, A.L. 'SWATH Structure: Navy Research and Development Applications', Marine Technology, Vol 27, No4, July, 1990, pp211-220.

9. Lee, C.M., and Curphey, R.M., 'Prediction of Motion, Stability and Wave Load of Small Waterplane-Area, Twin-Hull Ships', Transactions SNAME, Vol 85, 1977, pp94-130.

10. Jones, H., D. and Gerzina, D.M., 'Motions and Hul Induced Bridging Structure Loads for a Small Waterplane Area, Twin Hulled Attack Aircraft Carrier in Waves', DTNSRDC Report 3819, August, 1973.

11. Kallio, J.A. and Ricci, J.J., 'Seaworthiness Characteristics of a Small Waterplane Area Twin Hull (SWATH IV) Part II', DTNSRDC Report SPD 620-02, 1976.

12. Lee, C.M. and Murray, L.O., 'Experimental Investigation of Hydrodynamic Coefficients of a Small Waterplane Area, Twin Hull Model (SWATH 6A)' DTNSRDC Report SPD 747-01, 1977.

13. Kallio, J.A., 'Seaworthiness Characteristics of a 2900 ton Small Waterplane Area Twin Hull (SWATH)', DTNSRDC Report SPD 620-03, 1977.

14. Nethercote, W.C.E. and Schmitke, R.T., 'A Concept Exploration Model for SWATH Ships', Transactions RINA, Vol. 124, pp. 113-130, 1982.

15. Koops, A. and Nethercote, W.C.E., 'An Extended SWATH Concept Exploration Model', Proceedings of the RINA 2nd International Conference on SWATH Ships and Advanced Multi-Hulled Vessels, London, November, 1988.

16. Pattison D.R., Rose, P.H.A., and Harris, S.A., 'SWATH - The UK MOD Design and Assessment Program', Proceedings of the RINA 2nd International Conference on SWATH Ships and Advanced Multi-Hulled Vessels, London, November, 1988.

17. Djatmiko, E.B., 'Experimental Investigation into SWATH Ship Motions and Loadings', MSc Thesis, Department of Naval Architecture, University of Glasgow, UK, November, 1987.

18. Djatmiko, E.B., 'Experimental and Theoretical Studies of SWATH Behaviours', Annual Report, Department of Naval Architecture, University of Glasgow, UK, May, 1989.

19. Chun, H.H., Djatmiko, E.B., McGregor, R.C. and Ferguson, A.M., 'SWATH Resistance in Waves with Associated Steady and Dynamic Responses', Proceedings, 22nd ATTC, St John's, Newfoundland, Canada, August, 1989.

20. Djatmiko, E.B., Chun, H.H., McGregor, R.C. and MacGregor, J.R., 'Hydrodynamic Behaviour of a SWATH Fishing Vessel', Proceedings, Mechanical Engineering Forum 1990, Paper No. SOD-1, University of Toronto, Canada, June, 1990.

21. Mabuchi, T., Kunitake, Y. and Nakamura, H., 'A Status Report on Design and Operational Experiences with the Semi-Submerged Catamaran (SSC) Vessels', Proceedings, International Conference on SWATH Ships and Advanced Multi-Hulled Vessels, RINA, London, April, 1985.

22. Oshima, M., Narita, H. and Kunitake, Y., 'Experiences with 12 Meter Long Semi-Submerged Catamaran (SSC) 'Marine Ace' and Building of SSC Ferry for 446 Passengers', Proceedings, AIAA/SNAME Advanced Marine Vehicles Conference, Paper No. 79-2019, Baltimore, Maryland, USA, 1979.

23. Lee, C.M., Jones, H.D. and Curphey, R.M., 'Prediction of Motion and Hydrodynamic Loads of Catamarans', Marine Technology, SNAME, Vol. 10, No. 4, October, 1973.

24. Curphey, R.M. and Lee, C.M., 'Analytical Determination of Structural Loading on ASR Catamaran in Beam Waves', DTNSRDC, Ship Performance Department, R&D, Report No. 4267, Bethesda, Maryland, USA, April, 1974.

25. Hooft, J.P., 'Hydrodynamic Aspects of Semi-Submersible Platforms', Publication No 400, Netherlands Ship Model Basin , Wageningen, Netherlands.

26. Chan, H.S., 'A 3D Technique for Predicting First and Second Order Hydrodynamic Forces on a Marine Vehicle Advancing in Waves', PhD Thesis, Department of Naval Architecture, Glasgow University, August, 1990.

27. Chun, H.H., 'First and Second Order Forces on SWATH Ships in Waves', Dynamics of Marine Vehicles and Structures in Waves - Proceedings of the IUTAM Symposium, Brunel University, Uxbridge, June, 1990.

28. Keane, A.J., Price, W.G., Temarel, P., Wu, X-J and Wu, Y., 'Seakeeping and Structural Responses of SWATH Ships in Waves', Proceedings, International. Conference on SWATH Ships and Advanced Multi-Hulled Vessels II, RINA, London, November, 1988.

29. Price, W.G., Temarel, P. and Yousheng, W., "Structural Responses of a SWATH or Multi-Hull Vessel Travelling in Waves", Proceedings, International Conference on SWATH Ships and Advanced Multi-Hulled Vessels, Paper No. 15, RINA, London, UK, April, 1985.

30. Bishop, R.E.D., Price, W.G. and Temarel, P., 'On the Hydroelastic Response of a SWATH to Regular Oblique Waves', Proceedings, Advances in Marine Structures, ARE, Dunfermline, Scotland, May 1986.

31. Price, W.G., Temarel, P. and Wu, Y., 'Responses of a SWATH Travelling in Unidirectional Irregular Seas', Underwater Technology, SUT, Vol. 13, No. 4, pp. 2-10, 1987.

32. Clayton, B.R. and Bishop, R.E.D., 'Mechanics of Marine Vehicles', E.&F.N. Spon Ltd., London, 1982.

33. Price, W.G. and Wu, Y., 'The Influence of Non-Linear Fluid Forces in the Time Responses of Flexible SWATH Ships Excited by a Seaway', Proceedings, 8th Int. Conference on OMAE, pp. 125-135, the Hague, the Netherlands, March, 1987.

34. Ochi, M.K., 'Wave Statistics for the Design of Ships and Ocean Structures', Transactions SNAME , Vol 86,1978, pp47-76.

35. Betts, C.V., 'A Review of Developments in SWATH Technology', Proceedings, International Conference on SWATH Ships and Advanced Multi-Hulled Vessels II, RINA, London, November 1988.

36. Luedeke, G. and Montague, J., 'RMI's Small-Waterplane-Area-Twin-Hull (SWATH) Boat Project', Section Meeting, SNAME, San Diego Section, November 1984.

37. Luedeke, G., Montague, J., Posnansky, H. and Lewis, Q., 'The RMI SD-60 SWATH Demonstration Project', Proceedings, International Conference on SWATH Ships and Advanced Multi-Hulled Vessels, RINA, London, April, 1985.

38. American Bureau of Shipping, 'Preliminary Guide For Building and Classing Small Waterplane Area Twin Hull (SWATH) Vessels', Provisional 1990.

39. Lloyds Register of Shipping, 'Provisional Rules for the Classification of High Speed Catamarans', Provisional 1990.

40. Det norske Veritas, 'Rules for the Classification of High Speed Light Craft, 1985.

41. Det norske Veritas, 'Rules for the Classification of High Speed Light Craft, 1991.

42. Andrews, J.N., and Sikora, J.P., 'Determination of Wave Induced Loads on a 3,000-ton, SWATH Ship', DTNSRDC report, August, 1979.

43. Stirling, A.G., Jones G.L., and Clarke, J.D., 'Development of a SWATH Structural Design Procedure For Royal Navy Vessels', Proceedings of the RINA 2nd International Conference on SWATH Ships and Advanced Multi-Hulled Vessels, London, November, 1988.

44. Reilly, E.T., Shin, Y.S. and Kotte, E.H., 'A Prediction of Structural Load and Response of a SWATH Ship in Waves', Naval Engineers Journal, ASNE, May, 1988, pp. 251-264.

45. Kadala, E., Discussion to:- Reilly, E.T., Shin, Y.S. and Kotte, E.H., 'A Prediction of Structural Load and Response of a SWATH Ship in Waves', Naval Engineers Journal, July 1988, pp162-166.

46. Meyerhoff, W.K. et al, Report of Commitee V.4. 'Novel Design Concepts - SWATH', Proceedings of the 10th International Ship and Offshore Structures Congress, Denmark,1988.

47. Allen, R.G. and Holcomb, R.S., 'The Application of Small SWATH Ships to Coastal and Offshore Patrol Missions', Symposium on Small Fast Warships and Security Vessels, London, 1982.

CHAPTER 6

DESIGN EVALUATION

6.1 Introduction

Evolution of the SWATH concept has been well charted in many discussion and review papers. Until recently however most SWATH research has been directed towards establishing and subsequently improving individual aspects of SWATH performance relative to monohulls. A position has now been reached where the primary advantages and disadvantages of the concept are recognised and are no longer in dispute. Consequently the current requirement is for a balanced overview of the "total performance" of the concept relative to monohull "equivalents". This is clearly necessary in order to enable the designer to select the hullform best suited to a given role.

6.2 Aims and Objectives

The objective for the final phase of the project was to provide a balanced assessment of the relative merits of both monohull and SWATH designs. This comparison is based on all relevant features of the two concepts. Features and characteristics of both hullforms are identified and assigned a priority level. The priority level assigned includes consideration of the vessel's intended role and operating profile. Through application of this technique the chapter aims to provide guidance for the designer selecting hullforms for both general and specific roles.

6.3 Basis for Comparison

In order to perform any comparison we first require to define the basis for comparison. In this case this involves defining the terms "Total Performance" and "Equivalence" : -

Total Performance

The "Total Performance" of a vessel is defined as a measure of the overall capability

of that vessel to perform the mission for which it was designed. The overall capability is a function of all individual performance parameters for that design. Individual performance parameters include items such as seakeeping, powering and survivability. The function relating Total Performance to individual parameters is a unique feature of the vessel's operational profile.

Equivalence

Traditional estimates of equivalence (for monohulls) are often based on displacement and/or length (Ref 1). However since SWATH vessels are shorter than monohulls of equal displacement, comparisons based on these criteria are frequently misleading. More importantly, owing to the greatly improved seakeeping performance of SWATH vessels, it is often possible to perform a given role using a SWATH vessel of displacement considerably less than that of the monohull required for the same task. Consequently a comparison of overall performance based on equal displacement will penalize the SWATH heavily whilst disguising the greatly increased seakeeping capability afforded by the configuration.

For this reason any meaningful comparison between SWATH and monohull must be performed on the basis of capability or 'mission equivalence' .

Kennel et al (Ref 2) illustrate the importance of selecting realistic definitions of equivalence. This paper compares designs for two monohull and one SWATH frigate developed on the basis of equivalent payload, and equivalent seakeeping performance. Results from this study lead to the conclusion that the only correct basis for comparison is that of 'mission equivalence'.

6.4 Previous Work

The bulk of previous comparative work relates to the specific differences in SWATH / monohull behaviour. Since the primary reason for the existence of SWATH ships is seakeeping, it is perhaps not surprising that considerable attention has been devoted towards quantifying the increase in seakeeping performance afforded by the concept (Ref 3-17). Resistance and build cost are other "favourite" parameters for comparing SWATH and monohull vessels (Ref 1,7,17-22).

Unfortunately very few direct overall comparisons of SWATH and monohull vessels have been published. Notable exceptions to this include papers on a cruise liner

by Jones (Ref 23), Anti Submarine Frigates by Kennell et al (Ref 2) and a Deep Ocean Survey vessel T-AGS 38/39 by Kaysen (Ref 24,25). Eames (Ref 26,27) additionally offers a wider view of several advanced naval vehicles proposed for the role of 'Future Naval Surface Ships'. The scarcity of such comparisons is largely due to the difficulty of performing such a task objectively, and to the reluctance of some agencies to publish such potentially valuable commercial information.

6.5 Design Evaluation Techniques

The importance of comparing vessels on a mission basis has already been stressed. In order to compare SWATH and monohull contenders for a given role, the vessel features and characteristics applicable to that role must first be selected. In this study the performance parameters required to successfully fulfil the specified role were selected from those reviewed in Chapter 2.

Next the relevant performance parameters were listed together with corresponding mission weightings. These weightings reflect the importance of individual performance parameters to the success of the overall mission. An accurate estimate of mission weightings is vital to the realistic comparison of SWATH and monohull designs.
The selection of these values relies heavily on experience and therefore remains highly subjective. This leaves the designer / procurer in control to make decisions based on particular features of the mission requirement.

Once performance parameters and corresponding mission weightings have been established, the next step requires "scoring" both monohull and SWATH contenders against each parameter on the list. The complexity of this task depends on the parameter in question, and the amount of design information available. In some cases e.g. powering requirements, actual values may be available for both designs, in such cases direct comparison is readily possible. However, in the majority of instances precise information will be unavailable, in these cases the engineer must use his or her judgement and experience to arrive at a feasible, if subjective, value.

The Total Performance figure for both designs, is then given by the summation of all individual parameter and mission weighting products. It should be stressed that the figures produced are only a guide to the hullform best suited to perform that role, since the procedure contains many uncertainties and subjective estimates. It does however provide a starting point for more detailed design evaluations.

It should be recognised that the developed method exists to compare viable alternative designs. If one hullform fails to satisfy a vital or specified design requirement, then the comparison is void and its solution becomes academic.

6.5.1 Mathematical Evaluation Model

The simplified design evaluation procedure described, may conveniently be illustrated mathematically :-

Once the relevant performance parameters are selected,

$$P_1 , P_2 , P_3 , \ldots , P_n$$

and the relative mission weighting of the parameters defined,

$$w_1 , w_2 , w_3 , \ldots , w_n$$

each vessel is "scored" to reflect performance in individual areas,

$$p_1 , p_2 , p_3 , \ldots , p_n$$

The SWATH / Monohull performance ratio may then be calculated,

$$\frac{\text{SWATH} \quad p_1 - \text{Mono} \quad p_1}{\min(\text{SWATH} \quad p_1 , \text{Mono} \quad p_1)} \qquad \text{etc}$$

The individual role performances (RP 's) are then given by:-

$$RP_i = \left[\frac{\text{SWATH} \quad p_i - \text{Mono} \quad p_i}{\min(\text{SWATH} \quad p_i , \text{Mono} \quad p_i)} \right] \times w_i$$

The overall performance figure for the SWATH vessel relative to the monohull is therefore:-

$$\text{Overall Performance} \quad \frac{\text{SWATH}}{\text{Mono}} = \frac{\sum_{i=1}^{n} RP_i}{\sum_{i=1}^{n} w_i}$$

6.5.2 Sample Design Evaluations

The following examples illustrate the design evaluation procedure. The roles selected; that of Sonar Surveillance and Ocean Survey, are two of those for which SWATH vessels are most commonly advocated. Other commonly suggested applications for SWATH craft include:-

- Ferries (Ref 28-33)
- Small Cruise Liners (Ref 23,29,34)
- Offshore Patrol Vessels (Ref 35,36-39)
- Diving Support Ships (Ref 40,41)
- Small Air Support Vessels (Ref 42-44)
- Offshore Supply Boats (Ref 41)
- Frigates (Ref 45-47)
- Fishing Vessels (Ref 48,49)
- Research Ships (Ref 50-52)

Sonar Surveillance Vessel

The following comparison was based on published data for the existing monohull U.S. Navy T-AGOS sonar surveillance vessels and the recently completed SWATH T-AGOS 19 (Ref 53-55).

The Sonar Surveillance Vessel (SSV) role requires the vessel to remain at sea and operational in extreme weather for long periods. The vessels are designed to be fully operable at all headings in severe sea conditions. Previous vessels of the class have experienced difficulty in maintaining the required level of operability, hence the decision was taken to design and build a SWATH vessel for the purpose.

A typical mission profile for a SSV vessel involves 2-4 days steaming at 7-8 knots, over the side or through deck deployment of the towed array, 20-30 days slow speed (2-3 knots) steaming on all headings, recovery of array and return to port at 7-8 knots cruising speed.

From the foregoing it is obviously desirable to maximise percentage operability. Since seakeeping has the greatest influence on operability, the highest parameter weighting is therefore attached to it.

The operation of onboard systems is also of particular importance for a sonar support vessel. The performance of the towed array together with the system used for its deployment and recovery is central to the success of the mission.

The other parameters which influence the vessels ability to perform the mission are similarly listed and assigned a parameter weighting commensurate with their importance.

Fig 6.1 Gives the main particulars and seakeeping performance of the T-AGOS ships.
Table 6.1 Illustrates the evaluation procedure for T-AGOS 18/19.

For each parameter, cost, seakeeping etc, both monohull and SWATH are 'scored' . This value may be real e.g. in the case of percentage operability, or it may be a perceived relative quantity. The ratio of SWATH/monohull scores is then noted in the centre column. A negative value indicates that the SWATH is less able in that area. This figure is then multiplied by the mission weighting assigned to that parameter. The sum of these values divided by the sum of the mission weightings gives the overall SWATH/monohull performance ratio for that role.

In this case the SWATH has 95% operability compared with 57% for the monohull (Ref 53). The SWATH/Monohull ratio is therefore 0.667 ((95-57)/57) i.e. the SWATH has 66% greater operability. The parameter mission weightings were simply determined by arithmetically rating the parameters in descending order of importance, thus seakeeping is rated =14 and manoeuvrability =2. The final result of +0.09 implies that overall the SWATH is more capable of performing the S.S.V. mission than its monohull counterpart.

T-AGOS CLASS SHIP COMPARISON

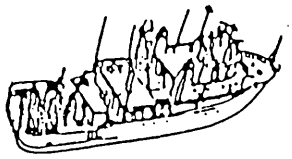

DESIGN	COMMERCIAL	COMMERCIAL
LENGTH (O.A.)	224 FT	232 FT
BEAM	43 FT	94 FT
DRAFT (F.L)	14 FT 11 IN	24 FT 9 IN
PROPULSION		
DIESEL ELECTRIC	1600 HP	1600 HP
ELECTRICAL POWER	(4) 600 Kw, 600 VAC DIESEL GENERATORS	(4) 835 Kw, 600 VAC DIESEL GENERATORS
DISPLACEMENT		
LIGHT SHIP	1587 LT.	2608 LT.
FULL LOAD	2236 LT.	3370 LT.
OPERABILITY/SURVIVABILITY	SS 5/8	SS 6/9
DAYS ON STATION	90	90
SUSTAINED SPEED	11 KTS	9.6 KTS
ENDURANCE	3000 NM	3000 NM
ICE STRENGTHENING	CLASS C	CLASS C
SURTASS OPERATIONS CENTER	1400 SQ. FT.	1400 SQ. FT.
PAYLOAD	130 TONS	130 TONS
ACCOMMODATIONS	33	33

MONOHULL AND SWATH T-AGOS

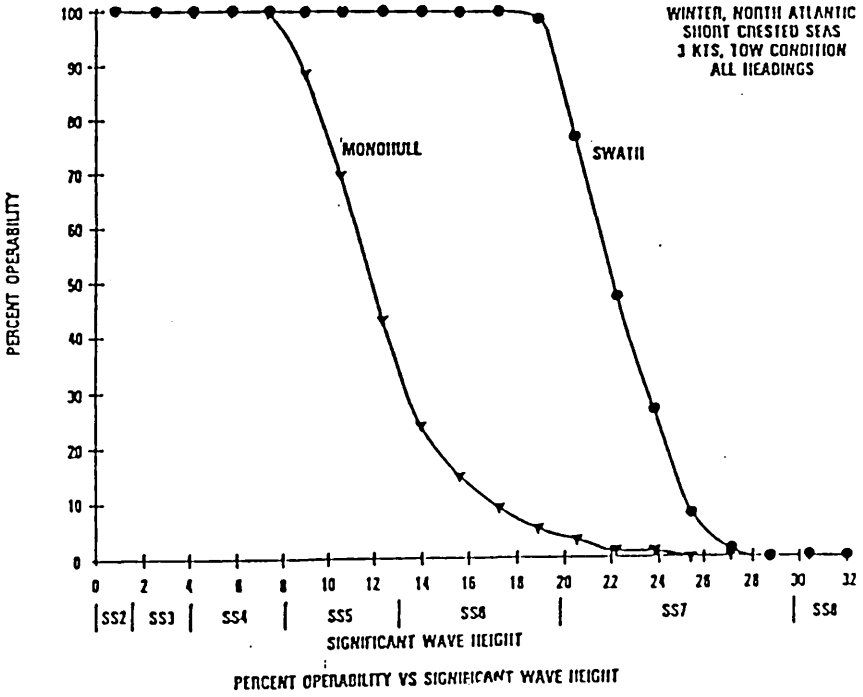

PERCENT OPERABILITY VS SIGNIFICANT WAVE HEIGHT

Fig 6.1 T-AGOS 18 / 19 - Principal and Operability Characteristics (Ref 53)

Mission :- S.S.V. Performance Parameter	Real or Perceived Scores Monohull	 SWATH	Performance Ratio SWATH/Monohull	Mission Weighting	Individual Role Performance
Seakeeping - Motions % OPERABILITY Loading W.N.N.A. Deck Wetness Slamming Speed/Course Maintenance	57	95	0.667	14	9.33
Operation Onboard Systems - Surface	3	5	0.667	8	5.33
(Independant of Motions) Air	-	-		2	0.00
Scale 1-5 Worst-Best Underwater	2	5	1.500	3	4.50
Cost - Design $ MILLION Construction Unit Build Operation	12	25.4	-1.117	12	-13.40
Endurance / Range 3000nM+90days @ 3kts	1	1	0.000	11	0.00
Survivability - SCALE 1-5					
Signature - Infra Red	4	5	0.250	1	0.25
Acoustic	3	5	0.667	2	1.33
Radar	5	3	-0.667	1	-0.67
Damage Resistance - Missile	3	5	0.667	1	0.67
Torpedo	3	5	0.667	1	0.67
Mine	4	5	0.250	1	0.25
Damage Stability -	3	5	0.667	2	1.33
N.B.C.W -	-	-		1	0.00
Reliability - Hull	5	3	-0.667	4	-2.67
Machinery	3	5	0.667	5	3.33
Interfacing Ability - Length	224'	232'	-0.667	8	-5.33
Beam	43'	94'			
Draught	14'11"	24'9"			
Freeboard					
Deck Area					
Habitabilty - Noise	4	5	0.250	3	0.75
Working Conditions	3	5	0.667	4	2.67
Stability - Intact	4	5	0.250	6	1.50
Payload % Displacement	0.058	0.038	-0.519	5	-2.59
Layout - Machinery Ratios /Total Vol Outfit "Usability Factor" Void Space	4	5	0.250	4	1.00
Powering - High Design Speed	4	5	0.250	1	0.25
Low Design Speed	3	5	0.667	2	1.33
Maneuvrability - High Speed	5	3	-0.667	1	-0.67
Low Speed	4	5	0.250	1	0.25
			Total -	104	9.42

Overall Mission Performance

SWATH/MONO = Positive 0.09

Table 6.1 Sample Design Evaluation for T-AGOS 19 and It's Monohull Counterpart

Oceanographic (Deep Ocean) Survey Ship

The Deep Ocean Survey (D.O.S.) mission involves surveying the vast areas of ocean floor beyond the continental shelves, to gather seabed profile information together with magnetic and gravimetric data. The U.S. Navy use auxiliary ships designated T-AGS to perform this task. The data collected is primarily used for the fleet ballistic missile program.

The D.O.S. operational profile is relatively straightforward. The vessel steers a predetermined course at constant speed, while acoustic depth measurements are taken by a large precision depth sounding sonar system. Co-ordinated gravity meter and magnetometer data is also recorded. Data collection starts when the vessel crosses the 600 feet contour and continues for the duration of the mission - usually about 30 days. During that period the vessels must operate completely independently.

Seakeeping obviously plays a major part in the vessels ability to maintain speed and heading over the 30 day operation. T-AGS require good seakeeping performance in order to remain operational throughout the duration of their mission. In addition, low ship motions result in an increase in the quality of information recorded by the onboard sensors.

A performance comparison was undertaken for a 12,500 Ton SWATH T-AGS design and the existing 15,000 Ton monohull T-AGS 39. The data used for this evaluation was taken from Ref 24 and 25. Fig 6.2 illustrates the main particulars for both monohull and SWATH designs. The order of parameter weighting is again similar to that for the S.S.V. mission. Premiums are placed on seakeeping performance and the operation of onboard systems. Given the civilian nature of the crew considerations of outfit are also important, e.g. union regulations concerning accommodation requirements are easier to implement on a SWATH. Endurance and range feature too although in this case both monohull and SWATH were designed to have equal endurance. Table 6.2 illustrates the T-AGS evaluation performed.

These evaluations were performed mainly to demonstrate the procedure suggested in section 6.5 and 6.5.1. They also indicate which features are most beneficial / damaging and indicate where design effort may most effectively be concentrated. The figures produced are the result of many subjective decisions and assessments. They should not therefore be relied upon or assumed accurate. They may however be taken as a reasonable indication of the suitability of SWATH ships for the roles considered.

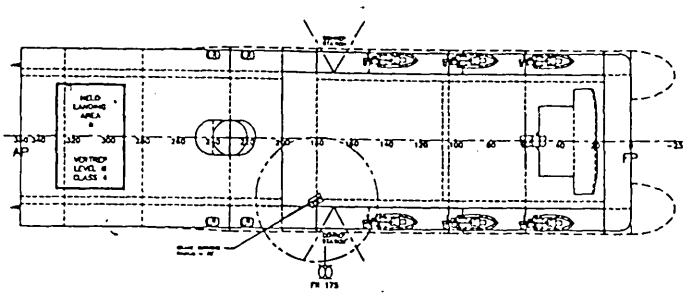

SWATH AGS
DEEP OCEAN SURVEY
(DOS)
SHIP

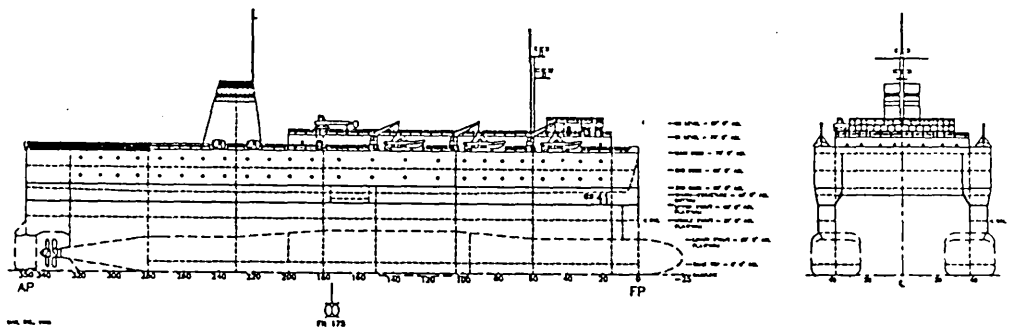

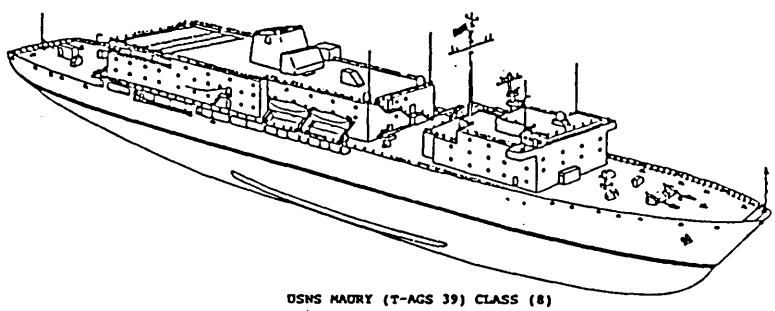

USNS MAURY (T-AGS 39) CLASS (8)

DEEP OCEAN SURVEY SHIP
PRINCIPAL CHARACTERISTICS COMPARISON

PRINCIPAL CHARACTERISTIC	T-AGS 39 (13)	SWATH AGS
Length Overall	499 ft 10 in	381 ft 0 in (lower hulls)
Length Between Perpendiculars (ABS)	462 ft 1-1/8 in	350 ft 0 in
LWL at Design Draft	476 ft 0 in at 30 ft 0 in	350 ft 0 in
Beam, Molded	72 ft 0 in	96 ft 0 in (at DWL)
(Beam)	--	104 ft 0 in (lower hulls)
(Beam)	--	100 ft 0 in (cross structure)
Draft, design	30 ft 0 in	31 ft 0 in
Depth, molded	42 ft 0 in(to main deck, side)	70 ft 0 in
(Depth)	51 ft 0 in(to 01 level, side)	--
Displacement, design draft	15,821 LT	12,585 LT
Light ship weight with margin	8,810 LT	8,738 LT
Type of Machinery	Medium Speed Diesel	Integrated Diesel Electric
Power-ABS Maximum Continuous Rating (MCR)	23,584 BHP	17,500 SHP
Power, 80% ABS MCR	19,039 BHP with PTO generator at full load	14,000 SHP
Speed, sustained operating, at 80% ABS MCR	20 knots	20 knots
Endurance at design draft and sustained operating speed	34 days plus 1500 nm	34 days plus 1500 nm
Total Accommodations	108 (SEE TABLE 2)	108 (SEE TABLE 2)

Enclosed Volume 1.5 million cu ft.

Fig 6.2 SWATH and Monohull T-AGS Principal Characteristics (Ref 24,25)

Mission :- D.O.S. Performance Parameter	Real or Perceived Scores		Performance Ratio	Mission	Individual Role
	Monohull	SWATH	SWATH/Monohull	Weighting	Performance
Operation Onboard Systems - Surface	4	5	0.250	3	0.75
(Independant of Motions) Air	3	5	0.667	3	2.00
Scale 1-5 Worst-Best Underwater	2	5	1.500	6	9.00
Seakeeping - Motions	4	5	0.250	2	2.75
Loading				1	
Deck Wetness				2	
Slamming				2	
Speed/Course Maintenance				4	
Cost - Design Total over Lifecycle	5	4	-0.250	2	-2.50
Construction				4	
Unit Build				2	
Operation				2	
Endurance / Range	34	34	0.000	9	0.00
Reliability - Hull	5	4	-0.250	3	-0.75
Machinery	5	2	-1.500	5	-7.50
Interfacing Ability - Length	5	4	-0.250	7	-1.75
Beam					
Draught					
Freeboard					
Deck Area					
Habitability - Noise	4	5	0.250	2	0.50
Working Conditions	3	5	0.667	4	2.67
Stability - Intact	4	5	0.250	3	0.75
Damaged	3	5	0.667	2	1.33
Powering - High Design Speed				n/a	
Low Design Speed (Installed)	24000	17500	0.371	4	1.49
Payload % Displacement	0.418	0.306	-0.367	3	-1.10
Maneuvrability - High Speed	5	4	-0.250	1	-0.25
Low Speed	4	5	0.250	1	0.25
Layout - Machinery Ratios /Total Vol					
Outfit "Usability Factor"					
Void Space	4	5	0.250	1	0.25
			Total -	78	7.88

Overall Mission Performance

SWATH/MONO = Positive 0.1

Table 6.2 Sample Design Evaluation for T-AGS 39 and Equivalent SWATH AGS

6.6 Conclusions

A comprehensive study of the advantages and disadvantages associated with both monohull and SWATH vessels has been undertaken. The parameters of primary importance for comparative purposes have been identified, and a framework suggested for the basic evaluation of alternative SWATH and monohull designs. Several simplified design evaluations have been performed, two of which are presented here to illustrate the developed method.

It was found that SWATH vessels prove superior to monohulls when performing missions dominated by seakeeping considerations, however it must be remembered that few missions are dictated solely by considerations of seakeeping. In particular when comparing 'seakeeping equivalent' vessels, it is important to recognise the additional payload capability of the larger monohull. In the same way the additional seakeeping performance of SWATH should not be overlooked when comparing equivalent displacement vessels. SWATH ships are unlikely to exceed 15,000 Tonnes displacement, since above this limit monohulls offer adequate seakeeping performance.

Survivability and operation of onboard systems are the two other principal areas where SWATH ships lead their monohull counterparts, while the cost of SWATH ships is presently estimated to be approximately 5-10% more than mission equivalent monohulls. This value is based on current U.S. Navy data and is subject to revision. Future advances in SWATH structures are likely to improve the perceived reliability of the concept and reduce design and fabrication costs while further advances in fabrication and outfit technology may ultimately remove any remaining SWATH/monohull cost differential.

Based on the results of, and the knowledge gained performing this study, the author recommends the SWATH concept for the following roles:-

- Sonar Surveillance SSV
- Oceanographic and Deep Ocean Survey DOS
- Offshore Patrol OPV
- Passenger Ferry (Exposed Route)
- Small Vehicle Ferry (Exposed Route)
- Diving Support and Salvage
- Light Displacement Air Support

All these roles require (relatively) small vessels with good seakeeping capabilities and / or large usable deck areas. The SWATH ship is therefore ideally suited to these missions although the final choice of vessel type will inevitably depend on many other indefinable factors not the least of which are cost and 'fashion'.

References to Chapter 6

1. Gupta, S.K., and Schimdt, T.W., 'Developments in SWATH Technology', Naval Engineers Journal, May 1986, pp171-187.

2. Kennell, C., White, B.L. and Comstock, E.N., 'Innovative Naval Design for North Atlantic Operations', Transactions, SNAME, Vol. 93, pp. 261-281, 1985.

3. Pollack, C.G.,' Motion Comparison Between 64-Foot SWATH and a 65-Foot Monohull', Report of the Naval Biodynamics Laboratory, New Oreleans, U.S.A. February 1985.

4. McGregor, R.C., Arthur, E.K., Djatmiko, E., Drysdale, L.H. and Zheng, X., 'Comparative Study of SWATH Seakeeping', Proceedings, International High-Performance Vehicle Conf., CSNAME, Shanghai, China, November, 1988.

5. Olson, LCDR S.R,'An Evaluation of the Seakeeping Qualities of Naval Combatants', Naval Engineers Journal, February, 1978.

6. Olson, LCDR S.R,'Seakeeping- and the SWATH Design', U.S. Naval Institute, Proceedings, March, 1978.

7. Olson, S.R., 'The Military Utility of the Small Waterplane Area Twin Hull (SWATH) Concept', Proceedings, AIAA/SNAME Advanced Marine Vehicles Conference, San Diego, California, April, 1978.

8. Comstock, E.N., Bales, S.L. and Gentile, D.M., 'Seakeeping Performance Comparison of Air Capable Ships', Naval Engineers Journal, ASNE, April, 1982.

9. Hosoda, R. and Kunitake, Y., 'Seakeeping Evaluation in SWATH Ship Design', Proceedings International Conference of SWATH Ships and Advanced Multi-Hulled Vessels, London, April, 1985.

10. McCreight, K.K. and Stahl, R.G.,'Recent Advances in the Seakeeping Assessment of Ships', Naval Engineers Journal, ASNE, May 1985.

11. McCreight, K.K., 'Assessing the Seaworthiness of SWATH Ships',Transactions SNAME, Vol. 95, pp. 189-214, 1987.

12. Djatmiko, E.B., 'Comparitive Evaluation of some Slamming Prediction Methods for SWATH Type Vessels', Departmental Report, Department of Naval Architecture, University of Glasgow, March 1991.

13. Chilo, B. and Santos, R.T.C., 'Seakeeping Assessment and Criteria of Naval Combatant SWATH Vehicles', Proceedimgs High-Speed Surface Craft Conference, London, May 1983.

14. Salvesen, N., 'Seakeeping Characteristics of Small Waterplane Area Twin Hull Ships', Proceedings AIAA/SNAME Advanced Marine Vehicles Conference, Annapolis, U.S.A., July, 1972.

15. Chun, H.H., Djatmiko, E.B. and McGregor, R.C., 'A Wide Ranging Study on the Motions of SWATH Ships with and without Forward Speeds', Proceedings, 9th International Conference on OMAE, Houston, Texas, USA, February, 1990.

16. Fang, M-C., 'The Motions of SWATH Ships in Waves', Journal Of Ship Research, Vol. 32, No. 4, December 1988, pp. 238-245.

17. Seren, D.B., Miller, N.S., Ferguson, A.M. and McGregor, R.C., 'Some Motion and Resistance Aspects of SWATH-Ship Design', Proceedings International Conference on SWATH Ships and Advanced Multi-Hulled Vessels , London, April, 1985.

18. Lin, W-C and Day, W.G. Jr., 'The Still-Water Resistance and Propulsion Characteristics of Small-Waterplane-Area Twin-Hull (SWATH) Ships', Proceedings AIAA/SNAME Advanced Marine Vehicles Conference, San Diego, California, February 1974.

19. Chun, H.H., Djatmiko, E.B., McGregor, R.C. and Ferguson, A.M., 'SWATH Resistance in Waves with Associated Steady and Dynamic Responses', Proceedings 22nd American Towing Tank Conference, St. John's, Newfoundland,

Canada, August 1989.

20. Chun, H.H., Ferguson, A.M. and McGregor, R.C., 'A New Computational Tool to Estimate the Resistance of SWATH Ships', Proceedings International High-Performance Vehicle Conference, CSNAME, Shanghai, China, November, 1988.

21. Bertram, V., and Jensen, G., 'A Practical Method for Wave Resistance Prediction for SWATH Ships', Proceedings International High-Performance Vehicle Conference, CSNAME, Shanghai, China, November, 1988.

22. Koops, A. and Nethercote, W.C.E., 'SWATH Model Resistance Experiments', Proceedings International Conference of SWATH Ships and Advanced Multi-Hulled Vessels , RINA, London, April, 1985.

23. Jones, A.H., 'A Comparison Between Royal Princess and an Equivalent SWATH Ship', Proceedings, IMAS'88, The Design and Development of Passenger Ships, IME, London, May 1988.

24. Kaysen, H.D., 'SWATH AGS Deep Ocean Survey Ship', The SNAME, The Chesapeake Section, October, 1985.

25. Kaysen, H.D. and Limpus, L.S., 'O'Neill Hullform (OHF) AGS Deep Ocean Survey Ship for the U.S. Navy', Proceedings, Intersociety Advanced Marine Vehicles Conference, Arlington, VA, USA, June 1989.

26. Eames, M.C., 'Future Naval Surface Ships', Naval Engineers Journal, Feb 1985.

27. Eames, M.C., 'Advances in Naval Architecture for Future Surface Warships', Transactions RINA, 1980.

28. Milner, R., 'The World's First 30 Knot Fast Displacement Catamaran (SWATH) Ferry', Proceedings, 7th International High Speed Surface Craft Conference, London, UK, 1990.

29. Routa, T., 'Application of the SWATH Principle to Passenger Vessels', Proceedings International Confernce of SWATH Ships and Advanced Multi-Hulled Vessels , RINA, London, April, 1985.

30. Dunlei, Y. and Linhuai, B., 'The Design of a 500 Passengers SWATH for Service Between Dalian and Yantai', Proceedings of International High-Performance Vehicle Conference, CSNAME, Shanghai, China, November, 1988.

31. Papanikolaou, A., Zaraphonitis, G. and Androulakakis, M., 'Preliminary Design of a High-Speed SWATH Passenger/Car Ferry', Proceedings 5th International Congress on Marine Technology, Athens, Greece, May, 1990.

32. The Editor of the Shipping World and Shipbuilder, 'Patria', Shipping World and Shipbuilder, September, 1989.

33. Kelley, T.D., 'Performance Comparisons of Selected Fast Ferries', Proceedings, 7th International High Speed Surface Craft Conference, London, UK, 1990.

34. Lovie, P.M. and Lang, T.G., 'Commercial Opportunities for SWATH Vessels', Proceedings International Conference on SWATH Ships and Advanced Multi-Hulled Vessels II, London, November, 1988.

35. Coe, T. J., 'A Technical Evaluation of the 60 Foot SWATH Ship Halcyon to Determine Utility in Coast Guard Operations', Proceedings Intersociety Advanced Marine Vehicles Conference, Washington, June, 1989.

36. Warren, N., 'SWATH Design for Offshore Patrols', Small Craft, Supplement to The Naval Architect, RINA, May, 1982.

37. Fernandez-Gonzalez, F. and Bazan, E.N., 'Mission Related Preliminary Design Solutions for Small SWATH Ocean Patrol Vessels', Proceedings International Conference on SWATH Ships and Advanced Multi-Hulled Vessels , RINA, London, April, 1985.

38. Holcomb, R.S., and Allen, R.G., 'Investigation of the Characteristics of Small SWATH Ships Configured for United States Coast Guard Operations', DTNSRDC Report No SDD-83-3, June 1983.

39. Holcomb, R.S., and Allen, R.G., 'The Application of Small SWATH ships to Coastal and Offshore Patrol Missions', Proceedings, RINA, Symposium on Small Fast Warships and Security Vessels, 1982.

40. Oshima, M., Narita, H. and Kunitake, Y., 'Experiences with 12 Meter Long Semi-Submerged Catamaran (SSC) 'Marine Ace' and Building of SSC Ferry for 445 Passengers', Proceedings AIAA/SNAME Advanced Marine Vehicles Conference, Baltimore, Maryland, USA, 1979.

41. McClure, A.C. 'Design for a Semi-Submersible Support Ship', Ocean Industry, August, 1972.

42. Childers, K.C., RAdm., Gloeckler, F.M. and Stevens, R.M., 'SWATH-The VSTOL Aircraft Carrier for the Post-1990's', Naval Engineers Journal, ASNE, February, 1977.

43. Pieroth, C.G. and Lamb, G.R., 'The SWATH Option as a V/STOL Aircraft Carrier', The SNAME, Hampton Roads Section, March, 1985.

44. Lang, T.G., Hightower, J.D., and Strickland, A.T., 'Design and Development of the 190 Ton Stable Semisubmerged Platform (SSP)', Transactions ASME, December, 1973.

45. Betts, C.V., Ferreiro, L.D., Grzeskowiak, S.R., McDonald, N.A. and Parlett, P.J. , 'Design Study for an Anti-Submarine Warfare SWATH Frigate', Proceedings, International Conference on Anti-Submarine Warfare, RINA, London, UK, May 1987.

46. Serter, E.H., 'Comparitive Studies for new U.S. Frigate Hull', International Defense Review 2, 1988.

47. Kennell, C.G., 'Small Waterplane Area twin Hull (SWATH) Combatant Ship Parametric Study', Naval Engineers Journal, ASNE, October, 1979.

48. Rice, M.S. and Harmon, J., 'Prospects for the Development of a SWATH Fishing Vessel', Proceedings, Ocean'78 Conference, IEEE, Washington D.C., USA, September, 1978.

49. MacGregor, J.R., Bose, N., and Small, G., 'Design and Construction of a Small Waterplane Area Twin Hull (SWATH) Vessel', Proceedings of World Symposium on Fishing Gear and Fishing Vessel Design, St Johns, Newfoundland , Canada, November, 1988.

50. Smith, S.N., 'Design and Hydrodynamic Performance of a Small-Submersible (SWATH) Research Vessel', Transactions, RINA, Vol. 125, 1983.

51. Oehlmann, H. and Knupffer, K., 'A New SWATH Naval Research Vessel for the Federal Republic of Germany', Proceedings, Intersociety Advanced Marine Vehicles Conf., Arlington, VA, USA, June, 1989.

52. Dinsmore, R.P., and Lang,T.G., 'Replacement of the University Research Fleet and a 2,500 Ton SWATH Ship Candidate', Proceedings AIAA 8th Advanced Marine Systems Conference, San Diego, California, U.S.A., September,1986.

53. T-AGOS 19 Unclassified U.S. Navy Data and Drawings.

54. Covich, P., 'SWATH T-AGOS 19 A Producible Design', Proceedings AIAA 8th Advanced Marine Systems Conference, San Diego, California, U.S.A. September 1986.

55. Covich, P., 'T-AGOS 19 : An Innovative Program for an Innovative Design', Naval Engineers Journal, ASNE, pp. 99-106, May 1987.

56. Cannon, T.R., and McKesson, C.B., 'Large SWATHS A Discussion of the Diminishing Returns of Increasing Ship Size', Proceedings AIAA 8th Advanced Marine Systems Conference, San Diego, California, U.S.A., Sept,1986.

CHAPTER 7

CONCLUSIONS

This thesis reports work intended to enhance presently available SWATH design capabilities and to extend the application of existing design programs. Following a general review of relevant design aspects, SWATH damaged stability, manoeuvring and wave load response are investigated. In addition a simplified method is developed for the overall mission based evaluation of alternative SWATH and monohull designs.

Results from these investigations are presented in detail at the end of the relevant chapters, however for reference purposes the principal conclusions are grouped and restated in the following pages.

7.1 Aspects of Design

This section is intended to highlight the range and extent of the variations existing in SWATH / monohull design and operability characteristics. It will be noted that the principal advantages / disadvantages of the SWATH concept are now recognised and therefore no longer in dispute. Consequently attention may be redirected towards previously neglected aspects of the design and towards establishing a measure of the concepts overall performance relative to that of monohull counterparts.

Damage stability, manoeuvring and wave loading were the priority areas identified for in depth study. The value of an accurate assessment of construction costs is also recognised, however this was not attempted owing to the availability and inevitably subjective quality of the required data.

7.2 Damage Stability

This phase of the project aimed to establish links between survivability and vessel geometry and to utilize this information by constructing a program intended to estimate damage stability using only preliminary design information.

The damaged stability characteristics of SWATH vessels were investigated by means of an extensive parametric study. Complete damage stability calculations were performed for 900 combinations of initial ship condition and flooding scenario.

Results from these calculations were processed and analysed exhaustively. The data obtained illustrates the dominance of cross structure effects on SWATH damaged behaviour. Overall the results confirm what is intuitively expected; initial flooding leads to rapid heeling/trimming which eases upon the immersion of the cross deck structure due to the massive rise of waterplane area and hence stability.

From the data collected to date it appears that SWATH vessels possess acceptable damaged stability characteristics, and indeed survivability which is likely to be ultimately superior to that of an equivalent monohull. It should be noted that the maximum angle of heel attained by the testcase vessel was only fractionally greater than 20 degrees. This corresponded to asymmetric flooding amidships of extent equal to 25 % of the vessels length. Clearly this is an extreme damage condition and one which very few conventional monohull vessels could hope to survive.

Using the database created, a program was developed which allows the user to estimate at the preliminary design stage, a vessels ability to survive in the event of it sustaining damage leading to partial flooding. This program has been validated, using flooded stability results calculated using commercial software, for a variety of combinations of design parameter.

In addition a limited investigation into the effects of varying the height of the vessels centre of gravity has been performed. Results from this investigation have been incorporated in the above program.

This project was intended to provide the foundations for a computer augmented damage stability estimation tool for SWATH vessels. With the creation and validation of 'FSEP1' and 'FSEP2' this aim has been accomplished.

7.3 Manoeuvring

The manoeuvring characteristics of SWATH vessels have been studied, demonstrated and simulated. This was achieved by means of literature review, full scale tests and the development of a manoeuvring prediction tool incorporating the best elements of currently available and accepted manoeuvring theory, suitably adapted for the novel geometry of the SWATH form.

Principal conclusions from the literature review may be summarised as follows :-

1. SWATH vessels are inherently very directionally stable. This is an advantage for missions requiring good course keeping in rough seas e.g. Sonar Surveillance Vessels.

2. In spite of this SWATH vessels can possess turning diameters equivalent to comparable monohulls. However this can only be achieved by careful design of the control surfaces.

3. Slow speed manoeuvring is excellent due to the availability of large amounts of differential thrust from widely spaced propellers.

4. Unlike monohulls turning performance is very speed dependent for most SWATH designs. Turning diameters increase with speed as we move from the medium to high speed range, particularly for designs with surface piercing rudders.

A manoeuvring prediction program was developed for SWATH vessels operating in the low to medium speed range. This program determines the rudder size required for a given vessel, and estimates the resulting turning performance for that vessel. The program may be applied to SWATH vessels fitted with rudders both in and out of the propeller slipstream and possessing widely different resistance and propulsive characteristics.

The program has been run for a number of existing SWATH designs for which full scale trials information is available. The results/predictions from the program were found to agree closely with the actual values observed on trials.

In addition full scale manoeuvring trials on the 20 ton SWATH fishing vessel "Ali" have been conducted and data on the turning performance collected. This data will be analysed and the results reported in greater detail in due course.

7.4 Environmental Loading

Chapter 5 reviews aspects of wave loading in the structural design of SWATH ships. The primary wave induced global loads were identified for SWATH vessels and

a thorough review of the techniques employed to predict these loads was undertaken.

It is widely acknowledged that wave induced side force leading to a transverse bending moment is the dominant form of environmental loading for these vessels. All available methods for the calculation / estimation of this force were therefore identified and applied to the vessels T-AGOS 19 and the M.V. Patria. Short term extreme value prediction methods were applied in order to determine likely lifetime values of design extreme loading. Empirically derived estimates were compared with those produced by the application of rigorous three dimensional potential theory, and conclusions on the applicability of the methods drawn.

The results obtained were on the whole encouraging although it appears that SWATH ships are still not adequately catered for by the classification societies. ABS are to date the only society to propose rules suitable for the design of general SWATH vessels. For vessels in the T-AGOS size range it appears that the capability presently exists to predict design extreme values of wave induced side load with reasonable certainty. This is unfortunately not the case for vessels of the M.V. Patria's size however it must be remembered that the structural scantlings of these vessels are nearly always driven by considerations of secondary loading. The accuracy of presently available estimates is therefore quite adequate for design purposes.

Based on these findings the author concludes that currently available methods for predicting extreme design global loads on SWATH ships are satisfactorily accurate for design purposes. The author subsequently recommends that attention be redirected towards incorporating the effect of weather and trade routing into the calculations, and to the investigation of structural response and stress transfer within the vessel.

7.5 Design Evaluation

In the final phase of the work the parameters of primary importance for comparative purposes were identified, and a framework was suggested for the basic evaluation of alternative SWATH and monohull designs.

This study highlighted the importance of making comparisons on the basis of mission equivalence. It must be stressed that no other definitions of equivalence are appropriate.

It was found that SWATH vessels prove superior to monohulls when performing missions dominated by seakeeping considerations, however it must be remembered that few missions are dictated solely by considerations of seakeeping. In particular when comparing 'seakeeping equivalent' vessels, it is important to recognise the additional payload capability of the larger monohull. In the same way the additional seakeeping performance of SWATH should not be overlooked when comparing equivalent displacement vessels. SWATH ships are unlikely to exceed 15,000 Tonnes displacement, since above this limit monohull vessels possess adequate seakeeping performance.

Survivability and operation of onboard systems are the two other principal areas where SWATH ships lead their monohull counterparts, while the cost of SWATH ships is presently estimated to be approximately 5-10% more than mission equivalent monohulls. This value is based on current U.S. Navy data and is subject to revision. Future advances in SWATH structures are likely to improve the perceived reliability of the concept and reduce design and fabrication costs while further advances in fabrication and outfit technology may ultimately remove any remaining SWATH / monohull cost differential.

Based on the results of, and the knowledge gained performing this study, the author recommends serious consideration be given to the SWATH concept to perform the following roles:-

- Sonar Surveillance SSV
- Oceanographic and Deep Ocean Survey DOS
- Offshore Patrol OPV
- Passenger Ferry (Exposed Route)
- Small Vehicle Ferry (Exposed Route)
- Diving Support and Salvage
- Light Displacement Air Support

All these roles require (relatively) small vessels with good seakeeping capabilities and / or large usable deck areas. The SWATH ship is therefore ideally suited to these missions although the final choice of vessel type will inevitably depend on many other indefinable factors not the least of which are cost and 'fashion'.

7.6 Closure

It is now almost 20 years since the U.S. Navy launched S.S.P. Kaimalino. The development pace of SWATH technology has since been rapid and continues to accelerate in spite of initial resistance to the concept from within the marine community. Many of the reasons for this resistance have now been removed with the result that the number of SWATH vessels has gradually risen and recently expanded rapidly. The current orderbook may be taken as an indication that the marine world is at last ready to accept the SWATH concept.

Although design information is still limited in monohull terms, the database is expanding continuously and confidence is gained with every newly built vessel. This thesis has broadened the scope of an existing SWATH design capability and forms a modest addition to the armoury of the naval architect engaged in the design of these unorthodox and intriguing vehicles.

Appendix A. Full Damage Stability Results

Flooded stability data output by the Wolfson Unit programs was processed to give values for Heel, Trim, Max GZ and area under the GZ curve for the two regions 0-45 and 0-20 degrees heel.

These values were plotted against flooding extent for each combination of flooding location, box clearance, design displacement and operating draught. Standard regression routines were applied to these plots and the polynomial coefficients of the equations thus produced were stored.

These equations form the database upon which 'FSEP1' is based.

DISPLACEMENT 950.0 TONNES DAMAGE LOCATION PORT AND STARBOARD FORWARD

BOX CLEARANCE 3.40 METRES TRIM
Y=-0.1576E-01 -0.2537E+00*X -0.2254E-01*X^2 +0.6209E-03*X^3

BOX CLEARANCE 2.21 METRES TRIM
Y=0.8241E-02 -0.3171E+00*X -0.1780E-01*X^2 +0.7211E-03*X^3

BOX CLEARANCE 3.40 METRES HEEL
Y=0

BOX CLEARANCE 2.21 METRES HEEL
Y=0

BOX CLEARANCE 3.40 METRES MAXIMUM Gz
Y=0.7097E+01 -0.6137E-02*X -0.5152E-03*X^2 -0.4143E-04*X^3

BOX CLEARANCE 2.21 METRES MAXIMUM Gz
FOR FLOODING EXTENT LESS THAN OR EQUAL TO 6.25%
Y=0.7217E+01 +0.8000E-03*X
FOR FLOODING EXTENT GREATER THAN 6.25%
Y=0.7217E+01 +0.6064E-02*X -0.2377E-02*X^2 +0.3418E-03*X^3 -0.1540E-04*X^4

BOX CLEARANCE 3.40 METRES AREA UNDER THE Gz CURVE TO 20 DEGREES
Y=0.4410E+00 +0.1077E-02*X -0.6543E-03*X^2 +0.5374E-04*X^3

BOX CLEARANCE 2.21 METRES AREA UNDER THE Gz CURVE TO 20 DEGREES
Y=0.5800E+00 -0.1510E-02*X +0.9122E-04*X^2 +0.2330E-04*X^3

BOX CLEARANCE 3.40 METRES AREA UNDER THE Gz CURVE TO 45 DEGREES
Y=0.2994E+01 -0.6566E-03*X -0.2243E-03*X^2 +0.2532E-04*X^3

BOX CLEARANCE 2.21 METRES AREA UNDER THE Gz CURVE TO 45 DEGREES
Y=0.3167E+01 -0.4833E-02*X +0.9277E-03*X^2 -0.1946E-04*X^3

DISPLACEMENT 1000.0 TONNES DAMAGE LOCATION PORT AND STARBOARD FORWARD

BOX CLEARANCE 3.40 METRES TRIM
Y=0.1952E-01 -0.2465E+00*X -0.3615E-01*X^2 +0.1263E-02*X^3

BOX CLEARANCE 2.21 METRES TRIM
Y=0.9784E-01 -0.5044E+00*X +0.5218E-02*X^2

BOX CLEARANCE 3.40 METRES HEEL
Y=0

BOX CLEARANCE 2.21 METRES HEEL
Y=0

BOX CLEARANCE 3.40 METRES MAXIMUM Gz
Y=0.6895E+01 -0.1163E-01*X +0.4741E-04*X^2

BOX CLEARANCE 2.21 METRES MAXIMUM Gz
Y=0.7205E+01 -0.2221E-02*X +0.2765E-03*X^2 +0.8333E-04*X^3 -0.8691E-05*X^4

BOX CLEARANCE 3.40 METRES AREA UNDER THE Gz CURVE TO 20 DEGREES
Y=0.3550E+00 -0.9518E-03*X -0.2424E-03*X^2 +0.4756E-04*X^3

BOX CLEARANCE 2.21 METRES AREA UNDER THE Gz CURVE TO 20 DEGREES
Y=0.5200E+00 -0.4176E-02*X +0.7000E-03*X^2 +0.2415E-05*X^3

BOX CLEARANCE 3.40 METRES AREA UNDER THE Gz CURVE TO 45 DEGREES
Y=0.2901E+01 -0.3347E-02*X +0.4033E-03*X^2 +0.8592E-05*X^3

BOX CLEARANCE 2.21 METRES AREA UNDER THE Gz CURVE TO 45 DEGREES
Y=0.3102E+01 -0.5803E-03*X +0.4330E-03*X^2

DISPLACEMENT 1050.0 TONNES DAMAGE LOCATION PORT AND STARBOARD FORWARD

BOX CLEARANCE 3.40 METRES TRIM
Y=0.1409E+00 -0.4943E+00*X -0.1296E-02*X^2

BOX CLEARANCE 2.21 METRES TRIM
Y=0.1327E+00 -0.4830E+00*X +0.4255E-02*X^2

BOX CLEARANCE 3.40 METRES HEEL
Y=0

BOX CLEARANCE 2.21 METRES HEEL
Y=0

BOX CLEARANCE 3.40 METRES MAXIMUM Gz
Y=0.6735E+01 -0.4035E-02*X +0.1520E-02*X^2 -0.7537E-04*X^3

BOX CLEARANCE 2.21 METRES MAXIMUM Gz
Y=0.7188E+01 -0.4749E-02*X +0.2017E-02*X^2 -0.1765E-03*X^3

BOX CLEARANCE 3.40 METRES AREA UNDER THE Gz CURVE TO 20 DEGREES
Y=0.2931E+00 -0.3305E-02*X +0.3287E-03*X^2 +0.3021E-04*X^3

BOX CLEARANCE 2.21 METRES AREA UNDER THE Gz CURVE TO 20 DEGREES
Y=0.4821E+00 -0.3089E-02*X +0.7499E-03*X^2 -0.1240E-05*X^3

BOX CLEARANCE 3.40 METRES AREA UNDER THE Gz CURVE TO 45 DEGREES
Y=0.2829E+01 -0.4097E-02*X +0.8367E-03*X^2 -0.7145E-05*X^3

BOX CLEARANCE 2.21 METRES AREA UNDER THE Gz CURVE TO 45 DEGREES
Y=0.3065E+01 +0.1730E-02*X +0.2868E-03*X^2

DISPLACEMENT 1900.0 TONNES DAMAGE LOCATION PORT AND STARBOARD FORWARD

BOX CLEARANCE 4.27 METRES TRIM
Y=0.3122E-01 -0.1314E+00*X -0.3653E-01*X^2 +0.9457E-03*X^3

BOX CLEARANCE 2.77 METRES TRIM
Y=0.9469E-01 -0.3073E+00*X -0.7965E-02*X^2

BOX CLEARANCE 4.27 METRES HEEL
Y=0

BOX CLEARANCE 2.77 METRES HEEL
Y=0

BOX CLEARANCE 4.27 METRES MAXIMUM Gz
Y=0.7170E+01 -0.1248E-01*X +0.5041E-03*X^2 -0.1186E-03*X^3

BOX CLEARANCE 2.77 METRES MAXIMUM Gz
Y=0.6996E+01 +0.5541E-02*X -0.2211E-02*X^2 +0.4175E-03*X^3 -0.2307E-04*X^4

BOX CLEARANCE 4.27 METRES AREA UNDER THE Gz CURVE TO 20 DEGREES
Y=0.3241E+00 -0.2910E-02*X +0.2613E-03*X^2 +0.1987E-04*X^3

BOX CLEARANCE 2.77 METRES AREA UNDER THE Gz CURVE TO 20 DEGREES
Y=0.3900E+00 -0.1918E-02*X +0.1752E-03*X^2 +0.2319E-04*X^3

BOX CLEARANCE 4.27 METRES AREA UNDER THE Gz CURVE TO 45 DEGREES
FOR FLOODING EXTENT LESS THAN OR EQUAL TO 8.33%
Y=0.2810E+01
FOR FLOODING EXTENT GREATER THAN 8.33%
Y=0.2740E+01 +0.1080E-01*X -0.2879E-03*X^2

BOX CLEARANCE 2.77 METRES AREA UNDER THE Gz CURVE TO 45 DEGREES
FOR FLOODING EXTENT LESS THAN OR EQUAL TO 6.25%
Y=0.2956E+01

FOR FLOODING EXTENT GREATER THAN 6.25%
Y=0.2957E+01 -0.6747E-02*X +0.1337E-02*X^2 -0.4947E-04*X^3

DISPLACEMENT 2000.0 TONNES DAMAGE LOCATION PORT AND STARBOARD FORWARD

BOX CLEARANCE 4.27 METRES TRIM
Y=0.1335E+00 -0.2778E+00*X -0.1415E-01*X^2

BOX CLEARANCE 2.77 METRES TRIM
Y=0.9662E-01 -0.2939E+00*X -0.8445E-02*X^2

BOX CLEARANCE 4.27 METRES HEEL
Y=0

BOX CLEARANCE 2.77 METRES HEEL
Y=0

BOX CLEARANCE 4.27 METRES MAXIMUM Gz
Y=0.6900E+01 -0.1280E-01*X +0.7810E-03*X^2 -0.8289E-04*X^3

BOX CLEARANCE 2.77 METRES MAXIMUM Gz
Y=0.7032E+01 -0.7262E-02*X +0.3328E-02*X^2 -0.2924E-03*X^3

BOX CLEARANCE 4.27 METRES AREA UNDER THE Gz CURVE TO 20 DEGREES
Y=0.2611E+00 -0.3504E-02*X +0.5713E-03*X^2 +0.9029E-05*X^3

BOX CLEARANCE 2.77 METRES AREA UNDER THE Gz CURVE TO 20 DEGREES
Y=0.3451E+00 -0.2332E-02*X +0.3672E-03*X^2 +0.1748E-04*X^3

BOX CLEARANCE 4.27 METRES AREA UNDER THE Gz CURVE TO 45 DEGREES
FOR FLOODING EXTENT LESS THAN OR EQUAL TO 6.25%
Y=0.2710E+01
FOR FLOODING EXTENT GREATER THAN 6.25%
Y=0.2680E+01 +0.4800E-02*X

BOX CLEARANCE 2.77 METRES AREA UNDER THE Gz CURVE TO 45 DEGREES
FOR FLOODING EXTENT LESS THAN OR EQUAL TO 6.25%
Y=0.2887E+01
FOR FLOODING EXTENT GREATER THAN 6.25%
Y=0.2887E+01 -0.6018E-02*X +0.1289E-02*X^2 -0.4901E-04*X^3

DISPLACEMENT 2100.0 TONNES DAMAGE LOCATION PORT AND STARBOARD FORWARD

BOX CLEARANCE 4.27 METRES TRIM
Y=0.1044E+00 -0.2428E+00*X -0.1631E-01*X^2

BOX CLEARANCE 2.77 METRES TRIM
Y=0.5036E-01 -0.2354E+00*X -0.1006E-01*X^2

BOX CLEARANCE 4.27 METRES HEEL
Y=0

BOX CLEARANCE 2.77 METRES HEEL
Y=0

BOX CLEARANCE 4.27 METRES MAXIMUM Gz
FOR FLOODING EXTENT LESS THAN OR EQUAL TO 6.33%
Y=0.6720E+01 +0.3200E-02*X
FOR FLOODING EXTENT GREATER THAN 6.33%
Y=0.6720E+01 +0.2561E-01*X -0.8626E-02*X^2 +0.1072E-02*X^3 -0.4241E-04*X^4

BOX CLEARANCE 2.77 METRES MAXIMUM Gz
Y=0.7043E+01 -0.1033E-01*X +0.2211E-02*X^2 -0.2552E-03*X^3

BOX CLEARANCE 4.27 METRES AREA UNDER THE Gz CURVE TO 20 DEGREES
Y=0.2300E+00 +0.1439E-02*X -0.3097E-03*X^2 +0.4711E-04*X^3

BOX CLEARANCE 2.77 METRES AREA UNDER THE Gz CURVE TO 20 DEGREES
Y=0.3221E+00 -0.2623E-02*X +0.6261E-03*X^2 +0.4294E-05*X^3

BOX CLEARANCE 4.27 METRES AREA UNDER THE Gz CURVE TO 45 DEGREES
FOR FLOODING EXTENT LESS THAN OR EQUAL TO 6.25%
Y=0.2640E+01
FOR FLOODING EXTENT GREATER THAN 6.25%
Y=0.2592E+01 +0.8134E-02*X -0.9548E-04*X^2

BOX CLEARANCE 2.77 METRES AREA UNDER THE Gz CURVE TO 45 DEGREES
FOR FLOODING EXTENT LESS THAN OR EQUAL TO 6.25%
Y=0.2839E+01
FOR FLOODING EXTENT GREATER THAN 6.25%
Y=0.2839E+01 -0.6302E-02*X +0.1389E-02*X^2 -0.5829E-04*X^3

DISPLACEMENT 2850.0 TONNES DAMAGE LOCATION PORT AND STARBOARD FORWARD

BOX CLEARANCE 4.91 METRES TRIM
Y=0.3468E-01 -0.2455E+00*X -0.3076E-01*X^2 +0.7518E-03*X^3

BOX CLEARANCE 3.17 METRES TRIM
Y=0.8767E-01 -0.3955E+00*X -0.6105E-02*X^2

BOX CLEARANCE 4.91 METRES HEEL
Y=0

BOX CLEARANCE 3.17 METRES HEEL
Y=0

BOX CLEARANCE 4.91 METRES MAXIMUM Gz
Y=0.7456E+01 +0.8948E-02*X +0.1575E-02*X^2 -0.2245E-03*X^3

BOX CLEARANCE 3.17 METRES MAXIMUM Gz
Y=0.7671E+01 -0.1217E-02*X +0.2887E-03*X^2 -0.2187E-03*X^3

BOX CLEARANCE 4.91 METRES AREA UNDER THE Gz CURVE TO 20 DEGREES
Y=0.3081E+00 -0.3872E-02*X +0.4304E-03*X^2 +0.1708E-04*X^3

BOX CLEARANCE 3.17 METRES AREA UNDER THE Gz CURVE TO 20 DEGREES
Y=0.3671E+00 -0.3795E-02*X +0.5002E-03*X^2 +0.1369E-04*X^3

BOX CLEARANCE 4.91 METRES AREA UNDER THE Gz CURVE TO 45 DEGREES
FOR FLOODING EXTENT LESS THAN OR EQUAL TO 6.25%
Y=0.2922E+01 -0.3200E-03*X
FOR FLOODING EXTENT GREATER THAN 6.25%
Y=0.2922E+01 -0.7517E-02*X +0.1545E-02*X^2 -0.6434E-04*X^3

BOX CLEARANCE 3.17 METRES AREA UNDER THE Gz CURVE TO 45 DEGREES
FOR FLOODING EXTENT LESS THAN OR EQUAL TO 6.25%
Y=0.3095E+01 -0.8000E-03*X
FOR FLOODING EXTENT GREATER THAN 6.25%
Y=0.3095E+01 -0.9013E-02*X +0.1817E-02*X^2 -0.8219E-04*X^3

DISPLACEMENT 3000.0 TONNES DAMAGE LOCATION PORT AND STARBOARD FORWARD

BOX CLEARANCE 4.91 METRES TRIM
Y=0.1405E+00 -0.3807E+00*X -0.1269E-01*X^2

BOX CLEARANCE 3.17 METRES TRIM
Y=0.1160E+00 -0.4016E+00*X -0.6342E-02*X^2

BOX CLEARANCE 4.91 METRES HEEL
Y=0

BOX CLEARANCE 3.17 METRES HEEL
Y=0

BOX CLEARANCE 4.91 METRES MAXIMUM Gz
Y=0.7569E+01 +0.5024E-03*X +0.2269E-02*X^2 -0.3007E-03*X^3

BOX CLEARANCE 3.17 METRES MAXIMUM Gz
Y=0.7396E+01 -0.9882E-02*X +0.1541E-02*X^2 -0.2405E-03*X^3

BOX CLEARANCE 4.91 METRES AREA UNDER THE Gz CURVE TO 20 DEGREES
Y=0.2421E+00 -0.4937E-02*X +0.7605E-03*X^2 +0.8462E-05*X^3

BOX CLEARANCE 3.17 METRES AREA UNDER THE Gz CURVE TO 20 DEGREES
Y=0.3131E+00 -0.4017E-02*X +0.7084E-03*X^2 +0.7403E-05*X^3

BOX CLEARANCE 4.91 METRES AREA UNDER THE Gz CURVE TO 45 DEGREES
FOR FLOODING EXTENT LESS THAN OR EQUAL TO 6.25%
Y=0.2809E+01 +0.1600E-03*X
FOR FLOODING EXTENT GREATER THAN 6.25%
Y=0.2809E+01 -0.6044E-02*X +0.1314E-02*X^2 -0.5383E-04*X^3

BOX CLEARANCE 3.17 METRES AREA UNDER THE Gz CURVE TO 45 DEGREES
FOR FLOODING EXTENT LESS THAN OR EQUAL TO 6.25%
Y=0.2986E+01 +0.1600E-03*X
FOR FLOODING EXTENT GREATER THAN 6.25%
Y=0.2986E+01 -0.9482E-02*X +0.2163E-02*X^2 -0.1013E-03*X^3

DISPLACEMENT 3150.0 TONNES DAMAGE LOCATION PORT AND STARBOARD FORWARD

BOX CLEARANCE 4.91 METRES TRIM
Y=0.1656E+00 -0.3860E+00*X -0.1334E-01*X^2

BOX CLEARANCE 3.17 METRES TRIM
Y=-0.1290E-02 -0.7444E-01*X -0.5517E-01*X^2 +0.1858E-02*X^3

BOX CLEARANCE 4.91 METRES HEEL
Y=0

BOX CLEARANCE 3.17 METRES HEEL
Y=0

BOX CLEARANCE 4.91 METRES MAXIMUM Gz
Y=0.7554E+01 -0.4731E-02*X +0.1557E-02*X^2 -0.2832E-03*X^3

BOX CLEARANCE 3.17 METRES MAXIMUM Gz
Y=0.7122E+01 -0.1040E-01*X +0.4499E-02*X^2 -0.4002E-03*X^3

BOX CLEARANCE 4.91 METRES AREA UNDER THE Gz CURVE TO 20 DEGREES
Y=0.2021E+00 -0.3343E-02*X +0.6474E-03*X^2 +0.1318E-04*X^3

BOX CLEARANCE 3.17 METRES AREA UNDER THE Gz CURVE TO 20 DEGREES
Y=0.2840E+00 -0.2796E-02*X +0.6767E-03*X^2 +0.6623E-05*X^3

BOX CLEARANCE 4.91 METRES AREA UNDER THE Gz CURVE TO 45 DEGREES
FOR FLOODING EXTENT LESS THAN OR EQUAL TO 6.25%
Y=0.2711E+01 +0.1600E-03*X
FOR FLOODING EXTENT GREATER THAN 6.25%
Y=0.2711E+01 -0.7522E-02*X +0.1653E-02*X^2 -0.6994E-04*X^3

BOX CLEARANCE 3.17 METRES AREA UNDER THE Gz CURVE TO 45 DEGREES
FOR FLOODING EXTENT LESS THAN OR EQUAL TO 6.25%
Y=0.2898E+01 +0.1120E-02*X
FOR FLOODING EXTENT GREATER THAN 6.25%
Y=0.2898E+01 -0.6324E-02*X +0.1830E-02*X^2 -0.9676E-04*X^3

DISPLACEMENT 3800.0 TONNES DAMAGE LOCATION PORT AND STARBOARD FORWARD

BOX CLEARANCE 5.38 METRES TRIM
Y=0.5415E-01 -0.1511E+00*X -0.4099E-01*X^2 +0.9484E-03*X^3

BOX CLEARANCE 3.48 METRES TRIM
Y=0.1064E+00 -0.3576E+00*X -0.9770E-02*X^2

BOX CLEARANCE 5.38 METRES HEEL
Y=0

BOX CLEARANCE 3.48 METRES HEEL
Y=0

BOX CLEARANCE 5.38 METRES MAXIMUM Gz
Y=0.7687E+01 +0.5051E-01*X -0.6694E-02*X^2

BOX CLEARANCE 3.48 METRES MAXIMUM Gz
Y=0.7458E+01 +0.4426E-02*X +0.1841E-02*X^2 -0.3242E-03*X^3

BOX CLEARANCE 5.38 METRES AREA UNDER THE Gz CURVE TO 20 DEGREES
Y=0.2687E+00 -0.8957E-02*X +0.1356E-02*X^2 -0.1965E-04*X^3

BOX CLEARANCE 3.48 METRES AREA UNDER THE Gz CURVE TO 20 DEGREES
Y=0.3106E+00 -0.5843E-02*X +0.8975E-03*X^2

BOX CLEARANCE 5.38 METRES AREA UNDER THE Gz CURVE TO 45 DEGREES
FOR FLOODING EXTENT LESS THAN OR EQUAL TO 6.25%
Y=0.2813E+01 -0.1120E-02*X
FOR FLOODING EXTENT GREATER THAN 6.25%
Y=0.2813E+01 -0.8753E-02*X +0.1718E-02*X^2 -0.8213E-04*X^3

BOX CLEARANCE 3.48 METRES AREA UNDER THE Gz CURVE TO 45 DEGREES
FOR FLOODING EXTENT LESS THAN OR EQUAL TO 6.25%
Y=0.2975E+01 -0.1600E-03*X
FOR FLOODING EXTENT GREATER THAN 6.25%
Y=0.2975E+01 -0.8052E-02*X +0.1913E-02*X^2 -0.1035E-03*X^3

DISPLACEMENT 4000.0 TONNES DAMAGE LOCATION PORT AND STARBOARD FORWARD

BOX CLEARANCE 5.38 METRES TRIM
Y=0.7228E-01 -0.1030E+00*X -0.5229E-01*X^2 +0.1321E-02*X^3

BOX CLEARANCE 3.48 METRES TRIM
Y=0.1149E+00 -0.3566E+00*X -0.1031E-01*X^2

BOX CLEARANCE 5.38 METRES HEEL
Y=0

BOX CLEARANCE 3.48 METRES HEEL
Y=0

BOX CLEARANCE 5.38 METRES MAXIMUM Gz
Y=0.7455E+01 +0.2985E-02*X -0.3663E-03*X^2 -0.1774E-03*X^3

BOX CLEARANCE 3.48 METRES MAXIMUM Gz
Y=0.7404E+01 -0.3860E-02*X +0.1201E-02*X^2 -0.3035E-03*X^3

BOX CLEARANCE 5.38 METRES AREA UNDER THE Gz CURVE TO 20 DEGREES
Y=0.2109E+00 -0.9898E-02*X +0.1687E-02*X^2 -0.2986E-04*X^3

BOX CLEARANCE 3.48 METRES AREA UNDER THE Gz CURVE TO 20 DEGREES
Y=0.2661E+00 -0.3940E-02*X +0.7782E-03*X^2 +0.4012E-05*X^3

BOX CLEARANCE 5.38 METRES AREA UNDER THE Gz CURVE TO 45 DEGREES
FOR FLOODING EXTENT LESS THAN OR EQUAL TO 6.25%
Y=0.2677E+01 -0.4800E-03*X

FOR FLOODING EXTENT GREATER THAN 6.25%
Y=0.2677E+01 -0.7863E-02*X +0.1675E-02*X^2 -0.8016E-04*X^3

BOX CLEARANCE 3.48 METRES AREA UNDER THE Gz CURVE TO 45 DEGREES
FOR FLOODING EXTENT LESS THAN OR EQUAL TO 6.25%
Y=0.2860E+01 -0.4800E-03*X
FOR FLOODING EXTENT GREATER THAN 6.25%
Y=0.2860E+01 -0.9551E-02*X +0.2216E-02*X^2 -0.1206E-03*X^3

DISPLACEMENT 4200.0 TONNES DAMAGE LOCATION PORT AND STARBOARD FORWARD

BOX CLEARANCE 5.38 METRES TRIM
Y=0.3778E+00 -0.4905E+00*X -0.4504E-02*X^2

BOX CLEARANCE 3.48 METRES TRIM
Y=0.4099E-03 -0.1017E+00*X -0.4509E-01*X^2 +0.1273E-02*X^3

BOX CLEARANCE 5.38 METRES HEEL
Y=0

BOX CLEARANCE 3.48 METRES HEEL
Y=0

BOX CLEARANCE 5.38 METRES MAXIMUM Gz
Y=0.7455E+01 +0.2985E-02*X -0.3663E-03*X^2 -0.1774E-03*X^3

BOX CLEARANCE 3.48 METRES MAXIMUM Gz
Y=0.7157E+01 -0.6505E-03*X +0.3018E-03*X^2 -0.2715E-03*X^3

BOX CLEARANCE 5.38 METRES AREA UNDER THE Gz CURVE TO 20 DEGREES
Y=0.1756E+00 -0.5291E-02*X +0.1202E-02*X^2 -0.1781E-04*X^3

BOX CLEARANCE 3.48 METRES AREA UNDER THE Gz CURVE TO 20 DEGREES
Y=0.2460E+00 -0.1646E-02*X +0.5545E-03*X^2 +0.9595E-05*X^3

BOX CLEARANCE 5.38 METRES AREA UNDER THE Gz CURVE TO 45 DEGREES
FOR FLOODING EXTENT LESS THAN OR EQUAL TO 6.25%
Y=0.2557E+01 +0.5184E-03*X
FOR FLOODING EXTENT GREATER THAN 6.25%
Y=0.2557E+01 -0.7343E-02*X +0.1875E-02*X^2 -0.9869E-04*X^3

BOX CLEARANCE 3.48 METRES AREA UNDER THE Gz CURVE TO 45 DEGREES
Y=0.2753E+01 -0.5045E-02*X +0.1571E-02*X^2 -0.1027E-03*X^3

DISPLACEMENT 4750.0 TONNES DAMAGE LOCATION PORT AND STARBOARD FORWARD

BOX CLEARANCE 5.94 METRES TRIM
Y=0.4231E-01 -0.1720E+00*X -0.3860E-01*X^2 +0.8325E-03*X^3

BOX CLEARANCE 3.88 METRES TRIM
Y=0.1341E+00 -0.1421E+00*X -0.2250E-01*X^2

BOX CLEARANCE 5.94 METRES HEEL
Y=0

BOX CLEARANCE 3.88 METRES HEEL
Y=0

BOX CLEARANCE 5.94 METRES MAXIMUM Gz
Y=0.7563E+01 +0.4874E-01*X -0.3361E-02*X^2 -0.1370E-03*X^3

BOX CLEARANCE 3.88 METRES MAXIMUM Gz
Y=0.7709E+01 +0.2128E-02*X +0.1475E-02*X^2 -0.3370E-03*X^3

BOX CLEARANCE 5.94 METRES AREA UNDER THE Gz CURVE TO 20 DEGREES
Y=0.1819E+00 +0.1295E-01*X -0.1728E-03*X^2 +0.1164E-04*X^3

BOX CLEARANCE 3.88 METRES AREA UNDER THE Gz CURVE TO 20 DEGREES
Y=0.2969E+00 -0.9361E-03*X -0.6806E-04*X^2 +0.3581E-04*X^3

BOX CLEARANCE 5.94 METRES AREA UNDER THE Gz CURVE TO 45 DEGREES
Y=0.2557E+01 +0.7216E-01*X -0.5360E-02*X^2 +0.1071E-03*X^3

BOX CLEARANCE 3.88 METRES AREA UNDER THE Gz CURVE TO 45 DEGREES
Y=0.2977E+01 -0.5112E-02*X +0.1206E-02*X^2 -0.6103E-04*X^3 -0.1282E-05*X^4

DISPLACEMENT 5000.0 TONNES DAMAGE LOCATION PORT AND STARBOARD FORWARD

BOX CLEARANCE 5.94 METRES TRIM
Y=0.5858E-01 -0.1196E+00*X -0.5041E-01*X^2 +0.1216E-02*X^3

BOX CLEARANCE 3.88 METRES TRIM
Y=-0.3263E-02 +0.2492E+00*X -0.8250E-01*X^2 +0.2230E-02*X^3

BOX CLEARANCE 5.94 METRES HEEL
Y=0

BOX CLEARANCE 3.88 METRES HEEL
Y=0

BOX CLEARANCE 5.94 METRES MAXIMUM Gz
Y=0.7526E+01 +0.3246E-01*X -0.2230E-02*X^2 -0.1719E-03*X^3

BOX CLEARANCE 3.88 METRES MAXIMUM Gz
Y=0.7417E+01 +0.1236E-02*X +0.1266E-02*X^2 -0.3275E-03*X^3

BOX CLEARANCE 5.94 METRES AREA UNDER THE Gz CURVE TO 20 DEGREES
Y=0.2138E+00 -0.8758E-02*X +0.1561E-02*X^2 -0.2717E-04*X^3

BOX CLEARANCE 3.88 METRES AREA UNDER THE Gz CURVE TO 20 DEGREES
Y=0.2598E+00 -0.1209E-02*X +0.7556E-04*X^2 +0.3013E-04*X^3

BOX CLEARANCE 5.94 METRES AREA UNDER THE Gz CURVE TO 45 DEGREES
Y=0.2689E+01 -0.5979E-02*X +0.1470E-02*X^2 -0.8095E-04*X^3

BOX CLEARANCE 3.88 METRES AREA UNDER THE Gz CURVE TO 45 DEGREES
Y=0.2845E+01 -0.5075E-02*X +0.1438E-02*X^2 -0.1001E-03*X^3

DISPLACEMENT 5250.0 TONNES DAMAGE LOCATION PORT AND STARBOARD FORWARD

BOX CLEARANCE 5.94 METRES TRIM
Y=0.3689E-01 -0.7266E-01*X -0.5768E-01*X^2 +0.1430E-02*X^3

BOX CLEARANCE 3.88 METRES TRIM
Y=0.8950E-01 +0.1067E+00*X -0.5090E-01*X^2 +0.8840E-03*X^3

BOX CLEARANCE 5.94 METRES HEEL
Y=0

BOX CLEARANCE 3.88 METRES HEEL
Y=0

BOX CLEARANCE 5.94 METRES MAXIMUM Gz
Y=0.7558E+01 +0.2683E-01*X -0.3865E-02*X^2 -0.1170E-03*X^3

BOX CLEARANCE 3.88 METRES MAXIMUM Gz
Y=0.6990E+01 +0.7346E-03*X +0.1273E-02*X^2 -0.3107E-03*X^3

BOX CLEARANCE 5.94 METRES AREA UNDER THE Gz CURVE TO 20 DEGREES
Y=0.1812E+00 -0.8610E-02*X +0.1656E-02*X^2 -0.3146E-04*X^3

BOX CLEARANCE 3.88 METRES AREA UNDER THE Gz CURVE TO 20 DEGREES
Y=0.2471E+00 -0.1808E-02*X +0.3128E-03*X^2 +0.1683E-04*X^3

BOX CLEARANCE 5.94 METRES AREA UNDER THE Gz CURVE TO 45 DEGREES
Y=0.2556E+01 -0.5642E-02*X +0.1347E-02*X^2 -0.7540E-04*X^3

BOX CLEARANCE 3.88 METRES AREA UNDER THE Gz CURVE TO 45 DEGREES
Y=0.2724E+01 -0.2801E-02*X +0.1049E-02*X^2 -0.8944E-04*X^3

DISPLACEMENT 950.0 TONNES DAMAGE LOCATION STARBOARD FORWARD

BOX CLEARANCE 3.40 METRES TRIM
Y=0.5768E-01 -0.1860E+00*X -0.2724E-02*X^2

BOX CLEARANCE 2.21 METRES TRIM
Y=0.2009E-01 -0.1392E+00*X -0.1545E-01*X^2 +0.5014E-03*X^3

BOX CLEARANCE 3.40 METRES HEEL
Y=-0.5759E-01 +0.1928E+00*X +0.7805E-02*X^2

BOX CLEARANCE 2.21 METRES HEEL
Y=-0.2173E-01 +0.1606E+00*X +0.1765E-01*X^2 -0.4828E-03*X^3

BOX CLEARANCE 3.40 METRES MAXIMUM Gz
Y=0.7104E+01 -0.5664E-02*X -0.1251E-02*X^2

BOX CLEARANCE 2.21 METRES MAXIMUM Gz
Y=0.7216E+01 -0.1409E-01*X +0.3811E-02*X^2 -0.2237E-03*X^3

BOX CLEARANCE 3.40 METRES AREA UNDER THE Gz CURVE TO 20 DEGREES
Y=0.4412E+00 -0.1138E-02*X -0.5497E-03*X^2

BOX CLEARANCE 2.21 METRES AREA UNDER THE Gz CURVE TO 20 DEGREES
Y=0.5798E+00 +0.1008E-02*X -0.8021E-03*X^2 +0.1518E-04*X^3

BOX CLEARANCE 3.40 METRES AREA UNDER THE Gz CURVE TO 45 DEGREES
Y=0.2993E+01 +0.2573E-02*X -0.1004E-02*X^2

BOX CLEARANCE 2.21 METRES AREA UNDER THE Gz CURVE TO 45 DEGREES
Y=0.3167E+01 -0.3446E-02*X +0.2962E-03*X^2 -0.4256E-04*X^3

DISPLACEMENT 1000.0 TONNES DAMAGE LOCATION STARBOARD FORWARD

BOX CLEARANCE 3.40 METRES TRIM
Y=0.2926E-01 -0.1546E+00*X -0.1237E-01*X^2 +0.3336E-03*X^3

BOX CLEARANCE 2.21 METRES TRIM
Y=0.2009E-01 -0.1392E+00*X -0.1545E-01*X^2 +0.5014E-03*X^3

BOX CLEARANCE 3.40 METRES HEEL
Y=-0.2850E-01 +0.2005E+00*X +0.2046E-01*X^2 -0.5126E-03*X^3

BOX CLEARANCE 2.21 METRES HEEL
Y=-0.1528E+00 +0.4110E+00*X -0.4016E-02*X^2

BOX CLEARANCE 3.40 METRES MAXIMUM Gz
Y=0.6895E+01 -0.1236E-01*X +0.9330E-04*X^2

BOX CLEARANCE 2.21 METRES MAXIMUM Gz
Y=0.7202E+01 -0.3030E-02*X +0.2047E-02*X^2 -0.1761E-03*X^3

BOX CLEARANCE 3.40 METRES AREA UNDER THE Gz CURVE TO 20 DEGREES
Y=0.3550E+00 +0.6052E-03*X -0.9255E-03*X^2 +0.2483E-04*X^3

BOX CLEARANCE 2.21 METRES AREA UNDER THE Gz CURVE TO 20 DEGREES
Y=0.5228E+00 -0.3383E-02*X -0.1808E-03*X^2

BOX CLEARANCE 3.40 METRES AREA UNDER THE Gz CURVE TO 45 DEGREES
Y=0.2900E+01 +0.1203E-02*X -0.7944E-03*X^2

BOX CLEARANCE 2.21 METRES AREA UNDER THE Gz CURVE TO 45 DEGREES
Y=0.3104E+01 -0.4447E-02*X +0.5340E-03*X^2 -0.4970E-04*X^3

DISPLACEMENT 1050.0 TONNES DAMAGE LOCATION STARBOARD FORWARD

BOX CLEARANCE 3.40 METRES TRIM
Y=0.3940E-01 -0.1306E+00*X -0.1949E-01*X^2 +0.5780E-03*X^3

BOX CLEARANCE 2.21 METRES TRIM
Y=0.1996E-01 -0.8138E-01*X -0.2286E-01*X^2 +0.7106E-03*X^3

BOX CLEARANCE 3.40 METRES HEEL
Y=-0.5314E-01 +0.2171E+00*X +0.2827E-01*X^2 -0.8517E-03*X^3

BOX CLEARANCE 2.21 METRES HEEL
Y=-0.1457E+00 +0.3880E+00*X -0.3200E-02*X^2

BOX CLEARANCE 3.40 METRES MAXIMUM Gz
Y=0.6735E+01 -0.5005E-02*X +0.1736E-02*X^2 -0.8657E-04*X^3

BOX CLEARANCE 2.21 METRES MAXIMUM Gz
Y=0.7184E+01 +0.7768E-02*X +0.1388E-03*X^2 -0.1232E-03*X^3

BOX CLEARANCE 3.40 METRES AREA UNDER THE Gz CURVE TO 20 DEGREES
Y=0.2930E+00 +0.9092E-03*X -0.8913E-03*X^2 +0.2968E-04*X^3

BOX CLEARANCE 2.21 METRES AREA UNDER THE Gz CURVE TO 20 DEGREES
Y=0.4821E+00 +0.1317E-03*X -0.4677E-03*X^2 +0.8129E-05*X^3

BOX CLEARANCE 3.40 METRES AREA UNDER THE Gz CURVE TO 45 DEGREES
Y=0.2828E+01 +0.1851E-02*X -0.7210E-03*X^2

BOX CLEARANCE 2.21 METRES AREA UNDER THE Gz CURVE TO 45 DEGREES
Y=0.3067E+01 -0.2358E-02*X +0.3709E-03*X^2 -0.4748E-04*X^3

DISPLACEMENT 1900.0 TONNES DAMAGE LOCATION STARBOARD FORWARD

BOX CLEARANCE 4.27 METRES TRIM
Y=0.2184E-01 -0.6973E-01*X -0.1773E-01*X^2 +0.3975E-03*X^3

BOX CLEARANCE 2.77 METRES TRIM
Y=0.2031E-01 -0.5917E-01*X -0.1961E-01*X^2 +0.5129E-03*X^3

BOX CLEARANCE 4.27 METRES HEEL
Y=-0.4835E-01 +0.1826E+00*X +0.2384E-01*X^2 -0.5574E-03*X^3

BOX CLEARANCE 2.77 METRES HEEL
Y=-0.5281E-01 +0.1646E+00*X +0.2429E-01*X^2 -0.6340E-03*X^3

BOX CLEARANCE 4.27 METRES MAXIMUM Gz
Y=0.7171E+01 -0.1759E-01*X +0.1446E-02*X^2 -0.1692E-03*X^3

BOX CLEARANCE 2.77 METRES MAXIMUM Gz
Y=0.6989E+01 +0.5189E-02*X +0.1632E-02*X^2 -0.2055E-03*X^3

BOX CLEARANCE 4.27 METRES AREA UNDER THE Gz CURVE TO 20 DEGREES
Y=0.3240E+00 +0.1242E-02*X -0.9309E-03*X^2 +0.2524E-04*X^3

BOX CLEARANCE 2.77 METRES AREA UNDER THE Gz CURVE TO 20 DEGREES
Y=0.3901E+00 +0.3485E-03*X -0.7055E-03*X^2 +0.1441E-04*X^3

BOX CLEARANCE 4.27 METRES AREA UNDER THE Gz CURVE TO 45 DEGREES
Y=0.2812E+01 -0.3043E-02*X +0.3416E-04*X^2 -0.5051E-04*X^3

BOX CLEARANCE 2.77 METRES AREA UNDER THE Gz CURVE TO 45 DEGREES
Y=0.2957E+01 -0.4683E-02*X +0.4872E-03*X^2 -0.6895E-04*X^3

DISPLACEMENT 2000.0 TONNES DAMAGE LOCATION STARBOARD FORWARD

BOX CLEARANCE 4.27 METRES TRIM
Y=0.1959E-01 -0.1184E-01*X -0.2738E-01*X^2 +0.6817E-03*X^3

BOX CLEARANCE 2.77 METRES TRIM
Y=0.7430E-02 -0.1304E-01*X -0.2578E-01*X^2 +0.6870E-03*X^3

BOX CLEARANCE 4.27 METRES HEEL
Y=-0.3790E-01 +0.4164E-01*X +0.4372E-01*X^2 -0.1110E-02*X^3

BOX CLEARANCE 2.77 METRES HEEL
Y=-0.3040E-01 +0.9025E-01*X +0.3250E-01*X^2 -0.8396E-03*X^3

BOX CLEARANCE 4.27 METRES MAXIMUM Gz
Y=0.6903E+01 -0.3536E-01*X +0.5080E-02*X^2 -0.2773E-03*X^3

BOX CLEARANCE 2.77 METRES MAXIMUM Gz
Y=0.7025E+01 +0.2072E-01*X -0.1339E-02*X^2 -0.1265E-03*X^3

BOX CLEARANCE 4.27 METRES AREA UNDER THE Gz CURVE TO 20 DEGREES
Y=0.2610E+00 -0.4278E-03*X -0.5634E-03*X^2 +0.1504E-04*X^3

BOX CLEARANCE 2.77 METRES AREA UNDER THE Gz CURVE TO 20 DEGREES
Y=0.3453E+00 -0.5611E-03*X -0.5090E-03*X^2 +0.1037E-04*X^3

BOX CLEARANCE 4.27 METRES AREA UNDER THE Gz CURVE TO 45 DEGREES
Y=0.2706E+01 -0.4894E-02*X +0.4788E-03*X^2 -0.6772E-04*X^3

BOX CLEARANCE 2.77 METRES AREA UNDER THE Gz CURVE TO 45 DEGREES
Y=0.2887E+01 -0.4256E-02*X +0.4173E-03*X^2 -0.6735E-04*X^3

DISPLACEMENT 2100.0 TONNES DAMAGE LOCATION STARBOARD FORWARD

BOX CLEARANCE 4.27 METRES TRIM
Y=0.4423E-02 +0.3698E-01*X -0.3401E-01*X^2 +0.8666E-03*X^3

BOX CLEARANCE 2.77 METRES TRIM
Y=-0.9631E-02 +0.1813E-01*X -0.2709E-01*X^2 +0.6949E-03*X^3

BOX CLEARANCE 4.27 METRES HEEL
Y=-0.9753E-02 -0.4824E-01*X +0.5243E-01*X^2 -0.1316E-02*X^3

BOX CLEARANCE 2.77 METRES HEEL
Y=0.3130E-02 +0.2900E-01*X +0.3211E-01*X^2 -0.7198E-03*X^3

BOX CLEARANCE 4.27 METRES MAXIMUM Gz
Y=0.6718E+01 -0.3471E-02*X +0.3196E-02*X^2 -0.2495E-03*X^3

BOX CLEARANCE 2.77 METRES MAXIMUM Gz
Y=0.7037E+01 +0.1683E-01*X -0.2358E-02*X^2 -0.9339E-04*X^3

BOX CLEARANCE 4.27 METRES AREA UNDER THE Gz CURVE TO 20 DEGREES
Y=0.2299E+00 +0.2059E-02*X -0.8686E-03*X^2 +0.2546E-04*X^3

BOX CLEARANCE 2.77 METRES AREA UNDER THE Gz CURVE TO 20 DEGREES
Y=0.3221E+00 -0.2891E-03*X -0.4251E-03*X^2 +0.7548E-05*X^3

BOX CLEARANCE 4.27 METRES AREA UNDER THE Gz CURVE TO 45 DEGREES
Y=0.2636E+01 -0.4374E-02*X +0.4862E-03*X^2 -0.7198E-04*X^3

BOX CLEARANCE 2.77 METRES AREA UNDER THE Gz CURVE TO 45 DEGREES
Y=0.2839E+01 -0.2979E-02*X +0.1961E-03*X^2 -0.6239E-04*X^3

DISPLACEMENT 2850.0 TONNES DAMAGE LOCATION STARBOARD FORWARD

BOX CLEARANCE 4.91 METRES TRIM
Y=0.5008E-02 -0.1193E+00*X -0.1070E-01*X^2

BOX CLEARANCE 3.17 METRES TRIM
Y=0.2502E-02 -0.3963E-01*X -0.2790E-01*X^2 +0.7433E-03*X^3

BOX CLEARANCE 4.91 METRES HEEL
Y=-0.9664E-01 +0.2905E+00*X +0.8621E-02*X^2

BOX CLEARANCE 3.17 METRES HEEL
Y=-0.5519E-02 +0.6076E-01*X +0.4025E-01*X^2 -0.1051E-02*X^3

BOX CLEARANCE 4.91 METRES MAXIMUM Gz
Y=0.7462E+01 -0.1129E-01*X +0.2988E-02*X^2 +0.4145E-04*X^3 -0.1855E-04*X^4

BOX CLEARANCE 3.17 METRES MAXIMUM Gz
Y=0.7670E+01 +0.1161E-01*X -0.2215E-02*X^2 -0.1170E-03*X^3

BOX CLEARANCE 4.91 METRES AREA UNDER THE Gz CURVE TO 20 DEGREES
Y=0.3096E+00 -0.3279E-02*X -0.2749E-03*X^2

BOX CLEARANCE 3.17 METRES AREA UNDER THE Gz CURVE TO 20 DEGREES
Y=0.3670E+00 +0.1844E-03*X -0.7910E-03*X^2 +0.1714E-04*X^3

BOX CLEARANCE 4.91 METRES AREA UNDER THE Gz CURVE TO 45 DEGREES
Y=0.2922E+01 -0.6236E-02*X +0.7878E-03*X^2 -0.1010E-03*X^3

BOX CLEARANCE 3.17 METRES AREA UNDER THE Gz CURVE TO 45 DEGREES
Y=0.3095E+01 -0.4166E-02*X +0.3012E-03*X^2 -0.7904E-04*X^3

DISPLACEMENT 3000.0 TONNES DAMAGE LOCATION STARBOARD FORWARD

BOX CLEARANCE 4.91 METRES TRIM
Y=0.1264E+00 -0.1941E+00*X -0.7626E-02*X^2

BOX CLEARANCE 3.17 METRES TRIM
Y=0.1938E-02 -0.1206E-02*X -0.3488E-01*X^2 +0.9608E-03*X^3

BOX CLEARANCE 4.91 METRES HEEL
Y=-0.1283E+00 +0.3082E+00*X +0.1129E-01*X^2

BOX CLEARANCE 3.17 METRES HEEL
Y=-0.3507E-02 +0.4245E-01*X +0.4668E-01*X^2 -0.1265E-02*X^3

BOX CLEARANCE 4.91 METRES MAXIMUM Gz
Y=0.7569E+01 -0.2395E-02*X +0.3143E-02*X^2 -0.3648E-03*X^3

BOX CLEARANCE 3.17 METRES MAXIMUM Gz
Y=0.7396E+01 -0.5369E-02*X +0.5309E-03*X^2 -0.1928E-03*X^3

BOX CLEARANCE 4.91 METRES AREA UNDER THE Gz CURVE TO 20 DEGREES
Y=0.2433E+00 -0.3388E-02*X -0.1490E-03*X^2

BOX CLEARANCE 3.17 METRES AREA UNDER THE Gz CURVE TO 20 DEGREES
Y=0.3129E+00 -0.1797E-03*X -0.5992E-03*X^2 +0.1286E-04*X^3

BOX CLEARANCE 4.91 METRES AREA UNDER THE Gz CURVE TO 45 DEGREES
Y=0.2809E+01 -0.4647E-02*X +0.5296E-03*X^2 -0.9335E-04*X^3

BOX CLEARANCE 3.17 METRES AREA UNDER THE Gz CURVE TO 45 DEGREES
Y=0.2986E+01 -0.3049E-02*X +0.2119E-03*X^2 -0.7622E-04*X^3

DISPLACEMENT 3150.0 TONNES DAMAGE LOCATION STARBOARD FORWARD

BOX CLEARANCE 4.91 METRES TRIM
Y=0.6597E-02 +0.1043E+00*X -0.5311E-01*X^2 +0.1515E-02*X^3

BOX CLEARANCE 3.17 METRES TRIM
Y=0.8370E-03 -0.1835E-01*X -0.2959E-01*X^2 +0.7835E-03*X^3

BOX CLEARANCE 4.91 METRES HEEL
Y=-0.1239E+00 +0.2866E+00*X +0.1462E-01*X^2

BOX CLEARANCE 3.17 METRES HEEL
Y=-0.1087E-02 +0.7783E-01*X +0.3635E-01*X^2 -0.8954E-03*X^3

BOX CLEARANCE 4.91 METRES MAXIMUM Gz
Y=0.7554E+01 -0.3759E-02*X +0.1624E-02*X^2 -0.3111E-03*X^3

BOX CLEARANCE 3.17 METRES MAXIMUM Gz
Y=0.7121E+01 +0.9915E-02*X +0.2778E-03*X^2 -0.2030E-03*X^3

BOX CLEARANCE 4.91 METRES AREA UNDER THE Gz CURVE TO 20 DEGREES
Y=0.2026E+00 -0.2729E-02*X -0.1188E-03*X^2

BOX CLEARANCE 3.17 METRES AREA UNDER THE Gz CURVE TO 20 DEGREES
Y=0.2839E+00 +0.2783E-03*X -0.5640E-03*X^2 +0.1226E-04*X^3

BOX CLEARANCE 4.91 METRES AREA UNDER THE Gz CURVE TO 45 DEGREES
Y=0.2711E+01 -0.6352E-02*X +0.8376E-03*X^2 -0.1086E-03*X^3

BOX CLEARANCE 3.17 METRES AREA UNDER THE Gz CURVE TO 45 DEGREES
Y=0.2898E+01 +0.9028E-03*X -0.3361E-03*X^2 -0.6081E-04*X^3

DISPLACEMENT 3800.0 TONNES DAMAGE LOCATION STARBOARD FORWARD

BOX CLEARANCE 5.38 METRES TRIM
Y=0.1527E-01 +0.9192E-01*X -0.5133E-01*X^2 +0.1685E-02*X^3

BOX CLEARANCE 3.48 METRES TRIM
Y=0.2830E-01 -0.7891E-01*X -0.2151E-01*X^2 +0.5275E-03*X^3

BOX CLEARANCE 5.38 METRES HEEL
Y=0.2738E-02 -0.1213E+00*X +0.6825E-01*X^2 -0.2075E-02*X^3

BOX CLEARANCE 3.48 METRES HEEL
Y=-0.4352E-01 +0.1273E+00*X +0.2853E-01*X^2 -0.6278E-03*X^3

BOX CLEARANCE 5.38 METRES MAXIMUM Gz
Y=0.7721E+01 -0.8076E-03*X +0.9650E-03*X^2 -0.2952E-03*X^3

BOX CLEARANCE 3.48 METRES MAXIMUM Gz
Y=0.7451E+01 +0.4269E-01*X -0.4866E-02*X^2 -0.6826E-04*X^3

BOX CLEARANCE 5.38 METRES AREA UNDER THE Gz CURVE TO 20 DEGREES
Y=0.2679E+00 +0.2130E-02*X -0.1227E-02*X^2 +0.3871E-04*X^3

BOX CLEARANCE 3.48 METRES AREA UNDER THE Gz CURVE TO 20 DEGREES
Y=0.3099E+00 +0.1817E-02*X -0.1098E-02*X^2 +0.3340E-04*X^3

BOX CLEARANCE 5.38 METRES AREA UNDER THE Gz CURVE TO 45 DEGREES
Y=0.2813E+01 -0.6725E-02*X +0.8068E-03*X^2 -0.1186E-03*X^3

BOX CLEARANCE 3.48 METRES AREA UNDER THE Gz CURVE TO 45 DEGREES
Y=0.2975E+01 -0.4614E-02*X +0.6604E-03*X^2 -0.1200E-03*X^3

DISPLACEMENT 4000.0 TONNES DAMAGE LOCATION STARBOARD FORWARD

BOX CLEARANCE 5.38 METRES TRIM
Y=0.9848E-01 -0.1404E+00*X -0.1165E-01*X^2

BOX CLEARANCE 3.48 METRES TRIM
Y=0.1983E-01 -0.4719E-01*X -0.2654E-01*X^2 +0.6780E-03*X^3

BOX CLEARANCE 5.38 METRES HEEL
Y=0.6843E-02 -0.2001E+00*X +0.8516E-01*X^2 -0.2581E-02*X^3

BOX CLEARANCE 3.48 METRES HEEL
Y=-0.3342E-01 +0.1084E+00*X +0.3384E-01*X^2 -0.7898E-03*X^3

BOX CLEARANCE 5.38 METRES MAXIMUM Gz
Y=0.7459E+01 -0.2205E-01*X +0.4485E-02*X^2 -0.4036E-03*X^3

BOX CLEARANCE 3.48 METRES MAXIMUM Gz
Y=0.7404E+01 -0.8559E-03*X +0.7974E-03*X^2 -0.3055E-03*X^3

BOX CLEARANCE 5.38 METRES AREA UNDER THE Gz CURVE TO 20 DEGREES
Y=0.2110E+00 -0.3523E-02*X -0.1390E-03*X^2

BOX CLEARANCE 3.48 METRES AREA UNDER THE Gz CURVE TO 20 DEGREES
Y=0.2659E+00 +0.8457E-03*X -0.8103E-03*X^2 +0.2483E-04*X^3

BOX CLEARANCE 5.38 METRES AREA UNDER THE Gz CURVE TO 45 DEGREES
Y=0.2677E+01 -0.4330E-02*X +0.4282E-03*X^2 -0.1045E-03*X^3

BOX CLEARANCE 3.48 METRES AREA UNDER THE Gz CURVE TO 45 DEGREES
Y=0.2860E+01 -0.5501E-02*X +0.7202E-03*X^2 -0.1245E-03*X^3

DISPLACEMENT 4200.0 TONNES DAMAGE LOCATION STARBOARD FORWARD

BOX CLEARANCE 5.38 METRES TRIM
Y=0.2059E-01 +0.9780E-01*X -0.5181E-01*X^2 +0.1534E-02*X^3

BOX CLEARANCE 3.48 METRES TRIM
Y=-0.1399E-02 -0.6536E-02*X -0.2977E-01*X^2 +0.7478E-03*X^3

BOX CLEARANCE 5.38 METRES HEEL
Y=0.6406E-02 -0.2043E+00*X +0.8890E-01*X^2 -0.2692E-02*X^3

BOX CLEARANCE 3.48 METRES HEEL
Y=-0.3585E-02 +0.8498E-01*X +0.3391E-01*X^2 -0.7392E-03*X^3

BOX CLEARANCE 5.38 METRES MAXIMUM Gz
Y=0.7281E+01 +0.5205E-02*X +0.2062E-02*X^2 -0.3543E-03*X^3

BOX CLEARANCE 3.48 METRES MAXIMUM Gz
Y=0.7157E+01 +0.2281E-02*X -0.1613E-03*X^2 -0.2690E-03*X^3

BOX CLEARANCE 5.38 METRES AREA UNDER THE Gz CURVE TO 20 DEGREES
Y=0.1754E+00 -0.3846E-03*X -0.5277E-03*X^2 +0.1719E-04*X^3

BOX CLEARANCE 3.48 METRES AREA UNDER THE Gz CURVE TO 20 DEGREES
Y=0.2459E+00 +0.1490E-02*X -0.7892E-03*X^2 +0.2383E-04*X^3

BOX CLEARANCE 5.38 METRES AREA UNDER THE Gz CURVE TO 45 DEGREES
Y=0.2557E+01 -0.1426E-02*X -0.5699E-04*X^2 -0.8576E-04*X^3

BOX CLEARANCE 3.48 METRES AREA UNDER THE Gz CURVE TO 45 DEGREES
Y=0.2753E+01 -0.1235E-02*X +0.5173E-04*X^2 -0.1031E-03*X^3

DISPLACEMENT 4750.0 TONNES DAMAGE LOCATION STARBOARD FORWARD

BOX CLEARANCE 5.94 METRES TRIM
Y=0.2570E-01 -0.6487E-01*X -0.2329E-01*X^2 +0.5013E-03*X^3

BOX CLEARANCE 3.88 METRES TRIM
Y=0.1349E-01 +0.5060E-01*X -0.3319E-01*X^2 +0.7790E-03*X^3

BOX CLEARANCE 5.94 METRES HEEL
Y=-0.3665E-01 +0.8885E-01*X +0.3237E-01*X^2 -0.5991E-03*X^3

BOX CLEARANCE 3.88 METRES HEEL
Y=-0.2866E-01 -0.1551E+00*X +0.5319E-01*X^2 -0.1143E-02*X^3

BOX CLEARANCE 5.94 METRES MAXIMUM Gz
Y=0.7564E+01 +0.4110E-01*X -0.1639E-02*X^2 -0.2326E-03*X^3

BOX CLEARANCE 3.88 METRES MAXIMUM Gz
Y=0.7709E+01 +0.1278E-02*X +0.1811E-02*X^2 -0.3664E-03*X^3

BOX CLEARANCE 5.94 METRES AREA UNDER THE Gz CURVE TO 20 DEGREES
Y=0.1815E+00 +0.1983E-01*X -0.2045E-02*X^2 +0.4198E-04*X^3

BOX CLEARANCE 3.88 METRES AREA UNDER THE Gz CURVE TO 20 DEGREES
Y=0.2971E+00 +0.2728E-02*X -0.8585E-03*X^2 +0.1749E-04*X^3

BOX CLEARANCE 5.94 METRES AREA UNDER THE Gz CURVE TO 45 DEGREES
Y=0.2556E+01 +0.7536E-01*X -0.6583E-02*X^2 +0.8333E-04*X^3

BOX CLEARANCE 3.88 METRES AREA UNDER THE Gz CURVE TO 45 DEGREES
Y=0.2978E+01 -0.2472E-02*X +0.8555E-03*X^2 -0.1414E-03*X^3

DISPLACEMENT 5000.0 TONNES DAMAGE LOCATION STARBOARD FORWARD

BOX CLEARANCE 5.94 METRES TRIM
Y=0.2662E-01 -0.2138E-01*X -0.3117E-01*X^2 +0.7259E-03*X^3

BOX CLEARANCE 3.88 METRES TRIM
Y=0.4738E-03 +0.1171E+00*X -0.3966E-01*X^2 +0.9317E-03*X^3

BOX CLEARANCE 5.94 METRES HEEL
Y=-0.3025E-01 +0.1306E-01*X +0.4840E-01*X^2 -0.1080E-02*X^3

BOX CLEARANCE 3.88 METRES HEEL
Y=-0.9775E-02 -0.1909E+00*X +0.5919E-01*X^2 -0.1299E-02*X^3

BOX CLEARANCE 5.94 METRES MAXIMUM Gz
Y=0.7531E+01 +0.3312E-02*X +0.3309E-02*X^2 -0.4243E-03*X^3

BOX CLEARANCE 3.88 METRES MAXIMUM Gz
Y=0.7417E+01 +0.2930E-02*X +0.1092E-02*X^2 -0.3348E-03*X^3

BOX CLEARANCE 5.94 METRES AREA UNDER THE Gz CURVE TO 20 DEGREES
Y=0.2131E+00 -0.1787E-02*X -0.3631E-03*X^2 +0.6538E-05*X^3

BOX CLEARANCE 3.88 METRES AREA UNDER THE Gz CURVE TO 20 DEGREES
Y=0.2600E+00 +0.2067E-02*X -0.6980E-03*X^2 +0.1390E-04*X^3

BOX CLEARANCE 5.94 METRES AREA UNDER THE Gz CURVE TO 45 DEGREES
Y=0.2689E+01 -0.2411E-02*X +0.1251E-03*X^2 -0.1010E-03*X^3

BOX CLEARANCE 3.88 METRES AREA UNDER THE Gz CURVE TO 45 DEGREES
Y=0.2846E+01 -0.2935E-03*X +0.4327E-03*X^2 -0.1271E-03*X^3

DISPLACEMENT 5250.0 TONNES DAMAGE LOCATION STARBOARD FORWARD

BOX CLEARANCE 5.94 METRES TRIM
Y=0.1063E-01 +0.1583E-01*X -0.3687E-01*X^2 +0.8838E-03*X^3

BOX CLEARANCE 3.88 METRES TRIM
Y=0.7927E-01 +0.1332E+00*X -0.3895E-01*X^2 +0.8774E-03*X^3

BOX CLEARANCE 5.94 METRES HEEL
Y=-0.1601E-01 -0.2783E-01*X +0.5707E-01*X^2 -0.1338E-02*X^3

BOX CLEARANCE 3.88 METRES HEEL
Y=0.6757E-02 -0.1878E+00*X +0.5541E-01*X^2 -0.1131E-02*X^3

BOX CLEARANCE 5.94 METRES MAXIMUM Gz
Y=0.7563E+01 +0.5718E-03*X +0.1001E-02*X^2 -0.3337E-03*X^3

BOX CLEARANCE 3.88 METRES MAXIMUM Gz
Y=0.6990E+01 -0.1579E-02*X +0.1906E-02*X^2 -0.3555E-03*X^3

BOX CLEARANCE 5.94 METRES AREA UNDER THE Gz CURVE TO 20 DEGREES
Y=0.1804E+00 -0.1595E-02*X -0.2941E-03*X^2 +0.5142E-05*X^3

BOX CLEARANCE 3.88 METRES AREA UNDER THE Gz CURVE TO 20 DEGREES
Y=0.2470E+00 +0.2246E-02*X -0.6515E-03*X^2 +0.1206E-04*X^3

BOX CLEARANCE 5.94 METRES AREA UNDER THE Gz CURVE TO 45 DEGREES
Y=0.2556E+01 -0.1194E-02*X -0.2734E-03*X^2 -0.8238E-04*X^3

BOX CLEARANCE 3.88 METRES AREA UNDER THE Gz CURVE TO 45 DEGREES
Y=0.2724E+01 +0.2288E-02*X -0.6534E-04*X^2 -0.1092E-03*X^3

DISPLACEMENT 950.0 TONNES DAMAGE LOCATION STARBOARD MIDSHIPS

BOX CLEARANCE 3.40 METRES TRIM
Y=-0.8400E-04 +0.5599E-01*X -0.4136E-02*X^2 +0.6764E-04*X^3

BOX CLEARANCE 2.21 METRES TRIM
Y=0.6225E-02 +0.4990E-01*X -0.4723E-02*X^2 +0.8953E-04*X^3

BOX CLEARANCE 3.40 METRES HEEL
Y=0.5277E-01 +0.1401E+01*X -0.2862E-01*X^2

BOX CLEARANCE 2.21 METRES HEEL
Y=-0.3345E-01 +0.1846E+01*X -0.1021E+00*X^2 +0.2050E-02*X^3

BOX CLEARANCE 3.40 METRES MAXIMUM Gz
FOR FLOODING EXTENT LESS THAN OR EQUAL TO 6.25%
Y=0.7093E+01 -0.5968E-01*X
FOR FLOODING EXTENT GREATER THAN 6.25%
Y=0.6590E+01 +0.2392E-01*X -0.5743E-03*X^2

BOX CLEARANCE 2.21 METRES MAXIMUM Gz
Y=0.7216E+01 -0.3576E-02*X +0.4057E-03*X^2 -0.6098E-04*X^3

BOX CLEARANCE 3.40 METRES AREA UNDER THE Gz CURVE TO 20 DEGREES
Y=0.4402E+00 -0.3500E-01*X +0.7554E-03*X^2

BOX CLEARANCE 2.21 METRES AREA UNDER THE Gz CURVE TO 20 DEGREES
Y=0.5800E+00 -0.3151E-01*X +0.1043E-02*X^2 -0.2115E-04*X^3

BOX CLEARANCE 3.40 METRES AREA UNDER THE Gz CURVE TO 45 DEGREES
Y=0.2979E+01 -0.3449E-01*X +0.3811E-03*X^2

BOX CLEARANCE 2.21 METRES AREA UNDER THE Gz CURVE TO 45 DEGREES
Y=0.3167E+01 -0.3571E-01*X +0.1543E-02*X^2 -0.4248E-04*X^3

DISPLACEMENT 1000.0 TONNES DAMAGE LOCATION STARBOARD MIDSHIPS

BOX CLEARANCE 3.40 METRES TRIM
Y=0.4988E-02 +0.9411E-01*X -0.9204E-02*X^2 +0.1998E-03*X^3

BOX CLEARANCE 2.21 METRES TRIM
Y=0.6147E-02 +0.1933E-01*X -0.2952E-02*X^2 +0.5955E-04*X^3

BOX CLEARANCE 3.40 METRES HEEL
Y=0.5838E-01 +0.2134E+01*X -0.1019E+00*X^2 +0.1756E-02*X^3

BOX CLEARANCE 2.21 METRES HEEL
Y=0.1563E-01 +0.2018E+01*X -0.1234E+00*X^2 +0.2618E-02*X^3

BOX CLEARANCE 3.40 METRES MAXIMUM Gz
Y=0.6890E+01 -0.5303E-01*X +0.7212E-02*X^2 -0.3213E-03*X^3 +0.4200E-05*X^4

BOX CLEARANCE 2.21 METRES MAXIMUM Gz
Y=0.7203E+01 +0.1034E-01*X -0.2435E-02*X^2 +0.2761E-04*X^3

BOX CLEARANCE 3.40 METRES AREA UNDER THE Gz CURVE TO 20 DEGREES
Y=0.3553E+00 -0.3243E-01*X +0.1067E-02*X^2 -0.1147E-04*X^3

BOX CLEARANCE 2.21 METRES AREA UNDER THE Gz CURVE TO 20 DEGREES
Y=0.5199E+00 -0.2652E-01*X +0.8210E-03*X^2 -0.1677E-04*X^3

BOX CLEARANCE 3.40 METRES AREA UNDER THE Gz CURVE TO 45 DEGREES
Y=0.2899E+01 -0.4273E-01*X +0.1849E-02*X^2 -0.4430E-04*X^3

BOX CLEARANCE 2.21 METRES AREA UNDER THE Gz CURVE TO 45 DEGREES
Y=0.3104E+01 -0.2851E-01*X +0.1010E-02*X^2 -0.3256E-04*X^3

DISPLACEMENT 1050.0 TONNES DAMAGE LOCATION STARBOARD MIDSHIPS

BOX CLEARANCE 3.40 METRES TRIM
Y=0.1243E-01 +0.7331E-01*X -0.8779E-02*X^2 +0.2075E-03*X^3

BOX CLEARANCE 2.21 METRES TRIM
Y=0.1011E-01 -0.1523E-02*X -0.2152E-02*X^2 +0.5319E-04*X^3

BOX CLEARANCE 3.40 METRES HEEL
Y=0.3040E-01 +0.2317E+01*X -0.1181E+00*X^2 +0.2099E-02*X^3

BOX CLEARANCE 2.21 METRES HEEL
Y=0.1219E-01 +0.1700E+01*X -0.9490E-01*X^2 +0.1949E-02*X^3

BOX CLEARANCE 3.40 METRES MAXIMUM Gz
Y=0.6735E+01 +0.1951E-01*X -0.2321E-02*X^2 +0.1867E-03*X^3 -0.5636E-05*X^4

BOX CLEARANCE 2.21 METRES MAXIMUM Gz
Y=0.7184E+01 +0.1555E-01*X -0.4737E-02*X^2 +0.1080E-03*X^3

BOX CLEARANCE 3.40 METRES AREA UNDER THE Gz CURVE TO 20 DEGREES
Y=0.2936E+00 -0.2796E-01*X +0.1031E-02*X^2 +0.1339E-04*X^3

BOX CLEARANCE 2.21 METRES AREA UNDER THE Gz CURVE TO 20 DEGREES
Y=0.4820E+00 -0.2127E-01*X +0.4416E-03*X^2 -0.7444E-05*X^3

BOX CLEARANCE 3.40 METRES AREA UNDER THE Gz CURVE TO 45 DEGREES
Y=0.2827E+01 -0.3700E-01*X +0.1575E-02*X^2 -0.4135E-04*X^3

BOX CLEARANCE 2.21 METRES AREA UNDER THE Gz CURVE TO 45 DEGREES
Y=0.3067E+01 -0.2207E-01*X +0.2917E-03*X^2 -0.1559E-04*X^3

DISPLACEMENT 1900.0 TONNES DAMAGE LOCATION STARBOARD MIDSHIPS

BOX CLEARANCE 4.27 METRES TRIM
Y=-0.9702E-03 +0.7211E-01*X -0.6418E-02*X^2 +0.1491E-03*X^3

BOX CLEARANCE 2.77 METRES TRIM
Y=0.2315E-02 +0.3648E-01*X -0.3645E-02*X^2 +0.7117E-04*X^3

BOX CLEARANCE 4.27 METRES HEEL
Y=0.1878E-01 +0.2125E+01*X -0.1005E+00*X^2 +0.2090E-02*X^3

BOX CLEARANCE 2.77 METRES HEEL
Y=0.5592E-01 +0.1848E+01*X -0.8525E-01*X^2 +0.1545E-02*X^3

BOX CLEARANCE 4.27 METRES MAXIMUM Gz
FOR FLOODING EXTENT LESS THAN OR EQUAL TO 6.33%
Y=0.7168E+01 -0.7488E-01*X
FOR FLOODING EXTENT GREATER THAN 6.33%
Y=0.6588E+01 +0.1258E-01*X +0.1397E-02*X^2 -0.8565E-04*X^3

BOX CLEARANCE 2.77 METRES MAXIMUM Gz
Y=0.6990E+01 +0.5630E-01*X -0.7863E-02*X^2 +0.1567E-03*X^3

BOX CLEARANCE 4.27 METRES AREA UNDER THE Gz CURVE TO 20 DEGREES
Y=0.3245E+00 -0.3531E-01*X +0.1020E-02*X^2

BOX CLEARANCE 2.77 METRES AREA UNDER THE Gz CURVE TO 20 DEGREES
Y=0.3891E+00 -0.2771E-01*X +0.4450E-03*X^2 +0.3316E-05*X^3

BOX CLEARANCE 4.27 METRES AREA UNDER THE Gz CURVE TO 45 DEGREES
Y=0.2810E+01 -0.4854E-01*X +0.6178E-03*X^2

BOX CLEARANCE 2.77 METRES AREA UNDER THE Gz CURVE TO 45 DEGREES
Y=0.2948E+01 -0.3210E-01*X -0.1705E-03*X^2

DISPLACEMENT 2000.0 TONNES DAMAGE LOCATION STARBOARD MIDSHIPS

BOX CLEARANCE 4.27 METRES TRIM
Y=-0.1472E-02 +0.1047E+00*X -0.1303E-01*X^2 +0.4045E-03*X^3

BOX CLEARANCE 2.77 METRES TRIM
Y=0.1658E-02 +0.1364E-01*X -0.2351E-02*X^2 +0.4862E-04*X^3

BOX CLEARANCE 4.27 METRES HEEL
Y=0.1973E-01 +0.2106E+01*X -0.8413E-01*X^2 +0.1203E-02*X^3

BOX CLEARANCE 2.77 METRES HEEL
Y=0.4380E-01 +0.1779E+01*X -0.8146E-01*X^2 +0.1490E-02*X^3

BOX CLEARANCE 4.27 METRES MAXIMUM Gz
Y=0.6900E+01 -0.7047E-01*X +0.1052E-01*X^2 -0.4395E-03*X^3

BOX CLEARANCE 2.77 METRES MAXIMUM Gz
Y=0.7034E+01 +0.2353E-01*X -0.6642E-02*X^2 +0.1366E-03*X^3

BOX CLEARANCE 4.27 METRES AREA UNDER THE Gz CURVE TO 20 DEGREES
Y=0.2609E+00 -0.2905E-01*X +0.8631E-03*X^2

BOX CLEARANCE 2.77 METRES AREA UNDER THE Gz CURVE TO 20 DEGREES
Y=0.3446E+00 -0.2624E-01*X +0.6330E-03*X^2 +0.3814E-05*X^3

BOX CLEARANCE 4.27 METRES AREA UNDER THE Gz CURVE TO 45 DEGREES
Y=0.2704E+01 -0.4181E-01*X +0.3151E-03*X^2

BOX CLEARANCE 2.77 METRES AREA UNDER THE Gz CURVE TO 45 DEGREES
Y=0.2878E+01 -0.3068E-01*X -0.2919E-03*X^2

DISPLACEMENT 2100.0 TONNES DAMAGE LOCATION STARBOARD MIDSHIPS

BOX CLEARANCE 4.27 METRES TRIM
Y=0.1748E-02 +0.5907E-01*X -0.7478E-02*X^2 +0.2121E-03*X^3

BOX CLEARANCE 2.77 METRES TRIM
Y=-0.6649E-03 +0.1618E-02*X -0.1936E-02*X^2 +0.4522E-04*X^3

BOX CLEARANCE 4.27 METRES HEEL
Y=0.5845E-02 +0.2191E+01*X -0.9664E-01*X^2 +0.1576E-02*X^3

BOX CLEARANCE 2.77 METRES HEEL
Y=0.2467E-01 +0.1380E+01*X -0.4821E-01*X^2 +0.7674E-03*X^3

BOX CLEARANCE 4.27 METRES MAXIMUM Gz
Y=0.6724E+01 +0.1280E-01*X +0.1388E-02*X^2 -0.2145E-03*X^3

BOX CLEARANCE 2.77 METRES MAXIMUM Gz
Y=0.7055E+01 -0.5317E-01*X +0.2879E-03*X^2 -0.4368E-04*X^3

BOX CLEARANCE 4.27 METRES AREA UNDER THE Gz CURVE TO 20 DEGREES
Y=0.2299E+00 -0.3104E-01*X +0.1479E-02*X^2 -0.2324E-04*X^3

BOX CLEARANCE 2.77 METRES AREA UNDER THE Gz CURVE TO 20 DEGREES
Y=0.3215E+00 -0.2287E-01*X +0.5304E-03*X^2 -0.3682E-05*X^3

BOX CLEARANCE 4.27 METRES AREA UNDER THE Gz CURVE TO 45 DEGREES
Y=0.2633E+01 -0.4077E-01*X +0.2344E-03*X^2

BOX CLEARANCE 2.77 METRES AREA UNDER THE Gz CURVE TO 45 DEGREES
Y=0.2830E+01 -0.3068E-01*X -0.3987E-03*X^2

DISPLACEMENT 2850.0 TONNES DAMAGE LOCATION STARBOARD MIDSHIPS

BOX CLEARANCE 4.91 METRES TRIM
Y=-0.1128E-02 +0.6771E-01*X -0.4941E-02*X^2 +0.8700E-04*X^3

BOX CLEARANCE 3.17 METRES TRIM
Y=0.5016E-03 +0.5252E-01*X -0.4918E-02*X^2 +0.1011E-03*X^3

BOX CLEARANCE 4.91 METRES HEEL
Y=-0.4257E-03 +0.2007E+01*X -0.7412E-01*X^2 +0.1153E-02*X^3

BOX CLEARANCE 3.17 METRES HEEL
Y=0.6736E-01 +0.1986E+01*X -0.9336E-01*X^2 +0.1752E-02*X^3

BOX CLEARANCE 4.91 METRES MAXIMUM Gz
Y=0.7469E+01 +0.5994E-01*X -0.7694E-02*X^2 +0.1197E-03*X^3

BOX CLEARANCE 3.17 METRES MAXIMUM Gz
Y=0.7662E+01 -0.1114E+00*X +0.7728E-02*X^2 -0.2634E-03*X^3

BOX CLEARANCE 4.91 METRES AREA UNDER THE Gz CURVE TO 20 DEGREES
Y=0.3084E+00 -0.4051E-01*X +0.1802E-02*X^2 -0.2701E-04*X^3

BOX CLEARANCE 3.17 METRES AREA UNDER THE Gz CURVE TO 20 DEGREES
Y=0.3648E+00 -0.3082E-01*X +0.6673E-03*X^2

BOX CLEARANCE 4.91 METRES AREA UNDER THE Gz CURVE TO 45 DEGREES
Y=0.2911E+01 -0.4352E-01*X -0.3331E-03*X^2

BOX CLEARANCE 3.17 METRES AREA UNDER THE Gz CURVE TO 45 DEGREES
Y=0.3079E+01 -0.3773E-01*X -0.5417E-03*X^2

DISPLACEMENT 3000.0 TONNES DAMAGE LOCATION STARBOARD MIDSHIPS

BOX CLEARANCE 4.91 METRES TRIM
Y=0.4874E-02 +0.7062E-01*X -0.6462E-02*X^2 +0.1356E-03*X^3

BOX CLEARANCE 3.17 METRES TRIM
Y=0.2922E-02 +0.2717E-01*X -0.3444E-02*X^2 +0.7461E-04*X^3

BOX CLEARANCE 4.91 METRES HEEL
Y=0.1915E-01 +0.2343E+01*X -0.1051E+00*X^2 +0.1856E-02*X^3

BOX CLEARANCE 3.17 METRES HEEL
Y=0.5613E-01 +0.1982E+01*X -0.9278E-01*X^2 +0.1732E-02*X^3

BOX CLEARANCE 4.91 METRES MAXIMUM Gz
Y=0.7571E+01 -0.1479E-01*X -0.2349E-02*X^2

BOX CLEARANCE 3.17 METRES MAXIMUM Gz
Y=0.7385E+01 -0.1623E-01*X -0.2988E-02*X^2

BOX CLEARANCE 4.91 METRES AREA UNDER THE Gz CURVE TO 20 DEGREES
Y=0.2420E+00 -0.3532E-01*X +0.1777E-02*X^2 -0.3006E-04*X^3

BOX CLEARANCE 3.17 METRES AREA UNDER THE Gz CURVE TO 20 DEGREES
Y=0.3104E+00 -0.2634E-01*X +0.5726E-03*X^2

BOX CLEARANCE 4.91 METRES AREA UNDER THE Gz CURVE TO 45 DEGREES
Y=0.2799E+01 -0.4285E-01*X -0.4338E-03*X^2

BOX CLEARANCE 3.17 METRES AREA UNDER THE Gz CURVE TO 45 DEGREES
Y=0.2972E+01 -0.3581E-01*X -0.7352E-03*X^2

DISPLACEMENT 3150.0 TONNES DAMAGE LOCATION STARBOARD MIDSHIPS

BOX CLEARANCE 4.91 METRES TRIM
Y=0.8409E-02 +0.5261E-01*X -0.5717E-02*X^2 +0.1268E-03*X^3

BOX CLEARANCE 3.17 METRES TRIM
Y=0.2859E-02 +0.8167E-02*X -0.2508E-02*X^2 +0.6044E-04*X^3

BOX CLEARANCE 4.91 METRES HEEL
Y=0.4394E-01 +0.2453E+01*X -0.1172E+00*X^2 +0.2155E-02*X^3

BOX CLEARANCE 3.17 METRES HEEL
Y=0.3682E-01 +0.1719E+01*X -0.6948E-01*X^2 +0.1196E-02*X^3

BOX CLEARANCE 4.91 METRES MAXIMUM Gz
Y=0.7553E+01 -0.9601E-01*X +0.5026E-02*X^2 -0.1921E-03*X^3

BOX CLEARANCE 3.17 METRES MAXIMUM Gz
Y=0.7125E+01 +0.1634E-01*X -0,6918E-02*X^2 +0.8868E-04*X^3

BOX CLEARANCE 4.91 METRES AREA UNDER THE Gz CURVE TO 20 DEGREES
Y=0.2020E+00 -0.2891E-01*X +0.1424E-02*X^2 -0.2365E-04*X^3

BOX CLEARANCE 3.17 METRES AREA UNDER THE Gz CURVE TO 20 DEGREES
Y=0.2826E+00 -0.2314E-01*X +0.4885E-03*X^2

BOX CLEARANCE 4.91 METRES AREA UNDER THE Gz CURVE TO 45 DEGREES
Y=0.2702E+01 -0.4352E-01*X -0.4922E-03*X^2

BOX CLEARANCE 3.17 METRES AREA UNDER THE Gz CURVE TO 45 DEGREES
Y=0.2889E+01 -0.3718E-01*X -0.8241E-03*X^2

DISPLACEMENT 3800.0 TONNES DAMAGE LOCATION STARBOARD MIDSHIPS

BOX CLEARANCE 5.38 METRES TRIM
Y=0.1751E-01 +0.4365E-01*X +0.3969E-03*X^2 -0.3113E-03*X^3 +0.8920E-05*X^4

BOX CLEARANCE 3.48 METRES TRIM
Y=0.1688E-02 +0.8356E-01*X -0.1303E-01*X^2 +0.6679E-03*X^3 -0.1169E-04*X^4

BOX CLEARANCE 5.38 METRES HEEL
Y=-0.2076E-01 +0.2090E+01*X -0.7016E-01*X^2 +0.9524E-03*X^3

BOX CLEARANCE 3.48 METRES HEEL
Y=0.3588E-01 +0.2115E+01*X -0.9984E-01*X^2 +0.1911E-02*X^3

BOX CLEARANCE 5.38 METRES MAXIMUM Gz
FOR FLOODING EXTENT LESS THAN OR EQUAL TO 6.25%
Y=0.7722E+01 -0.1469E+00*X +0.1152E-01*X^2
FOR FLOODING EXTENT GREATER THAN 6.25%
Y=0.6022E+01 +0.3361E+00*X -0.2527E-01*X^2 +0.4374E-03*X^3

BOX CLEARANCE 3.48 METRES MAXIMUM Gz
Y=0.7477E+01 -0.2134E-01*X -0.3417E-02*X^2

BOX CLEARANCE 5.38 METRES AREA UNDER THE Gz CURVE TO 20 DEGREES
Y=0.2679E+00 -0.4169E-01*X +0.2167E-02*X^2 -0.3714E-04*X^3

BOX CLEARANCE 3.48 METRES AREA UNDER THE Gz CURVE TO 20 DEGREES
Y=0.3104E+00 -0.3386E-01*X +0.1251E-02*X^2 -0.1573E-04*X^3

BOX CLEARANCE 5.38 METRES AREA UNDER THE Gz CURVE TO 45 DEGREES
Y=0.2803E+01 -0.5200E-01*X -0.3905E-03*X^2

BOX CLEARANCE 3.48 METRES AREA UNDER THE Gz CURVE TO 45 DEGREES
Y=0.2963E+01 -0.4308E-01*X -0.7990E-03*X^2

DISPLACEMENT 4000.0 TONNES DAMAGE LOCATION STARBOARD MIDSHIPS

BOX CLEARANCE 5.38 METRES TRIM
Y=0.2612E-01 +0.6254E-01*X -0.6052E-02*X^2 +0.1328E-03*X^3

BOX CLEARANCE 3.48 METRES TRIM
Y=0.2733E-02 +0.5557E-01*X -0.1106E-01*X^2 +0.6280E-03*X^3 -0.1176E-04*X^4

BOX CLEARANCE 5.38 METRES HEEL
Y=-0.3909E-02 +0.2529E+01*X -0.1132E+00*X^2 +0.1976E-02*X^3

BOX CLEARANCE 3.48 METRES HEEL
Y=0.2015E-01 +0.2037E+01*X -0.9357E-01*X^2 +0.1782E-02*X^3

BOX CLEARANCE 5.38 METRES MAXIMUM Gz
Y=0.7455E+01 +0.1343E-02*X -0.4188E-02*X^2

BOX CLEARANCE 3.48 METRES MAXIMUM Gz
Y=0.7370E+01 -0.5432E-01*X -0.2781E-02*X^2

BOX CLEARANCE 5.38 METRES AREA UNDER THE Gz CURVE TO 20 DEGREES
FOR FLOODING EXTENT LESS THAN OR EQUAL TO 16.66%
Y=0.2099E+00 -0.3993E-01*X +0.2739E-02*X^2 -0.6584E-04*X^3
FOR FLOODING EXTENT GREATER THAN 16.66%
Y=0

BOX CLEARANCE 3.48 METRES AREA UNDER THE Gz CURVE TO 20 DEGREES
Y=0.2662E+00 -0.2874E-01*X +0.1055E-02*X^2 -0.1323E-04*X^3

BOX CLEARANCE 5.38 METRES AREA UNDER THE Gz CURVE TO 45 DEGREES
Y=0.2672E+01 -0.5363E-01*X -0.3790E-03*X^2

BOX CLEARANCE 3.48 METRES AREA UNDER THE Gz CURVE TO 45 DEGREES
Y=0.2853E+01 -0.4700E-01*X -0.7729E-03*X^2

DISPLACEMENT 4200.0 TONNES DAMAGE LOCATION STARBOARD MIDSHIPS

BOX CLEARANCE 5.38 METRES TRIM
Y=0.2511E-01 +0.7937E-01*X -0.1240E-01*X^2 +0.5866E-03*X^3 -0.9355E-05*X^4

BOX CLEARANCE 3.48 METRES TRIM
Y=0.5537E-02 -0.3728E-03*X -0.1368E-02*X^2 +0.2783E-04*X^3

BOX CLEARANCE 5.38 METRES HEEL
Y=0.5454E-01 +0.2442E+01*X -0.1075E+00*X^2 +0.1868E-02*X^3

BOX CLEARANCE 3.48 METRES HEEL
Y=0.1990E-01 +0.1764E+01*X -0.7085E-01*X^2 +0.1315E-02*X^3

BOX CLEARANCE 5.38 METRES MAXIMUM Gz
Y=0.7281E+01 -0.6470E-02*X -0.4524E-02*X^2

BOX CLEARANCE 3.48 METRES MAXIMUM Gz
Y=0.7136E+01 -0.6789E-01*X -0.2781E-02*X^2

BOX CLEARANCE 5.38 METRES AREA UNDER THE Gz CURVE TO 20 DEGREES
FOR FLOODING EXTENT LESS THAN OR EQUAL TO 16.66%
Y=0.1755E+00 -0.2901E-01*X +0.1709E-02*X^2 -0.3600E-04*X^3
FOR FLOODING EXTENT GREATER THAN 16.66%
Y=0

BOX CLEARANCE 3.48 METRES AREA UNDER THE Gz CURVE TO 20 DEGREES
Y=0.2436E+00 -0.2137E-01*X +0.4674E-03*X^2

BOX CLEARANCE 5.38 METRES AREA UNDER THE Gz CURVE TO 45 DEGREES
Y=0.2556E+01 -0.5608E-01*X -0.3353E-03*X^2

BOX CLEARANCE 3.48 METRES AREA UNDER THE Gz CURVE TO 45 DEGREES
Y=0.2750E+01 -0.5197E-01*X -0.6955E-03*X^2

DISPLACEMENT 4750.0 TONNES DAMAGE LOCATION STARBOARD MIDSHIPS

BOX CLEARANCE 5.94 METRES TRIM
Y=-0.4483E-02 +0.7982E-01*X -0.6012E-02*X^2 +0.1159E-03*X^3

BOX CLEARANCE 3.88 METRES TRIM
Y=0.7642E-03 +0.4596E-02*X -0.1010E-02*X^2 +0.1968E-04*X^3

BOX CLEARANCE 5.94 METRES HEEL
Y=-0.1099E-01 +0.2069E+01*X -0.6567E-01*X^2 +0.8554E-03*X^3

BOX CLEARANCE 3.88 METRES HEEL
Y=0.3425E-01 +0.2172E+01*X -0.1031E+00*X^2 +0.1987E-02*X^3

BOX CLEARANCE 5.94 METRES MAXIMUM Gz
Y=0.7569E+01 +0.4174E-01*X -0.6164E-02*X^2 +0.1632E-04*X^3

BOX CLEARANCE 3.88 METRES MAXIMUM Gz
Y=0.7706E+01 -0.8163E-01*X +0.1652E-04*X^2 -0.9239E-04*X^3

BOX CLEARANCE 5.94 METRES AREA UNDER THE Gz CURVE TO 20 DEGREES
FOR FLOODING EXTENT LESS THAN OR EQUAL TO 16.66%
Y=0.1804E+00 -0.1733E-01*X +0.3183E-04*X^2 +0.2165E-04*X^3
FOR FLOODING EXTENT GREATER THAN 16.66%
Y=0

BOX CLEARANCE 3.88 METRES AREA UNDER THE Gz CURVE TO 20 DEGREES
Y=0.2973E+00 -0.3524E-01*X +0.1441E-02*X^2 -0.2027E-04*X^3

BOX CLEARANCE 5.94 METRES AREA UNDER THE Gz CURVE TO 45 DEGREES
Y=0.2558E+01 +0.5439E-02*X -0.4844E-02*X^2 +0.9209E-04*X^3

BOX CLEARANCE 3.88 METRES AREA UNDER THE Gz CURVE TO 45 DEGREES
Y=0.2977E+01 -0.5666E-01*X -0.3111E-03*X^2 -0.1264E-04*X^3

DISPLACEMENT 5000.0 TONNES DAMAGE LOCATION STARBOARD MIDSHIPS

BOX CLEARANCE 5.94 METRES TRIM
Y=0.6084E-02 +0.7794E-01*X -0.7029E-02*X^2 +0.1530E-03*X^3

BOX CLEARANCE 3.88 METRES TRIM
Y=0.1357E-02 +0.1659E-02*X -0.9746E-03*X^2 +0.1621E-04*X^3

BOX CLEARANCE 5.94 METRES HEEL
Y=-0.9282E-02 +0.2486E+01*X -0.1066E+00*X^2 +0.1839E-02*X^3

BOX CLEARANCE 3.88 METRES HEEL
Y=-0.6537E-02 +0.1944E+01*X -0.8218E-01*X^2 +0.1517E-02*X^3

BOX CLEARANCE 5.94 METRES MAXIMUM Gz
Y=0.7535E+01 +0.7815E-02*X -0.5393E-02*X^2

BOX CLEARANCE 3.88 METRES MAXIMUM Gz
Y=0.7419E+01 -0.5907E-01*X -0.4000E-02*X^2 +0.1073E-04*X^3

BOX CLEARANCE 5.94 METRES AREA UNDER THE Gz CURVE TO 20 DEGREES
FOR FLOODING EXTENT LESS THAN OR EQUAL TO 16.66%
Y=0.2129E+00 -0.3976E-01*X +0.2607E-02*X^2 -0.5918E-04*X^3
FOR FLOODING EXTENT GREATER THAN 16.66%
Y=0

BOX CLEARANCE 3.88 METRES AREA UNDER THE Gz CURVE TO 20 DEGREES
Y=0.2599E+00 -0.2960E-01*X +0.1150E-02*X^2 -0.1526E-04*X^3

BOX CLEARANCE 5.94 METRES AREA UNDER THE Gz CURVE TO 45 DEGREES
Y=0.2687E+01 -0.6256E-01*X -0.2950E-03*X^2

BOX CLEARANCE 3.88 METRES AREA UNDER THE Gz CURVE TO 45 DEGREES
Y=0.2845E+01 -0.5788E-01*X -0.7322E-03*X^2 +0.2269E-05*X^3

DISPLACEMENT 5250.0 TONNES DAMAGE LOCATION STARBOARD MIDSHIPS

BOX CLEARANCE 5.94 METRES TRIM
Y=0.6030E-03 +0.9999E-01*X -0.1496E-01*X^2 +0.7323E-03*X^3 -0.1218E-04*X^4

BOX CLEARANCE 3.88 METRES TRIM
Y=0.9024E-01 -0.1330E-01*X -0.2626E-03*X^2

BOX CLEARANCE 5.94 METRES HEEL
Y=0.2632E-01 +0.2544E+01*X -0.1154E+00*X^2 +0.2094E-02*X^3

BOX CLEARANCE 3.88 METRES HEEL
Y=0.5396E-02 +0.1643E+01*X -0.5945E-01*X^2 +0.1056E-02*X^3

BOX CLEARANCE 5.94 METRES MAXIMUM Gz
Y=0.7518E+01 -0.4263E-01*X -0.4314E-02*X^2

BOX CLEARANCE 3.88 METRES MAXIMUM Gz
Y=0.7001E+01 -0.6926E-01*X -0.3601E-02*X^2

BOX CLEARANCE 5.94 METRES AREA UNDER THE Gz CURVE TO 20 DEGREES
FOR FLOODING EXTENT LESS THAN OR EQUAL TO 16.66%
Y=0.1802E+00 -0.3192E-01*X +0.1976E-02*X^2 -0.4250E-04*X^3
FOR FLOODING EXTENT GREATER THAN 16.66%
Y=0

BOX CLEARANCE 3.88 METRES AREA UNDER THE Gz CURVE TO 20 DEGREES
Y=0.2462E+00 -0.2192E-01*X +0.4843E-03*X^2

BOX CLEARANCE 5.94 METRES AREA UNDER THE Gz CURVE TO 45 DEGREES
Y=0.2570E+01 -0.7064E-01*X

BOX CLEARANCE 3.88 METRES AREA UNDER THE Gz CURVE TO 45 DEGREES
Y=0.2725E+01 -0.6511E-01*X -0.4772E-03*X^2

DISPLACEMENT 950.0 TONNES DAMAGE LOCATION STARBOARD AFT

BOX CLEARANCE 3.40 METRES TRIM
Y=-0.1300E-01 -0.2409E-01*X +0.2019E-01*X^2 -0.4235E-03*X^3

BOX CLEARANCE 2.21 METRES TRIM
Y=-0.1249E-01 -0.6073E-01*X +0.2901E-01*X^2 -0.7757E-03*X^3

BOX CLEARANCE 3.40 METRES HEEL
Y=-0.6517E-02 -0.6327E-01*X +0.2696E-01*X^2 -0.4505E-03*X^3

BOX CLEARANCE 2.21 METRES HEEL
Y=-0.1155E-01 -0.8777E-01*X +0.3664E-01*X^2 -0.8519E-03*X^3

BOX CLEARANCE 3.40 METRES MAXIMUM Gz
Y=0.7093E+01 +0.3458E-02*X -0.1629E-02*X^2 +0.2919E-03*X^3 -0.1588E-04*X^4

BOX CLEARANCE 2.21 METRES MAXIMUM Gz
Y=0.7217E+01 +0.1700E-01*X -0.4930E-02*X^2 +0.4593E-03*X^3 -0.1392E-04*X^4

BOX CLEARANCE 3.40 METRES AREA UNDER THE Gz CURVE TO 20 DEGREES
Y=0.4410E+00 +0.5613E-03*X -0.2869E-03*X^2 -0.1117E-04*X^3

BOX CLEARANCE 2.21 METRES AREA UNDER THE Gz CURVE TO 20 DEGREES
Y=0.5795E+00 +0.3098E-02*X -0.7082E-03*X^2 +0.9625E-05*X^3

BOX CLEARANCE 3.40 METRES AREA UNDER THE Gz CURVE TO 45 DEGREES
Y=0.2994E+01 -0.1601E-02*X +0.3293E-03*X^2 -0.4424E-04*X^3

BOX CLEARANCE 2.21 METRES AREA UNDER THE Gz CURVE TO 45 DEGREES
Y=0.3167E+01 -0.1166E-02*X +0.1889E-03*X^2 -0.3059E-04*X^3

DISPLACEMENT 1000.0 TONNES DAMAGE LOCATION STARBOARD AFT

BOX CLEARANCE 3.40 METRES TRIM
Y=-0.5706E-02 -0.8975E-01*X +0.3304E-01*X^2 -0.8342E-03*X^3

BOX CLEARANCE 2.21 METRES TRIM
Y=-0.1433E-01 -0.8273E-01*X +0.3417E-01*X^2 -0.9598E-03*X^3

BOX CLEARANCE 3.40 METRES HEEL
Y=-0.1697E-01 -0.1175E+00*X +0.4328E-01*X^2 -0.9719E-03*X^3

BOX CLEARANCE 2.21 METRES HEEL
Y=-0.4308E-01 -0.5949E-01*X +0.3889E-01*X^2 -0.9618E-03*X^3

BOX CLEARANCE 3.40 METRES MAXIMUM Gz
Y=0.6890E+01 +0.5767E-02*X -0.6590E-03*X^2 -0.1564E-04*X^3

BOX CLEARANCE 2.21 METRES MAXIMUM Gz
Y=0.7205E+01 +0.1989E-01*X -0.5666E-02*X^2 +0.5185E-03*X^3 -0.1554E-04*X^4

BOX CLEARANCE 3.40 METRES AREA UNDER THE Gz CURVE TO 20 DEGREES
Y=0.3550E+00 +0.2193E-02*X -0.6006E-03*X^2 +0.6099E-05*X^3

BOX CLEARANCE 2.21 METRES AREA UNDER THE Gz CURVE TO 20 DEGREES
Y=0.5198E+00 +0.2435E-02*X -0.5887E-03*X^2 +0.8328E-05*X^3

BOX CLEARANCE 3.40 METRES AREA UNDER THE Gz CURVE TO 45 DEGREES
Y=0.2901E+01 +0.6713E-04*X -0.6044E-04*X^2 -0.2255E-04*X^3

BOX CLEARANCE 2.21 METRES AREA UNDER THE Gz CURVE TO 45 DEGREES
Y=0.3105E+01 -0.3005E-02*X +0.5035E-03*X^2 -0.3941E-04*X^3

DISPLACEMENT 1050.0 TONNES DAMAGE LOCATION STARBOARD AFT

BOX CLEARANCE 3.40 METRES TRIM
Y=-0.7904E-02 -0.1343E+00*X +0.4211E-01*X^2 -0.1131E-02*X^3

BOX CLEARANCE 2.21 METRES TRIM
Y=0.2781E-02 -0.5531E-01*X +0.2731E-01*X^2 -0.7430E-03*X^3

BOX CLEARANCE 3.40 METRES HEEL
Y=-0.3915E-01 -0.1690E+00*X +0.5730E-01*X^2 -0.1426E-02*X^3

BOX CLEARANCE 2.21 METRES HEEL
Y=-0.2173E-01 -0.3273E-01*X +0.3211E-01*X^2 -0.7254E-03*X^3

BOX CLEARANCE 3.40 METRES MAXIMUM Gz
Y=0.6734E+01 +0.9770E-03*X +0.8049E-04*X^2

BOX CLEARANCE 2.21 METRES MAXIMUM Gz
Y=0.7188E+01 +0.1997E-01*X -0.5751E-02*X^2 +0.5299E-03*X^3 -0.1606E-04*X^4

BOX CLEARANCE 3.40 METRES AREA UNDER THE Gz CURVE TO 20 DEGREES
Y=0.2929E+00 +0.2888E-02*X -0.7436E-03*X^2 +0.1735E-04*X^3

BOX CLEARANCE 2.21 METRES AREA UNDER THE Gz CURVE TO 20 DEGREES
Y=0.4816E+00 +0.2757E-02*X -0.5468E-03*X^2 +0.7615E-05*X^3

BOX CLEARANCE 3.40 METRES AREA UNDER THE Gz CURVE TO 45 DEGREES
Y=0.2829E+01 +0.5809E-03*X -0.1058E-03*X^2 -0.1736E-04*X^3

BOX CLEARANCE 2.21 METRES AREA UNDER THE Gz CURVE TO 45 DEGREES
Y=0.3067E+01 -0.2708E-02*X +0.5999E-03*X^2 -0.4437E-04*X^3

DISPLACEMENT 1900.0 TONNES DAMAGE LOCATION STARBOARD AFT

BOX CLEARANCE 4.27 METRES TRIM
Y=-0.3717E-02 -0.1009E+00*X +0.3025E-01*X^2 -0.6701E-03*X^3

BOX CLEARANCE 2.77 METRES TRIM
Y=-0.2879E-02 -0.1089E+00*X +0.3224E-01*X^2 -0.8009E-03*X^3

BOX CLEARANCE 4.27 METRES HEEL
Y=-0.2291E-01 -0.1475E+00*X +0.4935E-01*X^2 -0.1117E-02*X^3

BOX CLEARANCE 2.77 METRES HEEL
Y=-0.2090E-01 -0.1402E+00*X +0.4666E-01*X^2 -0.1082E-02*X^3

BOX CLEARANCE 4.27 METRES MAXIMUM Gz
Y=0.7163E+01 -0.1435E-02*X +0.6566E-03*X^2 -0.1259E-03*X^3

BOX CLEARANCE 2.77 METRES MAXIMUM Gz
Y=0.7002E+01 -0.4137E-01*X +0.8111E-02*X^2 -0.3508E-03*X^3

BOX CLEARANCE 4.27 METRES AREA UNDER THE Gz CURVE TO 20 DEGREES
Y=0.3239E+00 +0.2684E-02*X -0.7378E-03*X^2 +0.1300E-04*X^3

BOX CLEARANCE 2.77 METRES AREA UNDER THE Gz CURVE TO 20 DEGREES
Y=0.3896E+00 +0.3410E-02*X -0.7961E-03*X^2 +0.1469E-04*X^3

BOX CLEARANCE 4.27 METRES AREA UNDER THE Gz CURVE TO 45 DEGREES
Y=0.2812E+01 -0.1671E-02*X +0.2415E-03*X^2 -0.4759E-04*X^3

BOX CLEARANCE 2.77 METRES AREA UNDER THE Gz CURVE TO 45 DEGREES
Y=0.2957E+01 -0.4114E-02*X +0.7357E-03*X^2 -0.6407E-04*X^3

DISPLACEMENT 2000.0 TONNES DAMAGE LOCATION STARBOARD AFT

BOX CLEARANCE 4.27 METRES TRIM
Y=0.1209E-01 -0.1527E+00*X +0.3769E-01*X^2 -0.8776E-03*X^3

BOX CLEARANCE 2.77 METRES TRIM
Y=0.1032E-01 -0.1271E+00*X +0.3400E-01*X^2 -0.8514E-03*X^3

BOX CLEARANCE 4.27 METRES HEEL
Y=0.1527E-01 -0.2469E+00*X +0.6127E-01*X^2 -0.1414E-02*X^3

BOX CLEARANCE 2.77 METRES HEEL
Y=-0.1683E-02 -0.1388E+00*X +0.4316E-01*X^2 -0.9225E-03*X^3

BOX CLEARANCE 4.27 METRES MAXIMUM Gz
Y=0.6907E+01 -0.3323E-01*X +0.5154E-02*X^2 -0.2439E-03*X^3

BOX CLEARANCE 2.77 METRES MAXIMUM Gz
Y=0.7035E+01 -0.3286E-01*X +0.6944E-02*X^2 -0.3309E-03*X^3

BOX CLEARANCE 4.27 METRES AREA UNDER THE Gz CURVE TO 20 DEGREES
Y=0.2611E+00 +0.1677E-02*X -0.5320E-03*X^2 +0.9381E-05*X^3

BOX CLEARANCE 2.77 METRES AREA UNDER THE Gz CURVE TO 20 DEGREES
Y=0.3446E+00 +0.3035E-02*X -0.7180E-03*X^2 +0.1402E-04*X^3

BOX CLEARANCE 4.27 METRES AREA UNDER THE Gz CURVE TO 45 DEGREES
Y=0.2706E+01 -0.2466E-03*X +0.3419E-05*X^2 -0.3411E-04*X^3

BOX CLEARANCE 2.77 METRES AREA UNDER THE Gz CURVE TO 45 DEGREES
Y=0.2887E+01 -0.4182E-02*X +0.7707E-03*X^2 -0.6612E-04*X^3

DISPLACEMENT 2100.0 TONNES DAMAGE LOCATION STARBOARD AFT

BOX CLEARANCE 4.27 METRES TRIM
Y=0.1432E-01 -0.1615E+00*X +0.3886E-01*X^2 -0.9170E-03*X^3

BOX CLEARANCE 2.77 METRES TRIM
Y=0.9872E-02 -0.8391E-01*X +0.2522E-01*X^2 -0.5843E-03*X^3

BOX CLEARANCE 4.27 METRES HEEL
Y=0.1812E-01 -0.2323E+00*X +0.5609E-01*X^2 -0.1217E-02*X^3

BOX CLEARANCE 2.77 METRES HEEL
Y=-0.4747E-02 -0.6253E-01*X +0.2607E-01*X^2 -0.3548E-03*X^3

BOX CLEARANCE 4.27 METRES MAXIMUM Gz
Y=0.6724E+01 +0.2312E-01*X -0.6852E-02*X^2 +0.6929E-03*X^3 -0.2167E-04*X^4

BOX CLEARANCE 2.77 METRES MAXIMUM Gz
Y=0.7041E+01 -0.2439E-01*X +0.5577E-02*X^2 -0.3020E-03*X^3

BOX CLEARANCE 4.27 METRES AREA UNDER THE Gz CURVE TO 20 DEGREES
Y=0.2300E+00 +0.2773E-03*X -0.1688E-03*X^2 -0.7076E-05*X^3

BOX CLEARANCE 2.77 METRES AREA UNDER THE Gz CURVE TO 20 DEGREES
Y=0.3216E+00 +0.2558E-02*X -0.5896E-03*X^2 +0.1042E-04*X^3

BOX CLEARANCE 4.27 METRES AREA UNDER THE Gz CURVE TO 45 DEGREES
Y=0.2636E+01 -0.2377E-02*X +0.4601E-03*X^2 -0.5406E-04*X^3

BOX CLEARANCE 2.77 METRES AREA UNDER THE Gz CURVE TO 45 DEGREES
Y=0.2839E+01 -0.3894E-02*X +0.7721E-03*X^2 -0.6842E-04*X^3

DISPLACEMENT 2850.0 TONNES DAMAGE LOCATION STARBOARD AFT

BOX CLEARANCE 4.91 METRES TRIM
Y=-0.1195E-01 -0.9011E-01*X +0.3208E-01*X^2 -0.6949E-03*X^3

BOX CLEARANCE 3.17 METRES TRIM
Y=-0.1161E-01 -0.9286E-01*X +0.3352E-01*X^2 -0.8090E-03*X^3

BOX CLEARANCE 4.91 METRES HEEL
Y=-0.2973E-01 -0.1352E+00*X +0.4804E-01*X^2 -0.1039E-02*X^3

BOX CLEARANCE 3.17 METRES HEEL
Y=-0.2797E-01 -0.1196E+00*X +0.4492E-01*X^2 -0.1003E-02*X^3

BOX CLEARANCE 4.91 METRES MAXIMUM Gz
Y=0.7464E+01 -0.3867E-01*X +0.8507E-02*X^2 -0.3981E-03*X^3

BOX CLEARANCE 3.17 METRES MAXIMUM Gz
Y=0.7666E+01 +0.7053E-02*X +0.1088E-02*X^2 -0.2008E-03*X^3

BOX CLEARANCE 4.91 METRES AREA UNDER THE Gz CURVE TO 20 DEGREES
Y=0.3079E+00 +0.3024E-02*X -0.8349E-03*X^2 +0.1608E-04*X^3

BOX CLEARANCE 3.17 METRES AREA UNDER THE Gz CURVE TO 20 DEGREES
Y=0.3667E+00 +0.3411E-02*X -0.8653E-03*X^2 +0.1653E-04*X^3

BOX CLEARANCE 4.91 METRES AREA UNDER THE Gz CURVE TO 45 DEGREES
Y=0.2922E+01 -0.3717E-02*X +0.7557E-03*X^2 -0.7964E-04*X^3

BOX CLEARANCE 3.17 METRES AREA UNDER THE Gz CURVE TO 45 DEGREES
Y=0.3095E+01 -0.3662E-02*X +0.8269E-03*X^2 -0.8497E-04*X^3

DISPLACEMENT 3000.0 TONNES DAMAGE LOCATION STARBOARD AFT

BOX CLEARANCE 4.91 METRES TRIM
Y=0.3409E-02 -0.1487E+00*X +0.4143E-01*X^2 -0.9668E-03*X^3

BOX CLEARANCE 3.17 METRES TRIM
Y=0.3832E-02 -0.1265E+00*X +0.3841E-01*X^2 -0.9585E-03*X^3

BOX CLEARANCE 4.91 METRES HEEL
Y=-0.1466E-01 -0.2142E+00*X +0.6256E-01*X^2 -0.1454E-02*X^3

BOX CLEARANCE 3.17 METRES HEEL
Y=-0.1790E-01 -0.1293E+00*X +0.4715E-01*X^2 -0.1045E-02*X^3

BOX CLEARANCE 4.91 METRES MAXIMUM Gz
Y=0.7566E+01 -0.1947E-01*X +0.5848E-02*X^2 -0.3411E-03*X^3

BOX CLEARANCE 3.17 METRES MAXIMUM Gz
Y=0.7399E+01 -0.1628E-01*X +0.3990E-02*X^2 -0.2713E-03*X^3

BOX CLEARANCE 4.91 METRES AREA UNDER THE Gz CURVE TO 20 DEGREES
Y=0.2423E+00 +0.1613E-02*X -0.5918E-03*X^2 +0.1181E-04*X^3

BOX CLEARANCE 3.17 METRES AREA UNDER THE Gz CURVE TO 20 DEGREES
Y=0.3129E+00 +0.2847E-02*X -0.7188E-03*X^2 +0.1390E-04*X^3

BOX CLEARANCE 4.91 METRES AREA UNDER THE Gz CURVE TO 45 DEGREES
Y=0.2809E+01 -0.2694E-02*X +0.6349E-03*X^2 -0.7535E-04*X^3

BOX CLEARANCE 3.17 METRES AREA UNDER THE Gz CURVE TO 45 DEGREES
Y=0.2986E+01 -0.3739E-02*X +0.8654E-03*X^2 -0.8579E-04*X^3

DISPLACEMENT 3150.0 TONNES DAMAGE LOCATION STARBOARD AFT

BOX CLEARANCE 4.91 METRES TRIM
Y=0.1307E-01 -0.1848E+00*X +0.4699E-01*X^2 -0.1137E-02*X^3

BOX CLEARANCE 3.17 METRES TRIM
Y=0.1476E-01 -0.1146E+00*X +0.3448E-01*X^2 -0.8357E-03*X^3

BOX CLEARANCE 4.91 METRES HEEL
Y=-0.4311E-03 -0.2577E+00*X +0.6862E-01*X^2 -0.1597E-02*X^3

BOX CLEARANCE 3.17 METRES HEEL
Y=-0.5118E-02 -0.9860E-01*X +0.3880E-01*X^2 -0.7377E-03*X^3

BOX CLEARANCE 4.91 METRES MAXIMUM Gz
Y=0.7547E+01 +0.2120E-02*X +0.2740E-02*X^2 -0.2608E-03*X^3

BOX CLEARANCE 3.17 METRES MAXIMUM Gz
Y=0.7124E+01 -0.2926E-01*X +0.6862E-02*X^2 -0.3604E-03*X^3

BOX CLEARANCE 4.91 METRES AREA UNDER THE Gz CURVE TO 20 DEGREES
Y=0.2022E+00 +0.1195E-02*X -0.4750E-03*X^2 +0.9726E-05*X^3

BOX CLEARANCE 3.17 METRES AREA UNDER THE Gz CURVE TO 20 DEGREES
Y=0.2838E+00 +0.2297E-02*X -0.5879E-03*X^2 +0.1076E-04*X^3

BOX CLEARANCE 4.91 METRES AREA UNDER THE Gz CURVE TO 45 DEGREES
Y=0.2711E+01 -0.3736E-02*X +0.9695E-03*X^2 -0.9203E-04*X^3

BOX CLEARANCE 3.17 METRES AREA UNDER THE Gz CURVE TO 45 DEGREES
Y=0.2898E+01 -0.1615E-02*X +0.6410E-03*X^2 -0.8065E-04*X^3

DISPLACEMENT 3800.0 TONNES DAMAGE LOCATION STARBOARD AFT

BOX CLEARANCE 5.38 METRES TRIM
Y=0.3954E-01 -0.1890E+00*X +0.4564E-01*X^2 -0.1056E-02*X^3

BOX CLEARANCE 3.48 METRES TRIM
Y=-0.3123E-02 -0.1199E+00*X +0.3591E-01*X^2 -0.8399E-03*X^3

BOX CLEARANCE 5.38 METRES HEEL
Y=0.2296E-01 -0.2873E+00*X +0.6751E-01*X^2 -0.1444E-02*X^3

BOX CLEARANCE 3.48 METRES HEEL
Y=-0.1262E-01 -0.1719E+00*X +0.5001E-01*X^2 -0.1075E-02*X^3

BOX CLEARANCE 5.38 METRES MAXIMUM Gz
Y=0.7277E+01 -0.1490E-01*X +0.5317E-02*X^2 -0.3351E-03*X^3

BOX CLEARANCE 3.48 METRES MAXIMUM Gz
Y=0.7453E+01 -0.1355E-01*X +0.5034E-02*X^2 -0.3314E-03*X^3

BOX CLEARANCE 5.38 METRES AREA UNDER THE Gz CURVE TO 20 DEGREES
Y=0.1751E+00 +0.1692E-02*X -0.5212E-03*X^2 +0.1097E-04*X^3

BOX CLEARANCE 3.48 METRES AREA UNDER THE Gz CURVE TO 20 DEGREES
Y=0.3098E+00 +0.3145E-02*X -0.8166E-03*X^2 +0.1599E-04*X^3

BOX CLEARANCE 5.38 METRES AREA UNDER THE Gz CURVE TO 45 DEGREES
Y=0.2557E+01 -0.4209E-02*X +0.1116E-02*X^2 -0.1104E-03*X^3

BOX CLEARANCE 3.48 METRES AREA UNDER THE Gz CURVE TO 45 DEGREES
Y=0.2974E+01 -0.1639E-02*X +0.5779E-03*X^2 -0.8467E-04*X^3

DISPLACEMENT 4000.0 TONNES DAMAGE LOCATION STARBOARD AFT

BOX CLEARANCE 5.38 METRES TRIM
Y=0.3644E-01 -0.1733E+00*X +0.4291E-01*X^2 -0.9707E-03*X^3

BOX CLEARANCE 3.48 METRES TRIM
Y=0.9670E-02 -0.1394E+00*X +0.3860E-01*X^2 -0.9264E-03*X^3

BOX CLEARANCE 5.38 METRES HEEL
Y=0.2365E-01 -0.2826E+00*X +0.6523E-01*X^2 -0.1395E-02*X^3

BOX CLEARANCE 3.48 METRES HEEL
Y=-0.2368E-02 -0.1705E+00*X +0.5017E-01*X^2 -0.1049E-02*X^3

BOX CLEARANCE 5.38 METRES MAXIMUM Gz
Y=0.7462E+01 -0.1588E-01*X +0.3951E-02*X^2 -0.2784E-03*X^3

BOX CLEARANCE 3.48 METRES MAXIMUM Gz
Y=0.7395E+01 +0.8480E-02*X +0.1794E-02*X^2 -0.2484E-03*X^3

BOX CLEARANCE 5.38 METRES AREA UNDER THE Gz CURVE TO 20 DEGREES
Y=0.2098E+00 +0.2108E-02*X -0.6525E-03*X^2 +0.1382E-04*X^3

BOX CLEARANCE 3.48 METRES AREA UNDER THE Gz CURVE TO 20 DEGREES
Y=0.2660E+00 +0.2445E-02*X -0.6629E-03*X^2 +0.1320E-04*X^3

BOX CLEARANCE 5.38 METRES AREA UNDER THE Gz CURVE TO 45 DEGREES
Y=0.2677E+01 -0.2254E-02*X +0.6693E-03*X^2 -0.8996E-04*X^3

BOX CLEARANCE 3.48 METRES AREA UNDER THE Gz CURVE TO 45 DEGREES
Y=0.2859E+01 +0.1736E-02*X +0.1353E-03*X^2 -0.7152E-04*X^3

DISPLACEMENT 4200.0 TONNES DAMAGE LOCATION STARBOARD AFT

BOX CLEARANCE 5.38 METRES TRIM
Y=0.3954E-01 -0.1890E+00*X +0.4564E-01*X^2 -0.1056E-02*X^3

BOX CLEARANCE 3.48 METRES TRIM
Y=0.1579E-01 -0.1118E+00*X +0.3250E-01*X^2 -0.7404E-03*X^3

BOX CLEARANCE 5.38 METRES HEEL
Y=0.2296E-01 -0.2873E+00*X +0.6751E-01*X^2 -0.1444E-02*X^3

BOX CLEARANCE 3.48 METRES HEEL
Y=0.5917E-03 -0.1072E+00*X +0.3868E-01*X^2 -0.6657E-03*X^3

BOX CLEARANCE 5.38 METRES MAXIMUM Gz
Y=0.7277E+01 -0.1490E-01*X +0.5317E-02*X^2 -0.3351E-03*X^3

BOX CLEARANCE 3.48 METRES MAXIMUM Gz
Y=0.7150E+01 +0.1431E-01*X +0.1766E-03*X^2 -0.1925E-03*X^3

BOX CLEARANCE 5.38 METRES AREA UNDER THE Gz CURVE TO 20 DEGREES
Y=0.1751E+00 +0.1692E-02*X -0.5212E-03*X^2 +0.1097E-04*X^3

BOX CLEARANCE 3.48 METRES AREA UNDER THE Gz CURVE TO 20 DEGREES
Y=0.2457E+00 +0.2507E-02*X -0.5967E-03*X^2 +0.1129E-04*X^3

BOX CLEARANCE 5.38 METRES AREA UNDER THE Gz CURVE TO 45 DEGREES
Y=0.2557E+01 -0.4209E-02*X +0.1116E-02*X^2 -0.1104E-03*X^3

BOX CLEARANCE 3.48 METRES AREA UNDER THE Gz CURVE TO 45 DEGREES
Y=0.2751E+01 +0.4106E-02*X -0.2366E-03*X^2 -0.5991E-04*X^3

DISPLACEMENT 4750.0 TONNES DAMAGE LOCATION STARBOARD AFT

BOX CLEARANCE 5.94 METRES TRIM
Y=0.4460E-03 -0.1294E+00*X +0.3641E-01*X^2 -0.7667E-03*X^3

BOX CLEARANCE 3.88 METRES TRIM
Y=0.1602E-02 -0.2010E+00*X +0.4346E-01*X^2 -0.9852E-03*X^3

BOX CLEARANCE 5.94 METRES HEEL
Y=0.9939E-04 -0.1997E+00*X +0.5242E-01*X^2 -0.1041E-02*X^3

BOX CLEARANCE 3.88 METRES HEEL
Y=-0.3734E-03 -0.1993E+00*X +0.5303E-01*X^2 -0.1111E-02*X^3

BOX CLEARANCE 5.94 METRES MAXIMUM Gz
Y=0.7567E+01 +0.3632E-01*X -0.2127E-03*X^2 -0.1975E-03*X^3

BOX CLEARANCE 3.88 METRES MAXIMUM Gz
Y=0.7710E+01 -0.2411E-01*X +0.7015E-02*X^2 -0.3752E-03*X^3 -0.7697E-05*X^4

BOX CLEARANCE 5.94 METRES AREA UNDER THE Gz CURVE TO 20 DEGREES
Y=0.1810E+00 +0.2435E-01*X -0.2359E-02*X^2 +0.4902E-04*X^3

BOX CLEARANCE 3.88 METRES AREA UNDER THE Gz CURVE TO 20 DEGREES
Y=0.2967E+00 +0.3236E-02*X -0.8487E-03*X^2 +0.1710E-04*X^3

BOX CLEARANCE 5.94 METRES AREA UNDER THE Gz CURVE TO 45 DEGREES
Y=0.2558E+01 +0.6862E-01*X -0.4793E-02*X^2 +0.3401E-04*X^3

BOX CLEARANCE 3.88 METRES AREA UNDER THE Gz CURVE TO 45 DEGREES
Y=0.2978E+01 -0.5352E-02*X +0.1458E-02*X^2 -0.1415E-03*X^3

DISPLACEMENT 5000.0 TONNES DAMAGE LOCATION STARBOARD AFT

BOX CLEARANCE 5.94 METRES TRIM
Y=0.1874E-01 -0.1789E+00*X +0.4400E-01*X^2 -0.9776E-03*X^3

BOX CLEARANCE 3.88 METRES TRIM
Y=0.8048E-02 -0.1542E+00*X +0.3895E-01*X^2 -0.8868E-03*X^3

BOX CLEARANCE 5.94 METRES HEEL
Y=0.2150E-01 -0.2861E+00*X +0.6715E-01*X^2 -0.1447E-02*X^3

BOX CLEARANCE 3.88 METRES HEEL
Y=0.3599E-02 -0.1697E+00*X +0.4812E-01*X^2 -0.9307E-03*X^3

BOX CLEARANCE 5.94 METRES MAXIMUM Gz
Y=0.7524E+01 -0.1103E-01*X +0.5123E-02*X^2 -0.3455E-03*X^3

BOX CLEARANCE 3.88 METRES MAXIMUM Gz
Y=0.7418E+01 -0.2325E-01*X +0.7060E-02*X^2 -0.5216E-03*X^3

BOX CLEARANCE 5.94 METRES AREA UNDER THE Gz CURVE TO 20 DEGREES
Y=0.2129E+00 +0.2048E-02*X -0.6560E-03*X^2 +0.1367E-04*X^3

BOX CLEARANCE 3.88 METRES AREA UNDER THE Gz CURVE TO 20 DEGREES
Y=0.2596E+00 +0.2623E-02*X -0.6918E-03*X^2 +0.1366E-04*X^3

BOX CLEARANCE 5.94 METRES AREA UNDER THE Gz CURVE TO 45 DEGREES
Y=0.2687E+01 +0.4494E-02*X -0.4669E-03*X^2 -0.5187E-04*X^3

BOX CLEARANCE 3.88 METRES AREA UNDER THE Gz CURVE TO 45 DEGREES
Y=0.2846E+01 -0.6550E-02*X +0.1734E-02*X^2 -0.1565E-03*X^3

DISPLACEMENT 5250.0 TONNES DAMAGE LOCATION STARBOARD AFT

BOX CLEARANCE 5.94 METRES TRIM
Y=0.1682E-01 -0.1936E+00*X +0.4662E-01*X^2 -0.1056E-02*X^3

BOX CLEARANCE 3.88 METRES TRIM
Y=0.1031E+00 -0.1000E+00*X +0.2995E-01*X^2 -0.6314E-03*X^3

BOX CLEARANCE 5.94 METRES HEEL
Y=0.2194E-01 -0.3069E+00*X +0.7166E-01*X^2 -0.1559E-02*X^3

BOX CLEARANCE 3.88 METRES HEEL
Y=0.4539E-02 -0.1077E+00*X +0.3541E-01*X^2 -0.4988E-03*X^3

BOX CLEARANCE 5.94 METRES MAXIMUM Gz
Y=0.7551E+01 +0.1802E-01*X +0.7896E-03*X^2 -0.2340E-03*X^3

BOX CLEARANCE 3.88 METRES MAXIMUM Gz
FOR FLOODING EXTENT LESS THAN OR EQUAL TO 8.33%
Y=0.6991E+01 -0.1662E-02*X
FOR FLOODING EXTENT GREATER THAN 8.33%
Y=0.6991E+01 +0.5053E-01*X -0.1917E-01*X^2 +0.2284E-02*X^3 -0.8831E-04*X^4

BOX CLEARANCE 5.94 METRES AREA UNDER THE Gz CURVE TO 20 DEGREES
Y=0.1801E+00 +0.1609E-02*X -0.5343E-03*X^2 +0.1108E-04*X^3

BOX CLEARANCE 3.88 METRES AREA UNDER THE Gz CURVE TO 20 DEGREES
Y=0.2467E+00 +0.2667E-02*X -0.6148E-03*X^2 +0.1089E-04*X^3

BOX CLEARANCE 5.94 METRES AREA UNDER THE Gz CURVE TO 45 DEGREES
Y=0.2554E+01 +0.7885E-02*X -0.9603E-03*X^2 -0.3546E-04*X^3

BOX CLEARANCE 3.88 METRES AREA UNDER THE Gz CURVE TO 45 DEGREES
Y=0.2725E+01 -0.8308E-02*X +0.2183E-02*X^2 -0.1808E-03*X^3

DISPLACEMENT 950.0 TONNES DAMAGE LOCATION PORT AND STARBOARD AFT

BOX CLEARANCE 3.40 METRES TRIM
Y=-0.3571E-02 -0.8011E-01*X +0.4630E-01*X^2 -0.1132E-02*X^3

BOX CLEARANCE 2.21 METRES TRIM
Y=-0.1366E+00 +0.1887E+00*X +0.1003E-01*X^2

BOX CLEARANCE 3.40 METRES HEEL
Y=0

BOX CLEARANCE 2.21 METRES HEEL
Y=0

BOX CLEARANCE 3.40 METRES MAXIMUM Gz
Y=0.7086E+01 +0.2049E-01*X -0.2428E-02*X^2 +0.2364E-04*X^3

BOX CLEARANCE 2.21 METRES MAXIMUM Gz
Y=0.7217E+01 -0.1671E-02*X +0.4940E-03*X^2 -0.3075E-04*X^3

BOX CLEARANCE 3.40 METRES AREA UNDER THE Gz CURVE TO 20 DEGREES
Y=0.4409E+00 +0.2204E-02*X -0.6317E-03*X^2 +0.3717E-04*X^3

BOX CLEARANCE 2.21 METRES AREA UNDER THE Gz CURVE TO 20 DEGREES
Y=0.5800E+00 -0.2270E-03*X -0.1337E-03*X^2 +0.2288E-04*X^3

BOX CLEARANCE 3.40 METRES AREA UNDER THE Gz CURVE TO 45 DEGREES
Y=0.2994E+01 +0.1538E-02*X -0.3473E-03*X^2 +0.1886E-04*X^3

BOX CLEARANCE 2.21 METRES AREA UNDER THE Gz CURVE TO 45 DEGREES
Y=0.3167E+01 +0.1309E-03*X -0.1270E-03*X^2 +0.2055E-04*X^3

DISPLACEMENT 1000.0 TONNES DAMAGE LOCATION PORT AND STARBOARD AFT

BOX CLEARANCE 3.40 METRES TRIM
Y=-0.2740E-01 -0.1227E+00*X +0.5811E-01*X^2 -0.1543E-02*X^3

BOX CLEARANCE 2.21 METRES TRIM
Y=-0.1429E+00 +0.2107E+00*X +0.8170E-02*X^2

BOX CLEARANCE 3.40 METRES HEEL
Y=0

BOX CLEARANCE 2.21 METRES HEEL
Y=0

BOX CLEARANCE 3.40 METRES MAXIMUM Gz
Y=0.6888E+01 +0.1162E-01*X -0.1589E-02*X^2 +0.1546E-04*X^3

BOX CLEARANCE 2.21 METRES MAXIMUM Gz
Y=0.7205E+01 -0.9656E-03*X +0.3934E-03*X^2 -0.2877E-04*X^3

BOX CLEARANCE 3.40 METRES AREA UNDER THE Gz CURVE TO 20 DEGREES
Y=0.3552E+00 -0.9472E-03*X -0.9510E-04*X^2 +0.2413E-04*X^3

BOX CLEARANCE 2.21 METRES AREA UNDER THE Gz CURVE TO 20 DEGREES
Y=0.5201E+00 -0.1355E-02*X +0.1120E-03*X^2 +0.1567E-04*X^3

BOX CLEARANCE 3.40 METRES AREA UNDER THE Gz CURVE TO 45 DEGREES
Y=0.2902E+01 -0.3090E-02*X +0.3752E-03*X^2

BOX CLEARANCE 2.21 METRES AREA UNDER THE Gz CURVE TO 45 DEGREES
Y=0.3104E+01 -0.2555E-02*X +0.4187E-03*X^2 +0.1376E-05*X^3

DISPLACEMENT 1050.0 TONNES DAMAGE LOCATION PORT AND STARBOARD AFT

BOX CLEARANCE 3.40 METRES TRIM
Y=-0.1896E+00 +0.1755E+00*X +0.1527E-01*X^2

BOX CLEARANCE 2.21 METRES TRIM
Y=-0.7806E-01 +0.2015E+00*X +0.5632E-02*X^2

BOX CLEARANCE 3.40 METRES HEEL
Y=0

BOX CLEARANCE 2.21 METRES HEEL
Y=0

BOX CLEARANCE 3.40 METRES MAXIMUM Gz
Y=0.6735E+01 +0.2674E-02*X -0.9437E-03*X^2 +0.1420E-03*X^3 -0.5584E-05*X^4

BOX CLEARANCE 2.21 METRES MAXIMUM Gz
Y=0.7188E+01 -0.1713E-02*X +0.5396E-03*X^2 -0.3723E-04*X^3

BOX CLEARANCE 3.40 METRES AREA UNDER THE Gz CURVE TO 20 DEGREES
Y=0.2930E+00 +0.2392E-02*X -0.6970E-03*X^2 +0.5438E-04*X^3

BOX CLEARANCE 2.21 METRES AREA UNDER THE Gz CURVE TO 20 DEGREES
Y=0.4820E+00 -0.9267E-03*X +0.2092E-03*X^2 +0.9584E-05*X^3

BOX CLEARANCE 3.40 METRES AREA UNDER THE Gz CURVE TO 45 DEGREES
Y=0.2829E+01 -0.6726E-03*X +0.1067E-03*X^2 +0.1244E-04*X^3

BOX CLEARANCE 2.21 METRES AREA UNDER THE Gz CURVE TO 45 DEGREES
Y=0.3067E+01 -0.2355E-02*X +0.5756E-03*X^2 -0.8560E-05*X^3

DISPLACEMENT 1900.0 TONNES DAMAGE LOCATION PORT AND STARBOARD AFT

BOX CLEARANCE 4.27 METRES TRIM
Y=-0.9702E-01 +0.3312E-01*X +0.2314E-01*X^2

BOX CLEARANCE 2.77 METRES TRIM
Y=-0.1137E+00 +0.8336E-01*X +0.1695E-01*X^2

BOX CLEARANCE 4.27 METRES HEEL
Y=0

BOX CLEARANCE 2.77 METRES HEEL
Y=0

BOX CLEARANCE 4.27 METRES MAXIMUM Gz
Y=0.7168E+01 -0.2341E-01*X +0.4438E-02*X^2 -0.2706E-03*X^3

BOX CLEARANCE 2.77 METRES MAXIMUM Gz
Y=0.6996E+01 +0.4279E-02*X -0.1488E-02*X^2 +0.2166E-03*X^3 -0.8848E-05*X^4

BOX CLEARANCE 4.27 METRES AREA UNDER THE Gz CURVE TO 20 DEGREES
Y=0.3240E+00 -0.9623E-03*X +0.2328E-03*X^2 -0.3580E-04*X^3 +0.2399E-05*X^4

BOX CLEARANCE 2.77 METRES AREA UNDER THE Gz CURVE TO 20 DEGREES
Y=0.3900E+00 +0.7784E-03*X -0.3281E-03*X^2 +0.3309E-04*X^3

BOX CLEARANCE 4.27 METRES AREA UNDER THE Gz CURVE TO 45 DEGREES
Y=0.2812E+01 +0.9221E-04*X -0.1829E-03*X^2 +0.1602E-04*X^3

BOX CLEARANCE 2.77 METRES AREA UNDER THE Gz CURVE TO 45 DEGREES
FOR FLOODING EXTENT LESS THAN OR EQUAL TO 6.50%
Y=0.2956E+01
FOR FLOODING EXTENT GREATER THAN 6.50%
Y=0.2957E+01 -0.2771E-02*X +0.4501E-03*X^2 -0.9037E-05*X^3

DISPLACEMENT 2000.0 TONNES DAMAGE LOCATION PORT AND STARBOARD AFT

BOX CLEARANCE 4.27 METRES TRIM
Y=-0.7760E-01 +0.2106E-02*X +0.2592E-01*X^2

BOX CLEARANCE 2.77 METRES TRIM
Y=-0.7854E-01 +0.7354E-01*X +0.1579E-01*X^2

BOX CLEARANCE 4.27 METRES HEEL
Y=0

BOX CLEARANCE 2.77 METRES HEEL
Y=0

BOX CLEARANCE 4.27 METRES MAXIMUM Gz
Y=0.6899E+01 +0.8341E-02*X -0.2376E-02*X^2 +0.6855E-04*X^3

BOX CLEARANCE 2.77 METRES MAXIMUM Gz
Y=0.7032E+01 +0.9582E-02*X -0.3659E-02*X^2 +0.4822E-03*X^3 -0.1945E-04*X^4

BOX CLEARANCE 4.27 METRES AREA UNDER THE Gz CURVE TO 20 DEGREES
Y=0.2610E+00 +0.1454E-02*X -0.5138E-03*X^2 +0.4699E-04*X^3

BOX CLEARANCE 2.77 METRES AREA UNDER THE Gz CURVE TO 20 DEGREES
Y=0.3450E+00 +0.5065E-03*X -0.2654E-03*X^2 +0.3332E-04*X^3

BOX CLEARANCE 4.27 METRES AREA UNDER THE Gz CURVE TO 45 DEGREES
Y=0.2706E+01 -0.8070E-03*X +0.2338E-04*X^2 +0.1360E-04*X^3

BOX CLEARANCE 2.77 METRES AREA UNDER THE Gz CURVE TO 45 DEGREES
FOR FLOODING EXTENT LESS THAN OR EQUAL TO 6.25%
Y=0.2887E+01 -0.3200E-03*X

FOR FLOODING EXTENT GREATER THAN 6.25%
Y=0.2887E+01 -0.4033E-02*X +0.7132E-03*X^2 -0.2006E-04*X^3

DISPLACEMENT 2100.0 TONNES DAMAGE LOCATION PORT AND STARBOARD AFT

BOX CLEARANCE 4.27 METRES TRIM
Y=0.8664E-02 -0.2914E+00*X +0.7712E-01*X^2 -0.2155E-02*X^3

BOX CLEARANCE 2.77 METRES TRIM
Y=-0.3465E-03 -0.9631E-01*X +0.4335E-01*X^2 -0.1276E-02*X^3

BOX CLEARANCE 4.27 METRES HEEL
Y=0

BOX CLEARANCE 2.77 METRES HEEL
Y=0

BOX CLEARANCE 4.27 METRES MAXIMUM Gz
Y=0.6724E+01 +0.2967E-03*X -0.2271E-03*X^2 +0.9497E-04*X^3 -0.4699E-05*X^4

BOX CLEARANCE 2.77 METRES MAXIMUM Gz
Y=0.7043E+01 +0.1493E-01*X -0.7414E-02*X^2 +0.9937E-03*X^3 -0.3953E-04*X^4

BOX CLEARANCE 4.27 METRES AREA UNDER THE Gz CURVE TO 20 DEGREES
Y=0.2300E+00 +0.4212E-03*X -0.1964E-03*X^2 +0.3187E-04*X^3

BOX CLEARANCE 2.77 METRES AREA UNDER THE Gz CURVE TO 20 DEGREES
Y=0.3220E+00 +0.1057E-02*X +0.1427E-03*X^2 +0.1577E-04*X^3

BOX CLEARANCE 4.27 METRES AREA UNDER THE Gz CURVE TO 45 DEGREES
Y=0.2636E+01 -0.1526E-02*X +0.2323E-03*X^2 +0.4722E-05*X^3

BOX CLEARANCE 2.77 METRES AREA UNDER THE Gz CURVE TO 45 DEGREES
FOR FLOODING EXTENT LESS THAN OR EQUAL TO 6.50%
Y=0.2838E+01
FOR FLOODING EXTENT GREATER THAN 6.50%
Y=0.2839E+01 -0.4615E-02*X +0.7813E-03*X^2 -0.9415E-05*X^3 -0.9009E-06*X^4

DISPLACEMENT 2850.0 TONNES DAMAGE LOCATION PORT AND STARBOARD AFT

BOX CLEARANCE 4.91 METRES TRIM
Y=-0.2402E-01 -0.1699E+00*X +0.6367E-01*X^2 -0.1508E-02*X^3

BOX CLEARANCE 3.17 METRES TRIM
Y=-0.3817E-01 -0.9843E-01*X +0.5410E-01*X^2 -0.1356E-02*X^3

BOX CLEARANCE 4.91 METRES HEEL
Y=0

BOX CLEARANCE 3.17 METRES HEEL
Y=0

BOX CLEARANCE 4.91 METRES MAXIMUM Gz
Y=0.7464E+01 -0.3566E-01*X +0.7842E-02*X^2 -0.3638E-03*X^3

BOX CLEARANCE 3.17 METRES MAXIMUM Gz
Y=0.7667E+01 +0.6481E-02*X +0.1010E-02*X^2 -0.1862E-03*X^3

BOX CLEARANCE 4.91 METRES AREA UNDER THE Gz CURVE TO 20 DEGREES
Y=0.3080E+00 +0.1645E-02*X -0.6360E-03*X^2 +0.4996E-04*X^3

BOX CLEARANCE 3.17 METRES AREA UNDER THE Gz CURVE TO 20 DEGREES
Y=0.3670E+00 +0.1471E-02*X -0.5576E-03*X^2 +0.4746E-04*X^3

BOX CLEARANCE 4.91 METRES AREA UNDER THE Gz CURVE TO 45 DEGREES
Y=0.2921E+01 -0.7730E-03*X +0.1311E-03*X^2

BOX CLEARANCE 3.17 METRES AREA UNDER THE Gz CURVE TO 45 DEGREES
Y=0.3095E+01 -0.1510E-03*X +0.5109E-04*X^2

DISPLACEMENT 3000.0 TONNES DAMAGE LOCATION PORT AND STARBOARD AFT

BOX CLEARANCE 4.91 METRES TRIM
Y=-0.1946E-01 -0.2439E+00*X +0.7722E-01*X^2 -0.1936E-02*X^3

BOX CLEARANCE 3.17 METRES TRIM
Y=-0.2894E-01 -0.7710E-01*X +0.4971E-01*X^2 -0.1219E-02*X^3

BOX CLEARANCE 4.91 METRES HEEL
Y=0

BOX CLEARANCE 3.17 METRES HEEL
Y=0

BOX CLEARANCE 4.91 METRES MAXIMUM Gz
Y=0.7567E+01 -0.1851E-01*X +0.5516E-02*X^2 -0.3183E-03*X^3

BOX CLEARANCE 3.17 METRES MAXIMUM Gz
Y=0.7399E+01 -0.1469E-01*X +0.3683E-02*X^2 -0.2561E-03*X^3

BOX CLEARANCE 4.91 METRES AREA UNDER THE Gz CURVE TO 20 DEGREES
Y=0.2421E+00 +0.9647E-03*X -0.4892E-03*X^2 +0.5009E-04*X^3

BOX CLEARANCE 3.17 METRES AREA UNDER THE Gz CURVE TO 20 DEGREES
Y=0.3130E+00 -0.4884E-02*X +0.6841E-03*X^2

BOX CLEARANCE 4.91 METRES AREA UNDER THE Gz CURVE TO 45 DEGREES
Y=0.2808E+01 -0.5988E-03*X +0.1799E-03*X^2

BOX CLEARANCE 3.17 METRES AREA UNDER THE Gz CURVE TO 45 DEGREES
Y=0.2986E+01 +0.6513E-03*X +0.3946E-04*X^2

DISPLACEMENT 3150.0 TONNES DAMAGE LOCATION PORT AND STARBOARD AFT

BOX CLEARANCE 4.91 METRES TRIM
Y=-0.1129E+00 +0.4812E-01*X +0.2738E-01*X^2

BOX CLEARANCE 3.17 METRES TRIM
Y=-0.1694E-01 -0.1417E-01*X +0.3622E-01*X^2 -0.7886E-03*X^3

BOX CLEARANCE 4.91 METRES HEEL
Y=0

BOX CLEARANCE 3.17 METRES HEEL
Y=0

BOX CLEARANCE 4.91 METRES MAXIMUM Gz
Y=0.7555E+01 +0.1849E-01*X -0.7302E-02*X^2 +0.1063E-02*X^3 -0.4715E-04*X^4

BOX CLEARANCE 3.17 METRES MAXIMUM Gz
Y=0.7125E+01 -0.3117E-01*X +0.7115E-02*X^2 -0.3657E-03*X^3

BOX CLEARANCE 4.91 METRES AREA UNDER THE Gz CURVE TO 20 DEGREES
Y=0.2020E+00 +0.2616E-03*X -0.2541E-03*X^2 +0.4109E-04*X^3

BOX CLEARANCE 3.17 METRES AREA UNDER THE Gz CURVE TO 20 DEGREES
Y=0.2840E+00 -0.4073E-02*X +0.6525E-03*X^2

BOX CLEARANCE 4.91 METRES AREA UNDER THE Gz CURVE TO 45 DEGREES
Y=0.2710E+01 +0.8602E-03*X +0.1148E-03*X^2

BOX CLEARANCE 3.17 METRES AREA UNDER THE Gz CURVE TO 45 DEGREES
Y=0.2898E+01 +0.2494E-02*X -0.1024E-03*X^2

DISPLACEMENT 3800.0 TONNES DAMAGE LOCATION PORT AND STARBOARD AFT

BOX CLEARANCE 5.38 METRES TRIM
Y=-0.4271E-02 -0.1945E+00*X +0.6517E-01*X^2 -0.1484E-02*X^3

BOX CLEARANCE 3.48 METRES TRIM
Y=-0.2659E-01 -0.1582E+00*X +0.6021E-01*X^2 -0.1461E-02*X^3

BOX CLEARANCE 5.38 METRES HEEL
Y=0

BOX CLEARANCE 3.48 METRES HEEL
Y=0

BOX CLEARANCE 5.38 METRES MAXIMUM Gz
Y=0.7718E+01 +0.1086E-02*X +0.1564E-02*X^2 -0.2093E-03*X^3

BOX CLEARANCE 3.48 METRES MAXIMUM Gz
Y=0.7455E+01 -0.1687E-01*X +0.5479E-02*X^2 -0.3410E-03*X^3

BOX CLEARANCE 5.38 METRES AREA UNDER THE Gz CURVE TO 20 DEGREES
Y=0.2689E+00 -0.3219E-02*X +0.2582E-03*X^2 +0.1343E-04*X^3

BOX CLEARANCE 3.48 METRES AREA UNDER THE Gz CURVE TO 20 DEGREES
Y=0.3110E+00 -0.4469E-02*X +0.5458E-03*X^2 +0.3597E-05*X^3

BOX CLEARANCE 5.38 METRES AREA UNDER THE Gz CURVE TO 45 DEGREES
FOR FLOODING EXTENT LESS THAN OR EQUAL TO 6.25%
Y=0.2813E+01
FOR FLOODING EXTENT GREATER THAN 6.25%
Y=0.2813E+01 -0.1932E-02*X +0.4446E-03*X^2 -0.2166E-04*X^3

BOX CLEARANCE 3.48 METRES AREA UNDER THE Gz CURVE TO 45 DEGREES
FOR FLOODING EXTENT LESS THAN OR EQUAL TO 6.25%
Y=0.2975E+01
FOR FLOODING EXTENT GREATER THAN 6.25%
Y=0.2975E+01 -0.5988E-02*X +0.1280E-02*X^2 -0.5738E-04*X^3

DISPLACEMENT 4000.0 TONNES DAMAGE LOCATION PORT AND STARBOARD AFT

BOX CLEARANCE 5.38 METRES TRIM
Y=0.1635E-01 -0.2625E+00*X +0.7626E-01*X^2 -0.1821E-02*X^3

BOX CLEARANCE 3.48 METRES TRIM
Y=-0.1158E-01 -0.1316E+00*X +0.5440E-01*X^2 -0.1272E-02*X^3

BOX CLEARANCE 5.38 METRES HEEL
Y=0

BOX CLEARANCE 3.48 METRES HEEL
Y=0

BOX CLEARANCE 5.38 METRES MAXIMUM Gz
Y=0.7465E+01 -0.2779E-01*X +0.5194E-02*X^2 -0.3048E-03*X^3

BOX CLEARANCE 3.48 METRES MAXIMUM Gz
Y=0.7397E+01 +0.3560E-02*X +0.2520E-02*X^2 -0.2691E-03*X^3

BOX CLEARANCE 5.38 METRES AREA UNDER THE Gz CURVE TO 20 DEGREES
Y=0.2111E+00 -0.4513E-02*X +0.5680E-03*X^2 +0.4831E-05*X^3

BOX CLEARANCE 3.48 METRES AREA UNDER THE Gz CURVE TO 20 DEGREES
Y=0.2670E+00 -0.5163E-02*X +0.7492E-03*X^2 -0.2980E-05*X^3

BOX CLEARANCE 5.38 METRES AREA UNDER THE Gz CURVE TO 45 DEGREES
FOR FLOODING EXTENT LESS THAN OR EQUAL TO 6.25%
Y=0.2677E+01 +0.3200E-03*X

FOR FLOODING EXTENT GREATER THAN 6.25%
Y=0.2677E+01 -0.1740E-02*X +0.4496E-03*X^2 -0.1920E-04*X^3

BOX CLEARANCE 3.48 METRES AREA UNDER THE Gz CURVE TO 45 DEGREES
FOR FLOODING EXTENT LESS THAN OR EQUAL TO 6.25%
Y=0.2860E+01 +0.6400E-03*X
FOR FLOODING EXTENT GREATER THAN 6.25%
Y=0.2860E+01 -0.6891E-02*X +0.1664E-02*X^2 -0.7868E-04*X^3

DISPLACEMENT 4200.0 TONNES DAMAGE LOCATION PORT AND STARBOARD AFT

BOX CLEARANCE 5.38 METRES TRIM
Y=0.1459E-01 -0.2311E+00*X +0.7293E-01*X^2 -0.1737E-02*X^3

BOX CLEARANCE 3.48 METRES TRIM
Y=-0.5905E-02 -0.4849E-01*X +0.3843E-01*X^2 -0.7728E-03*X^3

BOX CLEARANCE 5.38 METRES HEEL
Y=0

BOX CLEARANCE 3.48 METRES HEEL
Y=0

BOX CLEARANCE 5.38 METRES MAXIMUM Gz
Y=0.7277E+01 -0.1447E-01*X +0.5439E-02*X^2 -0.3412E-03*X^3

BOX CLEARANCE 3.48 METRES MAXIMUM Gz
Y=0.7152E+01 +0.6334E-02*X +0.1403E-02*X^2 -0.2309E-03*X^3

BOX CLEARANCE 5.38 METRES AREA UNDER THE Gz CURVE TO 20 DEGREES
Y=0.1760E+00 -0.4598E-02*X +0.7107E-03*X^2 -0.4204E-06*X^3

BOX CLEARANCE 3.48 METRES AREA UNDER THE Gz CURVE TO 20 DEGREES
Y=0.2466E+00 -0.4318E-02*X +0.7500E-03*X^2 -0.5316E-05*X^3

BOX CLEARANCE 5.38 METRES AREA UNDER THE Gz CURVE TO 45 DEGREES
FOR FLOODING EXTENT LESS THAN OR EQUAL TO 6.25%
Y=0.2557E+01 +0.6400E-03*X
FOR FLOODING EXTENT GREATER THAN 6.25%
Y=0.2557E+01 -0.4016E-02*X +0.1021E-02*X^2 -0.4424E-04*X^3

BOX CLEARANCE 3.48 METRES AREA UNDER THE Gz CURVE TO 45 DEGREES
FOR FLOODING EXTENT LESS THAN OR EQUAL TO 6.25%
Y=0.2753E+01 +0.8000E-03*X
FOR FLOODING EXTENT GREATER THAN 6.25%
Y=0.2753E+01 -0.6636E-02*X +0.1720E-02*X^2 -0.8599E-04*X^3

DISPLACEMENT 4750.0 TONNES DAMAGE LOCATION PORT AND STARBOARD AFT

BOX CLEARANCE 5.94 METRES TRIM
Y=-0.1800E-01 -0.2171E+00*X +0.6834E-01*X^2 -0.1520E-02*X^3

BOX CLEARANCE 3.88 METRES TRIM
Y=-0.1599E-01 -0.2625E+00*X +0.7113E-01*X^2 -0.1669E-02*X^3

BOX CLEARANCE 5.94 METRES HEEL
Y=0

BOX CLEARANCE 3.88 METRES HEEL
Y=0

BOX CLEARANCE 5.94 METRES MAXIMUM Gz
Y=0.7568E+01 +0.3275E-01*X +0.2885E-03*X^2 -0.2084E-03*X^3

BOX CLEARANCE 3.88 METRES MAXIMUM Gz
Y=0.7701E+01 +0.1832E-01*X +0.2056E-03*X^2 -0.2263E-03*X^3

BOX CLEARANCE 5.94 METRES AREA UNDER THE Gz CURVE TO 20 DEGREES
Y=0.1821E+00 +0.1749E-01*X -0.1149E-02*X^2 +0.4227E-04*X^3

BOX CLEARANCE 3.88 METRES AREA UNDER THE Gz CURVE TO 20 DEGREES
Y=0.2978E+00 -0.4417E-02*X +0.5622E-03*X^2 +0.2590E-05*X^3

BOX CLEARANCE 5.94 METRES AREA UNDER THE Gz CURVE TO 45 DEGREES
Y=0.2556E+01 +0.1172E+00*X -0.1785E-01*X^2 +0.1175E-02*X^3 -0.2826E-04*X^4

BOX CLEARANCE 3.88 METRES AREA UNDER THE Gz CURVE TO 45 DEGREES
Y=0.2978E+01 -0.1007E-02*X +0.4129E-03*X^2 -0.2721E-04*X^3

DISPLACEMENT 5000.0 TONNES DAMAGE LOCATION PORT AND STARBOARD AFT

BOX CLEARANCE 5.94 METRES TRIM
Y=0.2160E-02 -0.2849E+00*X +0.7947E-01*X^2 -0.1856E-02*X^3

BOX CLEARANCE 3.88 METRES TRIM
Y=-0.3889E-02 -0.1720E+00*X +0.5816E-01*X^2 -0.1295E-02*X^3

BOX CLEARANCE 5.94 METRES HEEL
Y=0

BOX CLEARANCE 3.88 METRES HEEL
Y=0

BOX CLEARANCE 5.94 METRES MAXIMUM Gz
Y=0.7526E+01 -0.1787E-01*X +0.6146E-02*X^2 -0.3757E-03*X^3

BOX CLEARANCE 3.88 METRES MAXIMUM Gz
Y=0.7412E+01 +0.1470E-01*X -0.8556E-04*X^2 -0.2098E-03*X^3

BOX CLEARANCE 5.94 METRES AREA UNDER THE Gz CURVE TO 20 DEGREES
Y=0.2139E+00 -0.5017E-02*X +0.6341E-03*X^2 +0.2897E-05*X^3

BOX CLEARANCE 3.88 METRES AREA UNDER THE Gz CURVE TO 20 DEGREES
Y=0.2609E+00 -0.6340E-02*X +0.9813E-03*X^2 -0.1124E-04*X^3

BOX CLEARANCE 5.94 METRES AREA UNDER THE Gz CURVE TO 45 DEGREES
Y=0.2689E+01 +0.1848E-02*X -0.7629E-03*X^2 +0.1111E-03*X^3 -0.4498E-05*X^4

BOX CLEARANCE 3.88 METRES AREA UNDER THE Gz CURVE TO 45 DEGREES
Y=0.2846E+01 +0.7462E-03*X -0.6911E-03*X^2 +0.1570E-03*X^3 -0.8520E-05*X^4

DISPLACEMENT 5250.0 TONNES DAMAGE LOCATION PORT AND STARBOARD AFT

BOX CLEARANCE 5.94 METRES TRIM
Y=0.8994E-02 -0.3094E+00*X +0.8309E-01*X^2 -0.1961E-02*X^3

BOX CLEARANCE 3.88 METRES TRIM
Y=0.8994E-01 -0.5456E-01*X +0.3731E-01*X^2 -0.6596E-03*X^3

BOX CLEARANCE 5.94 METRES HEEL
Y=0

BOX CLEARANCE 3.88 METRES HEEL
Y=0

BOX CLEARANCE 5.94 METRES MAXIMUM Gz
Y=0.7554E+01 +0.1085E-01*X +0.1908E-02*X^2 -0.2701E-03*X^3

BOX CLEARANCE 3.88 METRES MAXIMUM Gz
Y=0.6980E+01 +0.2007E-02*X +0.2358E-02*X^2 -0.2797E-03*X^3

BOX CLEARANCE 5.94 METRES AREA UNDER THE Gz CURVE TO 20 DEGREES
Y=0.1811E+00 -0.5262E-02*X +0.7711E-03*X^2 -0.2075E-05*X^3

BOX CLEARANCE 3.88 METRES AREA UNDER THE Gz CURVE TO 20 DEGREES
Y=0.2479E+00 -0.5576E-02*X +0.9947E-03*X^2 -0.1456E-04*X^3

BOX CLEARANCE 5.94 METRES AREA UNDER THE Gz CURVE TO 45 DEGREES
FOR FLOODING EXTENT LESS THAN OR EQUAL TO 6.25%
Y=0.2556E+01 -0.1401E-02*X +0.3410E-03*X^2
FOR FLOODING EXTENT GREATER THAN 6.25%
Y=0.2556E+01 -0.4508E-02*X +0.1214E-02*X^2 -0.6006E-04*X^3

BOX CLEARANCE 3.88 METRES AREA UNDER THE Gz CURVE TO 45 DEGREES
Y=0.2725E+01 -0.2090E-02*X +0.5472E-04*X^2 +0.1117E-03*X^3 -0.8096E-05*X^4

Appendix B Examples of SWATHMAN Output Data Files

M.V. PATRIA

VESSEL LENGTH IN METRES 37.000
HULL LENGTH IN METRES 32.000
STRUT LENGTH IN METRES 32.000
HULL CENTRELINE SPACING IN METRES 10.000
LOAD DRAUGHT IN METRES 2.700
MAX HULL DIAMETER IN METRES 1.850
MAX STRUT WIDTH IN METRES 1.000
LOAD DISPLACEMENT IN TONNES 180.
WATER DENSITY IN TONNES/M**31.025
MASS MOMENT OF INERTIA OF VESSEL ABOUT LCG IN METRES **4 11927.
POSITION OF VESSELS CENTRE OF GRAVITY IN METRES FORWARD OF AMMIDSHIPS 0.0000

EFFECTIVE BLOCK COEFF FOR THIS VESSEL = 0.64

VALUE OF RUDDER AREA SELECTED IS 1.120M**2
DISTANCE RUDDERS AFT AMMIDSHIPS 18.500

RUDDER HEIGHT IN METRES 1.850
GEOMETRIC ASPECT RATIO OF RUDDER(S) 3.056
TAYLOR WAKE FRACTION 0.185
FLOW ACCELERATION DUE TO PROP 1.800
FRACTION OF RUDDER SUBJECT TO ACCELERATED FLOW 0.750
BASIC LIFT CURVE SLOPE COEFFICIENT 1.301
MIRROR IMAGING FACTOR 1.000
MODIFIED LIFT CURVE SLOPE COEFFICIENT 1.301
VELOCITY RATIO COEFFICIENT 1.864
CLARKES PROPULSIVE COEFFICIENT 2.425

RUDDER DERIVATIVES ARE
YD_ = 0.00198405
ND_ = -0.00099203

CLARKES METHOD SELECTED
MANOEUVRING DERIVATIVES

YV_ = -0.020269
YR_ = 0.007739
NV_ = -0.010997
NR_ = -0.004310
Y_V_ = -0.017694
Y_R_ = -0.000535
N_V_ = -0.000450
N_R_ = -0.001243
K_= -0.435781
T_= 0.774360

NORBINS P NO = 0.281

DESIGN STABLE

RUDDER AREA = 1.120 M**2 NORBINS P NO = .281

ARE THESE VALUES SATISFACTORY ?
Y

RUDDER ANGLE (DEG)	RADIUS OF TURN (M)
1	4207.304
2	2103.652
3	1402.435
4	1051.826
5	841.461
6	701.217
7	601.043
8	525.913
9	467.478
10	420.730
11	382.482
12	350.609
13	323.639
14	300.522
15	280.487
16	262.957
17	247.488
18	233.739
19	221.437
20	210.365
21	200.348
22	191.241
23	182.926
24	175.304
25	168.292
26	161.819
27	155.826
28	150.261
29	145.079
30	140.243
31	135.719
32	131.478
33	127.494
34	123.744
35	120.209

END OF RUN - PROGRAM STOP
VMS3 $

S.S.P. KAIMALINO

VESSEL LENGTH IN METRES 26.410
HULL LENGTH IN METRES 24.380
STRUT LENGTH IN METRES 14.170
HULL CENTRELINE SPACING IN METRES 12.190
LOAD DRAUGHT IN METRES 4.660
MAX HULL DIAMETER IN METRES 1.970
MAX STRUT WIDTH IN METRES 1.000
LOAD DISPLACEMENT IN TONNES 193.
WATER DENSITY IN TONNES/M**31.025
MASS MOMENT OF INERTIA OF VESSEL ABOUT LCG IN METRES **4 6515.
POSITION OF VESSELS CENTRE OF GRAVITY IN METRES FORWARD OF AMMIDSHIPS 1.6600

EFFECTIVE BLOCK COEFF FOR THIS VESSEL = 0.71

VALUE OF RUDDER AREA SELECTED IS 3.890M**2

RUDDER HEIGHT IN METRES 4.420
GEOMETRIC ASPECT RATIO OF RUDDER(S) 5.022
TAYLOR WAKE FRACTION 0.185
FLOW ACCELERATION DUE TO PROP 1.800
FRACTION OF RUDDER SUBJECT TO ACCELERATED FLOW 0.400
BASIC LIFT CURVE SLOPE COEFFICIENT 1.301
MIRROR IMAGING FACTOR 1.000
MODIFIED LIFT CURVE SLOPE COEFFICIENT 1.301
VELOCITY RATIO COEFFICIENT 1.461
CLARKES PROPULSIVE COEFFICIENT 1.901

RUDDER DERIVATIVES ARE
YD_ = 0.01059965
ND_ = -0.00529982

CLARKES METHOD SELECTED
MANOEUVRING DERIVATIVES

YV_ = -0.112722
YR_ = 0.037752
NV_ = -0.088736
NR_ = -0.022774
Y_V_ = -0.099728
Y_R_ = -0.004831
N_V_ = -0.006330
N_R_ = -0.006239
K_= -0.374836
T_= 0.317976

NORBINS P NO = 0.589

RUDDER ANGLE (DEG)	RADIUS OF TURN (M)
1	3858.172
2	1929.086
3	1286.057
4	964.543
5	771.634
6	643.029

```
 7                          551.167
 8                          482.271
 9                          428.686
10                          385.817
11                          350.743
12                          321.514
13                          296.782
14                          275.584
15                          257.211
16                          241.136
17                          226.951
18                          214.343
19                          203.062
20                          192.909
21                          183.722
22                          175.371
23                          167.747
24                          160.757
25                          154.327
26                          148.391
27                          142.895
28                          137.792
29                          133.040
30                          128.606
31                          124.457
32                          120.568
33                          116.914
34                          113.476
35                          110.233
ITERATION NO -  1

VALUE OF RUDDER AREA SELECTED IS  3.696M**2

RUDDER HEIGHT IN METRES  4.420
GEOMETRIC ASPECT RATIO OF RUDDER(S)  5.287
TAYLOR WAKE FRACTION 0.185
FLOW ACCELERATION DUE TO PROP 1.800
FRACTION OF RUDDER SUBJECT TO ACCELERATED FLOW 0.400
BASIC LIFT CURVE SLOPE COEFFICIENT  1.301
MIRROR IMAGING FACTOR 1.000
MODIFIED LIFT CURVE SLOPE COEFFICIENT  1.301
VELOCITY RATIO COEFFICIENT  1.461
CLARKES PROPULSIVE COEFFICIENT  1.901

RUDDER DERIVATIVES ARE
YD_ =  0.01006967
ND_ = -0.00503483

CLARKES METHOD SELECTED
MANOEUVRING DERIVATIVES

YV_ = -0.112563
YR_ =  0.037673
NV_ = -0.088815
NR_ = -0.022735
Y_V_ = -0.099728
Y_R_ = -0.004831
```

N_V_ = -0.006330
N_R_ = -0.006239
K_= -0.357295
T_= 0.318881

NORBINS P NO = 0.560

RUDDER ANGLE (DEG)	RADIUS OF TURN (M)
1	4047.864
2	2023.932
3	1349.288
4	1011.966
5	809.573
6	674.644
7	578.266
8	505.983
9	449.763
10	404.786
11	367.988
12	337.322
13	311.374
14	289.133
15	269.858
16	252.991
17	238.110
18	224.881
19	213.045
20	202.393
21	192.755
22	183.994
23	175.994
24	168.661
25	161.915
26	155.687
27	149.921
28	144.567
29	139.582
30	134.929
31	130.576
32	126.496
33	122.663
34	119.055
35	115.653

VMS3 $

M.V. HALCYON

VESSEL LENGTH IN METRES 18.290
HULL LENGTH IN METRES 16.130
STRUT LENGTH IN METRES 16.780
HULL CENTRELINE SPACING IN METRES 7.470
LOAD DRAUGHT IN METRES 2.130
MAX HULL DIAMETER IN METRES 1.524
MAX STRUT WIDTH IN METRES 0.750
LOAD DISPLACEMENT IN TONNES 50.
WATER DENSITY IN TONNES/M**31.025
MASS MOMENT OF INERTIA OF VESSEL ABOUT LCG IN METRES **4 810.
POSITION OF VESSELS CENTRE OF GRAVITY IN METRES FORWARD OF AMMIDSHIPS 0.0000

EFFECTIVE BLOCK COEFF FOR THIS VESSEL = 0.54

VALUE OF RUDDER AREA SELECTED IS 0.840M**2

RUDDER HEIGHT IN METRES 1.200
GEOMETRIC ASPECT RATIO OF RUDDER(S) 1.714
TAYLOR WAKE FRACTION 0.185
FLOW ACCELERATION DUE TO PROP 1.800
FRACTION OF RUDDER SUBJECT TO ACCELERATED FLOW 0.750
BASIC LIFT CURVE SLOPE COEFFICIENT 1.301
MIRROR IMAGING FACTOR 1.000
MODIFIED LIFT CURVE SLOPE COEFFICIENT 1.301
VELOCITY RATIO COEFFICIENT 1.864
CLARKES PROPULSIVE COEFFICIENT 2.425

RUDDER DERIVATIVES ARE
YD_ = 0.00608962
ND_ = -0.00304481

CLARKES METHOD SELECTED
MANOEUVRING DERIVATIVES

YV_ = -0.051030
YR_ = 0.016845
NV_ = -0.032299
NR_ = -0.010309
Y_V_ = -0.043737
Y_R_ = -0.002307
N_V_ = -0.002655
N_R_ = -0.002658
K_= -0.634173
T_= 0.731586

NORBINS P NO = 0.433

RUDDER ANGLE (DEG)	RADIUS OF TURN (M)
1	1457.300
2	728.650
3	485.767
4	364.325
5	291.460

```
 6                          242.883
 7                          208.186
 8                          182.163
 9                          161.922
10                          145.730
11                          132.482
12                          121.442
13                          112.100
14                          104.093
15                           97.153
16                           91.081
17                           85.724
18                           80.961
19                           76.700
20                           72.865
21                           69.395
22                           66.241
23                           63.361
24                           60.721
25                           58.292
26                           56.050
27                           53.974
28                           52.046
29                           50.252
30                           48.577
31                           47.010
32                           45.541
33                           44.161
34                           42.862
35                           41.637

DESIGN STABLE

RUDDER AREA =    0.840 M**2  NORBINS P NO = .433

ARE THESE VALUES SATISFACTORY ?
Y

END OF RUN - PROGRAM STOP
 VMS3 $
```

S.S.C. MARINE ACE

VESSEL LENGTH IN METRES 12.340
HULL LENGTH IN METRES 10.470
STRUT LENGTH IN METRES 7.310
HULL CENTRELINE SPACING IN METRES 5.300
LOAD DRAUGHT IN METRES 1.550
MAX HULL DIAMETER IN METRES 1.240
MAX STRUT WIDTH IN METRES 0.570
LOAD DISPLACEMENT IN TONNES 18.
WATER DENSITY IN TONNES/M**31.025
MASS MOMENT OF INERTIA OF VESSEL ABOUT LCG IN METRES **4 136.
POSITION OF VESSELS CENTRE OF GRAVITY IN METRES FORWARD OF AMMIDSHIPS 0.0000

EFFECTIVE BLOCK COEFF FOR THIS VESSEL = 0.52

VALUE OF RUDDER AREA SELECTED IS 0.340M**2

RUDDER HEIGHT IN METRES 1.240
GEOMETRIC ASPECT RATIO OF RUDDER(S) 4.522
TAYLOR WAKE FRACTION 0.185
FLOW ACCELERATION DUE TO PROP 1.800
FRACTION OF RUDDER SUBJECT TO ACCELERATED FLOW 0.750
BASIC LIFT CURVE SLOPE COEFFICIENT 1.301
MIRROR IMAGING FACTOR 1.000
MODIFIED LIFT CURVE SLOPE COEFFICIENT 1.301
VELOCITY RATIO COEFFICIENT 1.864
CLARKES PROPULSIVE COEFFICIENT 2.425

RUDDER DERIVATIVES ARE
YD_ = 0.00541486
ND_ = -0.00270743

CLARKES METHOD SELECTED
MANOEUVRING DERIVATIVES

YV_ = -0.059377
YR_ = 0.017810
NV_ = -0.038913
NR_ = -0.011555
Y_V_ = -0.050288
Y_R_ = -0.003232
N_V_ = -0.003853
N_R_ = -0.002833
K_= -0.584395
T_= 0.844818

NORBINS P NO = 0.346

DESIGN STABLE

RUDDER AREA = 0.340 M**2 NORBINS P NO = .346

ARE THESE VALUES SATISFACTORY ?
Y

RUDDER ANGLE (DEG)	RADIUS OF TURN (M)
1	1026.509
2	513.254
3	342.170
4	256.627
5	205.302
6	171.085
7	146.644
8	128.314
9	114.057
10	102.651
11	93.319
12	85.542
13	78.962
14	73.322
15	68.434
16	64.157
17	60.383
18	57.028
19	54.027
20	51.325
21	48.881
22	46.659
23	44.631
24	42.771
25	41.060
26	39.481
27	38.019
28	36.661
29	35.397
30	34.217
31	33.113
32	32.078
33	31.106
34	30.191
35	29.329

END OF RUN - PROGRAM STOP
VMS3 $

S.S.C. OHTORI

VESSEL LENGTH IN METRES 27.000
HULL LENGTH IN METRES 24.000
STRUT LENGTH IN METRES 24.000
HULL CENTRELINE SPACING IN METRES 8.000
LOAD DRAUGHT IN METRES 3.400
MAX HULL DIAMETER IN METRES 2.300
MAX STRUT WIDTH IN METRES 0.600
LOAD DISPLACEMENT IN TONNES 239.
WATER DENSITY IN TONNES/M**31.025
MASS MOMENT OF INERTIA OF VESSEL ABOUT LCG IN METRES **4 8433.
POSITION OF VESSELS CENTRE OF GRAVITY IN METRES FORWARD OF AMMIDSHIPS 0.0000

EFFECTIVE BLOCK COEFF FOR THIS VESSEL = 0.82

VALUE OF RUDDER AREA SELECTED IS 1.380M**2

RUDDER HEIGHT IN METRES 2.300
GEOMETRIC ASPECT RATIO OF RUDDER(S) 3.833
TAYLOR WAKE FRACTION 0.185
FLOW ACCELERATION DUE TO PROP 1.800
FRACTION OF RUDDER SUBJECT TO ACCELERATED FLOW 0.750
BASIC LIFT CURVE SLOPE COEFFICIENT 1.301
MIRROR IMAGING FACTOR 1.000
MODIFIED LIFT CURVE SLOPE COEFFICIENT 1.301
VELOCITY RATIO COEFFICIENT 1.864
CLARKES PROPULSIVE COEFFICIENT 2.425

RUDDER DERIVATIVES ARE
YD_ = 0.00459082
ND_ = -0.00229541

CLARKES METHOD SELECTED
MANOEUVRING DERIVATIVES

YV_ = -0.062200
YR_ = 0.018957
NV_ = -0.039276
NR_ = -0.011736
Y_V_ = -0.052376
Y_R_ = -0.002768
N_V_ = -0.003286
N_R_ = -0.003217
K_= -0.593880
T_= 1.324413

NORBINS P NO = 0.224

DESIGN STABLE

RUDDER AREA = 1.380 M**2 NORBINS P NO = .224

ARE THESE VALUES SATISFACTORY ?
Y

RUDDER ANGLE (DEG)	RADIUS OF TURN (M)
1	2315.448
2	1157.724
3	771.816
4	578.862
5	463.090
6	385.908
7	330.778
8	289.431
9	257.272
10	231.545
11	210.495
12	192.954
13	178.111
14	165.389
15	154.363
16	144.716
17	136.203
18	128.636
19	121.866
20	115.772
21	110.259
22	105.248
23	100.672
24	96.477
25	92.618
26	89.056
27	85.757
28	82.695
29	79.843
30	77.182
31	74.692
32	72.358
33	70.165
34	68.101
35	66.156

END OF RUN - PROGRAM STOP
VMS3 $

S.S.C. SEAGULL

VESSEL LENGTH IN METRES 35.900
HULL LENGTH IN METRES 31.500
STRUT LENGTH IN METRES 32.140
HULL CENTRELINE SPACING IN METRES 13.500
LOAD DRAUGHT IN METRES 3.150
MAX HULL DIAMETER IN METRES 2.950
MAX STRUT WIDTH IN METRES 1.250
LOAD DISPLACEMENT IN TONNES 343.
WATER DENSITY IN TONNES/M**31.025
MASS MOMENT OF INERTIA OF VESSEL ABOUT LCG IN METRES **4 21396.
POSITION OF VESSELS CENTRE OF GRAVITY IN METRES FORWARD OF AMMIDSHIPS 0.0000

EFFECTIVE BLOCK COEFF FOR THIS VESSEL = 0.59

VALUE OF RUDDER AREA SELECTED IS 1.260M**2

RUDDER HEIGHT IN METRES 2.000
GEOMETRIC ASPECT RATIO OF RUDDER(S) 3.175
TAYLOR WAKE FRACTION 0.185
FLOW ACCELERATION DUE TO PROP 1.800
FRACTION OF RUDDER SUBJECT TO ACCELERATED FLOW 0.750
BASIC LIFT CURVE SLOPE COEFFICIENT 1.301
MIRROR IMAGING FACTOR 1.000
MODIFIED LIFT CURVE SLOPE COEFFICIENT 1.301
VELOCITY RATIO COEFFICIENT 1.864
CLARKES PROPULSIVE COEFFICIENT 2.425

RUDDER DERIVATIVES ARE
YD_ = 0.00237094
ND_ = -0.00118547

CLARKES METHOD SELECTED
MANOEUVRING DERIVATIVES

YV_ = -0.030271
YR_ = 0.009889
NV_ = -0.016831
NR_ = -0.005995
Y_V_ = -0.025503
Y_R_ = -0.001262
N_V_ = -0.001258
N_R_ = -0.001587
K_= -0.725619
T_= 2.033995

NORBINS P NO = 0.178

DESIGN STABLE

RUDDER AREA = 1.260 M**2 NORBINS P NO = .178

ARE THESE VALUES SATISFACTORY ?
Y

RUDDER ANGLE (DEG)	RADIUS OF TURN (M)
1	2487.281
2	1243.640
3	829.093
4	621.820
5	497.456
6	414.547
7	355.326
8	310.910
9	276.364
10	248.728
11	226.116
12	207.273
13	191.329
14	177.663
15	165.819
16	155.455
17	146.311
18	138.182
19	130.910
20	124.364
21	118.442
22	113.058
23	108.143
24	103.637
25	99.491
26	95.665
27	92.121
28	88.831
29	85.768
30	82.909
31	80.235
32	77.728
33	75.372
34	73.155
35	71.065

```
END OF RUN - PROGRAM STOP
 VMS3 $
```

S.S.C. SEAGULL - LCG @ 2.0 M FWD AMMIDSHIPS

```
 VESSEL LENGTH IN METRES  35.900
 HULL LENGTH IN METRES  31.500
 STRUT LENGTH IN METRES  32.140
 HULL CENTRELINE SPACING IN METRES 13.500
 LOAD DRAUGHT IN METRES 3.150
 MAX HULL DIAMETER IN METRES 2.950
 MAX STRUT WIDTH IN METRES 1.250
 LOAD DISPLACEMENT IN TONNES  343.
 WATER DENSITY IN TONNES/M**31.025
 MASS MOMENT OF INERTIA OF VESSEL ABOUT LCG IN METRES **4      21396.
 POSITION OF VESSELS CENTRE OF GRAVITY IN METRES FORWARD OF AMMIDSHIPS 2.0000

EFFECTIVE BLOCK COEFF FOR THIS VESSEL = 0.59

VALUE OF RUDDER AREA SELECTED IS  1.260M**2

RUDDER HEIGHT IN METRES  2.950
GEOMETRIC ASPECT RATIO OF RUDDER(S)  6.907
TAYLOR WAKE FRACTION 0.185
FLOW ACCELERATION DUE TO PROP 1.800
FRACTION OF RUDDER SUBJECT TO ACCELERATED FLOW 0.750
BASIC LIFT CURVE SLOPE COEFFICIENT  1.301
MIRROR IMAGING FACTOR 1.000
MODIFIED LIFT CURVE SLOPE COEFFICIENT  1.301
VELOCITY RATIO COEFFICIENT  1.864
CLARKES PROPULSIVE COEFFICIENT  2.425

RUDDER DERIVATIVES ARE
YD_ =  0.00237094
ND_ = -0.00118547

CLARKES METHOD SELECTED
MANOEUVRING DERIVATIVES

YV_ = -0.030271
YR_ =  0.009889
NV_ = -0.016831
NR_ = -0.005995
Y_V_ = -0.025503
Y_R_ = -0.001262
N_V_ = -0.001258
N_R_ = -0.001587
K_=  -0.725619
T_=   1.639184

NORBINS P NO =  0.221

DESIGN STABLE

RUDDER AREA =   1.260 M**2  NORBINS P NO = .221

ARE THESE VALUES SATISFACTORY ?
Y
```

RUDDER ANGLE (DEG)	RADIUS OF TURN (M)
1	3068.169
2	1534.085
3	1022.723
4	767.042
5	613.634
6	511.362
7	438.310
8	383.521
9	340.908
10	306.817
11	278.924
12	255.681
13	236.013
14	219.155
15	204.545
16	191.761
17	180.481
18	170.454
19	161.483
20	153.408
21	146.103
22	139.462
23	133.399
24	127.840
25	122.727
26	118.007
27	113.636
28	109.577
29	105.799
30	102.272
31	98.973
32	95.880
33	92.975
34	90.240
35	87.662

END OF RUN - PROGRAM STOP
VMS3 $

Appendix C Prediction of Extreme Value Loading Using Short Term Spectral Analysis

It is clearly desirable to predict the likely maximum value of loading to which a vessel may be subject during its lifetime. This extreme value must be determined by considering all sea condition, ship speed and heading combinations which may be encountered during that lifetime, together with the frequency of occurrence of each of these combinations.
N.B. Here sea condition is defined in terms of sea severity and spectral shape

Consideration of the foregoing implies that extreme value predictions may only be made utilizing a long term prediction method such as that described in section 5.3.3. However it has been discovered that predictions of extreme values by short term methods agree well with those evaluated using long term techniques.

The short term evaluation procedure is greatly simplified over long term approaches. Since numerical comparison of both techniques indicate that short term prediction in severe seas is much to be preferred, a short term approach was therefore adopted for this study.

Response amplitude operators obtained both experimentally and theoretically were combined with the 2 parameter Pierson Moskowitz sea spectra to obtain loading response spectra. Short term extreme value predictions were then made from these loading spectra.

The Pierson Moskowitz spectral density function is defined:-

$$S(\omega) = \frac{\alpha g^2}{\omega^5} \exp\left[-\beta(g / U\omega)^4\right]$$

(Eqn C1)

Where:-

$\alpha = 0.0081$

$\beta = 0.74$

U = Wind Speed ms^{-1} @ 19.5m above free surface

$g = 9.81 \quad ms^{-2}$

The response spectrum for the vessel operating in the sea condition defined by the above spectrum is then :-

$$RS = S(\omega) * (RAO)^2$$

(Eqn C2)

Where:-

RAO = Response Amplitude Operator = (Response / Wave Amplitude)

Assuming this spectrum to be defined by a Rayleigh distribution and applying probability theory gives the "most probable extreme" value in N waves to be :-

$$\text{Max Value} = \sqrt{(2m_0 \ln N)}$$

(Eqn C3)

Statistically the probability of exceeding this value is $1 - e^{-1}$ (=0.632), where N is large. This equates to a 63% probability of exceedence. For design purposes a more conservative criterion is obviously required.

For this purpose we define the "design extreme value" as the value that will be exceeded in N occurrences with the probability of only one percent.

$$\text{Design Extreme Value} = \sqrt{[2m_0 \ln(N/\alpha)]}$$

(Eqn C4)

Where:-

m_0 = Area under the distribution function

α = A risk parameter –

0.01 gives a 99% Survival Rate

$$N = \frac{3600T^*}{T_Z} = \frac{3600T^*}{2\pi}\sqrt{\frac{m_2}{m_0}}$$

T_Z = Upcross wave period Rad / sec

T^* = Duration of storm conditions hours

m_2 = Second moment of spectrum

For a response spectrum derived using the Pierson Moskowitz sea spectrum the ratio of second moment to area may be assumed:-

$$\sqrt{\frac{m_2}{m_0}} = 0.4$$

Tables C1-C5 illustrate the application of the technique in spreadsheet form. Short term extreme values are calculated for the T-AGOS 19 and the M.V. Patria using RAO values derived both experimentally and analytically.

N.B. The Pierson Moskowitz spectrum is applicable to a fully developed North Atlantic Sea State. The severe design condition resulting from short term analysis may therefore be taken as conservative.

Precise evaluation of maximum lifetime loading values by this method is not possible since the fully developed sea condition defined by the above spectrum exists only for relatively short periods of time. Similarly the effects of weather and service routing are not properly taken into consideration by the above method. Values produced by the above analysis may however be considered adequate for design purposes.

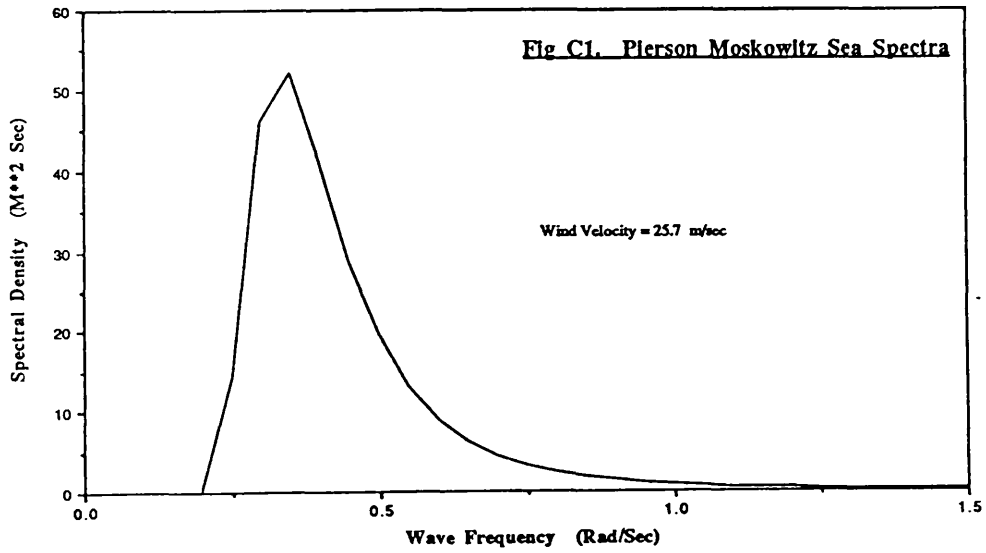

RAO Data Source:- Model Tests (Ref 51)

Wave Spectral Parameters		Wave Frequency Rad/Sec	Spectral Density M**2 Sec	Side Force RAO Tonnes/m	SF Response	Simpsons Multipliers	SM*SF Response
		0.20	0.133	124	2038.434	0.5	1019.217
alpha	0.0081	0.25	14.305	103	151765.480	2	303530.961
beta	0.74	0.30	46.121	119	653124.020	1	653124.020
Wind Velocity	25.7 m/s	0.35	52.098	134	935474.032	2	1870948.064
gravitational acceleration	9.81 m/s	0.40	41.211	117	564132.424	1	564132.424
number of waves	1400	0.45	28.799	78	175213.052	2	350426.104
(in a 6 hour storm)		0.50	19.400	69	92364.943	1	92364.943
		0.55	13.045	87	98738.742	2	197477.485
		0.60	8.880	141	176546.990	1	176546.990
		0.65	6.152	227	317019.958	2	634039.916
		0.70	4.344	331	475962.272	1	475962.272
		0.75	3.126	448	627349.390	2	1254698.780
		0.80	2.289	565	730824.142	1	730824.142
		0.85	1.705	470	376577.070	2	753154.140
		0.90	1.289	350	157887.455	1	157887.455
		0.95	0.988	310	94962.436	2	189924.872
		1.00	0.767	270	55940.689	1	55940.689
		1.05	0.603	232	32451.847	2	64903.693
		1.10	0.479	213	21724.950	1	21724.950
		1.15	0.384	195	14605.019	2	29210.038
		1.20	0.311	176	9630.567	1	9630.567
		1.25	0.254	158	6335.670	2	12671.340
		1.30	0.209	147	4511.824	1	4511.824
		1.35	0.173	139	3342.948	2	6685.897
		1.40	0.144	130	2439.459	1	2439.459
		1.45	0.121	121	1774.232	2	3548.463
		1.50	0.102	112	1283.675	0.5	641.837
						Summation =	8617970.541
						Total Area, mo =	287265.685
						Most Prob Ext. Side Force=	2040
						Design Ext. Side Force=	2609

RAO Data Source:- MARCHS 3D Program

Wave Spectral Parameters		Wave Frequency Rad/Sec	Spectral Density M**2Sec	Side Force RAO Tonnes/m	SF Response	Simpsons Multipliers	SM*SF Response
		0.20	0.133	1.795	0.427	0.5	0.214
alpha	0.0081	0.25	14.305	4.458	284.364	2	568.728
beta	0.74	0.30	46.121	9.436	4106.813	1	4106.813
Wind Velocity	25.7 m/s	0.35	52.098	18.053	16979.748	2	33959.496
gravitational acceleration	9.81 m/s	0.40	41.211	32.037	42296.411	1	42296.411
number of waves	1400	0.45	28.799	54.166	84495.282	2	168990.563
(in a 6 hour storm)		0.50	19.400	89.178	154284.337	1	154284.337
		0.55	13.045	147.552	284015.344	2	568030.689
		0.60	8.880	106.682	101065.637	1	101065.637
		0.65	6.152	380.878	892495.389	2	1784990.778
		0.70	4.344	775.994	2615975.386	1	2615975.386
		0.75	3.126	1663.136	8645876.563	2	17291753.125
		0.80	2.289	1146.494	3009257.161	1	3009257.161
		0.85	1.705	679.575	787287.038	2	1574574.076
		0.90	1.289	460.542	273369.141	1	273369.141
		0.95	0.988	395.454	154532.869	2	309065.738
		1.00	0.767	328.449	82782.240	1	82782.240
		1.05	0.603	307.560	57032.470	2	114064.940
		1.10	0.479	416.267	82974.413	1	82974.413
		1.15	0.384	401.717	61983.229	2	123966.457
		1.20	0.311	344.282	36851.524	1	36851.524
		1.25	0.254	292.694	21742.341	2	43484.682
		1.30	0.209	260.078	14122.878	1	14122.878
		1.35	0.173	241.823	10118.020	2	20236.039
		1.40	0.144	256.279	9480.541	1	9480.541
		1.45	0.121	260.573	8228.104	2	16456.208
		1.50	0.102	235.230	5662.457	0.5	2831.228
						Summation =	28479539.445
						Total Area, mo =	949317.981
						Most Prob Ext. Side Force=	3709
						Design Ext. Side Force=	4743

Tables C1 and C2. Short Term Extreme Value Predictions of Side Force for T-AGOS 19.

RAO Data Source:- Approximate Calculation

Wave Spectral Parameters		Wave Frequency Rad/Sec	Spectral density M**2Sec	Side Force RAO Tonnes/m	SF Response	Simpsons Multipliers	SM*SF Response
		0.20	0.133	41.491	228.220	0.5	114.110
alpha	0.0081	0.25	14.305	64.486	59487.630	2	118975.260
beta	0.74	0.30	46.121	92.261	392588.938	1	392588.938
Wind Velocity	25.7 m/s	0.35	52.098	124.625	809162.091	2	1618324.182
gravitational acceleration	9.81 m/s	0.40	41.211	161.360	1073002.933	1	1073002.933
number of waves	1400	0.45	28.799	202.220	1177675.424	2	2355350.847
(in a 6 hour storm)		0.50	19.400	246.939	1183009.123	1	1183009.123
		0.55	13.045	295.231	1137034.071	2	2274068.142
		0.60	8.880	346.796	1067998.226	1	1067998.226
		0.65	6.152	401.322	990877.749	2	1981755.499
		0.70	4.344	458.488	913213.301	1	913213.301
		0.75	3.126	517.971	838617.154	2	1677234.308
		0.80	2.289	579.445	768671.523	1	768671.523
		0.85	1.705	642.590	703923.653	2	1407847.306
		0.90	1.289	707.088	644403.509	1	644403.509
		0.95	0.988	772.631	589893.015	2	1179786.030
		1.00	0.767	838.925	540065.879	1	540065.879
		1.05	0.603	905.686	494559.588	2	989119.176
		1.10	0.479	972.646	453011.620	1	453011.620
		1.15	0.384	1039.556	415076.734	2	830153.469
		1.20	0.311	1106.182	380434.300	1	380434.300
		1.25	0.254	1172.312	348790.464	2	697580.927
		1.30	0.209	1237.751	319877.732	1	319877.732
		1.35	0.173	1302.325	293453.353	2	586906.705
		1.40	0.144	1365.880	269297.235	1	269297.235
		1.45	0.121	1428.279	247209.778	2	494419.555
		1.50	0.102	1489.405	227009.802	0.5	113504.901
						Summation =	24330714.734
						Total Area, mo =	811023.824
						Most Prob Ext Side Forces	3428
						Design Ext. Side Forces	4384

Table C3. Short Term Extreme Value Prediction of Side Force for T-AGOS 19.

RAO Data Source:- MARCHS 3D Program

Wave Spectral Parameters		Wave Frequency Rad/Sec	Spectral Density M**2 Sec	Side Force RAO Tonnes/m	SF Response	Simpsons Multipliers	SM*SF Response
		0.20	0.133	0.039	0.000	0.5	0.000
alpha	0.0081	0.25	14.305	0.095	0.129	2	0.258
beta	0.74	0.30	46.121	0.197	1.797	1	1.797
Wind Velocity	25.7 m/s	0.35	52.098	0.367	7.024	2	14.047
gravitational acceleration	9.81 m/s	0.40	41.211	0.630	16.331	1	16.331
number of waves	1400	0.45	28.799	1.015	29.643	2	59.287
(in a 6 hour storm)		0.50	19.400	1.558	47.081	1	47.081
		0.55	13.045	2.301	69.079	2	138.157
		0.60	8.880	3.294	96.366	1	96.366
		0.65	6.152	4.597	129.988	2	259.976
		0.70	4.344	6.282	171.426	1	171.426
		0.75	3.126	8.446	223.001	2	446.002
		0.80	2.289	11.093	281.707	1	281.707
		0.85	1.705	14.600	363.399	2	726.798
		0.90	1.289	19.046	467.525	1	467.525
		0.95	0.988	24.732	604.421	2	1208.842
		1.00	0.767	32.101	790.733	1	790.733
		1.05	0.603	41.786	1052.753	2	2105.506
		1.10	0.479	54.675	1431.453	1	1431.453
		1.15	0.384	71.809	1980.584	2	3961.168
		1.20	0.311	93.542	2720.430	1	2720.430
		1.25	0.254	116.7941745	3461.950	2	6923.899
		1.30	0.209	132.0474587	3640.638	1	3640.638
		1.35	0.173	132.4932701	3037.300	2	6074.600
		1.40	0.144	129.8561965	2434.065	1	2434.065
		1.45	0.121	73.22326919	649.737	2	1299.475
		1.50	0.102	77.43092846	613.547	0.5	306.774
						Summation =	35624.342
						Total Area, mo =	1187.478
						Most Prob Ext. Side Force=	131 Tonnes
						Design Ext. Side Force=	168 Tonnes

RAO Data Source:- Approximate Calculation

Wave Spectral Parameters		Wave Frequency Rad/Sec	Spectral Density M**2Sec	Side Force RAO Tonnes/m	SF Response	Simpsons Multipliers	SM*SF Response
		0.20	0.133	3.611	1.729	0.5	0.864
alpha	0.0081	0.25	14.305	5.633	453.950	2	907.899
beta	0.74	0.30	46.121	8.096	3023.047	1	3023.047
Wind Velocity	25.7 m/s	0.35	52.098	10.994	6297.335	2	12594.671
gravitational acceleration	9.81 m/s	0.40	41.211	14.322	8453.042	1	8453.042
number of waves	1400	0.45	28.799	18.072	9405.691	2	18811.383
(in a 6 hour storm)		0.50	19.400	22.237	9592.956	1	9592.956
		0.55	13.045	26.808	9374.879	2	18749.758
		0.60	8.880	31.775	8966.026	1	8966.026
		0.65	6.152	37.130	8481.553	2	16963.105
		0.70	4.344	42.860	7980.309	1	7980.309
		0.75	3.126	48.955	7491.108	2	14982.216
		0.80	2.289	55.403	7027.094	1	7027.094
		0.85	1.705	62.190	6593.330	2	13186.660
		0.90	1.289	69.305	6190.789	1	6190.789
		0.95	0.988	76.734	5818.442	2	11636.884
		1.00	0.767	84.463	5474.357	1	5474.357
		1.05	0.603	92.478	5156.276	2	10312.551
		1.10	0.479	100.763	4861.900	1	4861.900
		1.15	0.384	109.306	4589.042	2	9178.085
		1.20	0.311	118.091	4335.684	1	4335.684
		1.25	0.254	127.102	4099.997	2	8199.994
		1.30	0.209	136.325	3880.344	1	3880.344
		1.35	0.173	145.745	3675.268	2	7350.535
		1.40	0.144	155.347	3483.470	1	3483.470
		1.45	0.121	165.115	3303.801	2	6607.602
		1.50	0.102	175.035	3135.237	0.5	1567.619
						Summation =	224318.844
						Total Area, mo =	7477.295
						Most Prob Ext. Side Force=	329 Tonnes
						Design Ext. Side Force=	421 Tonnes

Tables C4 and C5. Short Term Extreme Value Predictions of Side Force for the M.V. Patria.

Appendix D Lloyds and DnV Service Restrictions

Lloyd's Register Provisional Rules for High Speed Catamarans

Craft built and classed in accordance with the rules will be assigned an operational envelope. This will be based on the design speeds, waveheights and displacements dependent on the criteria used to determine the loadings.

Lloyd's Service Group factors are given in Table D1.

These describe the service for which the craft has been approved and constructed. They will affect the scantlings of the craft, through the loads applied to it, and the equipment carried onboard.

The value of Significant Wave Height Hw used in the determination of accelerations and loads is, in general not to be less than K min for the appropriate group, and need not be taken as greater than K max for that group.

The service group notations are based on operation of the craft within its operational envelope in reasonable weather. Where conditions deteriorate beyond these limits the vessel is to be operated at reduced speed and is to seek shelter.

Reasonable weather is defined as winds less than Force 6, together with:-

1. Sea states within the operational envelope which result in green water being taken on board infrequently or not at all.
2. Motions which do not impair the efficient operation of the craft and do not significantly reduce passenger comfort or safety or impose any undue loads on vehicles carried.

Service Group 1 Covers craft intended for service in sheltered waters adjacent to sandbanks, reefs, breakwaters,or other coastal features and in similarly sheltered waters between islands where the range to refuge is in general 5 nautical miles or less. The geographical limits of the intended service are to be specified.

Service Group 2 Covers craft intended for service in waters where the range to refuge is 20 nm or less. This group usually covers craft intended for service in coastal waters.The geographical limits of the intended service are to be specified.

Service Group 3 Covers craft intended for service in waters where the range to refuge is 150 nm or less. The geographical limits of the intended service are to be specified.

Service Group 4 Covers craft intended for unrestricted sea-going service.

DnV Rules for Classification of High Speed Light Craft 1985

Craft built and classed in accordance with these rules are assigned a service restriction, in terms of the maximum distance at which they may operate in nautical miles from the nearest harbour or safe anchorage. The maximum service restriction notation is R280 nm.

The service restriction notation affects:-

1. Design pressure on the vessels sides above the waterline, superstructures and deckhouses, windows and deadlights.
2. Design hull girder loads for catamarans.
3. Anchoring and mooring equipment.

Further service restrictions are placed on the craft in terms of allowable speed / wave height or limits on vertical acceleration of the vessel. Such restrictions are stated in the 'Appendix to the Classification Certificate'.

Table D2 Relates Service Restriction to Load Factor.

DnV Rules for Classification of High Speed Light Craft 1991

The service restriction definitions in the 1991 version of the rules are essentially similar to the 1985 version.

It is interesting to note that the 1991 rules include more precise definitions of these operability limits than the previous (1985) rules. This presumably reflects a greater awareness on the part of DnV of the increasing range of applications and "rough water" roles now envisaged for catamarans and SWATH's.

Table D3 Defines the Service Restriction applicable and,
Table D4 Relates Service Restriction to Load Factor.

Service Group	K min	K max
1	0.6	1
2	1	2
3	2	4
4	4	See Note
NOTE		
Where the craft is intended for unrestricted service, the value of K max will be specially considered.		

Table D1. Lloyds Service Group Factors.

(Table 3.1.1 from Rules)

Service Restriction	s	q
<= R15	8.0	6.0
<= R45	7.5	5.5
<= R90	6.5	5.0
<= R150	5.5	4.0
<= R280	4.0	3.0

Table D2. 1985 DnV Service Restriction / Load Factor.

(Table D1 page 11 of 1985 Rules)

Service Notations	Seasons		
	Winter	Summer	Tropical
R0	300	No Restriction	No Restriction
R1	100	300	300
R2	50	100	250
R3	20	50	100
R4	Encl. fjords, rivers,lakes.	20	50

Table D3. 1991 DnV Service Restriction Definitions.

(Table B1 page 4, 1991 Rules)

Service Restriction	s	q
R4	8.0	6.0
R3	7.5	5.5
R2	6.5	5.0
R1	5.5	4.0
R0	4.0	3.0

Table D4. 1991 DnV Service Restriction / Load Factor.

(Table D1 page 11, 1991 Rules)

Appendix E An Approximation for Still Water Transverse Bending Moment

Idealising the structure as shown in Fig E1 and assuming that the weight of the box i.e. cross deck structure is approximately 40% of the total displacement. The weight of the hull and struts is therefore approximately 60% of the total displacement.

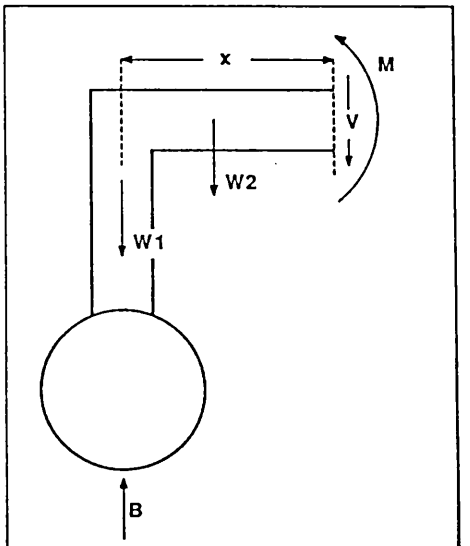

FIG E1. Forces acting on a SWATH in Still Water

For Equilibrium:-

$$M_B = Bx - W_1x - W_2\left(\frac{x}{2}\right)$$

$$= \left(\frac{\Delta}{2}\right)x - 0.6\left(\frac{\Delta}{2}\right)x - 0.4\left(\frac{\Delta}{2}\right)\left(\frac{x}{2}\right)$$

$$= \left(\frac{\Delta}{2}\right)x - \left(\frac{\Delta}{2}\right)0.6x - \left(\frac{\Delta}{2}\right)0.2x$$

$$= \left(\frac{\Delta}{2}\right)0.2x$$

(Eqn E1)

For M.V. Patria displacement is 180 Tonnes, and x=5m, the Still Water or Dead Load Transverse Bending Moment is therefore 90 Tm.

Appendix F Bending Moment Prediction using DnV'85 Rules

The following analysis is intended to illustrate the sensitivity of cross deck bending moment to service restrictions and vertical acceleration. It demonstrates that by careful selection of these parameters reasonable values of bending moment may be obtained using the 1985 formula, even though this formula was ostensibly developed for planing vessels.

The 1985 DnV rules state that,

Unless other values are justified by calculations according to accepted theories, model tests or full scale measurements, the vertical acceleration may be taken as :-

$$a_v = \frac{k_v g_0 V^{1.5}\left[\frac{H_s}{L}\right]}{1+0.04L}\left[1-\frac{1}{2.6\left(\frac{V}{\sqrt{L}}\right)}\right] \qquad \text{(Eqn F1)}$$

Where:-

a_v = Vertical Acceleration ms^{-2}

k_v = Longitudinal Distribution Factor (see Fig D1)

g_0 = Std Acceleration Gravity = $9.81 ms^{-2}$

H_s = Design Significant wave Height in metres

V and L are the crafts speed in knots and length in metres respectively

For the M.V. Patria operating at 30 knots in 4m significant wave heights, the acceleration at amidships according to the above formula is :-

$a_v = 40.98 ms^{-2}$

N.B. For the M.V. Patria operating at 30 knots in 4m significant wave heights corresponds to the limiting condition stated in the vessels classification certificate.
See Appendix D for details of Service Restrictions.

Applying the 1985 formula for transverse bending moment,
i.e. the 1991 formula given for planing craft:-

$$M_T = \frac{\Delta a_{cg} b}{s} \quad \text{kNm}$$

Where :-

a_v	Design Vertical Acceleration in m/s**2
b	Transverse Separation of Hull Longitudinal Centrelines in m
s	Factor 4-8 Depending on Service Restriction (see Appendix D)
q	Factor 3-6 Depending on Service Restriction (see Appendix D)
Δ	Fully Loaded Displacement in tonnes

Gives Transverse Bending Moment = 1003 Tm
for the M.V. Patria operating on a 43 nm crossing.
(i.e. s=7.5 from Table D2)

This value compares surprisingly favourably with estimates derived by more sophisticated formulae, and from those formulae derived specifically for fast displacement and SWATH vessels. It should however be noted that the agreement observed here is perhaps merely coincidental. Selection of s=4.0, (corresponding to the maximum 1985 limit of 280nm range from a safe haven), results in a moment value of 1880 Tm which is clearly over pessimistic.

It is perhaps more realistic to assume the vertical acceleration to be given by the 1991 rules formula:-

$$a_{cg} = k\frac{C_w}{L}\left(0.85 + 0.25\frac{V}{\sqrt{L}}\right)g_0 \quad \text{ms}^{-2}$$

Where:-

C_w = Wave Coefficient for HS Displacement Craft
= 0.08L for unrestricted service

k = 9 Aft of 0.2L from FP
= 15 Fwd of 0.2L from FP

Applying this formula to Patria gives a= 15.4 m/s**2.

Substituting this in to:-

$$M_T = \frac{\Delta a_{cg} b}{s} \quad \text{kNm}$$

Gives Transverse Bending Moment = 706 Tm for Patria operating up to 280 nm from port.

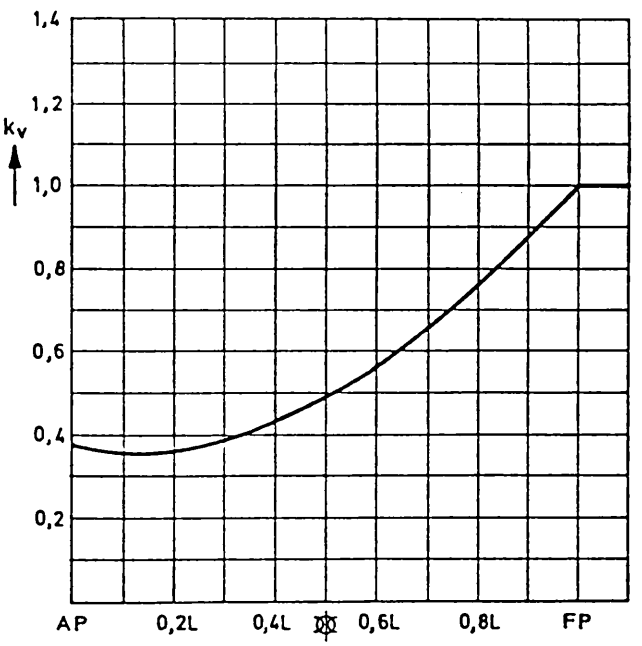

Fig F1

Appendix G. Simplified Direct Evaluation of Side Force

The wave forces acting on a SWATH vessel may be approximately evaluated using the following method. The hulls and struts are considered separately to determine the forces acting on each. These forces are then combined directly. Interference effects are assumed negligible and are neglected from this simplified analysis.

$$F_T = F_P + F_a$$

Where:-

F_P = Froude Krylov Force (dynamic water pressure force)

$= \rho \nabla a_x$

F_a = Diffraction Force (water particle acceleration force)

$= M_{AVM}\, a_x$

ρ = Water Density Tonne/m^3

∇ = Volume Displacement m^3

M_{AVM} = Added Virtual Mass Tonnes

$$a_x = 0.5\, H_w\, \omega^2 \int_{y=-d}^{y=0} e^{ky}\, dy$$

In order to simplify the problem the hulls are idealised as uniform circular cylinders with diameter equal to the maximum hull diameter.

Therefore for the hulls:-

$$F_T = 2\rho(0.5H_W)\omega^2 e^{-kd_0}\left[\frac{\pi D^2}{4}\right] L_H$$

For 'standard' struts of elliptical cross section:-

$$F_P = \rho\left(\frac{\pi Lt}{4}\right) 0.5\, H_w\, \omega^2 \int_{y=-d}^{y=0} e^{ky}\, dy$$

$$= \rho\left(\frac{\pi Lt}{4}\right) 0.5\, H_w \frac{\omega^2}{k}\left(1 - e^{-kd_1}\right)$$

$$F_s = \rho\pi\left(\frac{L}{2}\right)^2 0.5\, H_w\, \omega^2 \int_{y=-d}^{y=0} e^{ky}\, dy$$

$$= \rho\pi\left(\frac{L^2}{4}\right) 0.5\, H_w \frac{\omega^2}{k}\left(1 - e^{-kd_1}\right)$$

Where:-

H_w = Significant Wave Height m

ω = Wave Frequency Rad / Sec

L_H = Hull Length m

L_S = Strut Length m

D = Hull Diameter m

t = Strut Thickness m

d_0 = Hull Centreline Submergance m

d_1 = Depth Strut Submerged m

k = Wave No $= \omega^2 / g$

These formulae allow calculation of side force experienced by a vessel subject to regular waves with a specified significant wave height. The mechanics of the process are ideally suited to computer based spreadsheet packages. Tables G1 and G2 illustrate the spreadsheet calculation of wave induced side load on the T-AGOS 19 and the M.V. Patria.

To determine the maximum value of loading likely to be experienced by the vessel in a storm, recourse must be made to short term spectral analysis techniques.

Vessel Identifier:-	T-AGOS 19
water density	1.025 kg/m^3
gravitational acceleration	9.81 m/s^2
wave height	14 m
diameter of hull	4.88 m
length of hull	70.72 m
distance d(0)	5.11 m
distance d(1)	2.67 m
distance h	7.39 m
Strut Thickness	2.83
Strut Length	57.91 m

Wave Frequency (Rad/Sec)	Wave No	Side Force on Hull (kN)	Side Force on Strut (kN)	Total Side Force (kN)	Side Force RAO (Tonnes/Metre)
0.20	0.004	743.689	2105.472	2849.161	41.491
0.25	0.006	1148.474	3279.766	4428.240	64.486
0.30	0.009	1630.281	4705.282	6335.563	92.261
0.35	0.012	2181.744	6376.285	8558.029	124.625
0.40	0.016	2794.501	8286.087	11080.589	161.360
0.45	0.021	3459.353	10427.097	13886.450	202.220
0.50	0.025	4166.432	12790.864	16957.296	246.939
0.55	0.031	4905.384	15368.140	20273.524	295.231
0.60	0.037	5665.553	18148.936	23814.489	346.796
0.65	0.043	6436.171	21122.587	27558.758	401.322
0.70	0.050	7206.542	24277.819	31484.362	458.488
0.75	0.057	7966.219	27602.825	35569.044	517.971
0.80	0.065	8705.173	31085.331	39790.505	579.445
0.85	0.074	9413.951	34712.678	44126.629	642.590
0.90	0.083	10083.809	38471.892	48555.701	707.088
0.95	0.092	10706.837	42349.766	53056.604	772.631
1.00	0.102	11276.057	46332.935	57608.992	838.925
1.05	0.112	11785.501	50407.948	62193.449	905.686
1.10	0.123	12230.265	54561.348	66791.613	972.646
1.15	0.135	12606.547	58779.740	71386.287	1039.556
1.20	0.147	12911.651	63049.865	75961.516	1106.182
1.25	0.159	13143.984	67358.663	80502.648	1172.312
1.30	0.172	13303.022	71693.339	84996.361	1237.751
1.35	0.186	13389.262	76041.421	89430.683	1302.325
1.40	0.200	13404.158	80390.818	93794.976	1365.880
1.45	0.214	13350.045	84729.868	98079.914	1428.279
1.50	0.229	13230.047	89047.389	102277.437	1489.405

Vessel Identifier:-	M.V. Patria
water density	1.025 kg/m^3
gravitational acceleration	9.81 m/s^2
wave height	14 m
diameter of hull	1.8 m
length of hull	31.15 m
distance d(0)	1.8 m
distance d(1)	0.9 m
distance h	2.7 m
Strut Thickness	1
Strut Length	31.15 m

Wave Frequency (Rad/Sec)	Wave No	Side Force on Hull (kN)	Side Force on Strut (kN)	Total Side Force (kN)	Side Force RAO (Tonnes/Metre)
0.20	0.004	45.172	202.795	247.967	3.611
0.25	0.006	70.291	316.540	386.831	5.633
0.30	0.009	100.710	455.244	555.954	8.096
0.35	0.012	136.262	618.716	754.978	10.994
0.40	0.016	176.755	806.733	983.488	14.322
0.45	0.021	221.968	1019.038	1241.006	18.072
0.50	0.025	271.656	1255.343	1526.999	22.237
0.55	0.031	325.553	1515.327	1840.879	26.808
0.60	0.037	383.368	1798.638	2182.006	31.775
0.65	0.043	444.795	2104.894	2549.689	37.130
0.70	0.050	509.507	2433.685	2943.192	42.860
0.75	0.057	577.165	2784.569	3361.734	48.955
0.80	0.065	647.413	3157.081	3804.494	55.403
0.85	0.074	719.888	3550.726	4270.615	62.190
0.90	0.083	794.218	3964.986	4759.204	69.305
0.95	0.092	870.023	4399.316	5269.339	76.734
1.00	0.102	946.922	4853.152	5800.073	84.463
1.05	0.112	1024.530	5325.903	6350.434	92.478
1.10	0.123	1102.466	5816.963	6919.429	100.763
1.15	0.135	1180.350	6325.703	7506.053	109.306
1.20	0.147	1257.808	6851.478	8109.286	118.091
1.25	0.159	1334.474	7393.624	8728.098	127.102
1.30	0.172	1409.992	7951.465	9361.457	136.325
1.35	0.186	1484.017	8524.310	10008.327	145.745
1.40	0.200	1556.219	9111.454	10667.672	155.347
1.45	0.214	1626.279	9712.184	11338.463	165.115
1.50	0.229	1693.900	10325.775	12019.675	175.035

Tables G1 and G2, Approximate Calculation of Wave Induced Side Force RAO Values for T-AGOS 19 and M.V.Patria.